Muscle-tendon unit morphology, architecture and stiffness in relation to strength and responses to strength training

Muscle-Tendon Unit Morphology, Architecture and Stiffness in Relation to Strength and Responses to Strength Training

by

Garry John Massey

A Doctoral Thesis

Submitted in partial fulfilment of the requirements for the award of

Doctor of Philosophy of Loughborough University

March 2017

ABSTRACT

This thesis examined the change in skeletal muscle architecture with contractile force production, the relationship of architecture with muscle strength parameters and if muscle tendinous tissue stiffness determines *in vivo* explosive strength (i.e. rate of torque development, RTD). Muscle and tendinous tissue adaptations to contrasting strength training regimes, and the potential capacity of these tissues to adapt following chronic strength training were also explored. Quadriceps femoris fascicle length (FL) decreased, while the pennation angle (PA) increased in a curvi-linearly manner from rest to maximal voluntary contraction (MVC) torque. Consequently, effective physiological cross-sectional area ($_{eff}$PCSA) during MVC was 27% greater than at rest, although $_{eff}$PCSA measured at rest and during MVC had similar correlations to maximal strength. In the earliest phase of contraction, FL, but not PA, was negatively related (R^2=0.187) to voluntary RTD. Neither FL nor PA was related to maximal isometric or dynamic strength. Muscle-tendon unit (MTU) and patellar tendon (PT) stiffness were unrelated to voluntary and evoked RTD. Relative PT stiffness was also unrelated to relative RTD, although relative MTU stiffness was related to voluntary RTD (25-55%MVT, $R^2 \leq 0.188$) and evoked RTD (5-50%MVT, $R^2 \leq 0.194$). MTU stiffness increased after sustained-contraction (SCT, +21%), though not explosive-contraction strength training (ECT). PT stiffness increased similarly after ECT (+20%) and SCT (+16%), yet neither induced tendon hypertrophy. SCT produced modest muscle (+8%) and aponeurosis (+7%) hypertrophy. Chronic strength trained (CST: >3 years) males had substantially greater muscle and aponeurosis size, but similar tendon size as untrained controls (UNT) and short-term (12 weeks) strength trained (STT) individuals. Between these groups, at the highest common force, MTU stiffness was indifferent, while PT stiffness was similarly greater in STT and CST than UNT. These results suggest FL and PA have little influence on muscle strength and tendon stiffness has no influence on RTD. Maximum strength negated any qualitative influence of MTU stiffness on *in vivo* RTD. Component MTU tissues (muscle-aponeurosis vs. external tendon) adapt differentially depending on the strength training regime. Specifically, free tendon appeared to adapt to high magnitude loading, while loading duration is also an important stimulus for the muscle-aponeurosis. However, chronic strength training was not concordant with greater higher force MTU stiffness, and does not further increase higher force PT stiffness beyond the adaptations that occur after 12 weeks of strength training. Finally, no evidence was found for tendon hypertrophy in response to strength training.

Keywords: knee extensor, muscle-tendon unit, patellar tendon, stiffness, explosive strength, rate of torque development, muscle architecture, strength training, ultrasound

PUBLICATIONS

Massey G, Evangelidis P & Folland J. (2015). Influence of contractile force on the architecture and morphology of the quadriceps femoris. *Exp Physiol*, 100(11), 1342-1351.

Massey GJ, Balshaw TG, Maden-Wilkinson TM, Tillin NA & Folland JP. (2017). The influence of patellar tendon and muscle-tendon unit stiffness on quadriceps explosive strength in man. *Exp Physiol*, DOI: 0.1113/EP086190/full.

CONFERENCE PROCEEDINGS

G.Massey, P.Evangelidis & J.Folland (2013). Relationship between quadriceps femoris architecture and knee extension explosive force production. *Journal of Sports Sciences, 32:sup1,* s71-s72.

Massey G.J., Balshaw T.G., Maden-Wilkinson T.M., Tillin N.A., Folland J.P (2015). Differential tendinous tissue adaptations after conventional vs. explosive strength training *Book of Abstracts of the 20th Annual Congress of the European College of Sports Science in Malmö, Sweden, p416.*

G.Massey, T.G. Balshaw, T.Maden-Wilkinson, N.Tillin, J.Folland (2016). Do muscle-tendon unit and patellar tendon stiffness influence explosive strength in man? The Biomedical Basis of Elite Performance Conference. *Proceedings of the Physiological Society 35, PC38.*

Massey G.J., Balshaw T.G., Maden-Wilkinson T.M., Folland J.P (2016). Tendon size and stiffness: influence of short-term and chronic strength training. *Book of Abstracts of the 21st Annual Congress of the European College of Sports Science in Vienna, Austria, p128.*

- *Young Investigator Award Recipient*

ADDITIONAL CONTRIBUTIONS

Evangelidis PE, Massey GJ, Pain MT, & Folland JP. (2015). Biceps femoris aponeurosis size: a potential risk factor for strain injury? *Med Sci Sports Exerc*, 47(7), 1383-1389.

Evangelidis PE, Massey GJ, Pain MT, & Folland JP. (2016). Strength and size relationships of the quadriceps and hamstrings with special reference to reciprocal muscle balance. *Eur J Appl Physiol*, 116(3), 593-600.

Balshaw TG, Massey GJ, Maden-Wilkinson TM, Tillin NA, & Folland JP. (2016). Training-specific functional, neural, and hypertrophic adaptations to explosive- vs. sustained-contraction strength training. *J Appl Physiol*, 120(11), 1364-73.

ACKNOWLEDGEMENTS

Firstly I would like to extend my gratitude to my supervisor, Dr Jonathan Folland, for providing me the opportunity to undertake the work in this thesis and for his excellent advice and guidance throughout my studies.

A special thank you goes to Dr Pavlos Evangelidis for his friendship and collaboration with data collection and analysis in study chapters 1 and 2. I enjoyed working with him, which made the long hours of testing much easier.

A special thanks to Dr Thomas Balshaw. Working with him was a pleasure and without him studies 3-5 would not have been possible. He made the relentless testing sessions much more bearable.

Also, thank you to Dr Tom Maden-Wilkinson for his time in analysing the muscle MRI's for Chapters 6 and 7.

In addition, thank you to Dr Neale Tillin for his contribution to Chapters 5, 6 and 7.

I would also like to thank the MSc students Miss Alex McKeown, Mr Antonio Jesus Morales Artacho and Miss Clare Appleby for their valuable assistance with conducting the training study in Chapter 6. Thanks to Clare for also analysing some of the muscle MRI's.

And, of course I would very much like to express my sincere thanks to my mum and dad, Anne and Ronnie, as well as my sister Gemma for their love and support.

Finally, I would like to thank all those who were participants in my studies for their time and effort.

LIST OF ABBREVIATIONS

ACSA	Anatomical Cross-Sectional Area
Apon Area	Aponeurosis Area
BF	Biceps Femoris Muscle
CON	Control
CSA	Cross-Sectional Area
CST	Chronic Strength Trained
ECT	Explosive-Contraction Strength Training
$_{eff}$PCSA	Effective Physiological Cross-sectional Area
EMG	Electromyography
ES	Effect Size
FL	Fascicle Length
k	Stiffness
MET	Metabolic Equivalent
MRI	Magnetic Resonance Imaging
MTU	Muscle-Tendon Unit
MTUdt	Muscle-Tendon Unit Distal Tissue
MVC	Maximal Voluntary Contraction
MVT	Maximal Voluntary Torque
OCT	Octet
PA	Pennation Angle
PT	Patellar Tendon
QF	Quadriceps Femoris Muscle
QUADSvol	Quadriceps Femoris Muscle Volume
RF	Rectus Femoris
RTD	Rate of Torque Development
SCT	Sustained-Contraction Strength Training
ST	Semitendinosus Muscle
STT	Short-Term Strength Trained
TFCP	Tibio-Femoral Contact Point
UNT	Untrained

VI	Vastus Intermedius Muscle
VL	Vastus Lateralis Muscle
VM	Vastus Medialis Muscle
VOL	Voluntary

LIST OF TABLES

LIST OF FIGURES

TABLE OF CONTENTS

CHAPTER 1

General introduction

Strength defines the skeletal muscle force or torque produced under a given set of conditions and is fundamental to human physical capabilities. Various strength parameters can be characterised with careful laboratory measurements. Maximal isometric strength has been the most extensively studied aspect of neuromuscular function, and may relate well to athletic performance, or simply carrying out activities of daily living. Alternatively, maximal dynamic strength is considered more relevant to the performance of functional tasks such as balance, mobility and locomotion. In addition, the ability to increase torque as quickly as possible from low or resting levels (explosive strength, i.e. rate of torque development [RTD]) is considered particularly important in situations where the time to develop torque is limited: for instance, during athletic tasks such as sprinting and jumping (Weyand et al. 2010; Tillin et al. 2013a) and in injury-related situations (Izquierdo et al. 1999; Krosshaug et al. 2007). Further RTD deficits have a deleterious impact on physical function in musculoskeletal patients (e.g. osteoarthritis: Maffiuletti et al. 2010), and may predispose injury risk (Opar et al. 2013; Kline et al. 2015).

Skeletal muscle architecture refers to the spatial arrangement of muscle fibres and is commonly measured in *in vivo* as fascicle length (FL) and pennation angle (PA). FL is considered a major determinant of muscle's contractile speed and force-velocity properties (Lieber and Fridén 2000), though an anticipated positive relationship of FL to either RTD or high-velocity dynamic strength has not been demonstrated in the minimal number of *in vivo* investigations. Any possible influence of PA on dynamic strength (Azizi et al. 2008) or RTD is poorly documented. While the contractile elements of skeletal muscle ultimately generate the force to produce joint torque, this force is transmitted to the bone via the tendinous tissues (intramuscular aponeurosis and external free tendon) in order to produce torque and resultantly movement. The mechanical stiffness (resistance to deformation) of the tendinous tissues determines MTU interaction and modulates the contractile conditions (length and velocity); thus muscle force and joint torque production (Roberts 2002; Litchwark and Barclay 2010). Notably, greater tissue stiffness is thought to facilitate a higher RTD (Bojsen-Møller et al. 2005; Waugh et al. 2013), though evidence for this association *in vivo* is inconclusive.

An appreciation of tendon function has prompted relatively recent investigations into the adaptive response of tendinous tissues to altered patterns of mechanical loading (Magnusson et al. 2008; Heinemeier and Kjaer 2011). Most prominently the possibility of increased

tendinous tissue stiffness via strength training has been of interest, with studies examining relatively short-term (8-14 week) adaptations (Bohm et al. 2015; Wiesinger et al. 2015). However, the relative efficacy of contrasting training regimes, which impose distinct tissue mechanical loading patterns, to stimulate tendon adaptations has received minimal attention. Further, the potential capacity of tendons to continue to adapt to chronic strength training has been largely unexplored.

In vivo muscle architecture can be reliably estimated via ultrasonography. Substantial changes in FL (decreases) and PA (increases) occur even during isometric (constant length) contractions (Narici et al. 1996; Maganaris et al. 1998), and these changes may have important implications for our understanding of *in vivo* muscle function. The quadriceps femoris (QF) is a functionally important muscle group, however the architecture changes during contraction have only been reported within the component vastus lateralis muscle. Furthermore, the FL and PA changes during contraction result in an increase in the effective physiological cross-sectional area ($_{eff}$PCSA) of a muscle (Narici et al. 1996a). The functional significance being that $_{eff}$PCSA is proportional to the maximal isometric contractile force that can be exerted upon the tendon (Powell et al. 1984). Hitherto, *in vivo* studies have only established the relationship between isometric maximal voluntary torque (MVT) and $_{eff}$PCSA measured at rest. It is possible that $_{eff}$PCSA quantified during maximal voluntary contraction (MVC) may better reflect the inter-individual differences in muscle morphology during contraction and thus provide a better determinant of strength. The primary aim of study one was to document the architectural and $_{eff}$PCSA changes that occur within all four constituents of the QF and subsequently the whole muscle group throughout isometric contraction from rest to MVC. The secondary aim was to test whether there was stronger relationship between MVT and $_{eff}$PCSA measured during an MVC than for $_{eff}$PCSA measured at rest (Chapter 3).

Despite theoretical rationale, the influence of FL and PA on *in vivo* muscle strength characteristics has not been substantiated. A larger angle of fibre pennation permits a greater quantity of contractile material to attach to the aponeurosis, thus increases a muscles $_{eff}$PCSA. In this case, a greater PA may positively relate to higher MVT and might also be expected to influence later phase RTD, which is known to be dependent on MVT (Aagaard and Andersen 2006; Folland et al. 2014) and has similar physiological determinants as MVT (e.g. muscle size; Erskine et al. 2014). While there is some evidence supporting a moderate positive relation between PA and MVT (e.g. Wakahara et al. 2013; Ando et al. 2015), any

relation of PA to RTD has not been tested. A possible influence of PA on dynamic strength (Azizi et al. 2008) is unclear and any *in vivo* relationship has received minimal attention. Alternatively, FL is anticipated to have a profound influence on dynamic strength as longer fascicles possess more sarcomeres in-series which results in higher maximal shortening velocity potential and can thus likely generate a greater proportion of isometric with increasing contraction velocity (Bodine et al. 1982; Wickiewicz et al. 1984; Lieber and Fridén 2000). However, evidence to support an influence of FL on *in vivo* higher velocity dynamic strength is limited; a couple of studies report no correlation (Blazevich et al. 2009b; Baxter and Piazza 2014). Further to longer fascicles being capable of faster shortening, the time taken to stretch series elastic structures can slow RTD (Edman and Josephson 2007), and therefore longer fascicle might be positively associated with explosive strength. Contrarily, a preliminary report noted a negative association between the changes in FL (inferred from shifts in the optimal angle to develop joint torque) and RTD following strength training, implying longer fascicles slow torque development (Blazevich et al. 2009b). The second study aimed to directly assess the relationship between *in vivo* quadriceps femoris muscle architecture (measured at rest) and knee extension strength characteristics; maximal and explosive isometric strength, and dynamic strength at different velocities (Chapter 4).

Whether MTU and tendon stiffness are physiological determinants of RTD is unsubstantiated. During isometric contractions, the rate of muscle force production is slowed by the necessity of the muscle to shorten in order to stretch the tendinous tissues (Hill 1951; Edman and Josephson 2007); in accordance with the muscle force-velocity relationship (Wilkie 1949). Stiffer tissues also theoretically transmit force more quickly. Yet, these mechanisms may be inconsequential *in vivo*. To date no studies have examined whether tendon stiffness is related to human RTD. There is evidence of moderate positive correlations between MTU stiffness and RTD (R^2~0.10-0.30; Bojsen-Møller et al. 2005; Wang et al. 2012; Waugh et al. 2013; Hannah and Folland 2015), however these studies are mired by methodological issues (Seynnes et al. 2015). In particular, estimations of tissue stiffness have been acquired from tendon force-elongation measurements recorded under conditions of variable loading rates and within an absolute tendon force range relative to maximal strength (e.g. 50-90% MVT). Greater absolute forces and a faster RTD yield a stiffer tissue response, therefore the previous findings could be spurious owing to an inherent bias towards greater stiffness measurement in stronger (>MVT) individuals that also tend to display higher a RTD. The third study aimed to comprehensively examine the relationship between both

tendon and MTU stiffness, with voluntary and evoked RTD measurements of explosive strength recorded in duplicate measurement sessions. Correlations were performed between absolute and relative stiffness (to remove the influence of maximum strength) acquired from constant loading-rate ramp contractions, and RTD variables measured over the same torque range (Chapter 5).

Sustained-contraction strength training (SCT: ≥2 s duration) utilising high relative loads (>70% MVT) increases MTU (Kubo et al. 2001; 2006b; Arampatzis et al. 2007a, 2010; Bohm et al. 2014) and tendon stiffness after 8-14 weeks (Reeves et al. 2003; Kongsgaard et al. 2007; Seynnes et al. 2009; McMahon et al. 2013). Studies have typically assessed either MTU or tendon so the concordant changes are unclear. Interestingly a couple of studies have reported that explosive-contraction strength training (ECT: brief contractions [<1-second] with maximal/near maximal RTD) increased MTU stiffness after merely four (Tillin et al. 2012) or six weeks training (Burgess et al. 2007), suggesting ECT may be a time-efficient approach for providing a potent stimulus for tendon tissue adaptation. However, the efficacy of ECT vs. SCT has not been established. In addition, whether increased tissue stiffness is partially consequent to tendon/aponeurosis hypertrophy remains opaque. An increase in tendon CSA is controversial: a few studies found modest region-specific hypertrophy (Kongsgaard et al. 2007; Seynnes et al. 2009; Arampatzis et al. 2007a), while others showed no change (Arampatzis et al. 2010; Kubo et al. 2012; Bloomquist et al. 2013). A solitary report documents a small within-group increase in aponeurosis width after 12 weeks dynamic SCT (Wakahara et al. 2015). In contrast, tendon stiffness changes after SCT do appear to correspond with an improvement in tendon Young's modulus (material stiffness). The effect of ECT on tissue size and tendon Young's modulus is yet to be documented. The fourth study aimed to compare the mechanical (MTU stiffness, PT stiffness and PT Young's modulus), and morphological (quadriceps femoris muscle, VL aponeurosis and PT size) adaptations of the quadriceps MTU to 12 weeks isometric ECT vs. SCT vs. an untrained control group (Chapter 6).

A possible explanation for the uncertainty regarding tendon hypertrophy is the relatively slow turnover of tendon collagen (Smith and Rennie 2007; Heinemeier et al. 2013b). Modest changes in tendon size after 8-14 weeks may be on the threshold of what can be detected. More demonstrable hypertrophy could be evident after chronic (years) strength training. However, whether MTU and tendon stiffness undergo continued adaptation in response to

chronic exposure to high mechanical load is largely unexplored. The one published study found chronic strength trained males to have greater patellar tendon stiffness (measured at an equal absolute force), but similar Young's modulus compared to recreationally active males (Seynnes et al. 2013). The purpose of the fifth study was to compare the mechanical and morphological properties of the patellar tendon (stiffness, Young's modulus, CSA [mean and regional]) and quadriceps femoris muscle-tendon unit (stiffness, muscle volume, vastus lateralis aponeuroses area), between untrained controls, short-term strength trained (post-12 weeks training) and chronic-strength trained (>3 years of systematic training) groups (Chapter 7).

CHAPTER 2

Literature review

2.1. Introduction

The present thesis initially aimed to improve our understanding of the importance of muscle architecture to *in vivo* muscle strength characteristics, as well address the confusion regarding the influence of musculotendinous tissue stiffness as a determinant of explosive strength. Subsequently the effects of contrasting training regimes upon muscle-tendon unit (MTU) and tendon adaptations (morphology and stiffness) were examined, and finally the potential for tendinous tissue adaptations to chronic strength training was investigated. As pertinent to these aims, the theoretical influence and *in vivo* evidence to support muscle-tendon unit morphology and tendinous tissues stiffness as determinants for *in vivo* strength parameters will be outlined. In addition the MTU adaptations to strength training will be highlighted. The principal focus will be to appreciate the increasing evidence regarding the capacity of the tendon tissues to adapt to strength training and the possible training characteristics implicated in stimulating an adaptive response. Skeletal muscle and tendon structure and mechanical properties are covered in brief.

2.2. Basic Muscle-Tendon Unit Structure and Function

2.2.1. Muscle Structure

The functional unit that produces motion at a joint consists of the muscle and the tendon that attaches the muscle to the bone (i.e. the muscle-tendon unit). Skeletal muscle (Figure 2.1) is composed of the fibres that are linked together by a three-level network of collagenous intramuscular connective tissue: endomysium surrounds individual muscle fibres; perimysium collects bundles of fibres into fascicles; and epimysium ensheathes the entire muscle (Enoka 2008). The connective tissue connects muscle fibres to the tendon. Muscles fibres are long cylindrical, multi-nucleated cells filled with smaller units of filamentous structures, myofibrils. Myofibrils are composed of subunits, sarcomeres, arranged end to end the length of the myofibril. The sarcomere is the basic functional unit of muscle and contains thick and thin myofilaments composed of the contractile proteins myosin and actin. The sliding of actin myofilament on the myosin chain is the basic mechanism of muscle contraction (Oatis 2009).

2.2.2. Connective Tissue Structure

Skeletal muscle forces generated by the contractile apparatus are transmitted to the bone (to generate movement) via collagenous connective tissues:

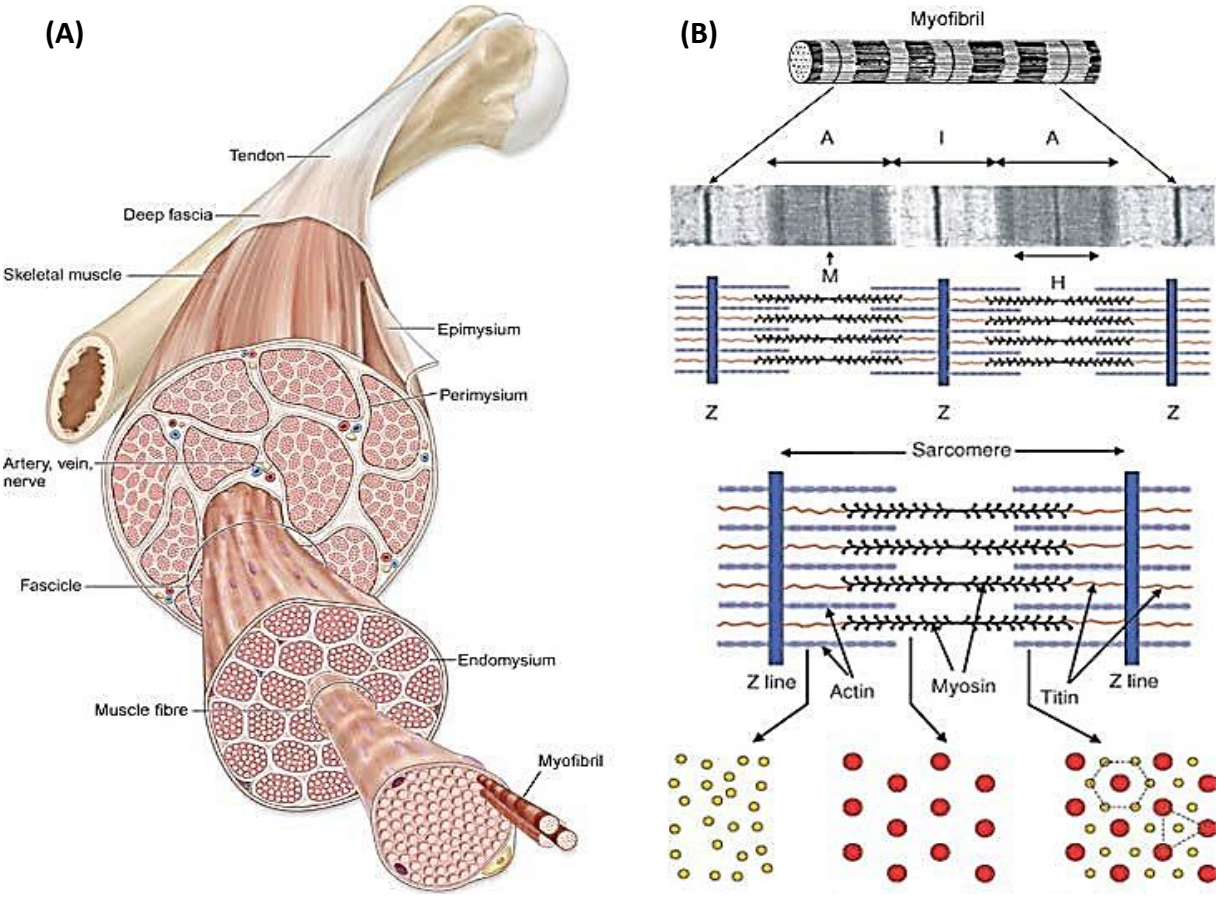

Figure 2.1. (A) An overview of the hierarchical structure of skeletal muscle from the whole muscle to the myofibril, and (**B)** the internal arrangement of the myofilaments within a sarcomere (Adapted from Jones et al. 2004).

2.2.2.1. Intramuscular Connective Tissues

Intramuscular connective tissues form the classical anatomical entities of endo-, peri-, and epimysium surrounding individual muscle fibres, bundles of muscle fibres (fascicles), and the whole muscle, respectively (Figure 2.2). Each muscle cell is surrounded by it's own plasma membrane and basement membrane. Filling the intervening region between the basement membrane and two adjacent muscle cells is the more substantial reticular layer comprised of a network of fine collagen fibrils and fibres (Purslow 2010). The collagen fibres form a seemingly quasi-random network of irregular wavy fibres; fibres appearing to run at all angles relative to the muscle fibre long axis (Purslow 2010). Though there is a preferred direction in the wide distribution of collagen fibre orientation that changes with muscle length, with more fibres being orientated to the long axis of the muscle fibres at longer lengths (Kovanen 2002; Purslow 2010). Different to the mesh-like structure of the endomysium, the perimysium consists of well-ordered sheets of wavy/crimped collagen

fibres (larger than endomysium) in a cross plied arrangement, all fibres within a ply being parallel to each other and lying at a common angle (±55°) to the muscle fibre direction at resting length (Purslow 2002). Collagen fibre orientation changes from 20-80° with short-long sarcomere lengths (Purslow 2002). The perimysium is considered continuous with the tendon (Gilles and Lieber 2010), as is the epimysium, which consists of two layers of large wavy collagen fibres aligned more parallel to the long axis of the muscle forming a dense sheet-like surface layer (Kjaer 2004; Gilles and Lieber 2010; Purslow 2010). The epimysium contains predominantly Type I collagen, perimysium Types I and III, and endomysium Types I, III, and V (Kovanen 2002).

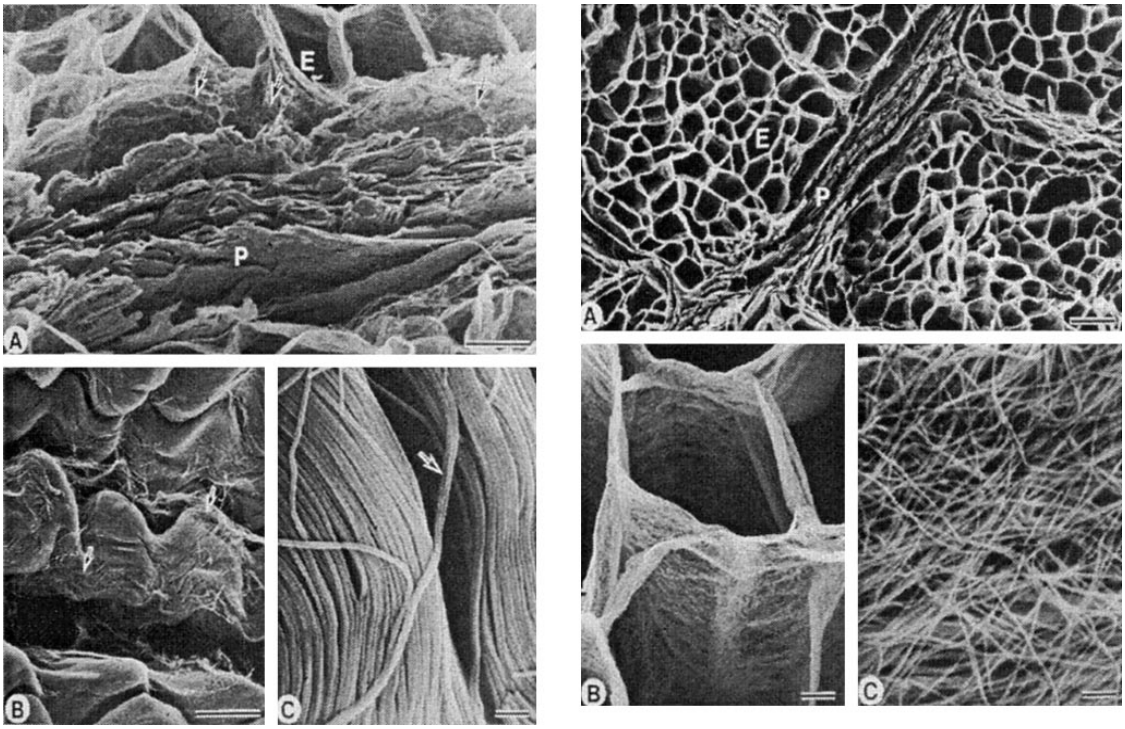

Figure 2.2. Scanning electron (SEM) micrographs of intramuscular connective tissue of bovine semitendinous muscle. Muscle samples have been treated by the cell-maceration method, which allows the examination of the three-dimensional arrangement of collagen fibrils in tissue sections. Perimysium (**P**) (panel A, left) is composed of several sheets of collagen fibres. Loose networks of collagen fibrils (**arrows**) appear to connect perimysium and endomysium (**E**). (Panel B, left). Higher magnification of perimysium showing bundles of collagen fibres in an extremely wavy pattern and covered with loose networks (**arrow**) of collagen fibrils. (Panel C, left) Higher magnification of the wavy perimysium shows the arrangement of collagen fibrils, some of them branching off the fibre and fusing into the adjacent fibre. (Panel A, right) Endomysium is a cylindrical sheath housing individual muscle fibres. The endomysial sheaths are membranous (panel B, right). (Panel C, right) A closer view of the endomysial sheath shows the arrangement of collagen fibrils (Kovanen 2002).

2.2.2.2. Tendinous Tissues (Aponeurosis and Tendon)

The sheet-like aponeurosis (internal tendon) surrounds the muscle belly and provides the attachment area for the muscle fibres. The external 'free' tendon provides the in-series structural link between the muscle and bone. The collagenous structure is considered similar in both aponeurosis and free tendon (Scott and Loeb 1995; Azizi et al. 2009) as both these tissues are primarily composed of collagen (mostly type I) organised in a hierarchical manner (collagen molecule [triple helix tropocollagen), micro-fibril, fibril, fibre, and fascicle; Screen 2009 [Figure 2.3]) primarily oriented along the longitudinal axis of the tendon. The collagen structure and biochemical composition of the tendon is considered principally responsible for the mechanical properties of tendinous tissues with the collagen fibril being the most basic load-bearing unit of the tendon (Kjaer 2004). The fibril consists of bundles of micro fibrils held together by biochemical bonds (cross-links) between the collagen molecules. In an unloaded condition collagen fibres display a characteristic wavy pattern (crimp) that disappears upon tendon stretch and collagen fibres straighten. The resistance to deformation provided by tendinous tissues is referred to as mechanical 'stiffness', which governs the effectiveness of tendons to transmit force and dictates muscle-tendon interaction.

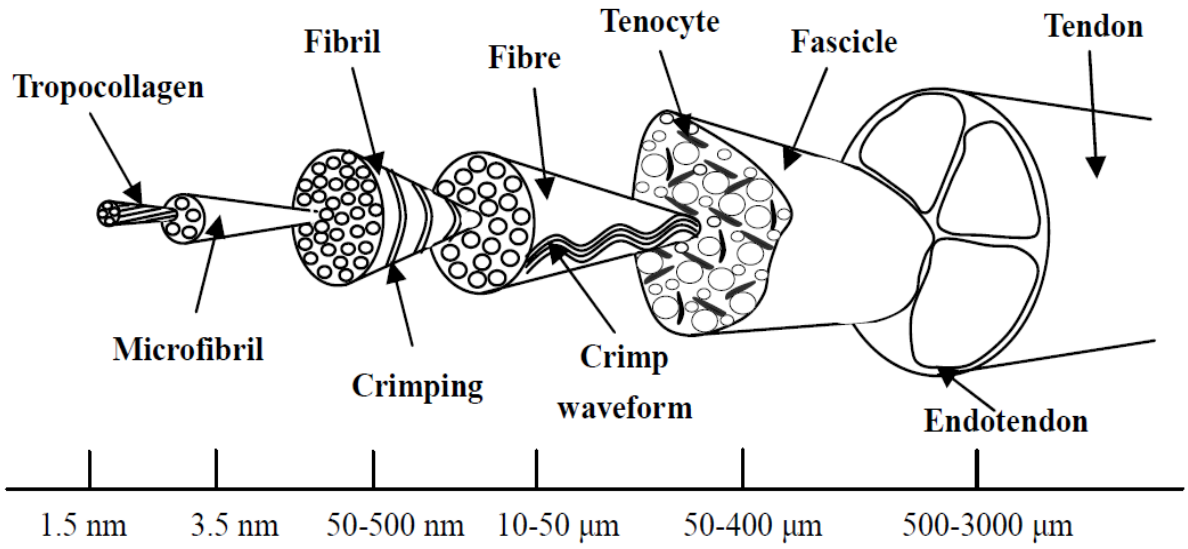

Figure 2.3. Schematic of the tendon hierarchical structure, highlighting the different collagen structures with a rough indication of the diameter (Adapted from Screen 2009).

2.2.3. Muscle Mechanical Properties

Muscle force production is intimately governed by the instantaneous contractile conditions determined by muscle fibre length (Gordon et al. 1966) and the rate of length change (velocity; Hill 1938; Katz 1939). *In vivo*, muscle force-length and force-velocity properties are transformed into torque-angle and torque-velocity relationships. Muscle moment arm (perpendicular distance from the line of action of muscle to the joint centre of rotation) transforms the linear movement of the muscle into rotation about the joint. The externally measurable quantity of torque results from the cross product of moment arm and force developed by the muscle. Muscle moment arm varies throughout the range of joint motion (Enoka 2008) and determines the muscle length change during joint rotation (Oatis 2009). In the relationships below, whole-muscle force-length/velocity properties are assumed to reflect those of scaled-up muscle fibres, which in turn are considered scaled versions of sarcomere properties.

2.2.3.1. Force-Length Relationship

In this relationship (Figure 2.4) skeletal muscle active force production is defined in terms of myofilament overlap, i.e. in terms of sarcomere length. At optimal length, where actin-myosin interactions (cross-bridges) are maximal, muscles generate force. As sarcomere length increases, force decreases owing to the decreasing number of interactions between actin and myosin myofilaments. At lengths shorter than the optimum, force decreases owing to the double interdigitation of actin filaments with both myosin and actin filaments from opposite sides of the sarcomere (Lieber and Ward 2011). At the muscle level, the active range force depends on number of sarcomeres in series. It is important to appreciate that the active force-length relationship is not a continuous curve and represents discrete data points observed when the muscle is held at different lengths and activated maximally. *In vivo* isometric torque-angle relationships are determined from maximal voluntary contractions performed at multiple joint angles throughout the range of motion.

2.2.3.2. Force-Velocity Relationship

This relationship (Figure 2.5) describes the dependence skeletal muscle force production on contraction velocity. When contraction velocity equals zero the maximal isometric force is developed. As contraction velocity increases during shortening (concentric) contractions during there is non-linear (hyperbolic) decrease in muscle force in accordance with a reduced probability of actin-myosin interactions (Lieber and Ward 2011); finite time is required for

cross-bridge attachment and detachment. At the muscle level, maximal shortening velocity depends on the number of sarcomeres in series. During lengthening (eccentric) contractions, increased contraction velocity yields greater contractile force than in isometric contractions, with a plateau of 1.5-1.9 times greater eccentric force regardless of further increases in lengthening velocity (Katz 1939). Force enhancement during active lengthening is thought to be most probably associated with the increased strain of attached cross-bridges as the sarcomeres are forcibly stretched (Edman 1999, Zatsiorsky and Prilutsky 2012). *In vivo*, the torque-velocity relationship is typically assessed using isovelocity dynamometry, and is formed from the maximum torques recorded during discrete contractions at distinct constant angular velocities. Volitional *in vivo* maximal eccentric torque may be similar to or slightly greater than maximal isometric torque, presumably due to neural inhibitory mechanism (Westing et al. 1988, 1990, 1991; Dudley et al. 1990; Seger and Thorstennsson 2000). (Figure 2.6).

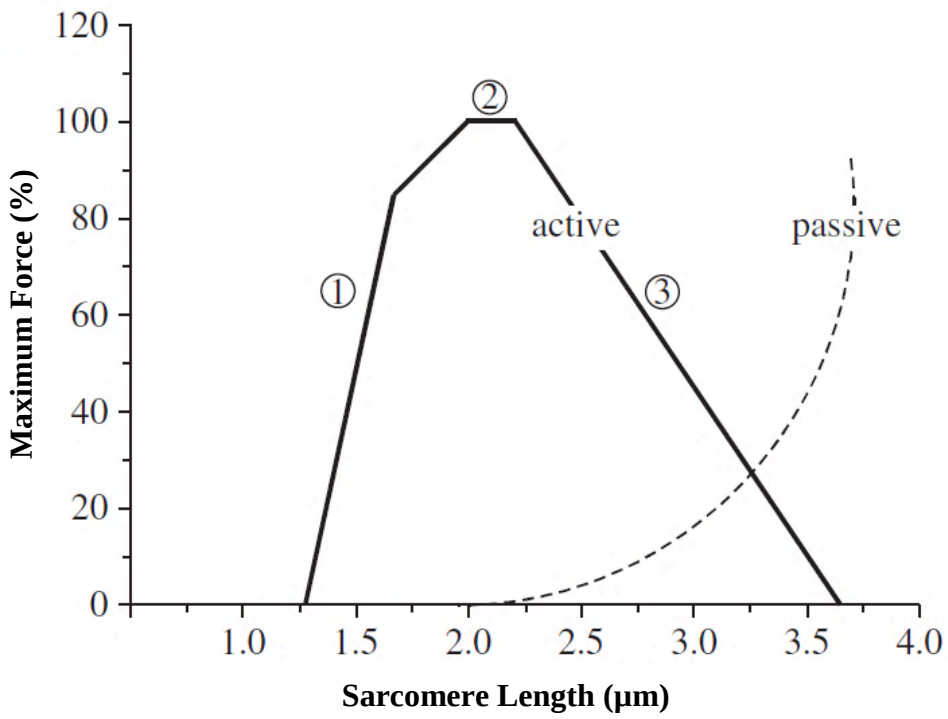

Figure 2.4 The isometric sarcomere force-length relationship obtained using sequential isometric contractions in single muscle fibres (solid line). Dotted line represents passive muscle tension borne by the muscle without activation. Number s above the active curve represent the three main regions of the force-length curve: (1) ascending region, (2) plateau and (3) descending region (Adapted from Lieber and Ward 2011).

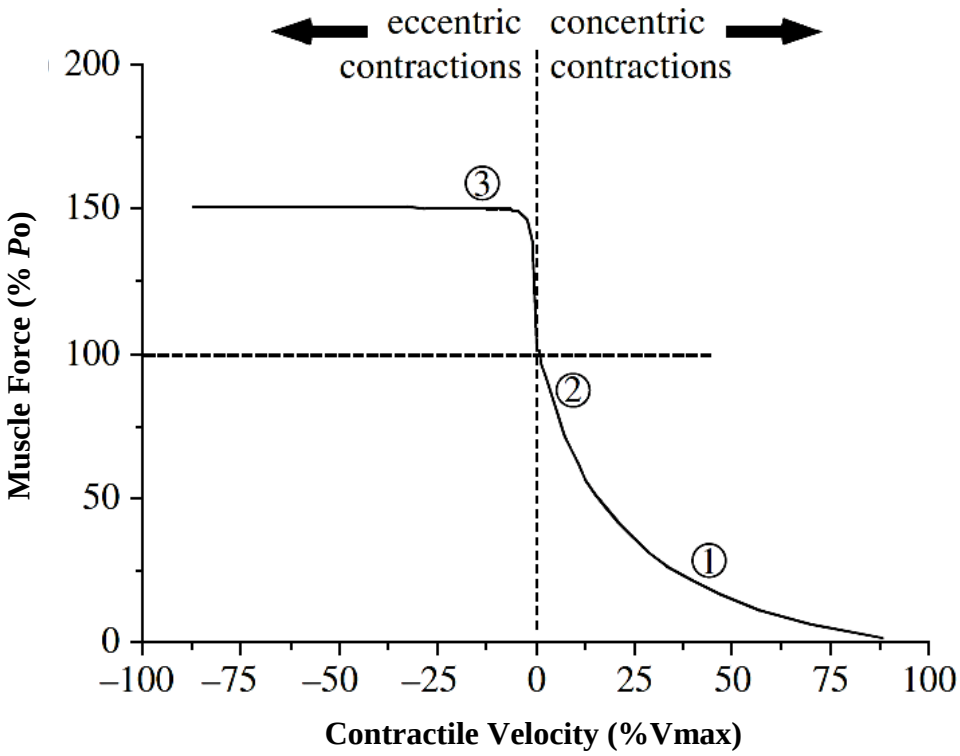

Figure 2.5. The muscle force-velocity relationship obtained using sequential contractions. (1) The circles numbers represent the force and velocity data from two concentric contractions (1, 2) and one eccentric contraction (3). *P*o, maximal isometric force. (Adapted from Lieber and Ward 2011).

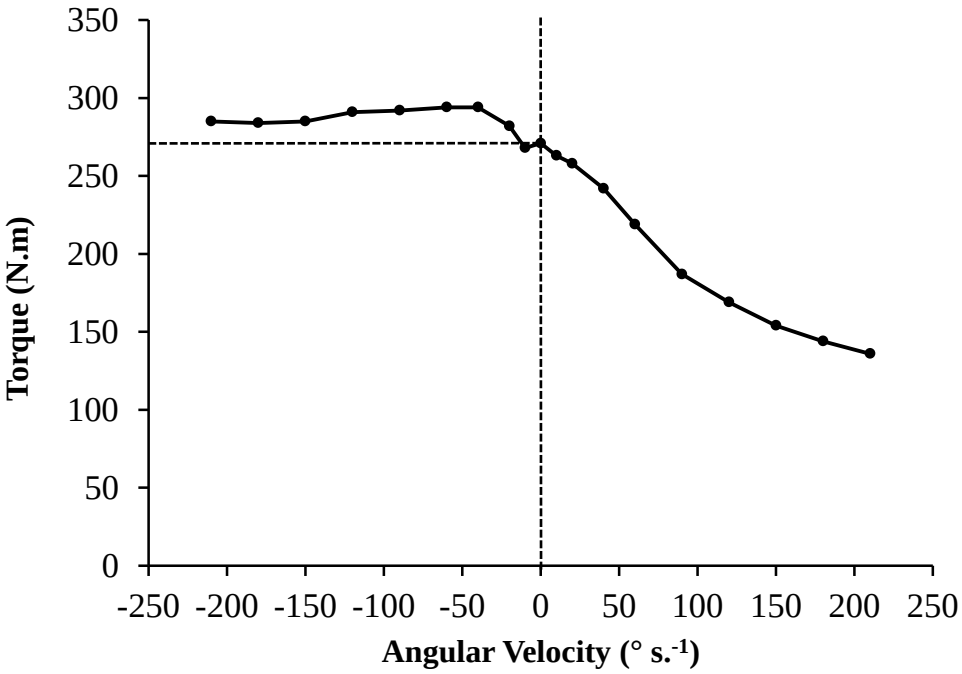

Figure 2.6. Example *In vivo* torque-velocity relationship obtained from discrete isovelocity knee extension maximal voluntary contractions. (Adapted from Dudley et al. 1990)

2.2.4. Basic Mechanisms of Tendon Elongation

In classical *in-vitro* mechanical tensile tests, the tendon force-elongation relationship displays a characteristic non-linearity at lower levels (slope increases) called the toe-region where relatively little force induces elongation. This region is associated with a structural change in fibril organisation from a crimped (wavy planar pattern) to a more straightened, parallel arrangement (Butler et al. 1978). Continued elongation elicits a stiffer response; greater increases in force are required for equivalent elongations, and there is a progressive recruitment of individual collagen fibrils at varying degrees of crimp (Zatsiorsky and Prilutsky 2012). With the increase in force additional collagen fibrils experience elongation, which accounts for the non-linearity (Hansen et al. 2002). With further applied force, a linear region (constant slope) is reached. This region reflects the stretching of the pre-aligned collagen fibers (Zatsiorsky and Prilutsky 2012).

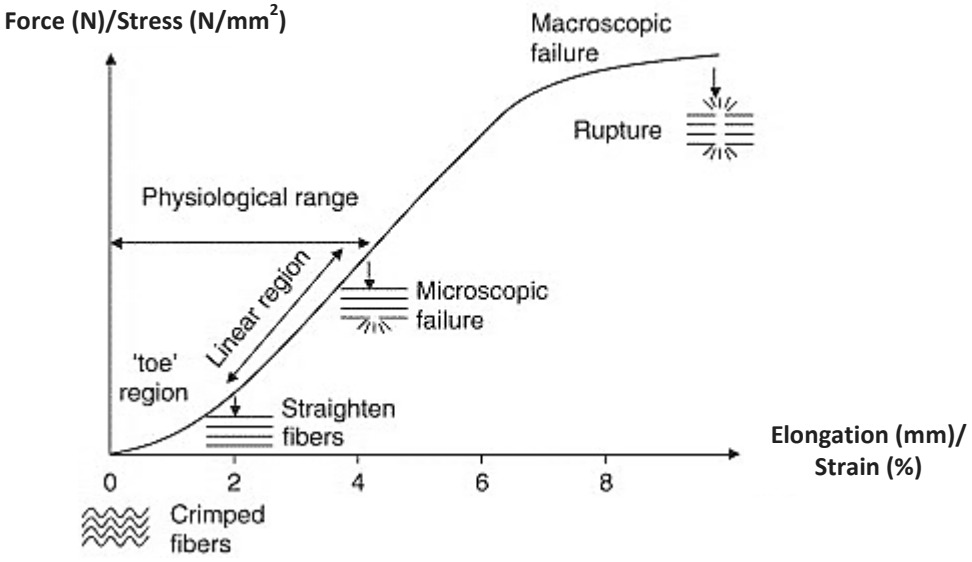

Figure 2.7. Schematic of the tendon force-elongation/stress-strain relationship (Adapted from Wang 2006).

2.3. Relation to Strength

The present thesis investigates maximal and explosive strength and adopts the following definitions: maximal strength (isometric and dynamic) is the greatest torque exerted during maximal voluntary contraction (i.e. Maximal Voluntary Torque [MVT]); explosive strength is the capability to increase torque from low or resting levels as quickly as possible as measured under isometric conditions and expressed as the rate of torque development (RTD) derived from the rising phase (i.e. slope) of the contraction torque-time curve. This section of the review outlines the determinants of strength to be examined in the ensuing experimental work.

2.3.1. Muscle Size

Muscle physiological cross-sectional area (PCSA) is the total cross-sectional area of the muscle fibres perpendicular to their line of action and represents the maximal number of sarcomeres in parallel; hence the possible number actin-myosin cross-bridges that can be formed. Accordingly, *in vitro*, the maximal tetanic tension transmitted along the tendon (i.e. the maximal isometric contractile force) is directly proportional to the PCSA once accounting for the angulation of the fibres relative to the muscle line of action (R^2 = 0.99; Powell et al. 1984). This effective ($_{eff}$) PCSA is therefore theoretically the most important determinant of maximal torque in vivo. Indeed studies have found strong correlations between PCSA and maximal isometric and concentric torque: plantar flexors r = 0.71 (Bamman et al. 2000); elbow flexors and extensors r = 0.91 and 0.95 (Fukunaga et al. 2001); knee extensors r = 0.72 and 0.62 (Blazevich et al. 2009b). A difficulty of estimating $_{eff}$PCSA *in vivo* is that it is a composite measure, calculated from the ratio of muscle volume (typically measured via magnetic resonance imaging) to fascicle length multiplied by the cosine of pennation angle, which can be measured via ultrasound imaging. Multiple measurement errors may affect the accuracy of the *in vivo* estimate and underpin why $_{eff}$PCSA may be no better a predictor of maximal strength than measures of total contractile material quantity. Further, $_{eff}$PCSA may be under or over estimated if regional FL and PA variation throughout the muscle volume is not captured and the generalized architectural data from single ultrasound images is used to derive $_{eff}$PCSA.

Measures of gross muscle size; anatomical cross-sectional area (ACSA; cross-sectional area perpendicular to the muscle length) and muscle volume, are essentially a structural proxy for

the $_{eff}$PCSA; thus number of parallel sarcomeres and hence maximal contractile force and resultant torque. Unsurprisingly, strong correlations have been equally reported between maximal isometric and concentric strength vs. ACSA: plantar flexors r = 0.73 (Bamman et al. 2000); elbow flexors and extensors r = 0.71 - 0.91 (Fukunaga et al. 2001; Akagi et al. 2009); knee extensors r = 0.73 (Blazevich et al. 2009b), and muscle volume: plantar flexors r = 0.47 – 0.65 (Bamman et al. 2000; Baxter and Piazza 2014); elbow flexors and extensors r = 0.76 – 0.94 (Fukunaga et al. 2001; Akagi et al. 2009; Erskine et al. 2014); knee extensors r = 0.55 – 0.86 (Blazevich et al. 2009b; Evangelidis et al. 2016); knee flexors r = 0.62 – 0.74, (Evangelidis et al. 2016). Though not typically considered, it is possible that the unaccounted for inter-individual differences in muscle fibre-type composition may partially confound the muscle strength-size (either volume, ACSA or $_{eff}$PCSA) relationship; potential differences in fibre-type specific force (force per unit cross-sectional area).

Muscle cross-sectional (anatomical and physiological) and volume will quantitatively impact explosive strength indirectly by virtue of the strong contribution of muscle size to maximal strength (Mirkov et al. 2004). Presuming equivalence of the other determinants of explosive strength and the resulting identical relative RTD (%MVT.s^{-1}), absolute explosive strength will merely scale with maximal strength. Maximal strength will exert a greater influence on explosive strength measured over longer durations/ later time periods as contraction approaches the peak of the torque-time curve, as stronger muscles will still be on the rising whereas the torque of a weaker muscle will be beginning the plateau as the contraction approaches the maximal voluntary level. Evidently the correlation coefficients between voluntary RTD (measured from 0-10, 0-20, … etc. up to 0-250 ms) and maximal strength increased as the time from the contraction onset increased, such that at time intervals later than 90 ms from contraction onset maximal strength could account for 52-81% of the variance in voluntary RTD (Andersen and Aagaard. 2006). Similarly, Folland et al. (2014) showed that maximal strength was correlated increasingly strongly with explosive strength (measured as force at specific times) as contraction progressed (r = 0.59-0.95), and explained 75 and 90% of later phase (100 and 150 ms) explosive strength. One study (Erskine et al. 2014) has reported lesser correlations for muscle size vs. explosive strength independent of maximal strength, with explosive strength during the initial phase of contraction (50 ms) being unrelated to muscle volume or ACSA, but the muscle size indices were increasingly correlated to explosive strength as the contraction progressed (100 ms: muscle volume r = 0.391; ACSA r = 0.428; 150ms: muscle volume r = 0.693; ACSA r = 0.725).

2.3.2. Muscle Architecture

In vivo skeletal muscle architecture is described by the spatial arrangement of muscle fascicles. Ultrasonography is typically used to visualise the greyscale contrast between intramuscular connective tissues and muscle tissue to reveal fascicle orientation. Fascicles either extend along the direction of the muscle (parallel muscles) or are orientated at an angle (pennate muscles). In a muscle of given volume a parallel arrangement can result in longer FL as fascicles extend the length of the muscle belly, where as in pennate muscles the fascicle angulation necessitates that fascicles only extend part of the muscle belly length (Narici and Maganaris 2006). This structural consequence results if fascicles follow a purely linear trajectory, however in pennate muscles there may evidently be some degree of muscle fascicle curvature (reciprocal of the radius of the fascicle circle; increased with contractile force and greater at shorter muscle lengths [Muramatsu et al. 2002]) that might somewhat dissociate the reciprocal relationship between fascicle angle and length. FL is the principal determinant of muscle maximal shortening velocity potential as it is considered coincidental with fibre length and thus number of sarcomeres in series (Lieber and Fridén 2000). Since pennation may result in a reduced muscle FL (in muscle of definite volume), pennate muscles are likely to have a slower maximal shortening velocity than parallel muscles. Some of this possible reduction in muscle shortening velocity secondary to reduced FL can be offset by the rotation of fascicles (about their insertion into the aponeurosis) that occurs in pennate muscle during contraction, which serves to amplify muscle shortening for a given degree of fascicle shortening (Narici 1999; Azizi et al. 2008).

FL defines the potential length change that can occur within a muscle: i.e. the summed displacement of more sarcomeres in-series equates to greater cumulative length change and subsequently dictates maximal shortening velocity because of the summed displacement of sarcomeres in series within a given time resulting in longer fascicles being able to shorten at higher velocities (Enoka 2008). For sarcomeres within longer fascicles, each individual sarcomere can operate at lower relative velocity for a given whole muscle shortening compared to sarcomeres of shorter, slower fascicles (Blazevich and Sharpe 2005); hence longer fascicles facilitate the maintenance of a higher proportion of isometric force capacity over boarder range of velocities. As such longer FL may positively influence *in vivo* dynamic strength, particularly as angular velocity increases. However, there is minimal evidence to affirm this postulation. A couple of studies reported no correlation between FL and dynamic strength (vastus lateralis FL vs. maximal concentric knee extension torque at 30 and 300^{o}.s^{1},

Blazevich et al. 2009b; medial gastrocnemius FL vs. maximal plantar flexion torque at 30, 120 and 210º.s^{-1}, Baxter and Piazza 2014). Alternatively, the longer fascicle lengths exhibited in sprinters than distance runners and controls (Abe et al. 2000), and the findings that greater FL was inversely correlated with 100-m sprint performance (vastus lateralis, r = -0.44 – -0.51 and gastrocnemius, r = -0.40 – -0.54; Kumagai et al. 2000; Abe et al. 2001), indirectly suggests that longer fascicles may benefit high velocity strength.

Equally as muscles shorten rapidly during the initial phases of explosive contractions owing to connective tissues compliance, a greater capacity for high velocity force production consequent to longer fascicle length may allow a higher RTD. The time taken to stretch the tissue compliance can account for ~40% of isometric force rise time in isolated muscle fibres (Edman and Josephson 2007) implying that longer, faster fascicles could theoretically facilitate explosive strength. Conversely, preliminary indirect evidence *in vivo* indicates a possible negative impact of longer muscle fascicle length on explosive strength. An inverse association was observed between the strength training induced shifts in the quadriceps femoris force-length relation towards longer muscle lengths (used as a measure of fascicle length changes) and increase in RTD in the initial 30 ms of an explosive isometric knee extensor contraction (R^2 = 0.50; Blazevich et al. 2009a). This finding was explained on the premise of longer fascicles possessing greater in series compliance, thereby slowing RTD.

Pennation permits a greater number of fascicles (or fascicles with greater cross sectional area) to be attached to a given tendon area thus increasing the number of parallel sarcomeres (Narici 1999). This increases the maximal isometric force the fascicles can exert on the tendon. However, only a component of the fascicle force that is exerted onto the tendon is transmitted in the longitudinal direction as a function of the cosine of the angle of pennation. The influence of pennation on the maximal isometric force generating capacity of a muscle is thus a trade-off between the increase in contractile material and the loss in fascicle force with increasing pennation angles. There is a net increase in muscle isometric force with increasing PA up to 45°, where the force transmission efficiency is reduced to effect of cancelling the force-augmenting effect of increased $_{eff}$PCSA (Alexander and Vernon 1975; Kawakami 2005). Muscle pennation angles are typically less than 30º (Ward et al. 2009), potentially leading to a net positive influence of PA on $_{eff}$PCSA and thus maximal strength in-vivo. Some studies have reported positive correlations (r = 0.471– 0.68) between maximal strength and the PA of the agonist muscles (Nagayoshi et al. 2003; Strasser et al. 2013; Wakahara et

al. 2013; Ando et al. 2015), which is indirect association owing to that greater PA's are generally concordant with larger muscle size (Kawakami et al. 2006). Presuming PA influences maximal strength, it is possible there will be a relationship between greater PA and later-phase RTD; however this has not been tested.

A functional consequence of the rotation of the fibres (increase PA) that occurs during muscle shortening is that muscle fascicles can shorten less and at a lower proportion of their maximal shortening capacity for a given muscle shortening velocity allowing greater force (Azizi et al 2008; Wakeling et al. 2011) and equally operate closer to the optimal length range that is conducive to sarcomere actin-myosin overlap (i.e. greater force). This mechanism is thought to be greater in muscles with higher resting PA's and be more prominent with increased contraction velocity (Brainerd and Azizi 2005; Azizi et al. 2008). Substantial architectural changes occur during muscle contraction, as the muscle shortens during force generation (Narici and Maganaris 2006; Azizi et al. 2008; Wakeling et al. 2011). Muscle shortening is accomplished via both muscle fascicle shortening and rotation (about their aponeurotic insertion), such that FL decreases (30-60%) and PA increases (60-160%) in the transition from rest to maximal voluntary force during isometric (constant muscle-tendon unit length) contractions (Herbert and Gandevia 1995; Narici et al. 1996a; Maganaris et al. 1998; Kawakami et al. 1998; Maganaris and Baltzapopoulos 1999; Hodges et al. 2003). Some studies report architectural changes to occur in a curvi-linear manner with the increase in contraction intensity; relatively greater changes are observed at lower forces and smaller changes at higher forces (Herbert and Gandevia, 1995; Ichinose et al. 1997; Maganaris et al. 1998; Hodges et al. 2003). Also, owing to the maintenance of muscle volume during contraction and the architecture changes, $_{eff}$PCSA will increase during isometric and concentric contractions (Narici et al. 1996a). Perhaps examining $_{eff}$PCSA during MVC will yield a higher correlation between $_{eff}$PCSA and MVT, than is reflected by $_{eff}$PCSA at rest.

2.3.3. Tendinous Tissue Stiffness

2.3.3.1. In Vivo Estimation of Stiffness

Muscle-tendon unit (including aponeurosis and tendon) and external 'free' in-series tendon force-elongation relationships are obtained *in vivo* by combining tissue elongation visualised via ultrasonography, with force measurements recorded during a ramp isometric contraction in which force is developed gradually up to maximal. The longitudinal displacement of either a muscle fascicle-aponeurosis cross-point or muscle-tendon junction (Bojsen-Møller et al.

2003; Maganaris et al. 2003; Stafilidis et al. 2005; Arampatzis et al. 2007a) defines muscle-tendon unit (MTU) elongation distal to the ultrasound measurement site. The typical capturing of ultrasound recordings to quantify aponeurosis elongation has the limitation that measurements are restricted to two-dimensional visualisation of longitudinal displacement, whereas aponeurosis deformation also occurs in the plane transverse (Iwanuma et al. 2011; Farris et al. 2013). Moreover, there may be heterogeneously distributed longitudinal displacement along the length of the aponeurosis and the observation that some parts of the aponeurosis may shorten during contraction (Finni et al. 2003; Kinugasa et al. 2008) questions the validity of using single point estimates of muscle aponeurosis elongation to derive MTU stiffness.

Some studies have measured patellar tendon elongation as either the displacement of the patella apex relative to an echo absorptive marker placed mid-tendon (Reeves et al. 2003) or as the increase in distance between the patella apex and tibia (Hansen et al. 2006). The former method however underestimates tendon elongation, as it does not capture tibial displacement. Tissue elongation (corrected for displacement due to joint angle rotation) measurements are plotted against the corresponding tendon force (corrected for antagonist co-activation) to derive a tendon force-tendinous tissue elongation relationship, the slope of which is defined as stiffness. Most commonly the slope between 50-90/100% MVT has been used to calculate the representative value of stiffness. It has been suggested that stiffness is linear over the high force range (Kubo et al. 2002b) and some studies similar report linear force-elongation relationships (Arampatzis et al. 2007b; Stenroth et al. 2012; Waugh et al. 2013). Measuring in a so-called linear region is in keeping with *in vitro* mechanical tensile tests where there is a distinct linear portion of the force-elongation curve that is used to define the elastic characteristics (stiffness) of tendon tissues (Butler et al. 1978). However, while the tendon-force elongation relationship may well fundamentally have a linear region, whether that region can always be expressed *in vivo* is uncertain. The tendons are capable of bearing much greater force than can be exerted by the muscle, thus the examined portion of the force-elongation curve during mechanical tests *in vivo* is dependent upon voluntary muscle strength. Therefore, adopting a measurement of stiffness over a narrow force range in the upper end of the voluntary force-elongation relationship provides the closest obtainable approximation of a linear value (e.g. 80-100%, Carroll et al. 2008; 90-100%, Seynnes et al. 2009).

2.3.3.2. Normalisation for Tendon Dimensions

As tendon dimensions markedly influence tendon stiffness, the tendon force-elongation relationship is typically normalised to tendon CSA and length respectively to yield a stress (F/CSA)-strain (elongation/initial resting length) relationship. The slope of which defines a dimensionless property referred to as the elastic modulus or Young's modulus. A difficultly with deriving accurate estimates of Young's modulus *in vivo* is the non-uniformity of tendon cross-sectional along the length of the tendon; e.g. patellar and achilles tendon CSA increases proximal-distal (Seynnes 2009; Arampatzis et al. Bohm et al. 2014). The Young's modulus defines the material stiffness and reflects the intrinsic tensile resistance of the tendon as determined by the tendons ultrastructure and composition: most prominently collagen content, collagen fibril size and collagen cross-links concentration (Buchanan and Marsh 2002; Heinemeier and Kjaer 2011; Kjaer et al. 2015). In particular, a greater proportion of larger collagen fibrils is associated with a stiffer tendon, owing to the greater possibility of cross-link formation between collagen molecules, while greater cross-link concentration likely increases intrinsic stiffness by preventing the slippage of the collagen molecule during mechanical loading (Heinemeier and Kjaer 2011).

2.3.3.3. Muscle-Strength Dependency

The maximal tendon strain prior to failure is considered a physiologically conserved (more or less constant) property (Matson et al. 2012). Therefore, greater muscle strength can expectedly necessitate a stiffer tendinous tissue to constrain tendon elongation to within sub-failure physiological limits. While an association between maximal strength and tendon stiffness is yet to be clearly documented, several cross-sectional studies report strong positive correlations between maximal voluntary isometric strength and MTU stiffness ($r = 0.58$-0.817: Arampatzis et al. 2007b; Kubo et al. 2011; Stenroth et al. 2012; Hannah and Folland 2015). However in these studies stiffness measurements correlated to strength were obtained over a force range relative to maximal (50-100% MVT, Arampatzis et al. and Kubo et al. or 10-80% MVT, Stenroth et al. 2012), and from force-elongation data acquired during constant ramp contraction times rest to peak e.g. 5-10 seconds). These approaches likely introduce a methodological artefact. For instance, due to the curvi-linear nature of the force elongation relationship in vivo: progressively increasing gradient of the *in-vivo* tendon tissue force-elongation relationship; e.g. tibialis anterior, Maganaris and Paul 1999; gastrocnemius, Maganaris and Paul 2002; patellar, Reeves et al. 2003), stronger individuals will inherently have a greater stiffness calculation.

2.3.3.4. Loading Rate-Sensitivity

The ramp isometric contractions performed to establish tendon stiffness are typically performed over a defined period (~3-10 seconds), however for obtaining comparative values across studies and also between individuals of vastly differing strength level, it is prudent to utilise a constant loading-rate. A few *in vivo* studies have addressed the postulation that tendinous tissue mechanical stiffness is strain-rate sensitive/ loading-rate dependent; meaning the estimated stiffness value is greater when the rate of force application during ramp contractions (i.e. shorter time to peak force), with conflicting results. Neither medial gastrocnemius muscle aponeurosis elongation nor Achilles tendon stiffness showed differences when calculated during ramp isometric plantar flexion contractions lasting 1-10-s (Kubo et al. 2002b; Peltonen et al. 2013). In contrary Achilles tendon did exhibit lower strain when maximal plantar flexion contractions were performed in minimal time (as fast as possible) as oppose to 1.5 s (Gerus et al. 2011). A further study indicated maximal patellar tendon elongation to be 42% lower during short (3 s) vs. long (10 s) maximal ramp isometric knee extensions, with patellar tendon stiffness calculated to be ~77% greater during short vs. long (Pearson et al. 2007). While controlling the contraction time is one step towards a standardised loading rate, individuals of differing strength will exhibit a greater rate of force development, therefore constant time contractions likely still lead to speciously stiffer tendon values in stronger individuals. Most recently, patellar tendon stiffness and modulus were demonstrated to be loading rate (ramp contraction RTD [$Nm.s^{-1}$]) dependent: stiffness and Young's modulus were significantly higher at 80 $Nm.s^{-1}$ (21.4% and 21.6%, respectively) and at 110 $Nm.s^{-1}$ (32.5% and 32.0%, respectively) than at 50 $Nm.s^{-1}$. Similarly, stiffness and Young's modulus were 9.9% and 8.8% higher, respectively, at 110 $Nm.s^{-1}$ than at 80 $Nm.s^{-1}$ (Kösters et al. 2014).

2.3.3.5 Muscle-Tendon Unit Interaction

During isometric muscle contraction, contractile force results in tendinous tissue elongation, the extent of which is determined by the tissue stiffness (> stiffness, less elongation). For a given contractile force, a more compliant (reciprocal of stiffness) tendon will allow the muscle to shorten more. This extra shortening would cause a shortening in the sarcomere of muscles, meaning that if the sarcomere is operating in the ascending limb of the force-length relation, having a more compliant tendon would result in lower force In contrast, if the sarcomere operates in the descending limb of the force-length relation, having a more complaint tendon would result in an increase in contractile force (Maganaris et al. 2008). In

effect, greater tendinous tissue compliance results in a rightward shift in the force-length relationship, towards longer optimal muscle lengths (Lieber et al. 1992; Lemos et al. 2008). Moreover, the rate of skeletal muscle isometric contractile force production is slowed by the necessity of the muscle to shorten in order to stretch the elastic components that transmit muscle force (Hill 1951; Edman and Josephson 2007). Stiffer tissues experience less elongation response to muscle force (provide greater mechanical resistance) and therefore constrain muscle shortening during the initial stages of contraction, permitting muscle fibres to operate in the higher force region of the force-velocity relationship (Wilson et al. 1994). Greater mechanical tendinous tissue stiffness could expectedly be associated with faster RTD *in vivo*. Hitherto no studies have examined the relationship of tendon stiffness to *in vivo* RTD. Some studies report moderate correlations between MTU stiffness and explosive strength: knee extensors (RTD 0-100ms r = 0.65 and 0-200ms r = 0.69 across divergent athletic subgroups, Bojsen-Møller et al. 2005; time taken to develop 150-300N external force r = -0.35 – -0.54, across equal n = male and females, Hannah and Folland 2015), and plantar flexors (in children of different ages RTD 0-50/200ms r = 0.42/0.42, and adult males and females RTD 0-50/200ms r = 0.45/0.47). However this evidence is unconvincing as these studies utilised either a relative force range for stiffness measurement and/or a constant time ramp contraction to acquire force-elongation data. As referred to (in sections 2.3.3.3 and 2.3.3.4.), such methods predispose stronger individuals to higher stiffness values. Relating biased estimated stiffness values to explosive strength, a variable known to be related to maximal strength (Andersen and Aagaard 2006; Folland et al. 2014), most likely renders a spurious relationship between stiffness and RTD. Indeed once examined with both variables expressed in relative terms, such relationships were abolished (Hannah and Folland 2015). This suggests that the relationships found between absolute MTU stiffness and explosive strength were coincidental and due to the influence of maximal strength on both RTD and a confounding effect on stiffness measurement.

2.4. Responses to Strength Training

Conventional strength training utilises high loads (≥70% MVT), with contractions performed in a controlled manner typically >2 s. This sustained-contraction strength training characteristically increases maximal strength (Rich and Cafarelli, 2000; Aagaard et al. 2002; Holtermann et al. 2007; Blazevich et al. 2008; Del Balso et al. 2007; Pucci et al. 2010; Andersen et al 2010; Tillin et al. 2011), with uncertainty as to the effectiveness on explosive

strength (Aagaard et al 2002; Del Balso et al. 2007; Blazevich et al, 2008; Andersen et al 2010; Tillin et al. 2011). Alternatively explosive-contraction strength training, focusing on brief contractions (~1 s) performed with maximal/near maximal RTD can induce observable improvements in maximal strength (though of lesser extent than sustained-contraction strength training) and substantially improves explosive strength (Van Cutsem et al. 1997; Barry et al. 2005; Geertsen et al. 2008; Tillin et al. 2012; Balshaw et al. 2016).

2.4.1. Muscle-Tendon Unit Hypertrophy

2.4.1.1. Muscle

The characteristic increase in muscle contractile material quantity (muscle size) following strength training is extensively reported in the literature: increases in muscle ACSA and volume are of around 5-15% with 8-14 weeks training (Narici et al. 1989, 1996: Roman et al. 1993; Aagaard et al. 2001; Wilkinson et al. 2006; Blazevich et al. 2007; Erskine et al. 2010). A significant hypertrophic response can be observed in as little as three weeks (Seynnes et al. 2007). A selective hypertrophic response has been observed, in terms of greater increases in ACSA at particular locations along the length of a given muscle and also larger gains ACSA and volume between constituent muscles of a muscle group (Folland and Williams 2007). Regional ACSA changes suggest that an accurate index of hypertrophy requires CSA measurements at multiple sites pre-post training, with muscle volume measurements providing the most thorough assessment. Whole muscle hypertrophy results primarily from a training-induced increase in muscle fibre CSA. A common finding is a preferential hypertrophy of type II fibres; type II fibre hypertrophy occurring in a shorter period of time and to a greater extent than type I (Roman et al, 1993; Andersen and Aagaard 2000; Aagaard et al. 2001, Wilkinson et al. 2006; Andersen and Aagaard 2010).

2.4.1.2. Intramuscular Connective Tissue

An increased muscle fibre CSA intimately necessitates an expansion of the intramuscular collagen network. In coordination with myofribrillar protein synthesis, resistance exercise stimulates an increased skeletal muscle collagen synthesis (Moore et al. 2005; Holm et al. 2010). Training-induced hypertrophy of muscle fibres will be accompanied by a proportional increase in intramuscular connective tissue. Evidently, there was remarkable similarity in the percentage of biceps brachii muscle samples comprised of connective tissue in bodybuilders and untrained controls (~13%: MacDougall et al. 1984). Likewise, biceps brachii connective tissue concentration was unchanged (~12%) after 12 weeks of heavy resistance elbow flexor

training in elderly males (Housh et al. 1992). Finding of a constant proportion of connective tissue regardless of muscle size or state of training indicates a greater absolute amount of collagen/ connective tissue after strength training.

2.4.1.3. Aponeurosis

An increase in muscle fibre CSA with strength training necessitates an increased quantity of contractile material to be attached to the aponeurosis. While the greater PA observed after strength training can partly accomplish this (Kawakami et al. 1995; Aagaard et al. 2001), it has been posited that a possible increase in aponeurosis size maybe needed to accommodate the greater fibre CSA (Abe et al. 2012). Supportively, a strong correlation between quadriceps femoris muscle volume and vastus lateralis deep aponeurosis area ($r = 0.85$), and the greater (32%) aponeurosis area in weightlifters than recreational active individuals was suggestive of a strength training adaptation in aponeurosis size (Abe et al. 2012). Subsequently, a solitary study found a small increase (1.9%) in vastus lateralis aponeurosis width to accompany an increased (10.7%) vastus lateralis ACSA after 12 weeks of dynamic (80% concentric one-repetition maximum) knee extension training (Wakahara et al. 2015). However, this study included a small cohort ($n = 11$) and reported only within-group (no comparison to the control group) changes that were deduced from paired-t-tests performed with no correction for multiple tests, and the result was of borderline statistical significance ($P = 0.05$). More robust evidence is required to affirm if aponeurosis hypertrophy is an adaptation to strength training.

2.4.1.4. Tendon

An increase in tendon stiffness could arise from an increase in tendon cross-sectional area (CSA: tendon stiffness will scale directly to CSA if all other structural and compositional factors influencing stiffness are equal; Butler et al. 1978). Hypothetically, strength training could increase tendon size via increases in strength imposing progressively greater mechanical load to the tendons which could initiate signalling cascades that stimulates cells located in the tissue to increase their production of extracellular matrix proteins, ultimately leading to tendon hypertrophy (Svensson et al. 2016). The evidence for tendon hypertrophy in response to strength training is rather equivocal. Using magnetic resonance imaging (MRI), several studies have documented modest increases in either Achilles or patellar tendon CSA (Kongsgaard et al. 2007; Arampatzis et al. 2007a; Seynnes et al. 2009; Farup et al. 2014; Bohm et al. 2014). Initially, Kongsgaard et al. 2007 suggested tendon hypertrophy

may be region specific (localised to proximal or distal regions). However it is important to appreciate that this conclusion is rather limited as the analysis was only performed at three specific sites along the PT length: proximal CSA, +6%; mid CSA, no change, distal CSA, +4% after 12 weeks heavy dynamic knee extensor training. Data from other studies are not so conducive. After 9 weeks dynamic knee extensor training, Seynnes et al. 2009 noted increases in patellar tendon CSA at 20-30, 60 and 90-100% of tendon length. Farup et al. 2012 measured patellar cross-sectional area pre-post 12-weeks training in accordance with the methods of Kongsgaard, finding only increased CSA at the proximal site. However, the data from Farup et al. indicate that patellar tendon CSA increased to a greater extent than quadriceps femoris muscle size, which given the slower tissue turnover of muscle vs. tendon (Miller et al. 2005; Smith and Rennie 2007; Heinemeier et al. 2013b), the finding seems dubious. Negatively each of these studies of the patellar tendon has neglected the inclusion of a control group. Following 14 weeks isometric plantar flexion strength training (90% MVC for 3 seconds), Achilles tendon hypertrophy was observed only at 60-70% (Arampatzis et al. 2007), while in response to the same protocol as Arampatzis et al. (2007a), Bohm et al. found AT hypertrophy across most of the tendon length (20-100%).

Conversely, a few other MRI studies found no changes in either patellar or Achilles tendon CSA measured at multiple sites along the lengths of the tendons (Arampatzis et al. 2010; Kubo et al. 2012; Bloomquist et al. 2013). In addition, there are multiple studies that equally report no change in Achilles, quadriceps or patellar tendon CSA after months of strength training (Kubo et al. 2001; 2006a, 2006b, 2007), although only a limited number of specified tendon were examined. Further these studies were deemed insufficient (Kongsgaard et al. 2007), based on their use of lower resolution MRI (≤ 0.5 Tesla) as oppose to the more commonly used 1.5 Tesla MRI. There are more studies that identified no change in patellar tendon CSA; albeit at selected locations (25, 50 and 75% of tendon length) which may not be conducive to hypertrophy (Reeves et al. 2003; Malliaras et al. 2012; McMahon et al. 2013; Kubo et al. 2009, 2010). Also these studies adopted ultrasound imaging for tendon CSA measurement. The accuracy of ultrasound has been questioned and suggested to be potentially unreliable owing to the perceived difficulty to precisely delineate the tendon boundary from surrounding tissue, and may not be a suitable method to detect relatively modest change in tendon size (Heinemeier and Kjaer 2011; Ezikos et al. 2013). Although good inter-day reliability has been reported in some studies (Rieder et al. 2015; Kruse et al. 2017).

2.4.2. Increased Tendinous Tissue Stiffness

2.4.2.1. Muscle-tendon unit (MTU: tendon-aponeurosis) and/ or 'free' tendon stiffness

It is a consistent observation that conventional strength training induces an increase in MTU stiffness (+16-60% [plantar flexor or knee extensor MTU] after 8-14 weeks: Arampatzis et al. 2007, 2010; Bohm et al. 2014; Kubo et al. 2001, 2002, 2006a, 2006b, 2010a, 2010b, 2012; Waugh et al. 2014). Interestingly, two studies reported notable increases in MTU stiffness following merely four (+34% [knee extensor MTU]: Tillin et al. 2012) and six weeks (+62% [plantar flexor MTU]; Burgess et al. 2007) of explosive strength training. Further, several studies have exclusively examined the patellar tendon adaptation to conventional strength training, likewise reporting a substantially increased stiffness after 8-14 (+15-83%: Reeves et al. 2003; Kongsgaard et al. 2007; Carroll et al. 2008; Seynnes et al. 2009; Malliaras et al. 2012; McMahon et al. 2013). Whether explosive strength training increases tendon stiffness is unknown. Hitherto, only a few serial studies (same group of authors) have simultaneously examined the changes in MTU and free tendon stiffness, showing inconsistent findings for the knee extensor MTU and PT stiffness after 12 weeks: isoinertial unilateral knee extension training (80% 1-RM) increased MTU, but not PT stiffness (Kubo et al. 2006a); isometric bi-lateral leg press training (70% MVC) increased knee extensor MTU but not PT stiffness (Kubo et al. 2006c), yet isometric and isoinertial knee unilateral extension training increased both PT and MTU (Kubo et al. 2009).

Evidently there is a wide variability in the findings from the cited studies. While this could to some extent simply be a consequence of inter-individual differences in the participants, it is also possible that the complexity of measuring *in vivo* tendon mechanical behaviour could contribute, along with a likely influence of the diversity of methods (Heinemeier and Kjaer 2011). Notable methodological differences between studies include: partial or full tissue length imaging and ramp contraction duration and loading rates. Further it is typical to calculate stiffness across an absolute force range that is expressed relative to maximal strength (e.g. 50-100% MVT) which means post strength training stiffness values will be calculated over higher absolute forces, exacerbating the stiffness changes. Differences in studies could thus be contingent upon strength changes. Further methodological discrepancies arise within the context of estimating tendon force in terms of the degree of control for antagonist co-activation and the validity of tendon moment arm measurements (Heinemeier and Kjaer 2011): e.g. direct MRI measure vs. estimation from limb length via cadaver data. A potential relative effectiveness of the varying training protocols employed notwithstanding.

2.4.2.2. Young's Modulus (material stiffness)

In the absence of changes in tendon size; and the disproportionate changes in tendon size and stiffness in studies finding tendon hypertrophy, the increased tendon stiffness post strength training appears predominantly ascribable to the approximately parallel improvement in the intrinsic material stiffness typically observed: similar increases in both tendon stiffness and Young's modulus; 65 and 69%, Reeves et al. 2003; 14.6 and 12.2% (only a tendency), Kongsgaard et al. 2007; +24 and 20%, Seynnes et al. 2009; +70.6 and 70.6%, Malliaras et al. 2012; +50 and 48%, McMahon et al. 2013).

2.4.2.3. Tendon Morphology and Composition Changes with Strength Training

As alluded to, the tendon collagenous structure and composition implicitly influence Young's modulus, however studies attempting to examine changes in collagen fibril morphology and cross-link density; that could be readily explicable mechanisms conferring the improved modulus, are sparse. Collagen concentration and inter-molecular crosslinks concentration was unchanged in patellar tendon biopsy samples from tendinopathy patients who underwent 12 weeks heavy slow resistance training (Kongsgaard et al. 2009). A further study in patellar tendinopathy patients equally showed no change in collagen concentration after 12 weeks HSR, although there was a notable change in collagen fibril morphology; fibril density increased while fibril mean area decreased (Kongsgaard et al. 2010). Whether healthy tendons likewise respond to strength training with alterations in collagen fibril morphology and cross-links concentration is yet to be investigated. Cross-link concentration changes maybe particularly important, as indicatively despite a 34% lower collagen concentration in old vs. young men, their *in vivo* patellar tendon Young's modulus was similar which was seemingly the result of a compensatory greater concentration of cross-links in the old men (Couppé et al. 2009).

2.4.2.4. Collagen Synthesis and Strength Training

Presumably alterations in tendon size and/or collagenous structure and composition would require an upregulation of tendon collagen synthesis. There is some evidence that increased mechanical loading can induce an increased collagen turnover (net synthesis: Langberg et al. 2001; Miller et al. 2005), though a collagen synthetic response after an acute bout of exercise is not a consistent finding (Dideriksen et al. 2013; Heinemeier et al. 2013b). However, more pertinently, an acute bout of resistance exercise (3 x 10 dynamic knee extensions at 70% one repetition maximum) was shown to not result in an increase in patellar tendon collagen

messenger RNA expression 24 hours post (Sullivan et al. 2009). Furthermore, the concentration of a peritendinous (outer region of tendon) tissue biomarker of collagen synthesis was reportedly unchanged after 12 weeks isoinertial squat training (Bloomquist et al. 2013).

2.4.2.5. Mechanical Loading Factors Influencing Tendinous Tissue Stiffness Changes

Changes in tendinous tissue stiffness (mechanical and material) may result from alterations in extracellular matrix protein (principally collagen) content and composition. Such changes necessitate the upregulation of protein expression by the resident tendon cells (tenocytes). Cellular responses ensue from the mechanotransduction pathways initiated by the cellular strain (Lavagnino et al. 2008). The important characteristics of the strength-training stimulus that will impact the loading (strain) applied to the tendon are magnitude and time-dependent: (i.e. rate and duration) loading characteristics (Lavagnino et al. 2008).

2.4.2.5.1. Magnitude

A couple of studies have compared the effects of high vs. lower relative intensity training (% MVT) finding only the high magnitude training induced tendon adaptation (Arampatzis et al. 2007a, 2010; Kongsgaard et al. 2007). In two different studies of isometric plantar flexion training (both n=11, 14 weeks, 4 times per week) involving contractions (either 3-s loading with 3-s relaxation, Arampatzis et al. 2007a or 1-s loading with 1-s relaxation, Arampatzis et al. 2010) of one leg at 55% maximal voluntary contraction (low strain, 2.5-3%) and the other leg at 90% maximal voluntary contraction (high strain, 4.5-5.0%) with matching training volume (equal accumulated torque-time integral), found an increase in Achilles tendon (aponeurotic and free tendon portions) stiffness of 36% (3-s protocol) and 16% (1-s protocol) in the high strain trained leg, with no significant changes in the low strain trained leg. Likewise, 12 weeks unilateral concentric-eccentric knee extensor training resulted in an increase (+15%) in patellar tendon stiffness in a heavy-load (70% 1-repetition maximum [RM]) vs. no change in a light load (40% 1-RM) trained leg. These studies are indicative of the need to utilise a relatively high loading intensity/magnitude in accordance with a supposed requirement to overcome an internal tendon strain threshold in order disturb the homeostasis of tenocytes and initiate mechanotransduction pathways (Arampatzis et al. 2009). Though the *in vivo* threshold has not been specifically defined studies showing an increase in tendon stiffness typically adopt ≥ 70% of maximum isometric/dynamic strength (Bohm et al. 2015). The importance of higher strain as a stimulus for adaptation is further

demonstrated by greater increases in tendinous tissue stiffness in response to strength training at longer muscle-tendon unit lengths (i.e. > strain: Kubo et al. 2006a; McMahon et al. 2013).

2.4.2.5.2. Rate

The findings of substantial increases in muscle-tendon unit stiffness in response to isometric explosive training utilising maximal/near maximal rates of force development (+62% after 6 weeks, Burgess et al. 2007; +34% after 4 weeks, Tillin et al. 2012) is suggestive that the imposed tendon strain rate is potentially a potent stimulus for tissue adaptation. However these studies investigated explosive training exclusively and could not directly compare the effects observed with explosive training to a contrastingly slower force-rise protocol. It was recently suggested that only a tendency for an increase in Achilles-tendon (aponeurosis and free tendon portions) stiffness in response to a high-strain rate training protocol in comparison to the increase in stiffness (+57%) after a reference protocol (isometric plantar flexion's: 3-s at 90% maximal voluntary force [time to target force, as short as possible]) was evidence that strain rate had a limited influence on tendon adaptation (Bohm et al. 2015). The high strain rate training was performed via multiple one-legged hops and the estimated tendon force was also 90% maximal voluntary isometric force with the number of contractions such to match the force-time integral of the reference training group. While perhaps indicative that higher strain rate may not necessarily be a beneficial mechanical stimuli for tissue adaptation, it is possible that the plyometric type exercise performed requires the tendinous tissues to function more in accordance with the requirement to store and release elastic energy. This mechanism could be potentially insufficient to promote adaptation towards force transmission effectiveness (i.e. stiffness). Incidentally, other studies examining the effects of plyometric training on tendon tissue adaptations have produced largely inconsistent findings (Burgess et al. 2007; Kubo et al. 2007; Foure et al. 2010, 2011).

2.4.2.5.3. Duration

Intuitively a greater loading duration may be expected to facilitate greater tendinous tissue adaptation. Surprisingly, there appears to be no apparent *in vivo* data that directly attempts to establish an association between total loading duration and subsequent changes in MTU or tendon stiffness. However, studies have been conducted that compared the effects of two muscle contraction duration protocols on MTU stiffness changes, while the free tendon has not been separately examined. Importantly in each study the contraction magnitude (%MVT) was matched in the contrasting duration conditions. Across two separate studies (Arampatzis

et al. 2007a, 2010 [details referred to previously]), 3-s contractions resulted in greater increase in Achilles tendon (combined soleus aponeurosis and free tendon components) stiffness than 1-s contractions, (+36 and 16% respectively). Subsequently 3-s loading was shown to be more effective than longer 12-s contractions (Achilles tendon stiffness, +57 vs 25%; Bohm et al. 2014). Collectively, these results indicated that a few seconds of constant force (isometric force hold) application is likely beneficial for promoting a tendon adaptive response. Importantly, in both these instances of comparison of the effects of contraction duration on tendinous tissue stiffness changes, the studies matched the total accumulated contraction duration (equated to 60-s) by varying the number of contractions (repetitions) performed per training set: Arampatzis et al. 2007a, 5 sets x 4 reps x 3-s vs. Arampatzis et al. 2010, 5 sets x 12 reps x 1-s; and Bohm et al. 2014, reference protocol 5 sets x 4 reps x 3-s vs. long duration protocol 5 sets x 1 reps 12-s). Therefore, while these studies indicated that accumulating an equivalent total contraction duration by partitioning the loading into repetitive briefly sustained efforts is perhaps more optimal that very brief or prolonged contractions, the question of whether differences is total loading duration influence tendinous tissue stiffness changes has not been appropriately established.

2.4.3. Chronic Strength Training Adaptations

Changes in tendon Young's modulus are suggested to be a short-term adaptive response to increased loading (strain in response to muscle contractile force), whereas tendon hypertrophy is considered more likely an accumulated adaptation that may require a prolonged period of time to manifest (Heinemeier and Kjaer 2011; Wiesinger et al. 2015; Kjaer et al. 2015). The supposition that tendon hypertrophy maybe a prolonged process is highlighted by a cross-sectional study (Couppé et al. 2008) comparing patellar tendon size and mechanical properties of the lead and non-lead extremity, in elite badminton and fencers expressing a ≥15% contralateral knee extension maximal strength imbalance showed that the greater muscle strength (average 22%) of the lead extremity was concordant with a 20-28% greater patellar tendon CSA (measured at proximal, mid and distal regions from MRI). PT mechanical stiffness measured between 90-100% of the highest common (all participants could achieve) tendon force was 36.4% higher in the lead extremity, whereas there was no difference in PT Young's modulus between extremities. The results of this study (Couppé et al. 2008) suggested that continued gains in strength with habitual training could promote long-term tendon adaptations. However, the tendon loading history experienced by the participants of the Couppé et al. study is predominantly of higher volume, and relatively

lower magnitude than would be elicited in regular strength training, and thus may not necessary reflect the potential of strength training to elicit tendon hypertrophy.

One published study has documented a 34% larger PT CSA in chronic strength trained (> 5 years) than untrained males; though measured via ultrasound (Seynnes et al. 2013). The PT stiffness at a common force level (3600-4000N) had a tendency (+21%, P = 0.06) to be greater in the chronic strength trained, which was probably precluded from significance as a result of the small cohorts (n = 8). Conversely, PT Young's modulus at the common force level was equivalent between chronic trained and untrained (Seynnes et al. 2013). However, though not discussed by the authors, no difference in Young's modulus could be consequent to the 33.7% lower stress reported at the common force level in the chronic strength than untrained. The curvi-linear nature of the stress-strain relationship potentially confounds the result. Alternatively this lack of difference in Young's modulus is possibly linked to the finding of no differences in the collagen content or collagen cross-link in the patellar tendon of chronically strength trained vs. untrained men shown in another study (LeMoine et al. 2009). Converse to earlier findings, Fukutani and Kurihara (2015) found that the tendon CSA in 5/6 MRI locations (Achilles, patellar and triceps brachii proximal and distal tendon sites) were no different in chronically strength trained (~10 years) vs. untrained controls. Therefore whether even chronic strength training can induced tendon hypertrophy is controversial. Alternatively, there is some limited suggestion of aponeurosis hypertrophy (see 2.4.1.3), data regarding tendon hypertrophy is more equivocal Studies to indicate MTU stiffness changes have been neglected.

2.5. Literature Review Summary

In summary, the importance of muscle architecture for *in vivo* muscle strength characteristics has not been well documented. Further, the influence of tendinous tissue stiffness to in vivo RTD is not wholly clear and a more methodological stringent study si required. Following recent findings that explosive contraction strength training maybe a potent stimulus to increase MTU stiffness, the relative efficacy of explosive vs. sustained contraction strength training needs to be established. In particular, external tendon adaptations (size and stiffness) to explosive strength training are yet to be documented. Currently, there is a lack of cross-sectional data concerning the MTU properties of chronic strength trained athletes which could provide insight into the potential further capacity of tendinous tissues to adapt increased mechanical load (muscle force induced tendon strain). Additional, robust tendon

size data are needed to affirm tendon hypertrophy as a potential adaptive response to strength training.

Therefore, the ensuing experimental chapters were designed in an attempt to: appropriately examine the relationship of *in vivo* muscle architecture to muscle strength; reconcile the influence of stiffness on RTD; establish the efficacy of explosive-contraction strength training to promote muscle-tendon unit adaptation; and appreciate whether tendinous tissues to continue to adapt to extended periods of strength training via cross-sectional comparison between groups of untrained, short-term strength trained and chronic strength trained individuals.

CHAPTER 3

Influence of contractile force on the architecture and morphology of the quadriceps femoris

3.1. INTRODUCTION

A skeletal muscle's force production capabilities are principally dependent on its architectural and morphological characteristics (Powell et al. 1984; Burkholder et al. 1994; Lieber and Fridén 2000). However the precise influence of these structural properties on function remains to be fully understood, perhaps because of the extensive changes in muscle architecture that occur during contraction. Therefore documenting the changes in muscle architecture and morphology during contraction may enhance our understanding of muscle function.

Several *in vivo* studies utilising ultrasonography have reported substantial changes in architectural parameters (fascicle length [FL] and pennation angle [PA]) in various skeletal muscles during contraction. Even during isometric contractions with constant muscle-tendon unit length, fascicles shorten and rotate about their aponeurotic insertion resulting in a reduction in FL (-30 to -60 %) and an increase in PA (+60 to +160%) during the transition from rest to maximal voluntary contraction (MVC) (Herbert and Gandevia 1995; Narici et al. 1996a; Maganaris et al. 1998; Kawakami et al. 1998). Fascicle shortening influences force production potential due to muscle fibre force-length relationship. An increase in the PA likely attenuates the extent of fascicle shortening (Azizi et al. 2008), but may compromise the transmission of force to the aponeurosis. The changes in architecture during contraction and their expected influence on muscle force production have implications for the accuracy of musculoskeletal models (Zajac, 1989) and the assessment of *in vivo* muscle mechanical properties (e.g. active force-length relationship; Ichinose et al. 1997; Muroaka et al. 2001). It is therefore crucial to have a thorough understanding of how architecture changes with contractile force.

The quadriceps femoris (QF) is a functionally important muscle group commonly studied in research, yet hitherto no studies have documented the architectural changes in this muscle group as contractile force increases. The QF comprises four constituent muscles; vastus lateralis (VL), vastus intermedius (VI), rectus femoris (RF) and vastus medialis (VM) whose tendons merge to form the patellar tendon and thus act collectively as knee extensors. Some studies have determined the FL and PA changes occurring in the component VL muscle (Ichinose et al. 1997; Chauhan et al. 2013), however, the architectural changes within the other constituent muscles remain unknown and it is unclear how the architecture changes

occurring in VL reflect those of the other constituent muscles and subsequently the whole QF.

Muscle size at rest is widely measured as it is considered a key physiological determinant of function. However a muscle's effective physiological cross-sectional area ($_{eff}$PCSA = muscle volume divided by FL x cosine PA; Lieber and Fridén 2000) is clearly influenced by the changes in architecture that occur during contraction. Only one study has documented the change in $_{eff}$PCSA during isometric contraction from rest to MVC, and these authors found a substantial increase in the $_{eff}$PCSA of the muscle (+35% in the gastrocnemius medialis; Narici et al. 1996). This increase appears functionally significant given the direct proportionality observed between skeletal muscle $_{eff}$PCSA and maximal isometric force-generating capacity *in vitro* (r = 0.99; Powell et al. 1984). In-vivo studies have identified a weaker but still clear association between muscle $_{eff}$PCSA and isometric maximal voluntary force/torque (MVF/T; r = 0.71–0.95; Fukunaga et al. 1996; Bamman et al. 2000; Fukunaga et al. 2001; Blazevich et al. 2009b). These *in vivo* studies assessed $_{eff}$PCSA at rest, and it is possible that this relationship with isometric strength could be even stronger if $_{eff}$PCSA were measured during a maximal voluntary contraction but this possibility has not been examined. Alternatively, if $_{eff}$PCSA measured during MVC did not explain a greater proportion of the variance in isometric strength than $_{eff}$PCSA at rest, this may validate the use of $_{eff}$PCSA measured at rest.

The primary aim of present study was to document the architectural and $_{eff}$PCSA changes that occur within all four constituents and thus the whole QF muscle throughout isometric contraction from rest to MVC. The secondary aim was to test whether there was stronger relationship between MVT and $_{eff}$PCSA measured during an MVC than for $_{eff}$PCSA measured at rest.

3.2. METHODS

3.2.1. Participants

Fifteen healthy young males (mean ± SD: age 20 ± 2 years, height 179 ± 7 cm, body mass 72 ± 7 kg) who gave their written informed consent prior to their participation in this study, which was approved by the Loughborough University Ethical Advisory committee and conformed to the declaration of Helsinki. Participants were free from musculoskeletal injury to the lower limb, had a low-moderate level of recreational physical activity (total ≤1500

Metabolic Equivalent [MET] minutes per week) as measured via the International Physical Activity Questionnaire: Short Format (Craig et al. 2003) and had not performed lower body strength/ power training in the previous 12 months. The present study included an original cohort of n = 31, although poor muscle image clarity during contraction for 16/31 meant only data for n = 15 were acquired in full.

3.2.2. Experimental Design

This study involved four separate laboratory visits; familiarisation, two test sessions and a magnetic resonance imaging (MRI) scan. During familiarisation participants practiced all tasks assessed during functional test sessions. The two muscle function and architecture measurement sessions were 7 days apart and conducted at a consistent time of day (between 11:00 and 18:00 hours), following at least 36 h without strenuous exercise with participants having consumed their normal diet. These sessions involved participants being seated in a custom-built isometric strength testing chair and completing a series of maximal and ramp (gradual increase in force level; test 1 only) voluntary knee extensor contractions of the dominant leg (defined as the leg that would be preferentially used as the kicking leg). Maximal voluntary contractions (MVCs) were performed to assess knee extension maximal voluntary torque (MVT). Ramp contractions involved a gradual increase in knee extensor torque up to >80% MVT over 8 s. Ultrasound images of the four constituent muscles of the quadriceps femoris were recorded at rest, throughout the ramp contractions and during the MVCs Architectural parameters (fascicle length [FL] and pennation angle [PA]) were measured from the ultrasound images during later off-line analysis. Architecture measurements at rest and MVC were averaged across the two test sessions. One week following the second muscle function and architecture session, an MRI scan of the upper leg (dominant leg used in functional testing) was conducted to assess quadriceps femoris muscle anatomical cross sectional area and volume.

3.2.3. Knee Extension Torque Measurement

Participants were firmly secured to the strength-testing chair with straps tightly fastened across the pelvis and shoulders to prevent any extraneous movement. Hip and knee angles at rest were 105° and 120° (180° = full extension), respectively. Extensive pilot work showed knee joint movement of ≤5° from rest to MVC. An ankle strap was placed 15% of tibial length proximal to the medial malleolus in series with a calibrated strain gauge (FBB universal S-Beam tension-compression load cell [linear response up to 1500 N], Force Logic,

Berkshire, UK) positioned perpendicular to the tibia. The distance from the centre of the ankle strap to the knee joint centre was measured in order to calculate knee extension torque. The force signal was amplified (A50 universal load cell amplifier, Force Logic UK) and sampled at 2000 Hz with an analogue-to-digital converter (Micro 1401, CED, Cambridge, UK) interfaced with a PC utilising Spike 2 software (CED). Prior to analysis, force signals were low-pass filtered at 500 Hz using a fourth order zero-lag Butterworth filter, and notch filtered in both directions at 50 Hz to remove mains frequency noise (q-factor = 10). To provide gravity correction baseline resting torque was subtracted from all contraction torque recordings.

3.2.4. Protocol

3.2.4.1. Knee extension maximal voluntary contractions

Participants performed a series of warm-up contractions at 50 (x3), 70 (x2) and 90% (x1) of perceived maximal voluntary effort before completing six MVCs, each separated by ~1 min rest. Participants were instructed to push as hard as possible for 3-5 s with verbal encouragement provided during contractions. Real-time force was displayed on a computer monitor in front of the participant to provide visual feedback during and between each MVC. The highest instantaneous torque achieved during any maximal contraction was defined as knee extension maximal voluntary torque (MVT) for that session. Ultrasound images were recorded during all six MVCs. Each of three muscle sites *(see muscle architecture below)*, capturing images for different constituent muscles, was recorded twice (in consecutive efforts) during the series of MVCs in a consistent order: VL, RF & VI, and VM.

3.2.4.2. Knee extension ramp voluntary contractions **(*test session 1 only)***

Participants performed six ramp contractions, each separated by a 30 s rest. Each contraction involved a progressive increase in torque from rest up to 80% MVT over 8 s by following a target line on the monitor. Ultrasound images were recorded from each recording site during 2 ramp contractions. The order of muscle imaging was the same as during MVCs.

3.2.5. Muscle Architecture

A 6 cm (8-MHz) linear array transducer was used to acquire B-mode ultrasound images (6-8 cm depth with imaging frequencies of 39-31 Hz; Toshiba Power Vision 6000, SSA-370A: Otawara-Shi, Japan). The transducer (coated with water soluble transmission gel) was held firmly over the skin, with minimal applied pressure. Images were recorded with the

transducer placed on the median longitudinal line of the muscle while positioned on the skin above the VL, VM and RF at 50, 25 and 60% of femur length (from the knee joint space to the greater trochanter), respectively. These positions correspond to the expected site along the femur where the anatomical cross-sectional area of each muscle was greatest (Erskine et al. 2009). The vastus intermedius was assessed from the images recorded over the rectus femoris. The transducer was orientated perpendicular to the lower aponeurosis and parallel to the fascicular path. Parallel fascicle alignment was presumed when transducer orientation (tilt and rotation angle; Bérnard et al. 2009) produced an image whereby the aponeuroses and the fascicle perimysium trajectory were clearly identified with no visible fascicle distortion at the image edges. The image recording sites were marked on the skin with a permanent marker. Participants were asked not to wash off the marks so that transducer placement could be accurately replicated during the second session. An echo absorbent marker (elastic band) was taped to the skin in the axial plane in order to provide a reference in the images of any transducer movement relative to the skin. Video output from the ultrasound machine was transferred (via S-video cable) to a digital video camcorder (Sony Walkman, GV-D900E) and images were recorded at 25 Hz and synchronised with force data via a pulse generated by the Micro 1401 and recorded in the ultrasound image. Images were imported into public domain software (Image J, v.1.46, National Institutes of Health, Bethesda, USA) to measure fascicle length (FL), pennation angle (PA). FL was measured as the length of the fascicular path between the superficial and deep aponeurosis. Any visible fascicle curvature was taken into account. If the fascicle extended off the image the missing portion was estimated via linearly extrapolating the fascicle and aponeuroses (Figure 3.1). Manual (fascicular line tracing) linear extrapolation approach was adopted from Muroaka et al. (2001). PA was measured as the angle between the fascicular path and their insertion into the deep aponeurosis. FL and PA were measured on three separate fascicles within a selected frame and the average of these fascicles accepted as the architecture measurement. Ultrasound frames selected for analysis were, 1) at rest - the image which had the clearest view of the fascicles and aponeurosis, 2) at each 20% torque increment during the ramp contraction (i.e. 1 frame at each of 20, 40, 60 and 80%MVT) and 3) during the two MVCs recorded at each site – ultrasound image recorded at the same time instant as peak torque during that MVC. Of the 2 MVCs per muscle, the MVC with the highest peak torque was analysed. Peak torque during architecture measurement was typically slightly less than actual MVT. For each individual, to calculate their whole quadriceps femoris muscle architecture measurements, their FL and PA of each constituent muscle was multiplied by their ratio of its respective effective PCSA

($_{eff}$PCSA) to total Quadriceps Femoris (QF) $_{eff}$PCSA (see below; *muscle morphology*). The sum of these values represented QF FL and PA expressed as the weighted mean of the constituent muscles based on their relative contribution to QF $_{eff}$PCSA. E.g., if FL (mm) of the constituent muscles was VL 100, VI 90, RF 85 and VM 105 mm and we utilise the average $_{eff}$PCSA ratios just indicated, QF FL as a weighted mean would equal, Σ (100*0.317) + (90*0.321) + (85*0.158) + (105*0.205).

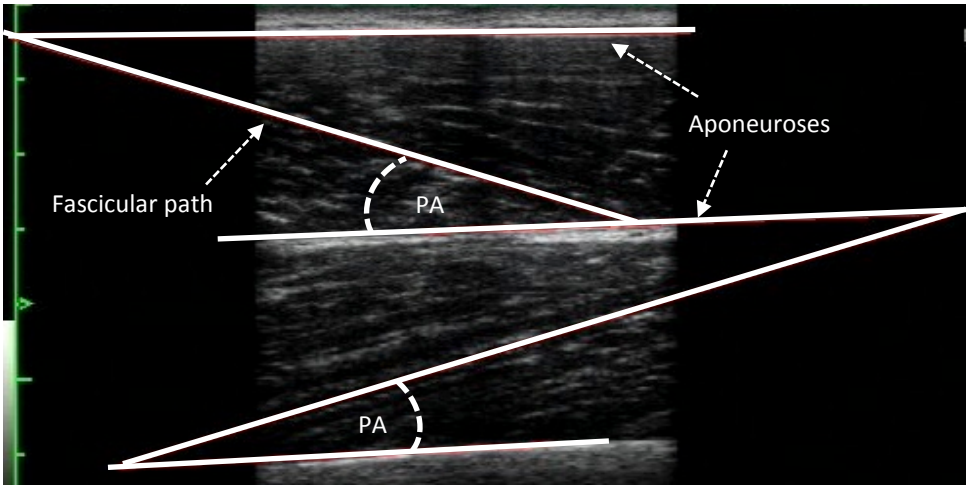

Figure 3.1. An ultrasound image of the rectus femoris and vastus intermedius muscles depicting the method used to measure architecture. Pennation angle, PA = the angle between the fascicular path and the deep aponeurosis. Fascicle length = length of the fascicular path between the aponeuroses. Typically fascicles extended off the image and the non-visible portion of the fascicle was estimated via manual linear extrapolation of the visible part of the fascicle and the aponeurosis. The scale on the left side of the image shows the ultrasound scan depth with each tick being 1 cm.

3.2.6. Muscle Morphology

Muscle anatomical cross sectional area (ACSA) and volume were measured from axial plane images generated from T1-weighted MRI scans (1.5 T Signa HDxt, GE Healthcare). Two overlapping scans of the thigh of each individual's dominant leg were recorded from the anterior superior iliac spine (ASIS) to mid-thigh, and mid-thigh to the knee joint space. Scans were taken at rest in the supine position with the knee of the scanned leg fully extended. Scans were performed with the following parameters: time of repetition = 600 ms, time to echo = 14 ms, image matrix = 512 x 512 pixels, field of view = 260 x 260 mm, slice thickness = 5 mm, inter-slice gap = 0 mm. The scans overlapped at mid-thigh and oil filled capsules were placed on the lateral aspect at mid-thigh. During analysis the capsules and

anatomical landmarks facilitated identification of identical slices within the two scans. MRI images were imported into OsiriX DICOM viewer (OsiriX v. 4.0; Pixmeo, Geneva, Switzerland). The ACSA of each of the four constituent muscles of the quadriceps femoris muscle (VL, VI, RF, and VM) was manually outlined (excluding visible external fat and connective tissue) on every third slice, starting from the most proximal axial MRI slice where the muscle could be outlined (Blazevich et al. 2009b; Erskine et al. 2009). Clear delineation of the individual vastii muscles was not always possible in the proximal parts of the muscle, therefore the muscle boundaries were estimated based on distal images where the muscle perimeters were easily identifiable. A cubic spline curve was fitted to the ACSA data points for each constituent muscle and the component muscle volume calculated as the area under the spline curve. Total quadriceps femoris muscle volume was provided by the sum of the four constituent muscle volumes. For each constituent muscle, the cross-sectional area of the muscle fascicles perpendicular to their line of action (i.e. physiological cross-sectional area, PCSA) was calculated by dividing its volume by its FL. Subsequently the $_{eff}$PCSA for each constituent muscle was determined by multiplying the PCSA of the muscle by its respective cosine PA (Erskine et al. 2009). Total quadriceps femoris $_{eff}$PCSA was provided by the sum of the constituent muscles respective $_{eff}$PCSA's.

3.2.7. Statistical Analysis

The reliability of architecture measures (VL, VI, RF, VM FL and PA) acquired in duplicate test sessions (at rest and during MVC) was calculated as the within-subject participant coefficient of variation (CVw, %, {[SD $_{(test1-2)}$/Mean $_{(test1-2)}$] x 100}). The architectural variables measured during duplicate test sessions were averaged to produce criterion values for statistical analysis. The reliability of the architecture measures was good at rest (CVw, FL & PA: VL 2.8 & 4.8, VI 4.5 &5.3, VM 4.7 & 5.5, RF 5.0 & 4.2%) and during MVC (CVw %, FL & PA: VL 2.0 & 4.2, VI 2.6 & 3.0, VM 2.1 & 2.6, RF 3.0 & 2.6%). QF LF, PA and $_{eff}$PCSA values at different torque levels (%MVT) and also relative (percentage) changes in FL/ PA/ $_{eff}$PCSA from rest to MVC between constituent muscles were compared using repeated measures one-way analysis of variance (ANOVA; within subject factor %MVT). Significant ANOVA were followed up with Bonferroni corrected pairwise comparisons to determine differences in FL, PA and $_{eff}$PCSA between specified torque levels. Second-order polynomial curves were used to describe the relationship between torque and FL, PA and $_{eff}$PCSA. Bivariate correlations were performed between QF FL vs. PA at rest, as well as FL vs. PA absolute and relative changes during the transition from rest to MVC. Bivariate

relationships were assessed with Pearson's product moment correlation (e.g. MVT and $_{eff}$PCSA measured at rest and MVT). Statistical significance test were conducted using SPSS version 19 (SPSS inc., Chicago, IL, U.S.A.) and a $P < 0.05$ denoted statistical significance. Descriptive statistics referred to in the text, table 1 and presented in figures (3.2 and 3.3) are mean ± standard deviation (SD).

3.3. RESULTS

Knee extension MVT was 268 ± 36 N.m. Architecture measurements during the MVCs were made when the torque level was 98.3 ± 0.018 (VL), 97.0 ± 0.018 (RF & VI), 97.5 ± 0.019 %MVT (VM), and on average 97.6 ± 0.018% MVT (QF). Group mean (± SD) constituent muscle $_{eff}$PCSA to total QF $_{eff}$PCSA ratios were VL 0.317 (0.030), VI 0.321 (0.036), RF 0.158 (0.026), VM 0.205 (0.027).

Within the constituent muscles of the QF (Figure 3.2), as torque production increased, FL decreased, PA increased and there was a resultant increase in $_{eff}$PCSA (Table 3.1.) From rest to MVC similar relative (%) decreases in FL occurred within each constituent muscle (ANOVA, % change $P = 0.214$). In contrast relative changes in PA between rest and MVC were smaller in VL than the other muscles (Bonferroni, $P < 0.001 – 0.05$), with no differences between RF, VI and VM ($P = 0.471 – 0.999$). Bonferroni pairwise comparisons indicated relative changes in $_{eff}$PCSA were greater in the VL than RF and VM ($P = 0.03$ and 0.004), while no other differences existed between any constituent muscles ($P = 0.058 – 0.999$).

Within the whole quadriceps femoris, as isometric knee extension torque increased, FL decreased and PA increased in a curvi-linear manner (Figure 3.3). From rest to MVC FL decreased from 93.7 ± 5.5 to 72.1 ± 3.4 mm (–23.5 ± 3.3%), while PA increased from 14.8 ± 1.3 to 20.3 ± 1.3º (+39.7 ± 6.6 %). Analysis of variance indicated a main effect of torque level on both FL and PA ($P < 0.001$) with differences in both measures of architecture observed between each incremental torque level; except FL at 40 vs. 60 %, P=0.056 (Figure 2). QF FL and PA at rest were highly inversely correlated ($r = – 0.845$, $P < 0.001$). During the transition from rest to MVC, no correlation existed between absolute changes in FL (mm) vs. PA (°), ($r = 0.303$, $P = 0.273$), although the relative (%) individual changes in FL vs. PA were positively related ($r = 0.517$, $P = 0.048$). The relative changes in architecture and morphology

from rest to MVC showed relatively limited variation between participants: between-participant coefficients of variation for FL 14.2%, PA 16.6% and $_{eff}$PCSA 21.3%.

QF $_{eff}$PCSA also increased curvi-linearly with torque level (Figure 3.3), with an increase from 192.5 ± 15.4 to 242.8 ± 18.9 cm^2 during the transition from rest to MVC (+26.5 ± 5.7 %). There was a main effect of torque level on $_{eff}$PCSA ($P < 0.001$), with significant differences between the $_{eff}$PCSA at each incremental torque level ($P \leq 0.002$).

There was a moderate correlation between MVT and $_{eff}$PCSA measured at rest ($r = 0.519$; $P = 0.047$), which was similar for MVT and $_{eff}$PCSA measured during MVC ($r = 0.530$; $P = 0.042$), (Figure 3.4). $_{eff}$PCSA measured at rest was highly correlated with $_{eff}$PCSA measured during MVC ($r = 0.853$, $P < 0.0001$).

Table 3.1. Percentage changes in muscle architecture and morphology within the constituent muscles of the quadriceps femoris (QF) muscle and whole QF during the transition from rest to isometric knee extension MVC.

	VL	VI	RF	VM	QF
Fascicle Length	– 24.1 ± 5.1	– 24.7 ± 6.3	– 20.6 ± 6.5	– 21.6 ± 6.0	– 23.5 ± 3.3
Pennation Angle	+ 24.1 ± 8.4	+ 47.1 ± 13.3***	+ 58.6 ± 22.6***	+ 45.1 ± 22.2*	+ 39.7 ± 6.6
Effective PCSA	+ 30.1 ± 9.0	+ 29.5 ± 10.4	+ 18.3 ± 8.8*	+ 23.1 ± 9.5**	+26.5 ± 5.7

Data are mean ± SD for n=15. VL = vastus lateralis, VI = vastus intermedius, RF = rectus femoris, VM = vastus medialis, QF = quadriceps femoris. QF effective physiological cross-sectional area ($_{eff}$PCSA) was measured (cm^2) as the sum of the $_{eff}$PCSA's of the constituent muscles. Percentage change data represent the change in the sum of the $_{eff}$PCSA's values of each constituent muscle. Significantly different to VL, ***P ≤0.001, **P<0.01, *P<0.05

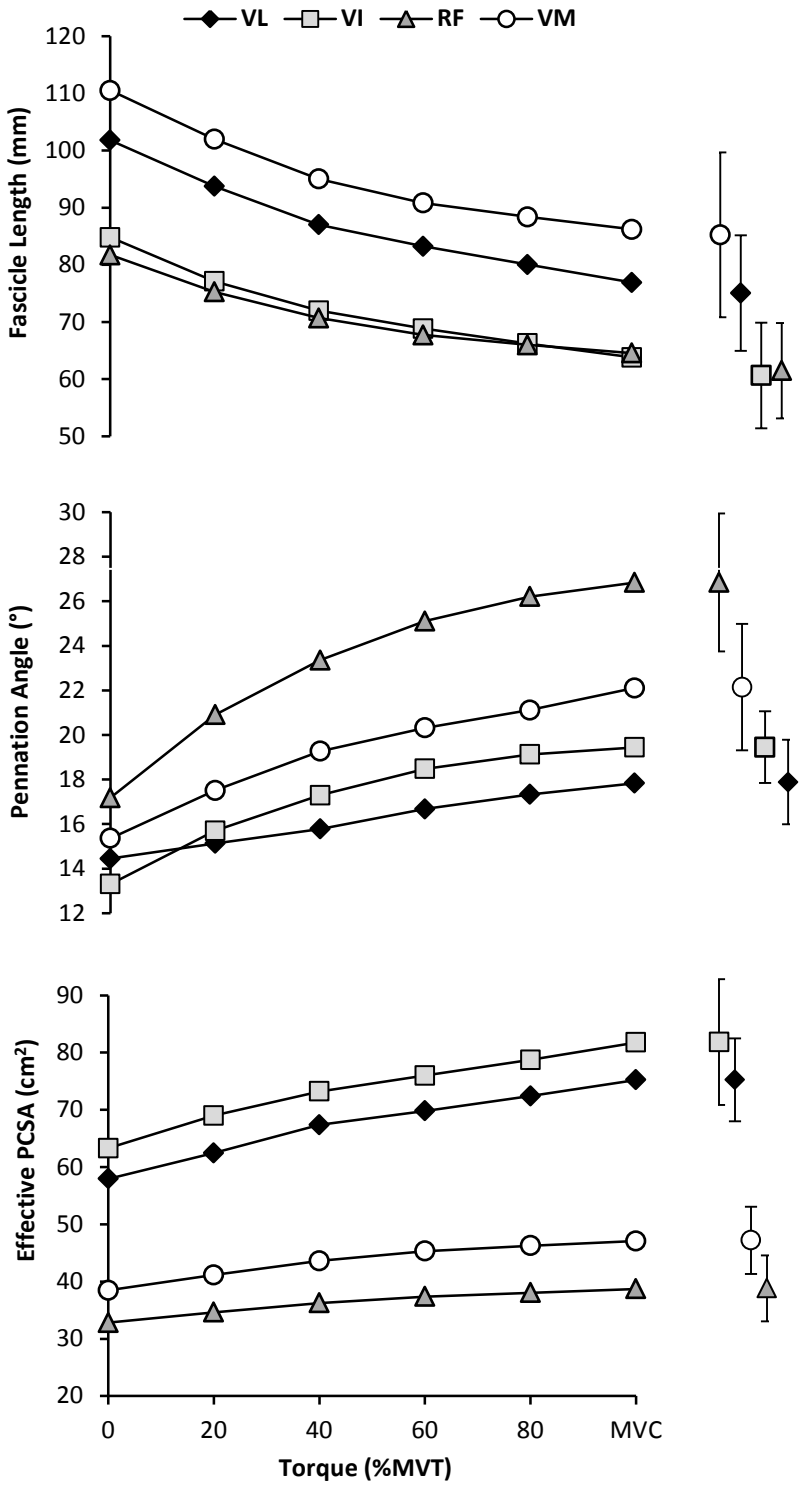

Figure 3.2. Muscle architecture (fascicle length and pennation angle) and morphology (effective physiological cross-sectional area, $_{eff}$PCSA) of the constituent muscles of the quadriceps femoris in relation to isometric knee extension torque (MVT = Maximal Voluntary Torque). Data are mean values at each torque level for n=15. The 'MVC' torque at which architecture/morphology measurements were made was on average ~98.3% (VL), 97.0% (RF & VI) and 97.5%MVT (VM). Vastus Lateralis (VL), Vastus Intermedius (VI), Rectus Femoris (RF) and Vastus Medialis (VM). Data points and error bars to the right of MVC show the mean standard deviation across torque levels.

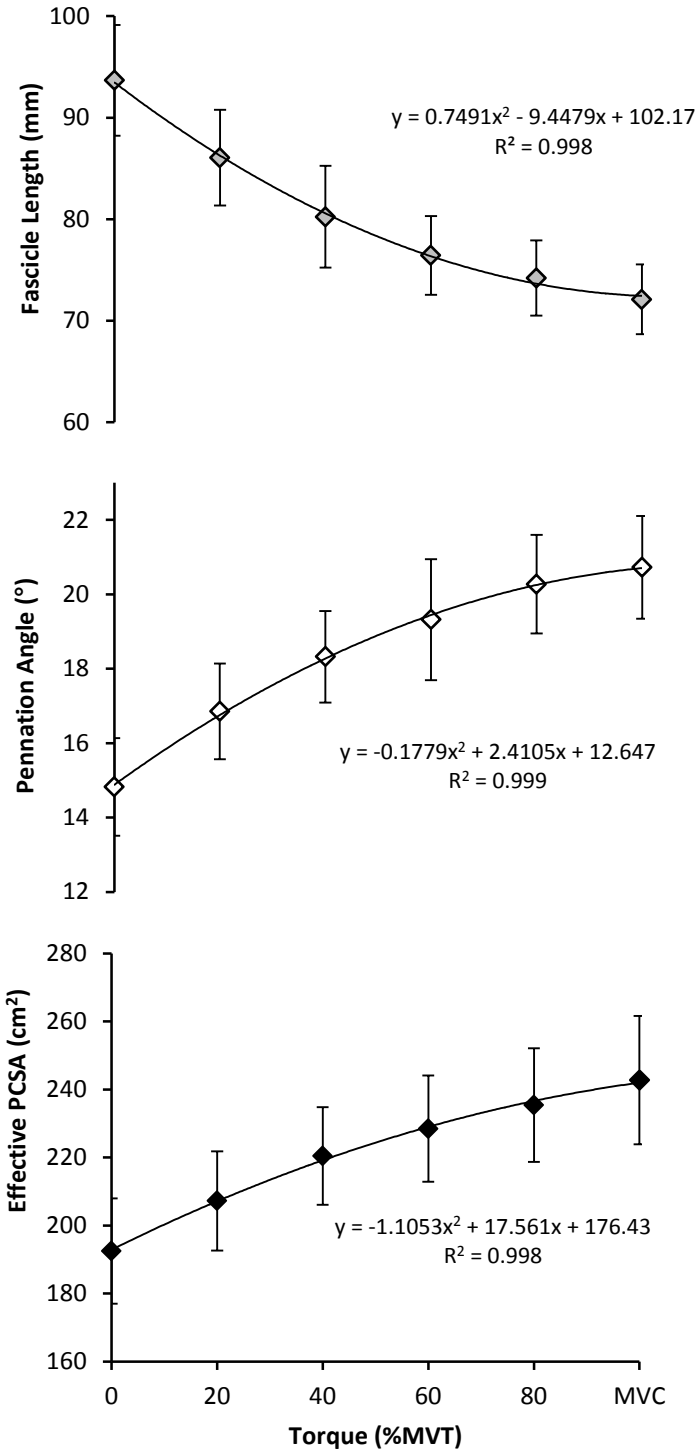

Figure 3.3 Quadriceps Femoris muscle architecture (fascicle length and pennation angle) and morphology (effective physiological cross-sectional area, $_{eff}$PCSA) in relation to isometric knee extension torque (MVT = Maximal Voluntary Torque). Data are mean ± SD (n =15); the mean values are fitted with a second order polynomial. 'MVC' torque level corresponds to the average %MVT achieved during the MVC's from which architecture was measured (97.6%MVT).

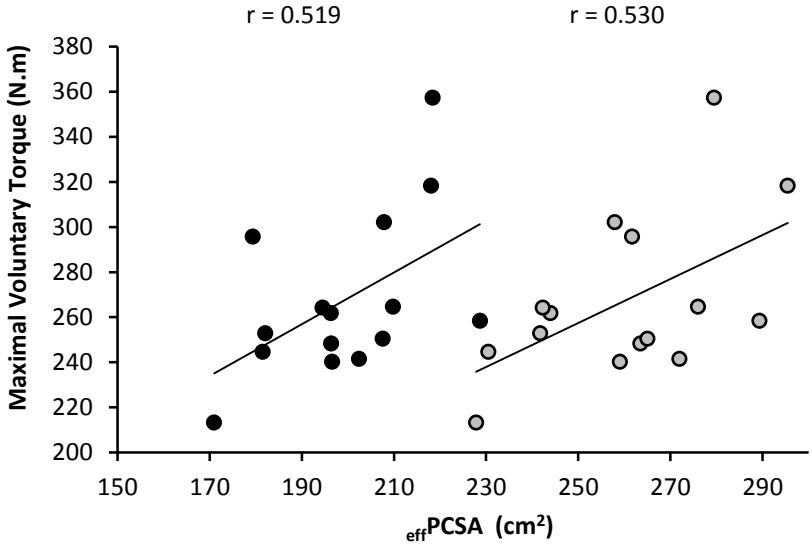

Figure 3.4. Scatterplot of the relationships between maximal voluntary torque and quadriceps femoris effective physiological cross-sectional area ($_{eff}$PCSA) measured at rest (black circles) or during isometric knee extension maximal voluntary contractions (grey circles) and (n = 15).

3.4. DISCUSSION

In the present study, within the whole QF muscle, as torque increased from rest up to MVC, there was a decrease in FL and increase in PA that occurred in a progressive curvi-linear manner. Resulting from these architectural changes, there was a corresponding curvi-linear relationship between torque and QF $_{eff}$PCSA (increase) during contraction. The relationship between MVT and $_{eff}$PCSA measured during an MVC was very similar to the relationship between MVT and $_{eff}$PCSA measured at rest, and thus $_{eff}$PCSA measured at rest appears a valid index of muscle size.

A number of studies have described substantial fascicle shortening and PA increase during isometric contractions in several muscles: triceps surae (Narici et al. 1996a; Maganaris et al. 1998; Kawakami et al. 1998), tibialis anterior (Ito et al. 1998; Maganaris et al. 1996; Hodges et al. 2003), biceps brachii and brachialis (Herbert and Gandevia 1995; Hodges et al. 2003) and vastus lateralis (Ichinose et al. 1997; Chauhan et al. 2013). Whilst no previous studies have examined the architectural changes within the whole quadriceps with contractile force, we found FL/ PA to be 24% shorter/greater at MVC than at rest in VL, which is comparable to previously reported values (FL, 20-35% and PA, 15-37%: Ichinose et al. 1997; Chauhan et al. 2013). However the relationship between force/torque and architecture in VL was not

representative of the changes in PA and $_{eff}$PCSA of the other constituent muscles of the QF group. Our study uniquely detailed the architecture changes within each constituent muscle (Figure 3.3) and therefore represents the first study to report to the architectural changes occurring in the whole QF (Figure 3.4). During an isometric MVC, QF FL was 24% shorter and PA 40% greater than at rest. The curvilinear changes in QF architecture with increased contraction intensity (i.e. greater changes at low torques and lesser changes at high torques) in the current study are in accordance with earlier reports (Herbert and Gandevia 1995; Ichinose et al. 1997; Ito et al. 1998; Maganaris et al. 1998; Hodges et al. 2003). Architecture changes reflect muscle shortening, which is thought to occur because of the initial slack and compliance of the force-transmitting tendinous tissues (Ito et al. l998; Maganaris et al. 2002). Therefore our torque–architecture relationship data conforms to the characteristic curvi-linear force-elongation relationship exhibited by tendinous tissues; greater elongation at lower forces with increased stiffness and resultant lower elongation at higher forces (Ito et al. 1998; Kubo et al. 2002b; Pearson et al. 2007).

Given the reciprocal relationship between muscle shortening and tendon elongation, the fascicle shortening and concurrent increase in PA that we have documented during contraction, are attributed to tendinous tissue compliance. Thus these changes in architecture would be expected to alter in proportion with tendinous tissue strain (elongation relative to initial length). Some previous studies have estimated muscle shortening by quantifying the difference in adjusted fascicle length (FL x cosine PA) between rest and MVC (Narici et al. 1996a; Ichinose et al. 1997; Kawakami et al. 1998). For our data this calculation yielded a group mean QF muscle shortening of ~7%. An appreciation of the fascicle/muscle shortening-tendinous tissue elongation interaction is important as it directly influences FL and thus force production via the force-length relationship. This has implications for the optimal muscle FL and thus the joint angle at which maximal voluntary torque is produced. For instance alterations in tendon stiffness (e.g. aging, resistance training or immobilisation) may increase/decrease the extent of muscle fascicle shortening and influence the angle-torque relationship. An additional concept to be aware of is how pennation angle changes effectively decouple fascicle and muscle displacements (muscle gearing), although such architectural interaction is principally considered a mechanism to augment force production during dynamic contractions (Azizi et al. 2008).

The $_{eff}$PCSA is considered the principal determinant of muscle force capability with previous studies finding 50-90 % of the variance in maximal muscle strength explained by the resting state $_{eff}$PCSA (Bamman et al. 2000; Fukunaga et al. 2001; Blazevich et al. 2009b). Our data indicate only a moderate albeit statistically significant association between $_{eff}$PCSA and MVT. This might reflect the fact that the current study involved a relatively small and homogenous cohort. Nevertheless, as consequence of the muscle architecture changes we have documented, and assuming a constant muscle volume during contraction (Azizi et al. 2008), QF $_{eff}$PCSA during an MVC was 26.5% greater than at rest.

We tested whether there was a stronger relation between MVT and $_{eff}$PCSA measured during an MVC, than $_{eff}$PCSA measured at rest. The measurement of $_{eff}$PCSA in a maximally contracted state (i.e. during an MVC) might be expected to more accurately reflect the actual effective force generating capacity of the sarcomeres (essentially the number of cross-bridges in parallel and their transmission of force in line with the tendon), and thus MVT, than $_{eff}$PCSA measured at rest. However, this was not the case, as MVT showed similar moderate correlations to both QF $_{eff}$PCSA measured at rest and during knee extension MVC. Therefore $_{eff}$PCSA during an MVC did not capture the variability in force generating capacity any better than $_{eff}$PCSA measured at rest. This may be because these two measures of muscle size are very highly correlated ($R^2 = 0.728$) and exhibited similar between participant variability (CV: $_{eff}$PCSA at rest 8.0%, $_{eff}$PCSA during an MVC 7.8%). Essentially the changes in architecture seemed relatively consistent for all individuals leading to a largely systematic change in $_{eff}$PCSA. The consistency of the change in $_{eff}$PCSA is likely due to the fact that tendon lengthening/muscle shortening are in proportion to relative force (%MVT) rather than being greater for stronger muscles. Tendon stiffness/compliance have been strongly correlated with maximal muscle strength (Arampatzis et al. 2007b; Stenroth et al. 2012; Hannah and Folland 2015), such that stronger muscles have stiffer tendons with less tendon lengthening/muscle shortening at the same absolute force, but equivalent length changes at the same relative force. This implies that muscle shortening and consequent architecture changes at MVT are similar for a range of different muscles. Furthermore if the architecture changes during contraction were similar for all participants it is not surprising that $_{eff}$PCSA measured at rest and during MVC were equally related to MVT. Evidently, compared to $_{eff}$PCSA at rest, measuring $_{eff}$PCSA during MVC did not improve the relationship with MVT, with the important implication of this finding being that it appears unnecessary to invest the additional time required to measure $_{eff}$PCSA during MVC if the aim is merely to utilise

$_{eff}$PCSA as a morphological descriptor of strength capability. Incidentally a recent study has reported practically very similar correlations between elbow flexor anatomical cross-sectional area measured at rest and at various sub-maximal torque levels, and maximal strength (Akagi et al. 2015). In summary resting measures of muscle size remain appropriate and no less relevant or valid for determining function than muscle size measured during MVCs.

The difficulty in clearly identifying the fascicular path in the constituent RF and VM muscles during contraction could have contributed to why $_{eff}$PCSA measured during MVC was no more predictive of MVT than resting muscle $_{eff}$PCSA. In addition muscle architecture was measured in 2-D within a single portion of each constituent muscle, which may be a significant oversimplification of the 3-D changes in architecture throughout each constituent muscle (Lee et al. 2015). Further work could establish the relationship between muscle strength and $_{eff}$PCSA derived from measurements of three-dimensional architecture.

In conclusion, the present study showed that quadriceps femoris FL, PA and $_{eff}$PCSA exhibited curvi-linear relationships with knee extension torque level. Consequently there were large substantial changes in FL (-24%), PA (+40%) and $_{eff}$PCSA (+27%) from rest to MVC. Interestingly, measuring $_{eff}$PCSA during a MVC was not related to MVT to a greater extent than measuring $_{eff}$PCSA under resting conditions, likely due to there being similar muscle shortening and architecture changes in all individuals during the transition from rest to MVC. Therefore resting measures of muscle size remain appropriate and no less relevant or valid, than muscle size measured at MVC, for determining function.

CHAPTER 4

Quadriceps femoris muscle architecture in relation to knee extension strength

4.1. INTRODUCTION

Skeletal muscle architecture (the spatial arrangement of muscle fibres) is considered an important determinant of a muscle's contractile properties (Lieber and Ward 2011). Unlike other muscle structural features (size and fibre-type), few studies have examined if architecture (fascicle length, FL; pennation angle, PA) is related to *in vivo* muscle function. Maximal isometric strength is the most commonly characterised aspect of neuromuscular function and relates well to performance of athletic (Stone et al. 2002), as well as daily life activities (Rantanen et al. 1994; Avlund et al. 1994; Schultz 1995). However, dynamic strength is widely considered to be more relevant to the performance of functional tasks such as mobility, locomotion and balance (Skelton et al. 2002; Bean et al. 2003; Cuoco et al. 2004). Further there has been a growing appreciation of the functional significance of the ability to increase torque as quickly as possible from low or resting levels (explosive strength), particular in situations where the time to generate torque is limited; for instance in sprinting and jumping (Weyand et al. 2010; Tillin et al. 2013a) and during injury related situations (e.g. anterior cruciate ligament tears in ≤50ms: Krosshaug et al. 2007; Koga et al. 2010). The importance of muscle architecture to inter-individual differences in these different measures of muscle function has not been well investigated.

The maximal isometric strength of isolated muscle is proportional to the muscle's physiological cross-sectional area (Powell et al. 1984). Pennation (angulation of muscle fibres) permits a greater amount of contractile material to attach to the aponeurosis thus increasing muscle physiological cross-sectional area (for a given muscle volume). Greater PA may therefore indirectly positively relate to maximal strength in vivo, although such evidence is not well documented. Assuming greater PA confers a higher maximal strength implies that, given the strong relationship between maximal and explosive strength, especially over extended time periods (Andersen and Aagaard 2006; Folland et al. 2014), PA may positively relate to later phase explosive strength, though this possibility has not been investigated. Further greater PA's are associated with more fascicle rotation (increase PA) during contraction that can amplify muscle-shortening velocity and allows fascicles to shorten at relatively slower velocities thereby permitting force production (Brainerd and Azizi 2005; Azizi et al. 2008). However, whether such a mechanism could noticeable enhance explosive and dynamic strength is unclear.

In vivo FL is thought to reflect muscle fibre length (Lieber and Fridén 2000) and thus serial sarcomere number; that largely dictates a muscles maximal shortening velocity (Bodine et al. 1982; Lieber and Fridén 2000). Long fascicles with a high maximal shortening velocity have an extended force-velocity relationship, compared to shorter slower fascicles, and consequently muscles with long fascicles can generate a relatively high proportion of isometric force at any given sub-maximal velocity (Wickiewicz et al. 1984; Lieber and Fridén 2000). On this basis the inter-individual differences in dynamic strength, both at high velocity and the ratio of strength at high to low velocity maybe partly explained by FL. Contrarily the couple of *in vivo* studies to date found no correlations between FL and high velocity strength (Blazevich et al. 2009b; Baxter and Piazza 2014). However only FL from one muscle contributing to joint torque was measured, which may not represent the whole muscle group.

Theoretically a muscle capable of higher shortening velocity might be expected to develop torque faster even in an isometric situation by more quickly taking up the inherent slack and compliance present within in-series force-transmitting structures (Edman and Josephson 2007). Preliminary indirect evidence actually suggests longer FL may negatively impact explosive strength; greater changes in FL with strength training have been associated with lesser increase in early phase explosive strength (Blazevich et al. 2009a). A direct investigation is now required. While much work has delineated neural and contractile determinants of explosive strength (Aagaard and Andersen 2006; Folland et al. 2014; Maffiuletti et al. 2016), the influence of muscle architecture has received little attention. Any influence of architecture on explosive strength might be expected to be most pronounced for evoked contractions that bypass the voluntary nervous system and drive the muscle at its maximal possible rate of force development (de Ruiter et al. 2004; Folland et al. 2014).

The present study aimed to assess the relationship between *in vivo* quadriceps femoris muscle architecture and knee extension strength capabilities; maximal and explosive isometric strength and dynamic strength at different velocities (50 and 350°s^{-1}). We hypothesized that fascicle length would be positively related to explosive strength; particularly during the initial phase of contraction, whereas pennation angle was expected to influence later phase explosive strength in accordance with positive correlations to maximal strength. Longer fascicle lengths were expected to facilitate greater higher velocity dynamic torque and subsequently positively relate to a high-low velocity strength ratio.

4.2. METHODS

4.2.1 Participants

Thirty-one healthy young males (mean ± SD: age 20 ± 2 years, height 179 ± 7 cm, body mass 72 ± 7 kg) gave their written informed consent prior to their participation in this study, which was approved by the Loughborough University Ethical Advisory committee. Participants had a low-moderate level of recreational physical activity (≤1500 MET minutes per week, measured via the International Physical Activity Questionnaire: Short Format (Craig et al. 2003), had not participated in any form of lower body strength/ power training in the previous 12 months and were free from musculoskeletal injury.

4.2.2. Experimental Design

Participants visited the laboratory for ~90 minutes on three separate occasions to complete a range of strength measurements of the knee extensors (dominant leg; preferred kicking leg). Each visit was 7 days apart and at a consistent time of day (between 11:00 and 18:00 hours), following at least 36 hours without strenuous exercise. Visit one involved familiarisation with the isometric and isovelocity contractions. Visit two involved (in this order): muscle architecture measurements (fascicle length, FL; pennation angle, PA) of all constituent muscles of the quadriceps femoris; isometric maximal voluntary contractions (MVCs); isometric voluntary and evoked explosive contractions, as well as a second familiarisation with the isovelocity contractions. Visit three was identical to visit 2, facilitating duplicate measurements of architecture and isometric contractions, but also included isovelocity strength measurements at high and low velocities.

4.2.3. Measurements

4.2.3.1. Muscle Architecture

In vivo FL and PA of the four constituent muscles of the quadriceps femoris group was measured from ultrasound images recorded at rest while participants were positioned in the strength-testing chair, prior to any contractions. Real-time B-mode ultrasound images were acquired with a 6 cm (8-MHz) linear array transducer (Toshiba Power Vision 6000, SSA-370A: Otawara-Shi, Japan). Image depth was 6 or 8 cm. The transducer (coated with water soluble transmission gel) was held firmly over the skin, but with only minimal pressure applied on the dermal surface. Separate images were recorded from the vastus lateralis (VL), vastus medialis (VM) and simultaneously from the rectus femoris (RF) and vastus intermedius (VI), with the transducer placed on the median longitudinal line of each

superficial muscle belly at 50 (VL), 25 (VM) and 60% (RF & VI) of femur length (greater trochanter to the tibio-femoral contact point [knee joint space]). These positions correspond to the expected site along the femur where the anatomical cross sectional area of the underlying muscles is greatest (Erskine et al. 2009). The transducer was orientated perpendicular to the lower aponeurosis and parallel to the fascicular path. Appropriate transducer orientation (tilt and rotation angle; Bénard et al. 2009) was defined as the orientation resulting in an image with the aponeuroses and the perimysium trajectory of several fascicles being clearly identifiable with no visible fascicle distortion at the edge of the image. Image acquisition sites were marked on the skin with a permanent marker. Participants were asked to not wash off the marks so ultrasound transducer placement could be accurately replicated during the second session. Video output from the ultrasound machine (S video cable) were recorded by a digital video camcorder (Sony Walkman, GV-D900E), and later imported into public domain software (Image J, v.1.46, National Institutes of Health, Bethesda, USA) for measurement of FL and PA. FL was measured as the length of the fascicular path between the superficial and deep aponeurosis. Any visible fascicle curvature was manually taken into account. In instances when fascicles extended off the acquired image, the missing portion was estimated via manual linear extrapolation of the fascicle and aponeurosis. PA was measured as the angle between the fascicular path and their insertion into the deep aponeurosis. FL and PA were measured on 2-3 clearly discernible fascicles within a selected ultrasound image, which was the image with the clearest view of the fascicles and aponeurosis. The average of these fascicles was the accepted architecture measurement. To provide a representative measure of whole quadriceps femoris muscle architecture, FL and PA of each constituent muscle was first multiplied by the fraction of total Quadriceps Femoris (QF) effective PCSA provided by that constituent muscle (VL = 0.317, VI = 0.321, RF = 0.158, VM = 0.205; Massey et al. 2015). The sum of these values represented QF FL and QF PA.

4.2.3.2. Isometric Torque

Participants were firmly secured to a custom built isometric strength-testing chair with tightly fastened straps placed across the pelvis and shoulder to prevent any extraneous movement. Hip and knee angles were 105° and 120° (180° = full extension), respectively. An ankle strap was placed 2 cm proximal to the medial malleolus in series with a calibrated strain gauge (FBB universal S-Beam tension-compression load cell [linear response up to 1500 N], Force Logic, Berkshire, UK) positioned perpendicular to the tibia. The distance from the center of

the ankle strap to the knee joint center was measured in order to calculate knee extension torque. The strain gauge signal was amplified (A50 universal load cell amplifier, Force Logic UK) and sampled at 2000 Hz with an analogue to digital converter (Micro 1401, CED, Cambridge, UK) interfaced with a PC utilising Spike 2 software (CED). In offline analysis force signals were systematically notch filtered in both directions 50 Hz (q-factor = 10) and low-pass filtered at 500 Hz using a fourth order zero-lag Butterworth filter, gravity corrected by subtracting baseline resting force and multiplied by external moment arm; the distance from the center of the ankle strap to the knee joint space, to calculate torque values.

4.2.3.3. Isovelocity Torque

Participants were seated on an isovelocity dynamometer (Con-Trex MJ, CMV AG, Dübendorf, Switzerland) with a hip angle of 120° (180° = full extension). Two 3-point belts secured the torso and additional straps tightly secured the pelvis and the distal thigh of their dominant leg to limit extraneous movement. A brace was placed in front of the non-involved leg. The knee joint center was aligned with the dynamometer rotational axis during isometric contractions of >50% maximal effort at a knee joint angle of ~115°. The dynamometer's shin brace was placed anterior to the shank ~2 cm above the medial malleolus before the shank was tightly secured to the dynamometer lever arm. An additional moulded rigid plastic shin pad, lined with 2 mm of high-density foam, was tightly secured to the tibia to avoid any discomfort to the shin during maximal contractions. Passive torque measurements were recorded while the tested leg was passively moved through the full range of motion. Thereafter active torque values were corrected for passive torque. Torque, crank angle and crank velocity signals were amplified (x1000) with an analogue-to-digital converter (Micro 1401-3, CED, Cambridge, UK) and sampled at 2000 Hz with a PC using Spike 2 software (CED, Cambridge, UK). The data were filtered at 15 Hz.

4.2.4. Protocol

Following a brief warm-up (3-s contractions at 50 [x3], 70 [x2] and 90% [x1] of perceived maximal) measurement contractions were performed in the following order:

4.2.4.1. Isometric Maximal Voluntary Contractions

Participants performed three MVCs (separated by ~1 min rest) and were instructed to push as hard as possible for 3-5 s with verbal encouragement provided during all MVCs. Real-time torque was displayed on a computer monitor in front of the participant to provide visual

feedback during and between each MVC. The highest instantaneous torque achieved during any maximal (or explosive) contraction was defined as knee extension maximal voluntary torque (MVT).

4.2.4.2. Isometric Explosive Voluntary Contractions

Participants performed a series of 10 explosive voluntary contractions each separated by 15 s. Participants were instructed to extend their knee 'as fast and as hard as possible'; with the emphasis on 'fast', for ~1 s from a relaxed state upon hearing an auditory signal. Contractions involving visible countermovement or pre-tension were discarded and another attempt made. To indicate if a countermovement or pre-tension had occurred, resting force was displayed on a sensitive scale. During each explosive contraction participants were required to exceed 80% MVT, which was depicted on screen with a horizontal cursor. To provide performance feedback the time taken to reach 80% MVT was shown after each contraction and the slope of the rising force-time curve (1 ms time constant) was displayed throughout contractions with the peak slope of the best effort indicated with an on-screen cursor. The three best explosive contractions (highest torque at 100 ms) and no discernible countermovement or pre-tension (change in baseline torque >0.17 Nm in the preceding 250 ms) of were analysed in detail. Contraction onset was defined as the last trough before the torque signal permanently deflected away from the envelope of the baseline noise; identified via manual inspection by a trained investigator using a systematic method, in accordance with previously published methods (Tillin et al. 2010). Manual onset detection is considered to provide greater accuracy and reliability than an automatic approach (see Tillin et al. 2013b). Briefly, the torque signal was initially viewed with y and x-axis scales of 0.34 Nm and 250 ms respectively (so the envelope of the baseline noise could be clearly discerned) and a vertical cursor placed on torque onset. Accurate placement of the cursor was verified by viewing the signal with a higher resolution. Voluntary explosive torque was measured at 50, 100 and 150 ms from contraction onset and rate of torque development (RTD; ΔTorque/ΔTime) calculated over sequential time periods 50-100 and 100-150ms. Values recorded from each of the three best contractions were averaged.

4.2.4.3. Isometric Evoked Contractions

The femoral nerve was electrically stimulated (constant current, variable voltage stimulator; DS7AH, Digitimer Ltd., UK) with square-wave pulses (0.2 ms duration) to elicit involuntary contractions of the knee extensors. Electrical stimuli were applied via a cathode stimulation

probe (1 cm diameter; Electro Medical Supplies, Wantage, UK) protruding 2 cm perpendicular from the center of a plastic base (4 x 5 cm), pressed into the femoral triangle and held firmly in position throughout contractions. An anode (carbon rubber electrode, 7 x10 cm; Electro Medical Supplies, Wantage, UK) was taped to the skin over the greater trochanter. The precise location of the cathode was determined as the position that evoked the greatest twitch response to single pulses applied at a particular submaximal electrical current. Twitch contractions were elicited at incremental currents until a maximal twitch force (plateau) occurred. Thereafter, the electrical current was reduced and octet stimulation (8 pulses at 300 Hz) was delivered in step-wise increments up to a supramaximal current (120% of the maximal twitch/plateau current). Real-time inspection of octet force and the slope of the rising force-time curve confirmed a plateau in both peak octet force and peak RFD during the incremental stimulation. Subsequently, three supramaximal (120% maximal current) octet contractions were elicited, separated by 12 s. Evoked octet torque was measured at 50 ms from contraction onset. Values recorded from each supramaximal contraction were averaged.

4.2.4.4. Isovelocity Contractions

After completing a standardised warm-up of five submaximal contractions of progressively higher intensity, participants performed 3 sets of 2, and 3 sets of 3, maximal concentric-eccentric contractions at $50°s^{-1}$ and $350°s^{-1}$ respectively (in this order), over ~100° range of motion. There was $\geq$ 1 min rest between each set and $\geq$ 2 min rest between velocities. Concentric-eccentric contractions were used to ensure full activation during the concentric phase of the movement. Participants were instructed to grasp the handles next to the seat during maximal contractions. Verbal encouragement was given and online visual feedback of the crank torque was provided on a computer screen. During later analysis, the acceleration and deceleration phases were excluded in order to disregard torque overshoot during these phases (Schwartz et al. 2010) and the constant isovelocity period (within ± 10% of the prescribed crank angular velocity) was identified. The highest instantaneous torque recorded within the isovelocity period of the concentric contractions at that velocity was defined as maximal torque. The ratio between concentric maximal torques at $350°s^{-1}$ vs. $50°s^{-1}$ was defined as the high velocity torque ratio ($ConT_{350}:T_{50}$). Reciprocal eccentric-concentric contractions were performed to ensure muscle-pre-activation prior to concentric phase initiation to maximise contractile performance and limit any differences of muscle neural activation between participants.

4.2.5. Statistical Analysis

Test re-test reliability of dependent variables measured during both test sessions (FL, PA, MVT, Torque at times) was calculated as within subject co-efficient of variation (CVw, %). Specifically, individual CVw's were calculated ([test 1 and 2 standard deviation / test 1 and 2 mean]*100) and the average of each participants value gave the group mean CVw. Prior to determining relationships between architecture and explosive torque, values recorded from the two test sessions were averaged and this value used in statistical tests. Pearson product moment bivariate correlations were performed to assess the relationship between quadriceps femoris muscle architecture (FL, PA) and the torque (absolute and relative) developed at specified time points during explosive voluntary and evoked octet contractions. Pearson's correlations were performed between architecture variables and isovelocity torques and the high-velocity torque ratio. Statistical analysis was conducted using SPSS version 20 (SPSS inc., Chicago, IL, U.S.A.). $P<0.05$ denoted a statistically significant correlation. Descriptive statistics are mean ± standard deviation (SD). Variability between subjects for architecture and strength measures is expressed as a co-efficient of variation (CVb, %).

4.3. RESULTS

4.3.1. Reliability of Measurements

Architecture measurements of the individual muscles during the two test sessions were highly reliable (CVw: FL 2.7 – 4.7%, PA 4.3 – 5.6%). Subsequently whole QF architecture also had excellent reliability (QF FL 2.6%, QF PA 2.2%). Likewise, isometric MVT had excellent reliability (CVw 2.3%). However, between-session reliability was not as good for early phase explosive voluntary torque at 50 ms (CVw 10.7 and 10.9%), though this improved for measurements later in the contraction (100 ms 4.7%, 150 ms 4.2%). Evoked octet torque (Nm) at 50ms had excellent reliability (CVw 3.1%).

4.3.2. Quadriceps Femoris (QF) Architecture (Table 4.1)

Fascicles lengths of individual muscles ranged from 83.6 ± 10.7 (VI) to 105.7 ± 17.7 mm (VM) and the between participant variability (CVb) was 12.0–16.7%. However whole QF FL showed less variability (91.7 ± 6.8 mm, CVb 7.4%). constituent muscles PA's were 13.7 – 17.8° and varied within muscles by 12.5 – 17.0% (CVb), whereas whole QF PA (group mean = 15.7°) showed less variability (CVb 8.8%). VI has equally the shortest fascicles and narrowest PA's. VL architecture (94.6 mm and 15.6°) was rather intermediate of the other constituent muscles and thus most resembled that of the whole QF. For each of the individual

muscles FL and PA had strong (RF, r = -0.745, P < 0.001; VM (r = -0.723, P < 0.001) or moderate inverse relationships (VL, r = -0.468, P = 0.008; VI, r = -0.382, P = 0.034). Whole QF FL and QF PA were also inversely related (r = -0.508, P = 0.005). The architecture values of individual muscles were unrelated; i.e. the FL/ PA of one muscle was not related to the FL/ PA of any other muscles (FL, r = -0.292 to 0.273; all P > 0.05; PA, r = -0.013 to 0.339, all P > 0.05).

Table 4.1. Architectural characteristics of the vastus lateralis (VL), vastus intermedius (VI), rectus femoris (RF), vastus medialis (VM) and whole quadriceps femoris (QF). Fascicle length and pennation angle measured at rest. QF architecture was calculated as a weighted mean of the constituent muscles based on each muscles contribution to total effective PCSA. Data are mean ± SD (n = 31).

Architecture					
Muscle:	**VL**	**VI**	**RF**	**VM**	**QF**
Fascicle Length (mm)					
Mean	94.6	83.8	83.6	105.7	91.7
SD	11.4	10.2	10.7	17.7	6.8
CVb (%)	12.0	12.2	12.8	16.7	7.4
Range	75.9 - 121	68.6 - 118.1	58.3 - 101.9	76.6 - 150.8	80.5 - 105.5
Pennation Angle (°)					
Mean	15.6	13.7	17.2	17.8	15.7
SD	1.9	2.2	2.9	3.0	1.4
CVb (%)	12.5	16.1	16.6	17.0	8.8
Range	12.3 - 19.8	9.5 - 19.3	13.0 - 25.5	12.4 - 25.0	12.9 -18.5

CVb = between subject coefficient of variation. Range (minimum - maximum values).

4.3.3. Maximal and Explosive Isometric Strength

Isometric MVT was 283 ± 41 Nm (range 213 – 388 Nm; CVb = 14.0%). The between participant variability in explosive voluntary torques (Figure 4.1) was greatest in the early phase of contraction for absolute and relative torque but decreased as the contractions progressed. Absolute and relative torques at 50ms during evoked octet contractions (120.4 ± 21.7 Nm, CVb 18.0% and 42.5 ± 4.5% MVT, CVb 10.6%) was 2.5-fold greater and exhibited 2-3 times less variability than voluntary torques at 50 ms.

4.3.4. Maximal Dynamic Strength

Knee extension maximal concentric torques at 50 and 350°s^{-1} were 166.5 ± 29.4 Nm (range 96.8 – 222.8 Nm; CVb 17.7%) and 97.4 ± 15.8 Nm (range 58.8 – 123.4 Nm; CVb 16.2%) respectively. The high-low velocity torque ratio (Con T_{350}:T_{50}) was 0.59 ± 0.07 (range 0.44 – 0.76; CVb 12.1%).

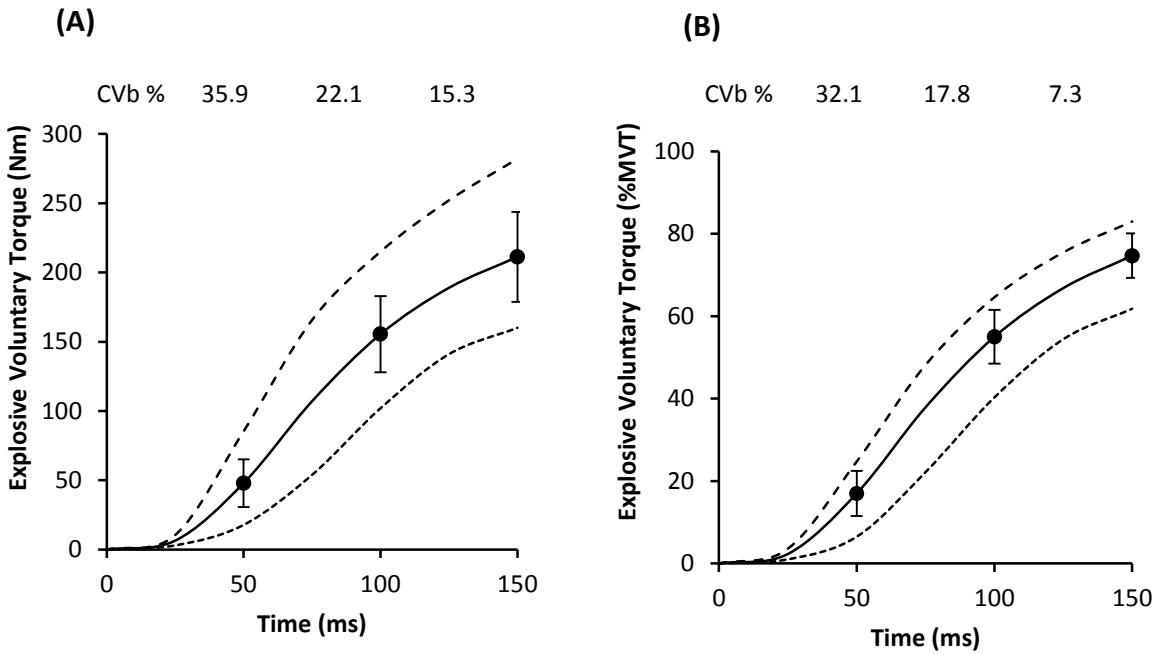

Figure 4.1. Absolute (Nm [A]) and Relative (%MVT [B]) torque developed at 50 ms intervals from torque onset during explosive voluntary contractions of the knee extensors. Black line and circles (bars) represent mean (± SD) and the dotted and dashed lines depict the minimum and values respectively (n = 31).

4.3.5. Bivariate Correlations: Relationships between Architecture and Muscle Strength

Isometric MVT was not related to QF FL nor PA (Both $r \leq 0.017$ and $P \geq 0.926$). Likewise, maximal concentric torque produced at $50°s^{-1}$, $350°s^{-1}$ or Con T_{350}:T_{50} were unrelated to neither QF FL nor PA (all $r \leq 0.273$ and $P \geq 0.137$). However, FL was inversely related to explosive voluntary absolute and relative torque at 50 ms (Figure 4.2 A and B) but was not subsequently related to absolute or relative torque at later times during the contraction or RTD (Table 4.2). Conversely FL was not related to absolute or relative evoked torque (tables 2). PA was similar unrelated to absolute and relative explosive voluntary torque and RTD, and absolute and relative evoked torque (Table 4.2).

Table 4.2. Pearson's product moment correlation coefficient (r-values) between quadriceps femoris architecture and measures of explosive strength: absolute (Nm) and relative (% maximal voluntary torque) isometric knee extension torque and sequential rate of torque development (RTD, $Nm.s^{-1}$ and $\%MVT.s^{-1}$) developed at specific time points during explosive voluntary contractions and evoked octet contractions (n = 31).

	Muscle Architecture			
	Fascicle Length		**Pennation Angle**	
	r	p	r	p
Explosive Voluntary				
Torque (Nm) at 50 ms	**-0.433***	0.015	0.118	0.529
Torque (Nm) at 100 ms	-0.176	0.343	0.096	0.606
Torque (Nm) at 150 ms	-0.105	0.574	0.087	0.643
RTD ($Nm.s^{-1}$) 50-100 ms	0.144	0.440	0.034	0.854
RTD ($Nm.s^{-1}$) 100-150 ms	0.130	0.486	0.015	0.938
Torque (%MVT) at 50 ms	**-0.442***	0.013	0.073	0.697
Torque (%MVT) at 100 ms	-0.227	0.219	0.070	0.708
Torque (%MVT) at 150 ms	-0.228	0.218	0.123	0.511
RTD (%MVT.s) 50-100 ms	0.236	0.201	0.017	0.927
RTD (%MVT.s) 100-150 ms	0.093	0.618	0.081	0.665
Evoked Octet				
Torque (Nm) at 50 ms	0.079	0.673	0.176	0.345
Torque (%MVT) at 50 ms	0.005	0.828	0.299	0.102

Significant *P<0.05

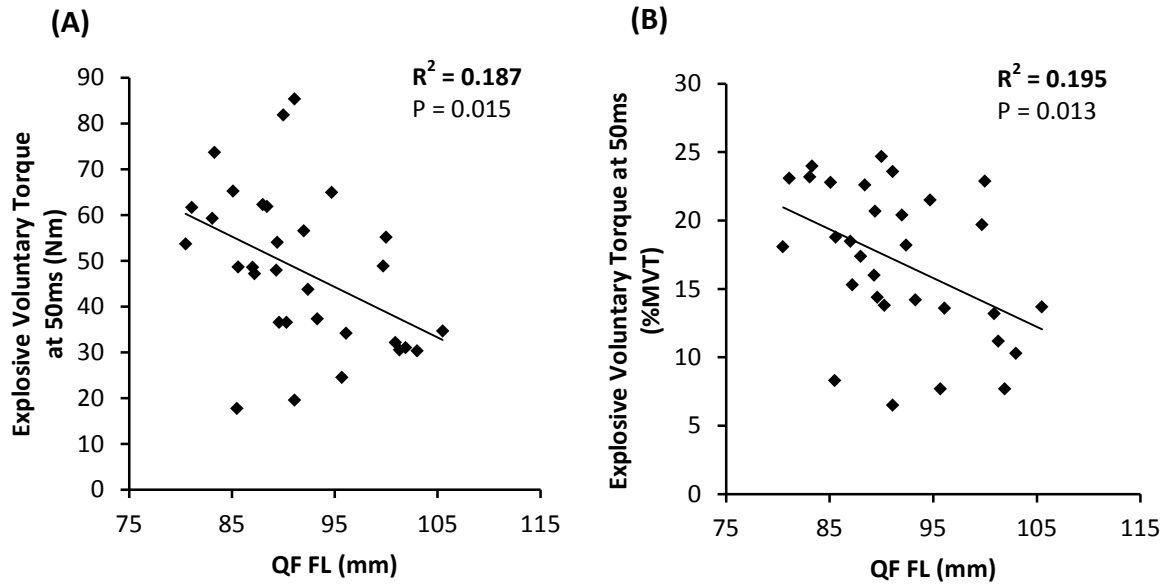

Figure 4.2. Scatterplots depicting the relationship between quadriceps (QF) fascicle length (FL) and absolute (A) and relative (B) torque produced at 50 ms during explosive voluntary isometric knee extension contractions (n = 31).

4.4. DISCUSSION

The present study investigated the relationship between quadriceps femoris (QF) *in vivo* muscle architecture (fascicle length [FL], pennation angle [PA]) and neuromuscular function, specifically maximal and explosive isometric knee extension strength, as well as dynamic strength; isovelocity concentric torque (50 and 350°s^{-1}) and the high-low velocity torque ratio (Con T_{350}:T_{50}). We found FL was negatively related to early phase (0-50 ms) absolute and relative explosive voluntary torque, though not evoked torque. Alternatively PA was unrelated to explosive voluntary or evoked torque and neither FL nor PA was related to maximal isometric or dynamic strength.

4.4.1 Quadriceps Femoris Muscle Architecture

Our data for *in vivo* QF architecture (Table 4.1) are in general agreement with the range of values typically observed (Blazevich et al. 2006, 2007b; O'Brien et al. 2010; Ema et al. 2013; Strasser et al. 2013; Ando et al. 2015). We found moderate inter-individual variability in FL and PA of the individual muscles (12 – 17% CVb, FL and PA) that was larger than the surprisingly low variability observed for the whole QF (FL and PA = 7-9 % CVb). The lower variability of whole QF architecture than the individual muscles is intriguing as variability of the whole muscle might be expected to be similar to the average variability of the individual constituent muscles. The relatively low variability in whole QF architecture may in part be due to the lack of relationship between the corresponding FL/PA of the constituent muscles. Such architectural dissimilarity between QF constituent muscles has been reported (Blazevich et al 2006). Though perhaps counterintuitive, architectural variability amongst muscles within a synergistic group is considered a design feature that broadens the functional capabilities of the muscle group (Lieber and Ward 2011).

4.4.2. Relationships between Muscle Architecture and Maximal Strength

An initial observation was the lack of correlation between PA and isometric MVT. As a higher PA increases a muscles effective physiological cross-sectional area; which is proportional to maximal isometric force *in vitro* (Powell et al. 1984), we might expect at least an indirect association between PA and maximal isometric strength *in vivo*. However the QF PA's measured in this study were quite acute (<20º), therefore the impact on muscle PCSA is likely limited. In contrast a few studies report positive correlations between maximal strength and the PA of the agonist muscles (r = 0.471 – 0.68: Nagayoshi et al. 2003; Strasser et al. 2013; Wakahara et al. 2013; Ando et al. 2015). Interestingly, QF studies found only lateral VI

PA was related to knee extension isometric strength, though these studies (Strasser et al. 2013; Ando et al. 2015) did not derive a whole QF measure as we did. We conducted a posteriori correlations in our data between individual constituent muscles PA and MVT, which yielded no significance.

Additionally PA had no apparent influence on maximal dynamic strength. The PA increases that occur during concentric contractions amplify the shortening of the muscle (Zuurbier et al. 1992), resulting in the possibility that a given muscle shortening velocity can be achieved with lesser contribution from fascicle excursion. This mechanism would subsequently allow greater force production and is hypothesised to be more prevalent in muscles possessing greater initial PA (Brainerd and Azizi 2005; Azizi and Brainerd 2007). Also, this effect of dissociating muscle and fascicle length/velocity is theoretically greater with increasing contraction velocity (Azizi et al. 2008; Wakeling et al. 2011). Likely the narrow PA's (and limited variability) we found induce a relatively small rotational effect, that subsequently has negligible influence on fascicle length changes during contraction as previously suggested (Ichinose et al. 2000), thus underpinning our findings. Furthermore it has been articulated that the initial PA is not independently responsible for a fascicle rotation effect. Instead fascicle shortening is driven principally by the extent of actual muscle shortening that is attributable to tendon compliance (Muraoka et al. 2001; Wakeling et al. 2011; Randhawa et al. 2013; Hauraix et al. 2013). Therefore a seeming inconsequentiality of PA is reasonable.

Similarly FL had no correlation with dynamic strength. Longer FL was hypothesized to facilitate dynamic strength as reflected by greater higher velocity torque and thus a higher torque ratio. However we found no such relationship. While theoretically counterintuitive (Wickiewicz et al. 1984), our data support other correlational studies that equally reported FL was unrelated to higher velocity torque (vastus lateralis FL vs. knee extension torque, Blazevich et al. 2009b; gastrocnemius medialis FL vs. plantar flexor torque, Baxter and Piazza 2014) or a high-low velocity torque ratio ($30{:}300^{o}\text{-}s^{-1}$: Blazevich et al. 2009b). These studies although only measured architecture from just one of the muscles contributing to joint torque. We can consider our inclusion of FL measures from each of the constituent muscles of the QF and subsequently the whole muscle group as a more representative measure. A mechanical premise to expect longer FL to facilitate greater higher velocity torque and ratio is that longer fascicles (faster shortening potential) could operate (more specifically the sarcomeres of longer fascicles; Lieber and Ward 2011) at relatively lower shortening

velocities during joint rotations at a given velocity, and thus maintain a greater proportion of slow velocity torque at higher velocities. However recent a study using high frame ultrasound to record actual fascicle shortening velocities during joint rotations at varying velocities (30-330º-s^{-1}) showed that possessing longer fascicles was not necessarily associated with a lower fascicle velocity for a given joint angular velocity: normalisation of fascicle velocity for resting fascicle length did not reduce the inter-individual difference in fascicle velocity (Hauraix et al. 2013). This finding perhaps accounts for why there was a theoretical and empirical discord in the present studies results. Also it is important to consider that the 'high' velocity utilised in the present study; in accordance with isovelocity dynamometry limitations, is essentially far removed from real-world joint velocities (e.g. ~750-1200ºs^{-1} knee extension angular velocity in jumping [Bobbert et al. 1986] and sprinting [Higashihara et al. 2010]) where longer fascicle lengths may expectedly influence performance. For instance longer FL's have been found in sprinters (athletes with an obvious propensity for high velocity torque) vs. distance runners and controls (Abe et al. 2000), and subsequently longer FL was related to faster sprint times (Kumagai et al. 2000; Abe et al. 2001).

4.4.3. Relationship between Muscle Architecture and Explosive Strength

In contrary to our hypothesis that FL would positively relate to explosive strength, we found an adverse association between FL and torque produced in the initial phase of explosive voluntary contraction (0-50 ms); with no subsequent relation thereafter, and no relation of FL to evoked torque. Our finding is however concordant with the negative correlation found between changes in fascicle length (though indirect inferred via torque-angle data) towards longer fascicles and changes in voluntary isometric RTD (Blazevich et al. 2009a). The inverse correlation was ascribed to a theoretical determinism equating longer fascicles to greater muscle compliance; longer fascicles possess more sarcomeres in series (each sarcomere having compliance). Greater compliance would reduce RTD (Wilkie 1949) and thus longer fascicles would exhibit lower RTD. Neither, Blazevich et al. nor our study measured muscle compliance, so the articulated supposition is untested. Incidentally, we are unaware of any study examining any architecture-muscle compliance association. It is sensible that our finding was localised to the earliest phase of the contraction, considering this is when compliance would be greatest as muscle forces are relatively low and therefore the need to stretch the compliance tissues will likely influence RTD.

A relation between FL and voluntary, but not evoked torque at 50 ms is perhaps surprising because evoked contractions bypass the nervous system to reveal MTU contractile capacity and highlight the influence of morphological and mechanical characteristics. A more profound relation of FL to evoked than voluntary explosive strength could thus have been expected. Overtly this was not the case. A possible explanation is that the substantially faster RTD in response to the octet stimulation will subsequently remove the tissue slack and compliance much sooner. This means that by the time (50 ms) evoked torque measures are then taken, contractile forces are much higher than in voluntary contractions, and evidently any influence of longer FL induced compliance is irrelevant to how quickly higher torques are produced. Thus the different findings for the voluntary and evoked contractions are effectually a measurement artefact. This explanation suggests that a possible implication of our finding is that by improving the capacity to rapidly activate the muscle at the onset of the voluntary contraction such that the RTD more replicates that possible under evoked condition, the small negative influence of FL on initial voluntary explosive strength we have documented could potentially be negated. Such improvements can be readily achieved with specific explosive training (Tillin et al. 2012; Balshaw et al. 2016). Interestingly, in the study by Blazevich et al. (2009a), the training program that induced supposed FL change had no impact on the rate of muscle activation.

A final simple hypothesis was that PA might be related to later phase voluntary explosive strength owing to a potential relationship to maximal strength and the known influence of maximal strength on RTD. However greater PA was not associated with higher voluntary RTD or later-phase explosive force, which is deemed ascribable to the lack of relation between PA and MVT.

4.4.4. Limitations

In the present study, resting architecture measures where acquired with the knee joint in a flexed position that is likely close to the optimal joint angle for joint production, with the view that such architecture measures would subsequently be deemed of particular functional relevance. However, it is possible that because muscle architecture variables are influenced by knee joint angle, any inter-individual differences in the extent of muscle stretch from the anatomical position (straight leg) to the knee joint angle of measurement in this study (120°) could adversely influence the validity of the acquired architecture measures to reflect true physiological differences between participants and subsequently the relationship to functional

performance. For instance, it is not necessarily clear whether a longer fascicle length reflects more sarcomeres in series or simply a greater stretch of existing sarcomeres. Finally, the QF muscle architecture measures derived in this study are a generalised estimate that may limit their applicability to complex whole muscle performance.

4.4.5. Conclusion

In conclusion, QF FL was negatively related to the explosive voluntary torque at the earliest measured time (50 ms), maybe due to previously postulated relation of FL to tissue compliance presumed to slow initial RTD. FL did not relate to voluntary torque/RTD after 50 ms, and was likewise unrelated to evoked torque at 50 ms. The difference between voluntary and evoked relations to FL is potentially a consequence of the supramaximal stimulation eliciting such a high (maximal) RTD to remove slack and compliance extremely quickly so evoked torque measures are performed at higher torque levels where earlier compliance has no residual influence. However FL was not related to high-velocity strength, potentially because the hypothesised mechanism to account for an expected relationship is secondary to the influence of muscle-tendon interaction driven by tendon compliance. Also we cannot preclude the possibility that the 'high' isovelocity was simply insufficiently rapid to detect a hypothesised influence of FL (or maybe PA) on high-velocity strength. Finally PA was inconsequential to *in vivo* muscle strength characteristics, possible due to the acuteness of the values measured indeed having genuinely minimal functional effect. The low inter-individual variability in FL and PA could additionally account for an overall limited relation of skeletal muscle architecture to *in vivo* muscle strength.

CHAPTER 5

The influence of muscle-tendon unit and patellar tendon stiffness on quadriceps explosive strength in man

5.1. INTRODUCTION

Explosive strength is the ability to increase torque from low or resting levels as quickly as possible. It is commonly examined under isometric conditions and expressed as the rate of torque development (RTD) derived from the rising phase (i.e. slope) of the contractile torque-time curve. Explosive strength is considered important in situations where the time to develop torque is limited: for instance in athletic activities such as sprinting and jumping (Weyand et al. 2010; Tillin et al. 2013a); and in injury-related situations such as maintaining balance (Izquierdo et al. 1999; Robinovitch et al. 2002) or stabilizing joints (e.g. anterior cruciate ligament tears [ACL] in ≤50ms: Krosshaug et al. 2007; Koga et al. 2010) following mechanical perturbation. Further, RTD deficits have a deleterious impact on physical function in musculoskeletal patients (e.g. osteoarthritis: Maffiuletti et al. 2010; Winters and Rudolph 2014) and impaired RTD post-ACL injury may increase the risk of developing post-traumatic osteoarthritis (Kline et al. 2015), and thus RTD is an important outcome for muscle function rehabilitation (Angelozzi et al. 2012). Developing a greater understanding of the determinants of RTD could therefore have potentially widespread functional and clinical implications.

During isometric contractions, the rate of skeletal muscle contractile force production is slowed by the necessity of the muscle to shorten in order to stretch the elastic components that transmit muscle force (Hill 1951; Edman and Josephson 2007). The mechanical stiffness (resistance to elongation) of the muscle-tendon unit (MTU) and particularly its tendinous tissue components (external 'free' tendon and aponeurosis) are therefore widely hypothesised to influence *in vivo* RTD (Wilson et al. 1994; Kubo et al. 2001; Reeves et al. 2003). Stiffer tissues are thought to provide greater mechanical resistance that can constrain muscle shortening during the initial stages of contraction thereby permitting muscle fibres to operate in the higher force region of the force-velocity relationship (Wilson et al. 1994). Moreover, the force transmission time of stiffer tissues is theoretically shorter (Waugh et al. 2013). This rationale suggests that stiffer tissues exert a substantial influence on explosive strength, however, the quantitative contribution of tendon and MTU stiffness to explosive strength remains opaque (Maffiuletti et al. 2016). In contrast, tissue elongation during the rising torque-time curve maybe sufficiently negligible and the duration of force transmission through connective tissues of such brevity (Nordez et al. 2009; DeWall et al. 2014), that the inter-individual differences in tendon/MTU stiffness could be practically irrelevant to the inter-individual variation in RTD.

To date no studies have examined the relationship of tendon stiffness to *in vivo* RTD. The relationship between MTU stiffness and RTD has been examined by several studies, typically reporting positive correlations (R^2~0.10-0.30) for cohorts incorporating heterogeneous subgroups: divergent athletic groups (Bojsen-Møller et al. 2005), tendinopathic and healthy limbs (Wang et al. 2012), children of different ages (Waugh et al. 2013), adult males and females (Waugh et al. 2013; Hannah and Folland 2015). However, these subgroups likely exhibit discrete characteristics (e.g. neuromuscular activation, maximal strength, muscle fibre type composition and pain) that are known to influence RTD (Maffiuletti et al. 2016) and may confound the relationship between tissue stiffness and RTD. One recent study found absolute MTU stiffness and explosive strength were correlated, at least at higher forces (i.e. later-phase RTD), though once the influence of maximal strength (maximal voluntary torque, MVT) was removed (via partial correlation or relative values) there was no independent relationship of stiffness and explosive strength (Hannah and Folland 2015). This suggests that the relationship of absolute MTU stiffness and explosive strength is coincidental and due to the influence of maximal strength on both variables.

Furthermore studies of musculotendinous tissue stiffness are mired by methodological shortcomings (Seynnes et al. 2015). In particular, the loading-rate sensitivity of stiffness measurements (i.e. faster rate yields greater stiffness: Lieber et al. 2000; Pearson et al. 2007; Theis et al. 2012; Kösters et al. 2014) necessitates a constant RTD during the ramp contractions used to measure stiffness. Nonetheless previous studies have tended to standardise contraction duration, which leads to different loading rates according to each individual's MVT and may bias stiffness measurements to stronger individuals contracting at higher loading rates (Bojsen-Møller et al. 2005, Wang et al. 2012; Waugh et al. 2013; Hannah and Folland 2015). Obtaining reliable measures of tissue stiffness requires numerous efforts (Schulze et al. 2013), though a limited number of contractions (~2), usually from just one test session, have been commonly used (Wang et al. 2012; Waugh et al. 2013; Hannah and Folland 2015). Further to circumvent the difficulty of judging the consistency of grey-scale ultrasound patterns for the points of interest and possible experimenter bias in tissue elongation measurements, some degree of automated analysis is recommended (Seynnes et al. 2015), though studies have often relied on manual procedures (Wang et al. 2012; Waugh et al. 2013; Hannah and Folland 2015).

Of specific concern for studies that have investigated the link between stiffness and RTD is that tissue stiffness is known to increase with torque (increasing gradient of the torque-elongation relationship; Maganaris and Paul 1999, 2002; Reeves et al. 2003). Yet stiffness has often been measured over a high torque increment (e.g. 50-90% MVT, Bojsen-Møller et al. 2005; 50-100%MVT, Kubo et al. 2001, Wang et al. 2012) even though RTD is usually measured from the lowest possible torque - rest (e.g. 0-50% MVT). Thus the relevance of high torque measures of stiffness to functional measurements starting from rest or low levels of torque, that are known to involve markedly lower stiffness properties, appears questionable. To avoid this dissociation between measured and functionally relevant stiffness, both variables could be measured over the same torque increment.

Any influence of tissue stiffness on explosive strength might be expected to be more pronounced for evoked contractions that drive the muscle at its maximal possible RTD (Deutekom et al. 2000; de Ruiter et al. 2004; Folland et al. 2014) and depend entirely on the characteristics of the MTU rather than the voluntary nervous system. The influence of tendon stiffness on evoked RTD has not been investigated and only Hannah and Folland (2015) have examined the relationship between MTU stiffness and evoked explosive strength, finding a stronger correlation for evoked than voluntary RTD.

The present study aimed to comprehensively examine the relationship between both tendon and MTU stiffness, with voluntary and evoked RTD measurements of explosive strength. All relationships between stiffness and RTD variables were examined over the same torque increment for both variables. In addition to evaluating the relationship of absolute measures of stiffness and RTD, the association of relative measures was examined to remove any influence of maximal strength. A large cohort of healthy young men were assessed in duplicate measurement sessions, with tendon and MTU stiffness determined during multiple ramp contractions performed at a constant loading rate.

5.2. METHOD

5.2.1. Participants

Fifty-two young men (age 25 ± 2 years, height 176 ± 7 cm, weight 72 ± 9 kg) provided written informed consent before participating in this study, which was approved by the Loughborough University Ethical advisory committee. Participants were healthy, free from musculoskeletal injury, and recreationally active (2160 ± 1309 MET minutes per week,

International Physical Activity Questionnaire short format; Craig et al. 2003), but not involved in any form of systematic training in the 18 months prior to the study.

5.2.2. Experimental Design

Participants completed a familiarisation session, involving practice of all voluntary contractions performed during subsequent measurement sessions and habituation with evoked (electrically stimulated) contractions, followed by two duplicate measurement sessions separated by 7-10 days. Measurement sessions involved a series of unilateral isometric contractions of the knee extensors of the dominant (preferred kicking) leg in the following order: maximal voluntary (MVCs) and explosive voluntary contractions, electrically evoked octet contractions (second measurement session only) and voluntary ramp contractions. Finally, knee flexor MVCs were also completed. Knee joint torque was recorded throughout contractions, and knee flexor surface electromyography (EMG) was recorded during knee flexor MVCs and knee extensor ramp contractions. MVT was determined from MVCs, while voluntary and evoked RTD measurements of explosive strength were determined from explosive voluntary and evoked octet contractions, respectively. Ramp contractions were performed to permit tissue stiffness measurements from simultaneous torque and elongation, via ultrasound imaging, recordings. Measurement sessions with each individual were performed at a consistent time of the day, and all sessions started between 12:00-19:00 hours. Participants were instructed not to participate in strenuous physical activity or consume alcohol for 36 hours, and refrain from caffeine consumption for 6 hours, before measurement sessions. On a separate occasion, sagittal plane MRI images of the knee joint were acquired to measure patellar tendon (PT) moment arm in order to convert external torques to tendon force.

5.2.3. Torque Measurement

Participants were positioned in an isometric strength-testing chair with knee and hip angles of 115° and 126° (180° = full extension), respectively. Adjustable straps were tightly fastened across the pelvis and shoulders to prevent extraneous movement. An ankle strap (35 mm width reinforced canvas webbing) was placed ~15% of tibial length (distance from lateral malleolus to knee joint space) above the medial malleolus, and positioned perpendicular to the tibia and in series with a calibrated S-Beam strain gauge (Force Logic, Berkshire, UK). The analogue force signal was amplified (x370; A50 amplifier, Force Logic UK) and sampled at 2,000 Hz using an A/D converter (Micro 1401; CED, Cambridge, UK) and

recorded with Spike 2 computer software (CED). In offline analysis, force signals were low-pass filtered at 500 Hz using a fourth order zero-lag Butterworth filter, gravity corrected by subtracting baseline force, and multiplied by lever length, the distance from the knee joint space to the center of the ankle strap, to calculate torque.

5.2.4. Knee Flexor Electromyography (EMG)

Surface EMG recordings over the biceps femoris (BF) and semitendinosus (ST) were made with a wireless EMG system (Trigno; Delsys Inc, Boston, MA) were made during knee flexor MVCs and knee extensor ramp contractions. Following preparation of the skin (shaving, abrading and cleansing with alcohol) single differential Trigno standard EMG sensors (1-cm inter electrode distance; Delsys Inc, Boston, MA) were attached over each muscle using adhesive interfaces. Sensors were positioned parallel to the presumed frontal plane orientation of the underlying muscle fibres at 45% of thigh length (distance from the greater trochanter to the lateral knee joint space) measured from the popliteal crease. EMG signals were amplified at source (x300; 20-450 Hz bandwidth) before further amplification (overall effective gain x 909) and sampled at 2000 Hz via the same A/D converter and computer software as the force signal, to enable data synchronization. In offline analysis, EMG signals were corrected for the 48-ms delay inherent to the Trigno EMG system and band-pass filtered (6-500 Hz) using a fourth-order, zero-lag Butterworth digital filter.

5.2.5. Knee Extension and Flexion Maximal Voluntary Contractions

Following a brief warm-up (3 s contractions at 50% [x3], 75% [x3] and 90% [x1] of perceived maximal), participants performed 3-4 MVCs and were instructed to either ‘push as hard as possible’ (knee extension) or ‘pull as hard as possible’ (knee flexion) for 3-5 s and rest ≥ 30 s. A horizontal cursor indicating the greatest torque obtained within the session was displayed for biofeedback and verbal encouragement was provided during all MVCs. The highest instantaneous torque recorded during any MVC was defined as MVT. During knee flexor MVCs EMG amplitude was calculated as the root mean square (RMS) of the filtered EMG signal of the BF and ST over a 500 ms epoch at knee flexion MVT (250 ms either side) and averaged across the two muscles to give EMG_{MAX}.

5.2.6. Explosive Voluntary Contractions

Participants performed a series of 10 explosive voluntary contractions each separated by 15 s. Participants were instructed to extend their knee 'as fast and as hard as possible'; with the emphasis on 'fast', for 1 s from a relaxed state upon hearing an auditory signal. Contractions involving a visible countermovement or pre-tension were discarded and another attempt made. To indicate if a countermovement or pre-tension had occurred, resting torque was displayed on a sensitive scale. During each explosive contractions participants were required to exceed 80%MVT, which was depicted by an on-screen marker. To provide performance feedback the time taken to reach 80%MVT was shown after each contraction and the slope of the rising torque-time curve (10 ms time constant) was displayed throughout these contractions with the peak slope of their best attempt indicated with an on-screen cursor. The three best explosive contractions (highest torque at 100 ms) and no discernible countermovement or pre-tension (change in baseline force <0.34 Nm in the preceding 300 ms) were analysed in detail. Contraction torque onset was defined as the last trough before the torque signal permanently deflected away from the envelope of the baseline noise; identified via manual inspection using a systematic standard method by the same trained investigator, in accordance with previously published methods (Tillin et al. 2010). Manual onset detection is considered to provide greater accuracy and reliability than an automatic approach (Tillin et al. 2013b). The torque signal was initially viewed with y and x-axis scales of 0.68 Nm and 300 ms respectively and a vertical cursor placed on torque onset. Accurate placement of the cursor was verified by viewing the signal with a higher resolution. RTD (ΔTorque or Δ%MVT /ΔTime) measurements of explosive strength were calculated from the time taken between contraction onset and absolute (50, 100 and 150 Nm [Vol $RTD_{0\text{-}50Nm}$, Vol $RTD_{0\text{-}100Nm}$, Vol $RTD_{0\text{-}150Nm}$) and relative (25, 50 and 75%MVT [Vol $RTD_{0\text{-}25\%MVT}$, Vol $RTD_{0\text{-}50\%MVT}$, Vol $RTD_{0\text{-}75\%MVT}$]) torques, as well as RTD between sequential torque levels (absolute 50-100 and 100-150 Nm [Vol $RTD_{50\text{-}100Nm}$ and Vol $RTD_{100\text{-}150Nm}$]; relative 25-50 and 50-75% MVT [Vol $RTD_{25\text{-}50\%MVT}$, Vol $RTD_{50\text{-}75\%MVT}$]). Values recorded from each of the three analysed (best) contractions were averaged.

5.2.7. Evoked Octet Contractions

The femoral nerve was electrically stimulated (constant current, variable voltage stimulator; DS7AH, Digitimer Ltd., UK) with square-wave pulses (0.2 ms duration) to elicit involuntary contractions of the knee extensors whilst the participant was voluntarily passive. Electrical stimuli were applied via a cathode probe (1-cm diameter; Electro Medical Supplies, Wantage,

UK) protruding 2 cm perpendicular from the center of a plastic base (4 x 5 cm). The cathode and an anode (carbon rubber electrode, 7 x10 cm; Electro Medical Supplies, Wantage, UK) were coated with electrode gel and securely taped to the skin over the femoral nerve in the femoral triangle and the greater trochanter respectively. The precise location of the cathode was determined as the position that evoked the greatest twitch response to a submaximal electrical current. Twitch contractions were elicited at incremental currents (~15 s apart) until a simultaneous plateau in peak torque and the peak slope of the rising twitch torque was observed. Thereafter, the electrical current was lowered and octet stimulation (8 pulses at 300 Hz) was delivered in step-wise increments until the stimulation intensity that elicited twitch force plateau (defined as the maximal stimulation intensity/ current) was reached. Real-time inspection of octet peak force and peak rate of force development (10 ms epoch) confirmed a plateau in both variables with incremental stimulation. Subsequently, three supramaximal (120% maximal current) octet contractions were elicited. Absolute and relative RTD (ΔTorque or Δ%MVT/ΔTime) measurements of evoked explosive strength were calculated from the time taken between contraction onset and absolute (50 and 100 Nm [Oct $RTD_{0\text{-}50Nm}$ and Oct $RTD_{0\text{-}100Nm}$) and relative (25 and 50%MVT [Oct $RTD_{0\text{-}25\%MVT}$ and Oct $RTD_{0\text{-}50\%MVT}$]) torques, as well as RTD between sequential torques (absolute 50-100Nm [Oct $RTD_{50\text{-}100Nm}$]; relative 25-50%MVT [Oct $RTD_{25\text{-}50\%MVT}$]). Values recorded from each of the three supramaximal contractions were averaged. Evoked measures were not acquired for three participants who did not tolerate the discomfort associated with the octet stimulation.

5.2.8. Ramp Contractions for Determination of Tissue Stiffness

Tissue stiffness was derived from synchronous recordings of torque and tissue elongation (see below, corrected for passive tissue displacement via video recording of knee joint changes) during isometric knee extension ramp contractions (experimental set-up; Figure 5.1). Participants completed two sub-maximum practice ramp contractions prior to five maximum attempts with 90 s rest between contractions. Prior to each ramp contraction participants were shown a target torque-time trace on a computer monitor that increased at a constant gradient (50 $Nm.s^{-1}$ loading rate) from zero up to MVT. They were instructed to match the target trace as closely as possible for as long as possible (i.e. up to MVT), and real-time torque was displayed over the target torque-time trace for feedback. The preceding knee extensor MVCs and sub-maximal contractions were considered sufficient to elicit tissue preconditioning. The three most suitable ramp contractions, according to highest peak torque,

the closeness to the target loading rate and ultrasound image clarity, were analysed and measurements averaged across these three contractions.

5.2.9. Measurement of Tissue Elongation

Video images from two ultrasound machines and one video camera were captured to obtain tissue and knee joint displacements during ramp contractions. An ultrasound probe (7.5 MHz linear array transducer, B-mode, scanning width 60mm and depth 50 mm; Toshiba Power Vision 6000, SSA-370A: Otawara-Shi, Japan) was fitted into a custom made high-density foam cast that was strapped to the lateral aspect of the thigh with the mid-point of the probe positioned at ~50 % thigh length. The probe was aligned so the fascicles inserting into the vastus lateralis (VL) muscle deep aponeurosis could be visualized at rest and during contraction. An echo-absorptive marker (multiple layers of transpore medical tape) was placed beneath the ultrasound probe to provide a reference for any probe movement over the skin. Another ultrasound probe (5-10 MHz linear array transducer, B-mode, scanning width 92 mm and depth 65 mm, EUP-L53L; Hitachi EUB-8500) was fitted into a custom made high-density foam cast that was held firmly over the anterior aspect of the knee with the probe aligned longitudinal to the patellar tendon such that the patella apex and insertion of the posterior tendon fibres at the tibia could be visualized at rest and throughout the contraction. The ultrasound machines were interfaced with the computer collecting torque data in Spike 2 and the video feeds were recorded synchronously with torque using Spike 2 video capture at 25 Hz. During off-line analysis tissue elongation was tracked frame-by-frame using public-domain semi-automatic video analysis software: Tracker, version 4.86 (www.cabrillo.edu/~dbrown/tracker). VL fascicle deep aponeurosis cross point displacement relative to the skin marker provided a measure of muscle-tendon unit (MTU) elongation (Figure 5.1). Patellar tendon elongation was determined by the longitudinal displacement of the patella apex and the tendon tibial insertion (Figure 5.1). The distal insertion of the patellar tendon was not monitored for the purpose of estimating overall MTU elongation. To enable correction of tissue displacement due to joint angle changes during ramp contractions individual ratios of tissue displacement relative to joint angular displacement (mm/°) were obtained from passive movements (i.e. plotting the tissue displacement-knee joint angle relationship). This ratio was used to determine tissue displacement resulting from knee angle change during ramp contractions, which was subsequently subtracted from total measured displacement. Corrections were only applied to aponeurosis displacement. Tendon elongation under passive conditions was deemed negligible. Passive movements were conducted prior to

the ramp contractions. Participants were instructed to completely relax as their knee was moved through 90 to 130°. During passive movements and ramp contractions, knee joint angle (angle between visible markers placed on the greater trochanter, lateral knee joint space and lateral malleolus) was derived from sagittal plane video recorded using a camera mounted on a tripod positioned (1.5 m) perpendicular to the strength-testing chair. The video camera was interfaced with a computer and recorded using spike 2 video capture at 25 Hz (simultaneously with force, EMG, and ultrasound images during the ramp contractions) and analysed via Tracker software.

5.2.10. Calculation of Tendon Force

PT force was calculated by dividing external absolute knee extensor torque by the patellar tendon moment arm length. The latter was measured from sagittal plane T1-weighted MR (1.5 T Signa HDxt, GE) images (time of repetition/time to echo 480/14, image matrix 512 x 512, field of view 160 x 160 mm, pixel size 0.313 x 0.313, slice thickness 2 mm, inter-slice gap = 0 mm) as the perpendicular distance from the PT line of action to the tibio-femoral contact point, which was the midpoint of the contact distance between the tibia and femur. Due to constraints in the size of the knee coil, sagittal images were acquired in an extended knee position (~163°). Moment arm length for any specific knee angle measured at rest or during ramp contraction was estimated from previously published data fitted with a quadratic function (Kellis and Baltzopoulos 1999), scaled to each participant's measured moment arm length at 163°. Absolute internal knee extensor torque was given by summing net knee extension torque and the estimated knee flexor co-contraction torque. Antagonist knee flexor torque was estimated by expressing the average knee flexor EMG amplitude (RMS 50 ms moving window) during ramp contractions relative to the knee flexor EMG_{MAX} and multiplying by the knee flexor MVT (assuming a linear relationship between EMG amplitude and torque). During analysis, torque and EMG amplitude were down-sampled to 25 Hz to match the ultrasound video frequency.

5.2.11. Calculation of Muscle-Tendon Unit and Patellar Tendon Stiffness

MTU (corrected for passive tissue displacement) and PT elongation were plotted (for each ramp contraction analysed) against tendon force. Tendon force-elongation plots were fitted with a second-order polynomial forced through zero. Using the associated quadratic equations MTU and PT elongation was determined at specific absolute (50, 100 and 150 Nm) and individual relative knee extension torques (25, 50 and 75% MVT). Absolute stiffness (Δ

tendon force [N]/Δ elongation [mm]; $N.mm^{-1}$) was calculated over 0-50, 0-100 and 0-150 Nm torque increments (MTU/PT $k_{0\text{-}50Nm}$, MTU/PT $k_{0\text{-}100Nm}$, MTU/PT $k_{0\text{-}150Nm}$) and sequential torque increments of 50-100 and 100-150 Nm (MTU/PT $k_{50\text{-}100Nm}$ and MTU/PT $k_{100\text{-}150Nm}$). MTU and PT elongation at relative torques were converted to strain (ε, %; ratio of Δ tissue length to resting tissue length). Relative stiffness (Δ%MVT/Δε [$\%MVT.\varepsilon^{-1}$]) was calculated over relative 0-25, 0-50, 0-75%MVT increments (MTU/PT $k_{0\text{-}25\%MVT}$, MTU/PT $k_{0\text{-}50\%MVT}$, MTU/PT $k_{0\text{-}75\%MVT}$) and sequential increments 25-50 and 50-75%MVT (MTU/PT $k_{25\text{-}50\%MVT}$ and MTU/PT $k_{25\text{-}75\%}$MVT). The stiffness measures derived from each of the three ramp contractions analysed was averaged to give each individuals representative values. MTU resting length was assessed with a tape measure over the surface of the skin from the tibial tuberosity to center of the measurement site over VL. PT length was taken as the distance between the patella apex and the insertion of the posterior fibres of the tendon on the tibia, measured from ultrasound images acquired at rest prior to the ramp knee extensions.

5.2.12. Statistical Analysis

MVT, RTD and tissue stiffness (k) measures from duplicate measurement sessions were averaged for criterion measures used in statistical tests. Using SPSS Version 20.0 (IBM Corp., Armonk, NY), Pearson's product moment bivariate correlations were performed to examine the relationships between absolute or relative RTD (voluntary or evoked) vs. tissue stiffness variables (MTU or PT) measured over equivalent torque increments; e.g. absolute PT $k_{0\text{-}100Nm}$ vs. Vol $RTD_{0\text{-}100Nm}$, relative MTU $k_{0\text{-}50\%MVT}$ vs. Vol $RTD_{0\text{-}50\%MVT}$. Absolute stiffness measures were also correlated against MVT. Additional (a posteriori) correlations were performed between matched relative torque increment voluntary/evoked octet RTD and MTU stiffness over 5% increments from contraction onset (e.g. Vol $RTD_{50\text{-}55\%MVT}$ [$\%MVT.s^{-1}$] vs. MTU $k_{50\text{-}55\%MVT}$ [$\%MVT.\varepsilon^{-1}$]), to more specifically characterise the relationships found between the relative RTD and relative MTU stiffness. Statistical significance level was $P<0.05$. Descriptive data are presented as mean ± standard deviation (SD). To provide an index of measurement reliability average within participant coefficient of variation (CVw, %) was calculated between the two measurement sessions, although it is worth noting that the criterion values (averaged across two sessions) will have higher reliability than each individual session. Inter-individual variability is reported as between participant coefficient of variation (CVb, %) of criterion measures.

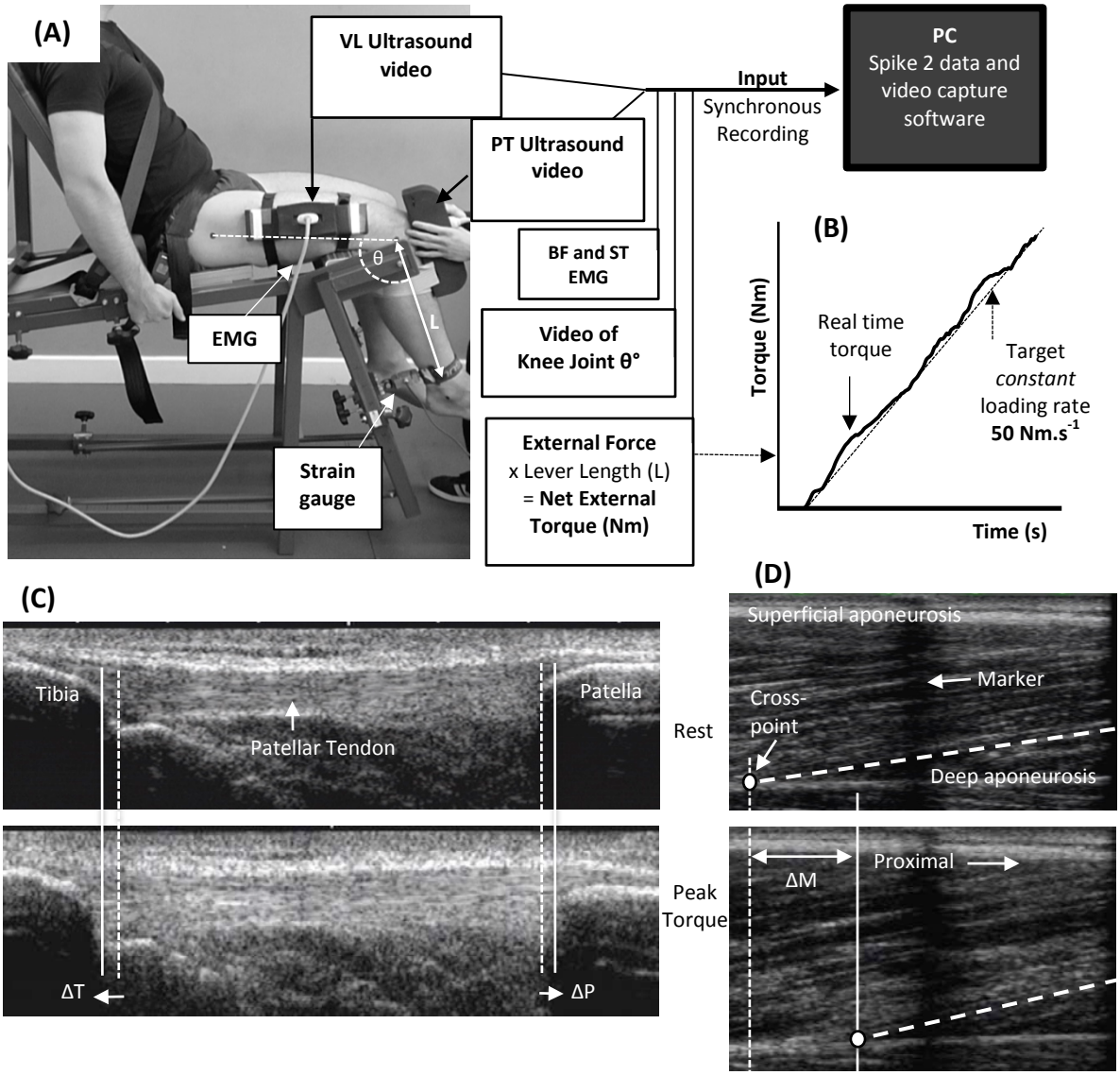

Figure 5.1. The experimental set-up and ultrasound imaging during ramp contractions. Participants were tightly fastened to a rigid isometric strength-testing chair with resting knee and hip angles of 115 and 126° respectively (A). Unilateral knee extensor torque, video of knee joint angle, antagonist muscle (biceps femoris [BF], semitendinosus [ST]) surface electromyography and ultrasound video images were recorded during constant-loading rate isometric ramp knee extensor contractions (example in B). Ultrasound images are of the patellar tendon (PT, C) and vastus lateralis (VL, D) muscle at rest (top) and at peak ramp torque (bottom) and indicate the measurement of PT (tibia-patellar displacement, ΔT + ΔP) and MTU (VL deep aponeurosis fascicle-cross point proximal displacement [ΔM] relative to the echo-absorptive skin marker) elongation.

5.3. RESULTS

5.3.1. Measurement Reliability

Within-participant test-retest reliability was excellent for MVT (CVw 3.0%), and good for voluntary RTD (CVw ≤ 8.6% for absolute and relative measures). Matched MTU and PT k measures were not as reliable, but improved at higher torque increments: MTU k and relative MTU k, CVw 15.4 to 9.7% and 14.1 to 11.0%; PT k and relative PT k, CVw 13.9 to 8.8% and 13.6 to 8.1%.

5.3.2. Inter-individual Variability

Knee extension MVT was 245.0 ± 41.8 Nm (CVb 17.1%, 2.3-fold range). Voluntary torque-time curves (Figure 5.2 A and C) exhibited similar between participant variability in absolute and relative RTD measures CVb of 14.4 to 20.5% (1.8- to 2.9-fold range). Voluntary sequential RTD was more variable (CVb 32.0-33.0%) as was relative sequential RTD (CVb 24.0-25.0%). Evoked octet torque-time curves (Figure 5.3 B and D) showed octet RTD and relative octet RTD varied much less than voluntary $RTD_{0\text{-}50Nm}$ and $_{0\text{-}25\%MVT}$. Octet sequential RTD/relative RTD was highly variable (CVb was 37.4 and 45.3%).

There was large inter-individual variability in external torque-elongation/strain relationships for both the PT and MTU as shown in Figure 5.3. The variability in elongation was greatest at the initial torque increment (50 Nm: MTU 7.6-fold range; PT 3.7-fold range), which progressively reduced at higher torque increments and sequential torques (e.g. 100-150 Nm: MTU 3.2-fold range; PT 2.4-fold range). Similarly, relative knee extensor torque-MTU/PT strain curves (Figure 5.4 C/D) showed tissue strain to be most variable at the initial relative torque level (25%MVT: MTU 6.6-fold range; PT 3.5-fold range), with less inter-individual variability at higher and sequential relative torques (e.g. 50-75%MVT: MTU 3.2-fold range; PT 2.4-fold range). PT elongation was 20% of MTU elongation at all torque increments. Alternatively, PT strain was 1.45-fold greater than MTU strain. For clarity, whilst the external torque-elongation/strain relationships are shown for illustrative purposes, individual stiffness values were derived from tendon force-elongation/strain relationships.

5.3.3. Bivariate Correlations of PT Stiffness and Explosive Strength

Voluntary and evoked RTD were unrelated to PT k measured over matching torque increment ($r = 0.02$ to 0.242, $P \geq 0.094$ [Figure 5.4]; e.g. scatterplot in Figure 5.5 B). Likewise, relative voluntary and evoked RTD were also unrelated to relative PT k ($r = 0.048$

to 0.255, P = 0.069 to 0.736; Figure 5.6). PT k measures were also unrelated to MVT (r = 0.094 to 0.127, all $P \geq 0.371$).

5.3.4. Bivariate Correlations of MTU Stiffness and Explosive Strength

Voluntary and evoked RTD were unrelated to MTU k measured over the same torque increment (r = 0.038 to 0.191, $P \geq 0.184$; e.g. scatterplot in Figure 5.5 A). In contrast, some voluntary and evoked relative RTD measures were positively associated with relative MTU k (Figure 6) e.g. relative Vol $RTD_{25\text{-}50\%MVT}$ r = 0.374, P = 0.007 (Figure 5.7 A) and Oct $RTD_{25\text{-}50\%MVT}$ r = 0.353, P = 0.014 (Figure 5.7 B). Following these associations a more detailed secondary analysis using 5%MVT increments (relative MTU k and relative RTD again measured over the same increments) showed that relative MTU k was positively related to relative voluntary RTD for the increments from 35-55%MVT (r = 0.312 to 0.434, $P \leq 0.026$; Figure 5.8). Relative evoked RTD was also positively related to relative MTU k from 5-45% MVT (r = 0.315 to 0.461, $P \leq 0.029$; Figure 5.8). Finally MTU k measures were unrelated to MVT (MTU, r = -0.124 to -0.09, all $P \geq 0.388$).

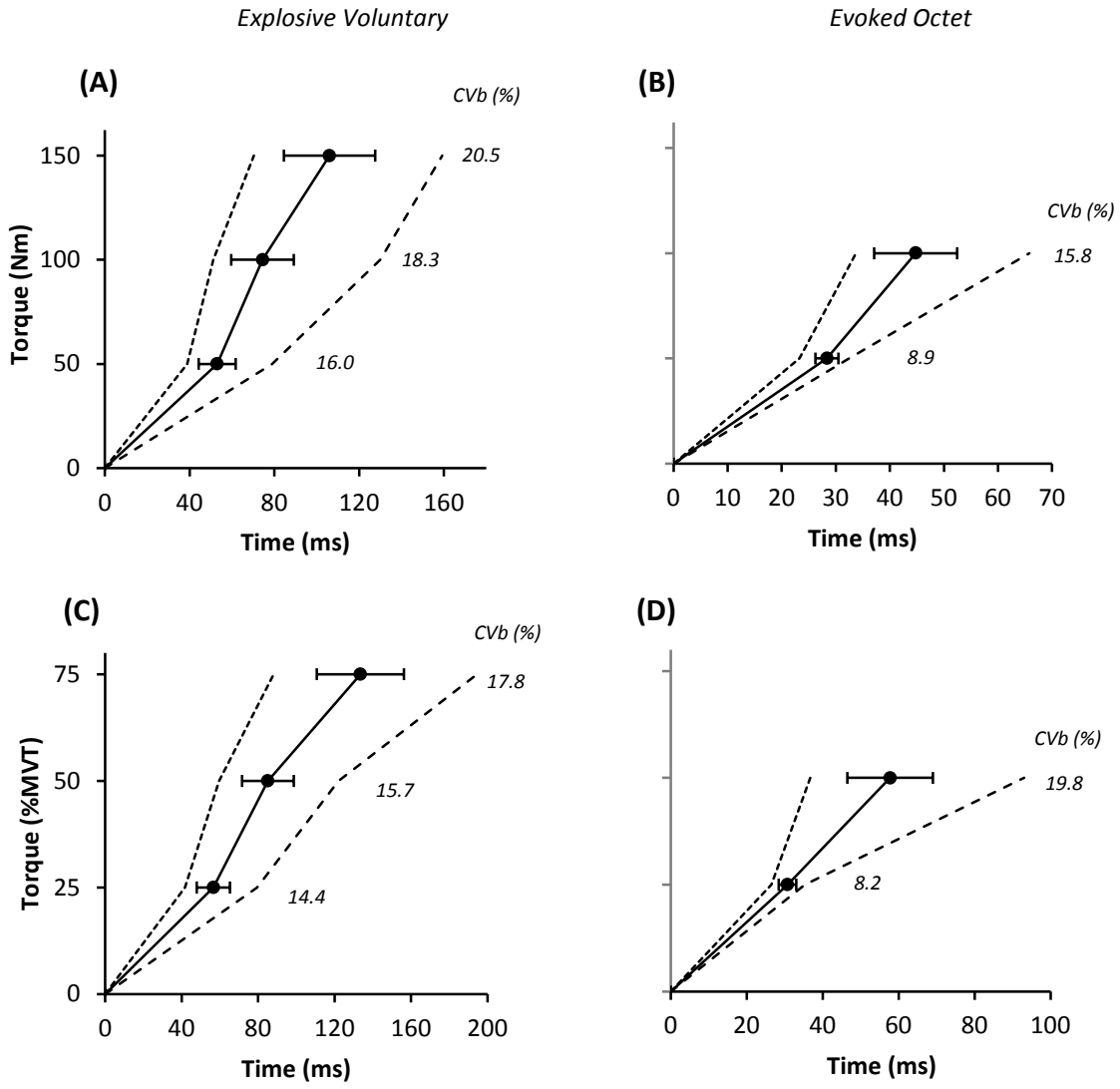

Figure 5.2. Inter-individual variability of torque-time curves during explosive voluntary (A, C; n=52) and evoked octet (B, D, n=49) contractions of the knee extensors expressed in absolute (Nm; A, B) and relative (% maximal voluntary torque, MVT; C, D) terms. Black line and circles (bars) are mean (± SD) and the dotted and dashed lines depict the minimum and maximum torque values respectively. *Italic* numbers give the between participant co-efficient of variation (CVb %) for the rate of torque development (absolute, ΔTorque/ΔTime [A and B]; relative, Δ%MVT/ΔTime [C and D]) calculated from 0 to the specified torque increment.

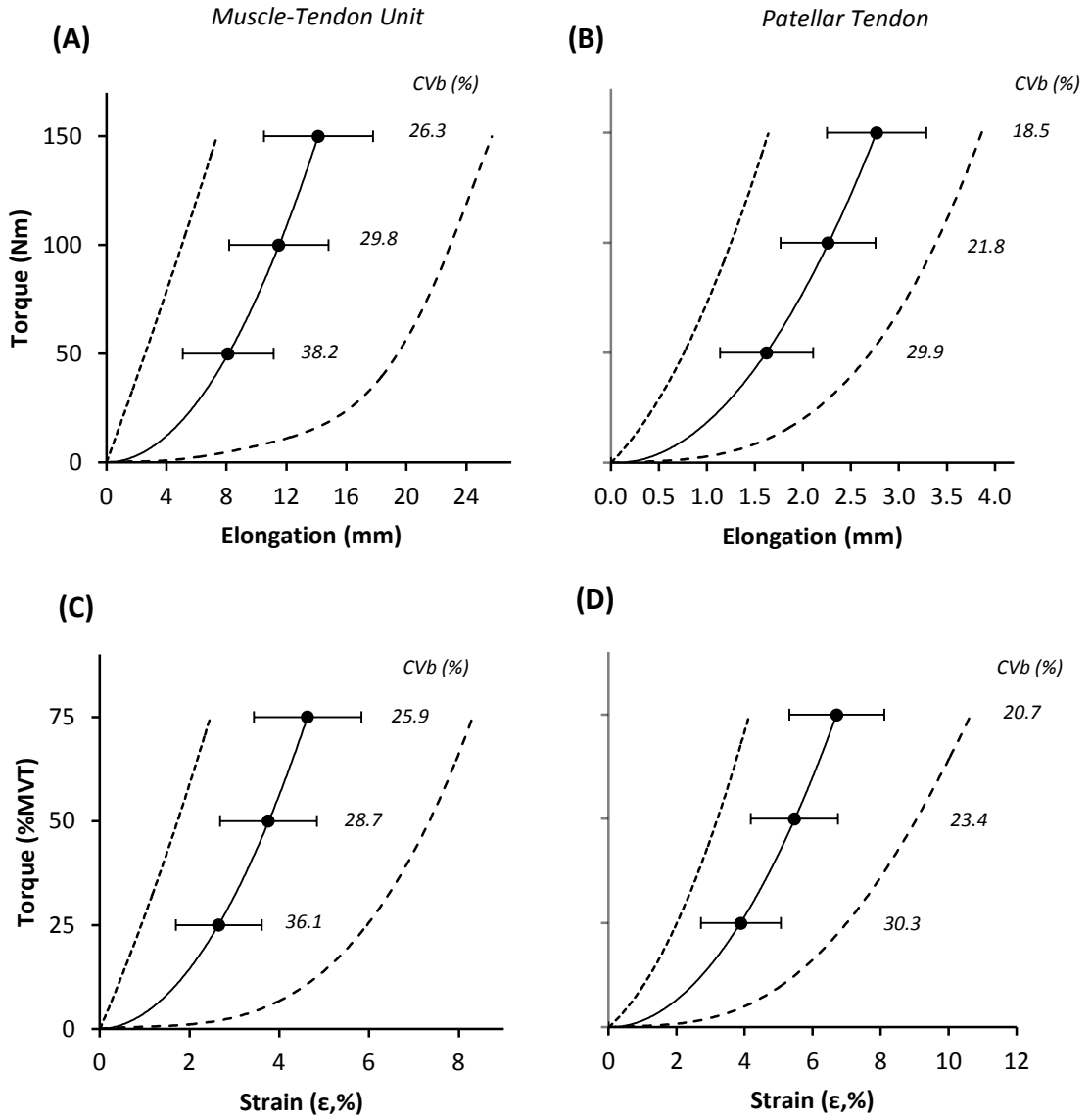

Figure 5.3. Inter-individual variability in absolute torque-tissue elongation and relative torque (%MVT)-tissue strain curves for the muscle-tendon unit (MTU; A and C) and patellar tendon (PT; B and D). Data acquired during isometric ramp knee extensor contractions. Black line and circles (bars) are mean (± SD) torque-elongation/strain curve, while dotted and dashed lines depict individuals with the minimum and maximum values of elongation/strain respectively. *Italic* numbers give between participant co-efficient of variation (CVb %) for elongation and strain measured from 0 to the specified torque level. Stiffness measurements were subsequently derived from individual tendon force-elongation/strain relationships

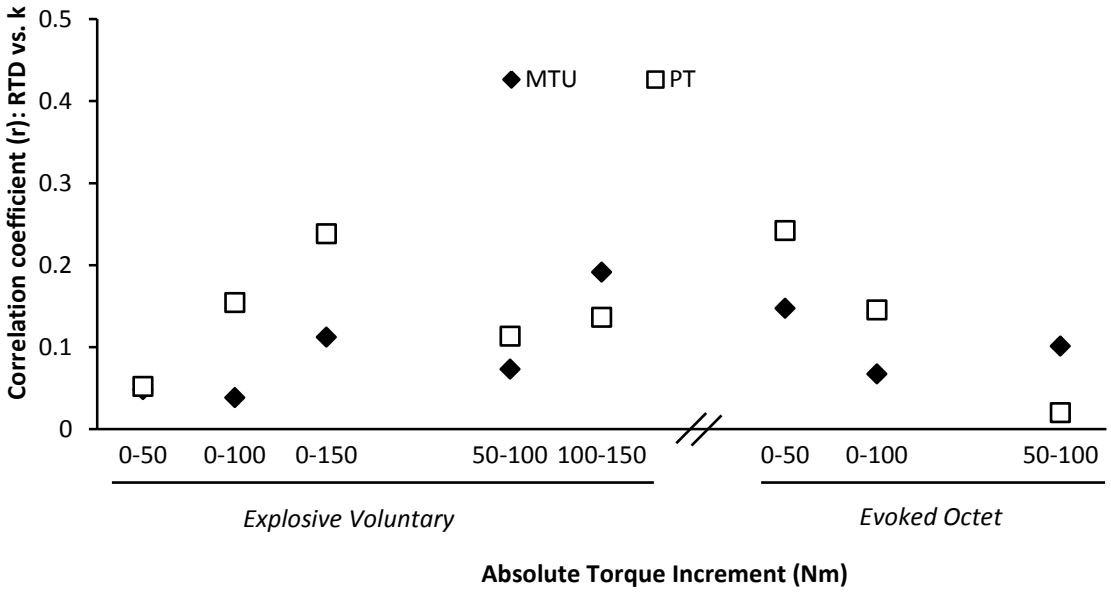

Figure 5.4. Pearson's product moment correlation coefficients between the rate of torque development (RTD) during explosive voluntary or evoked octet contractions and the muscle-tendon unit (MTU, black diamonds) and patellar tendon (PT, white squares) absolute stiffness (k; $N.mm^{-1}$) calculated across absolute tendon forces at the equivalent torque increment.

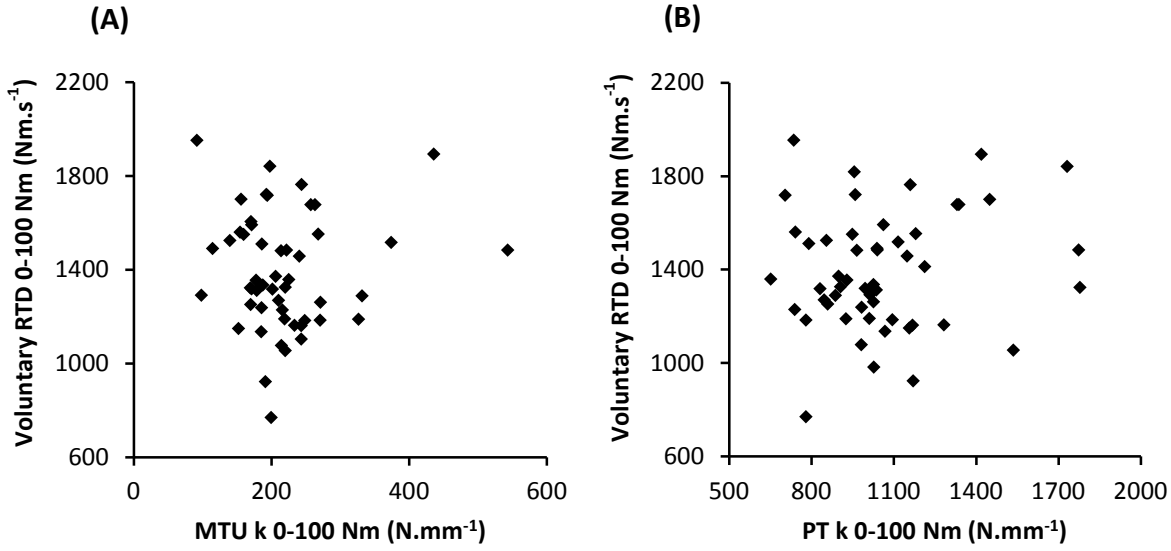

Figure 5.5. Example scatterplots showing bivariate relationships between the rate of torque development (RTD; $Nm.s^{-1}$) during explosive voluntary (A, [n=51]) contractions and the equivalent torque increment stiffness (k; $N.mm^{-1}$) of the muscle-tendon unit (MTU, A) and patellar tendon (PT, B).

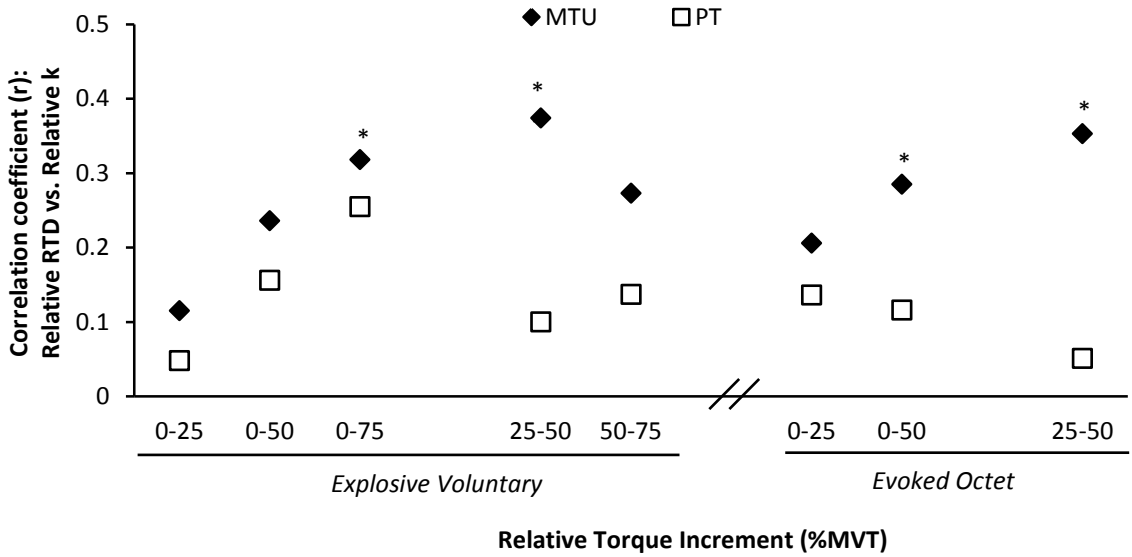

Figure 5.6. Pearson's product moment correlation coefficients between the relative rate of torque development (RTD) during explosive voluntary and evoked octet contractions and the muscle-tendon unit (MTU) and patellar tendon (PT) relative stiffness (k; %MVT/ε^{-1}) calculated across strain values determined at corresponding relative torques. **P<0.01, *P<0.05.

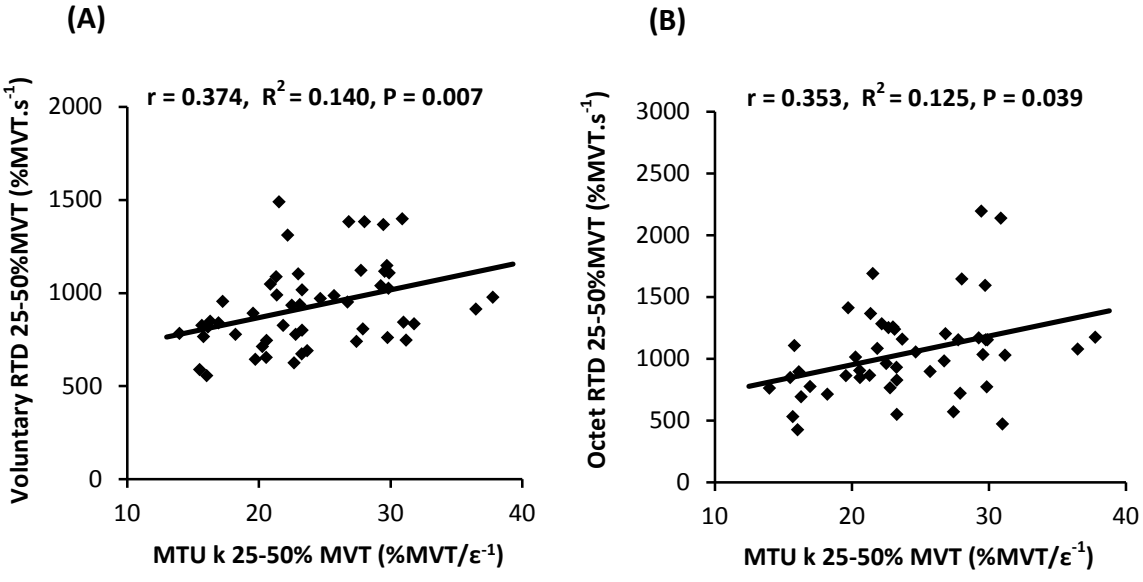

Figure 5.7. Scatterplots of the bivariate relationships between the relative rate of torque development (RTD; %MVT.s^{-1}) during explosive voluntary (Vol; A [n = 51]) and evoked octet (Oct; B [n = 48]) contractions and the equivalent relative torque increment relative stiffness (k; %MVT/ε^{-1}) of the muscle-tendon unit (MTU).

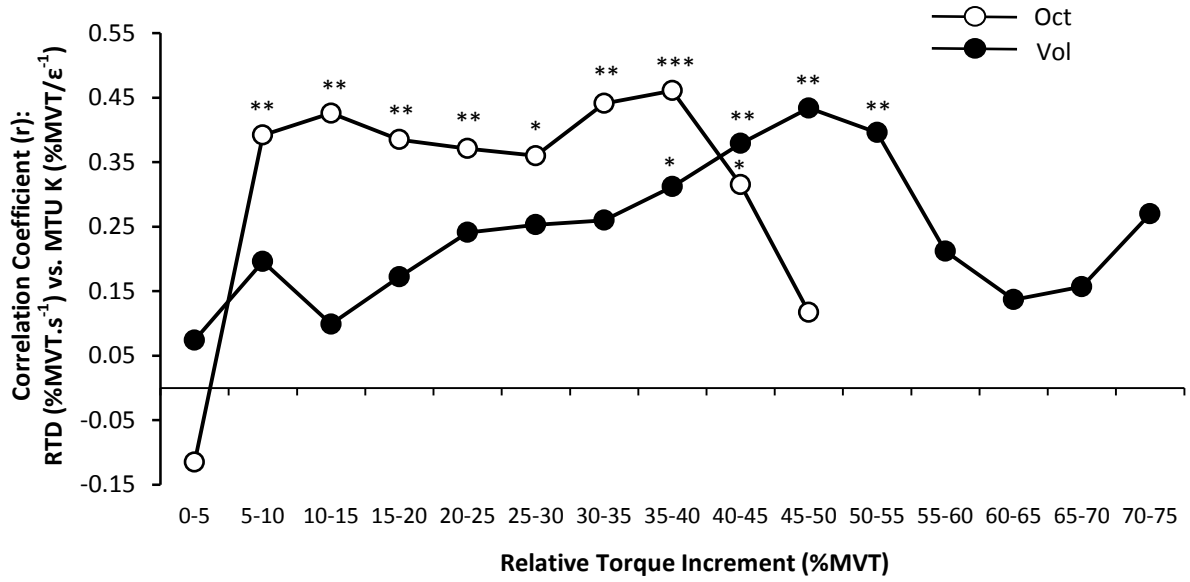

Figure 5.8. Bivariate correlations between relative RTD (%MVT.s^{-1}) and relative MTU K (%MVT/ε^{-1}) during matching %MVT torque increment. Correlations performed with n = 51 for voluntary [Vol] and n = 48 for evoked octet (Oct) contractions. Statistical significance level: *P<0.05, **P<0.01, ***P<0.001.

5.4. DISCUSSION

The present study carefully investigated whether both PT and MTU stiffness (k) were related to voluntary and evoked explosive muscle strength *in vivo*, with both variables assessed over the same torque increment, and expressed in absolute and relative terms. Bivariate correlations revealed no relationships between absolute PT and MTU k and voluntary and evoked RTD. Likewise relative PT k was unrelated to relative voluntary or evoked RTD. However, relative MTU k had modest positive relationships to some measures of relative RTD during explosive voluntary (Vol $RTD_{0\text{-}75\%MVT}$, R^2 = 0.101; Vol $RTD_{25\text{-}50\%MVT}$, R^2 = 0.140), and evoked octet (Oct $RTD_{0\text{-}50\%MVT}$, R^2 = 0.081; Oct $RTD_{25\text{-}50\%MVT}$, R^2 = 0.125) contractions. Subsequent correlations between relative RTD and MTU k in 5%MVT increments showed relative MTU k contributes to explaining voluntary relative RTD between 35-55%MVT (R^2 = 0.097 – 0.188), and relative RTD throughout evoked octet contraction (5-45%MVT; R^2 = 0.099 – 0.194).

Our finding of no relationships between MTU k and RTD measures is contrary to earlier work that generally supported weak-moderate positive relationships between MTU k and RTD (Bojsen-Møller et al. 2005; Waugh et al. 2013; Hannah and Folland 2015). However these studies used loading rates that were dependent upon and thus may have been confounded by MVT, did not match the torque increments of stiffness and RTD measurement (Bojsen-Møller et al. 2005; Waugh et al. 2013), and included heterogeneous sub-groups exhibiting differences in potentially confounding variables (Bojsen-Møller et al. 2005; Waugh et al. 2013; Hannah and Folland et al. 2015). These methodological issues may have skewed previous stiffness measurements in favour of stronger individuals who also tend to have higher RTD values (Andersen and Aagaard 2006; Folland et al. 2014). For example, calculating stiffness over a tendon force increment that is relative to maximal strength (e.g. 50-90%MVT, Bojsen-Møller et al. 2005; 50-100%MVT Wang et al. 2012; 10-80% MVT, Waugh et al. 2013) means the force increment for stiffness determination is higher for stronger individuals. As there is a well-documented force-stiffness relationship this method creates a methodological artefact whereby stronger individuals will inherently be measured to have a greater stiffness. In addition use of inconsistent loading rates, as a consequence of standardized duration ramp contractions to different force increments for each individual, would produce higher stiffness values for the higher loading rates of stronger individuals (Pearson et al. 2007; Theis et al. 2012; Kösters et al. 2014).

In contrast, stiffness measurements in the present study were more thorough: duplicate measurement sessions each involving multiple, standardised loading ramp contractions, measurements of stiffness and RTD over the same torque increment for all individuals, and use of a large cohort of exclusively young males with similar physical activity status. Nevertheless this approach revealed wide inter-individual variability in MTU k, yet such differences did not manifest into a noticeable association with absolute RTD. Seemingly the lack of relationship between MTU k and RTD could be ascribed to our avoidance of a specious association mediated by the confounding influence of maximal strength.

Some measures of relative MTU k and relative RTD were significantly associated. Specifically, during the initial analysis relative MTU k was related to Vol $RTD_{0\text{-}75\%MVT}$ and relative Vol $RTD_{25\text{-}50\%MVT}$, and during the secondary analysis of 5% torque increments relative MTU k and relative RTD were associated during the between 35-55%MVT. This contrasts with the results of a previous study that found no relationship between relative

MTU k and relative RTD (Hannah and Folland 2015). However, this previous study involved ramp contractions with a constant duration and thus variable loading rates that may introduce a bias as well as males and females that exhibit a number of distinct differences that might confound the relationship. In the current study the consistent significant relationship between relative MTU k and voluntary relative RTD from 35-55%MVT suggest a genuine systematic relationship, although the explained variance was small (≤18.8%). The logical explanation for these volitional relationships was via an effect of relative MTU k on the contractile capability for relative RTD as shown by the finding that relative MTU k was also significantly related to octet relative RTD; specifically octet $RTD_{0\text{-}50\%MVT}$, octet $RTD_{25\text{-}50\%MVT}$ and subsequently from the 5% torque increments RTD from 5-50%MVT. Furthermore the torque increment over which voluntary relative RTD was associated with relative MTU k (25-55%MVT) was on average 52-93 ms into the explosive contraction, which is consistent with the steepest phase of the voluntary contractions (50-100 ms) where voluntary RTD is primarily determined by the contractile capacity for RTD (Folland et al. 2014). The finding that relative RTD was in part explained by relative MTU k, despite no corresponding relationships for absolute measures suggests an overwhelming influence of maximal strength on absolute RTD that seemingly negated any qualitative influence of MTU k. Finally, the rather limited explained variance of relative octet RTD by MTU k (≤19.4%) indicates that contractile RTD is largely determined by other factors; such as activation kinetics (Edman and Josephson 2007), contractile protein composition (Harridge et al. 1996).

The present study was thus the first attempt to investigate if there is a relationship between *in vivo* free tendon k and RTD. We found PT k was not related to voluntary or evoked knee extensor RTD. The PT exhibited minimal elongation (~3 mm) that seems unlikely to appreciably influence muscle length changes and thus force-generating potential. Also, the rate of force transmission through tendons is exceptionally rapid (Nordez et al. 2009; DeWall et al. 2014) especially for short tendons such as the PT (length ~45-50mm), and likely explains the lack of a relationship between PT k and RTD. Furthermore PT k was unrelated to MVT and it is notable that we found no relation between relative PT k and voluntary/evoked relative RTD measures. Research with isolated muscles has found the force rise time under isometric conditions of fixed sarcomere length was not appreciably faster than during muscle-tendon unit fixed-end contractions, indicating a negligible impact of tendon compliance on isometric rate of force development (Haugen and Sten-Knudsen 1987). Similarly, Kawakami and Lieber (2000) showed that the internal sarcomere shortening during

fixed-end contractions of an isolated MTU was unchanged once the proximal and distal ends of the aponeurosis where clamped, indicating that the tendon did not impact muscle internal shortening during isometric force production. Whether our results can be generalised to other MTU's where the tendon may contribute more significantly to the overall MTU stiffness is uncertain and requires further research.

Our results imply the relationships we found between relative MTU k and RTD are due to the contribution of elastic tissues proximal to the tendon. Conceptually our method reflects the elongation of distal (to the ultrasound measurement site) tendinous tissues (aponeurosis-tendon). Thus our findings regarding relative MTU k and relative RTD are presumably consequent to aponeurosis force-length characteristics. Indeed, modelling studies demonstrate that greater aponeurosis stiffness results in a reduction in its stretch that decreases muscle fibre strains (Rehorn and Blemker 2010; Rahemi et al. 2014). Lesser strain permits slower fibre shortening and possibly places fibres at longer lengths on the ascending limb of their force-length curves (Lieber et al. 1992; Lemos et al. 2008), and may facilitate a more efficient longitudinal force transmission. More favourable fibre contractile conditions for force production permitted by a stiffer aponeurosis could account for our evidence of greater relative RTD (both voluntary and evoked) being associated with a stiffer relative MTU.

In conclusion, absolute MTU and PT k were not associated with voluntary or evoked RTD, and this was also the case for relative PT k and relative RTD. However greater relative MTU k was related to higher relative voluntary and evoked RTD. These results suggest a differential influence of MTU tissue components (muscle-aponeurosis vs. tendon) on relative RTD. An overriding influence of maximal strength is presumed to negate any relationship between absolute MTU k and RTD.

CHAPTER 6

Differential tendinous tissues adaptations following explosive- vs. sustained-contraction strength training

6.1. INTRODUCTION

The mechanical stiffness (resistance to deformation) of musculotendinous tissues is integral to the effectiveness of these tissues to transmit skeletal muscle force to the bone and thus generate movement. Stiffer tissues may be protective in injury-related situations, for instance maintaining balance in response to mechanical perturbation (Onambélé et al. 2006). Moreover, stiffer tendons are ultimately stronger (Matson et al. 2012; LaCroix et al. 2013), and undergo less strain in response to a given stress, which reduces their susceptibility to damage (Ker 1988; Buchanan and Marsh 2002). Likewise, stiffer tissues may limit injury risk by providing greater joint stability and theoretically reduce the loading imposed on passive joint tissue (meniscus, cartilage, ligaments) structures (McNair et al. 1992; Wojtys et al. 2002; Karamanidis et al. 2008; Blackburn et al. 2013; Lipps et al. 2014). A particular concern is that joint injuries predispose to degenerative disease (i.e. osteoarthritis), which constitutes a substantial burden to the quality of life. In overview, increasing muscle-tendon unit (MTU) stiffness may have widespread functional and clinical implications.

MTU stiffness has been repeatedly found to increase following conventional strength training with sustained contractions (≥2 s duration with loads of >70% maximal), e.g. 16-54% after 12-14 weeks (Arampatzis et al. 2007a, 2010; Kubo et al. 2001, 2006b, 2010, 2012). Interestingly, two recent studies reported that training with brief explosive-contractions (<1-s) characterised by maximal/near maximal rate of force development produced notable increases in MTU stiffness after merely four (34%; Tillin et al. 2012) and siz weeks (62%; Burgess et al. 2007) of training. This type of explosive-contraction strength training (ECT) appears to be a highly time-efficient training regime that is also relatively non-fatiguing and thus offers the possibility of better training adherence for older adults and patient groups (e.g. osteoarthritis, tendinopathy). These preliminary results suggest that ECT may be a potent stimulus for increasing MTU stiffness. However, a comprehensive longer-term investigation is required to validate the efficacy of ECT to increase musculotendinous tissue stiffness in comparison to more conventional sustained-contraction strength training (SCT). This may permit further understanding of the influence of loading rate (high for ECT, low for SCT) and loading duration (high for SCT, low for ECT) as mechanical stimuli for increases in tissue stiffness. Our previous work has found the contrasting mechanical stimuli of ECT vs. SCT to elicit distinct functional and neural adaptations (Tillin et al. 2014; Balshaw et al. 2016), suggesting the possibility that these alternate tissue-loading patterns may induce different musculotendinous adaptations.

Whilst changes in MTU stiffness in response to strength training have received considerable attention, which component of the MTU is responsible for this adaptation is unclear. For example, whether increased MTU stiffness is accompanied by changes in stiffness of the free tendon remains opaque with the only two studies reporting a simultaneous increase (Kubo et al. 2009) or no change (Kubo et al. 2006c) in patellar tendon (PT) stiffness. These studies however had only small numbers (n=8/10) and no control group, therefore the possible contribution of changes in PT stiffness to increased quadriceps MTU stiffness in response to any form of strength training remains to be elucidated.

Changes in MTU and tendon stiffness after strength training may depend upon the increase in the size of these tissues. Muscle hypertrophy is a well-recognised characteristic response to conventional strength training regimes (Hubal et al. 2005; Folland and Williams 2007; Erskine et al. 2010) that is suggested to be coincident with an increase in aponeurosis size (Abe et al. 2012), but changes in aponeurosis size are largely unknown. A solitary report documented a 1.9% increase in vastus lateralis aponeurosis width to accompany a 10.7% increase in quadriceps muscle size after 12 weeks of dynamic SCT (Wakahara et al. 2015). Evidence for tendon hypertrophy after SCT is much more equivocal. While some studies utilising magnetic resonance imaging have detected a modest increase in tendon cross-sectional area (~4-5%: Arampatzis et al. 2007a; Kongsgaard et al. 2007; Seynnes et al. 2009; Bohm et al. 2014) that may be region specific, others have reported no change (Arampatzis et al. 2010; Kubo et al. 2012; Bloomquist et al. 2013). The responses of muscle, aponeurosis and tendon size to ECT are unknown. Given the marginal changes in tendon size after SCT, the increases in tendon stiffness (e.g.15-65%; Reeves et al. 2003; Kongsgaard et al. 2007; Seynnes et al. 2009; Malliaras et al. 2012; McMahon et al. 2013) are predominantly attributed to the nearly parallel improvement in tendon Young's modulus (stiffness relative to tendon dimensions, i.e. material stiffness), although the changes in tendon modulus after ECT are yet to be documented.

The aim of the present study was to compare the mechanical (MTU stiffness, PT stiffness and PT Young's modulus), and morphological (quadriceps femoris muscle, vastus lateralis aponeurosis and PT size) adaptations of the quadriceps MTU to 12 weeks isometric ECT vs. SCT vs. an untrained control group.

6.2. METHODS

6.2.1. Participants

Forty-two young, healthy, asymptomatic, males who had not completed lower body-strength training for >18 months and were not involved in systematic physical training were randomly assigned to ECT (n = 14), SCT (n = 15) or CON (n = 13) groups. Each participant provided written informed consent prior to completing this study, which was approved by the Loughborough University Ethical advisory committee. Baseline recreational physical activity level was assessed with the International Physical Activity Questionnaire (IPAQ, short format; Craig et al. 2003).

6.2.2. Experimental Design

Participants visited the laboratory for a familiarisation session that included measurement of muscle strength and body mass to facilitate group allocation, as well as practice isometric ramp contractions. Thereafter, two duplicate laboratory measurement sessions were conducted both pre (sessions 7-10 days apart prior to the first training session) and post (2-3 days after the last training session, and 2-3 days later). MRI scans of the thigh and knee were conducted pre (5 days prior to the start of the first training session) and post (3 days after the final training session) to measure knee extensor MTU tissues size (quadriceps femoris muscle volume, vastus lateralis [VL] aponeurosis area, patellar tendon [PT] cross-sectional area) and PT moment arm. Measurement and training sessions were performed on the same isometric apparatus. Training for ECT and SCT groups involved unilateral isometric contractions of both legs three times a week for 12 weeks (36 sessions in total), whereas CON participants attended only the measurement sessions and maintained their habitual activity. All participants were instructed to maintain their habitual physical activity and diet throughout the study. Measurement sessions involved a series of contractions in the following order: maximal voluntary contraction (MVCs to establish maximal voluntary torque [MVT]); ramp voluntary contractions of the knee extensors to establish tendinous tissue properties, and knee flexor MVCs of the dominant (preferred kicking) leg. Knee joint torque was recorded throughout contractions. Knee flexor surface electromyography was recorded during knee flexor MVCs and knee extensor ramp contractions. Ultrasound images of the VL and PT were recorded to assess tissue elongation during the ramp contractions in order to derive force-elongation relationships (to determine stiffness) of the distal MTU and PT, as well as stress-strain relationships for the PT (to determine Young's modulus). Measurement sessions were at a consistent time of day and started between 12:00-19:00 hours.

6.2.3. Training

After a brief warm-up of sub-maximal contractions of both legs, participants completed four sets of ten unilateral isometric knee-extensor contractions of each leg; with sets alternating between legs. Each set took 60 s with 2 min between successive sets on the same leg. ECT involved short, explosive contractions with participants instructed to perform each contraction "as fast and hard as possible" up to ≥80%MVT for ~1 s, and then relax for 5 s between repetitions. A computer monitor displayed RTD (10 ms time epoch) to provide biofeedback of explosive performance, with a cursor indicating the highest peak RTD achieved throughout the session, participants were encouraged to achieve a higher peak RTD with each subsequent contraction. The torque-time curve was also shown: with a horizontal cursor at 80%MVT (target torque) to ensure sufficiently forceful contractions; and on a sensitive scale baseline torque was highlighted in order to observe and correct any pre-tension or countermovement. SCT involved sustained contractions at 75%MVT, with 2-s rest between contractions. In order to control the RTD these participants were presented with a target torque trace 2-s before every contraction and instructed to match this target, which increased torque linearly from rest to 75%MVT over 1-s before holding a plateau at 75%MVT for a further 3-s. All training participants (ECT and SCT) performed three maximal voluntary isometric contractions (MVCs, see below) at the start of each training week in order to re-establish MVT and prescribe training torques. Torque data from the first session of weeks 1, 6 and 12 were analysed for all training participants (i.e. ECT and SCT) in order to quantify peak loading magnitude (peak torque), loading rate (peak RTD [$Nm.s^{-1}$], 50 ms epoch), and loading duration (defined as time >65%MVT). All repetitions from the selected training sessions were analysed and an average across the three sessions determined for these loading indices.

6.2.4. Torque Measurement

Measurement and training sessions were completed in the same custom-made isometric strength-testing chair with knee and hip angles of 115° and 126° (180° = full extension), respectively. Adjustable straps were tightly fastened across the pelvis and shoulders to prevent extraneous movement. An ankle strap (35 mm width reinforced canvas webbing) was placed ~15% of tibial length (distance from lateral malleolus to knee joint space) above the medial malleolus, and positioned perpendicular to the tibia and in series with a calibrated S-Beam strain gauge (Force Logic, Berkshire, UK). The analogue force signal was amplified (x370; A50 amplifier, Force Logic UK) and sampled at 2,000 Hz using an A/D converter

(Micro 1401; CED, Cambridge, UK) and recorded with Spike 2 computer software (CED). In offline analysis, force signals were low-pass filtered at 500 Hz using a fourth order zero-lag Butterworth filter, gravity corrected by subtracting baseline force, and multiplied by lever length, the distance from the knee joint space to the centre of the ankle strap, to calculate torque values.

6.2.5. Knee Flexor Electromyography (EMG)

Surface EMG recordings over the biceps femoris (BF) and semitendinosus (ST) were made with a wireless EMG system (Trigno; Delsys Inc, Boston, MA) were made during knee flexor MVCs and knee extensor ramp contractions. Following preparation of the skin (shaving, abrading and cleansing with alcohol) single differential Trigno standard EMG sensors (1-cm inter electrode distance; Delsys Inc, Boston, MA) were attached over each muscle using adhesive interfaces. Sensors were positioned parallel to the presumed frontal plane orientation of the underlying muscle fibres at 45% of thigh length (distance from the greater trochanter to the lateral knee joint space) measured from the popliteal crease. EMG signals were amplified at source (x300; 20-450 Hz bandwidth) before further amplification (overall effective gain x 909) and sampled at 2000 Hz via the same A/D converter and computer software as the force signal, to enable data synchronization. In offline analysis, EMG signals were corrected for the 48 ms delay inherent to the Trigno EMG system and band-pass filtered (6-500 Hz) using a fourth-order, zero-lag Butterworth digital filter.

6.2.6. Knee Extension and Flexion Maximal Voluntary Contractions

Following a brief warm-up (3 s contractions at 50% [x3], 75% [x3] and 90% [x1] of perceived maximal), participants performed 3-4 MVCs and were instructed to either ‘push as hard as possible’ (knee extension) or ‘pull as hard as possible’ (knee flexion) for 3-5 s and rest ≥ 30 s. A horizontal cursor indicating the greatest torque obtained within the session was displayed for biofeedback and verbal encouragement was provided during all MVC’s. The highest instantaneous torque recorded during any MVC was defined as MVT. During knee flexor MVCs EMG amplitude was calculated as the root mean square (RMS) of the filtered EMG signal of the BF and ST over a 500 ms epoch at knee flexion MVT (250 ms either side) and averaged across the two muscles to give knee flexor EMG_{MAX}.

6.2.7. MRI measurement of Muscle Tendon Unit Morphology and Moment Arm

T1-weighted MR (1.5 T Signa HDxt, GE) images of the dominant leg (thigh and knee) were acquired in the supine position at a knee angle of 163° (due to constraints in knee coil size) and analysed using OsiriX software (Version 6.0, Pixmeo, Geneva, Switzerland). Using a receiver 8-channel whole body coil, axial images (time of repetition/time to echo 550/14, image matrix 512 x 512, field of view 260 x 260 mm, pixel size 0.508 x 0.508 mm, slice thickness 5 mm, inter-slice gap 0 mm) were acquired from the anterior superior iliac spine to the knee joint space in two overlapping blocks. Oil filled capsules placed on the lateral side of the thigh allowed alignment of the blocks during analysis. The quadriceps femoris (QF) muscles (vastus lateralis [VL] vastus intermedius [VI], vastus medialis, and rectus femoris) were manually outlined in every third image (i.e. every 15 mm) starting from the most proximal image in which the muscle appeared. The volume of each muscle was calculated using cubic spline interpolation (GraphPad Prism 6, GraphPad Software, Inc.). Total QF volume (QUADSvol) was the sum of the individual muscle volumes. As previously described (Abe et al. 2012), the deep aponeurosis of the VL muscle was defined as the visible dark black segment between the VL and VI muscles in the thigh MRI images. The tangent line of the VL muscle and the dark black segment in each cross-sectional image was traced manually. The length of the black line was defined as VL aponeurosis width and was measured on every third image (i.e. every 15 mm), starting in the most distal image were the aponeurosis was visible. Width measures were plotted against aponeurosis length (distance between most proximal and distal image where the aponeurosis was visible). The area under a spline curve fitted to data points was defined as the VL aponeurosis area (Apon Area).

Immediately after thigh imaging, a lower extremity knee coil was used to acquire axial (time of repetition/time to echo 510/14, image matrix 512 x 512, field of view 160 x 160 mm, pixel size 0.313 x 0.313, slice thickness 2 mm, inter-slice gap 0 mm) and sagittal images (time of repetition/time to echo 480/14, image matrix 512 x 512, field of view 160 x 160 mm, pixel size 0.313 x 0.313, slice thickness 2 mm, inter-slice gap 0 mm) of the knee joint. Contiguous axial images spanned patellar tendon length, which during analysis, were reconstructed to be aligned perpendicular to the line of action of the patellar tendon. Images spanned from 2 cm superior to the patella apex to 2 cm inferior to the tendon tibial insertion (Figure 6.1 A). Patellar tendon CSA was measured on each contiguous image along the tendon's length (first image where the patellar was no longer visible to the last image before the tibial insertion). Images, viewed in greyscale, were sharpened (Figure 6.1 B) and the perimeter manually

outlined (Figure 6.1 C). Mean tendon CSA (mm^2) was defined by the average of all measured images (14 to 24 images). Sagittal plane images were used to determined patellar tendon moment arm, the perpendicular distance from the patellar tendon line of action to the tibio-femoral contact point, which was the midpoint of the distance between the tibio-femoral contact points of the medial and lateral femoral condyles (Figure 6.2).

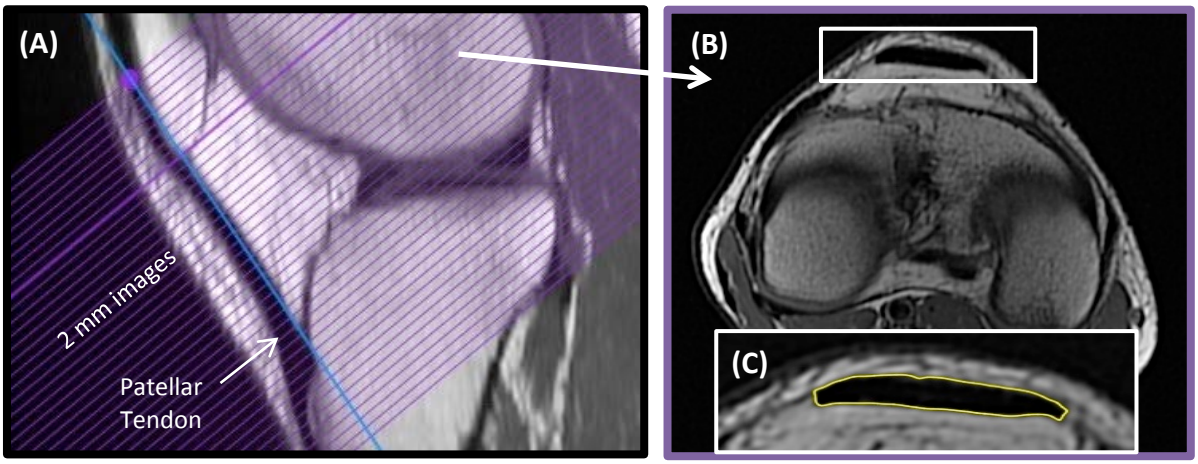

Figure 6.1. Patellar Tendon (PT) Cross-Sectional Area (CSA, mm^2) measurement. Axial MRI images spanning tendon length in contigous 2 mm thick slices aligned perpendicular to the tendon (A). In each axial image (e.g. B), the perimeter of the PT which was manually outlined (C).

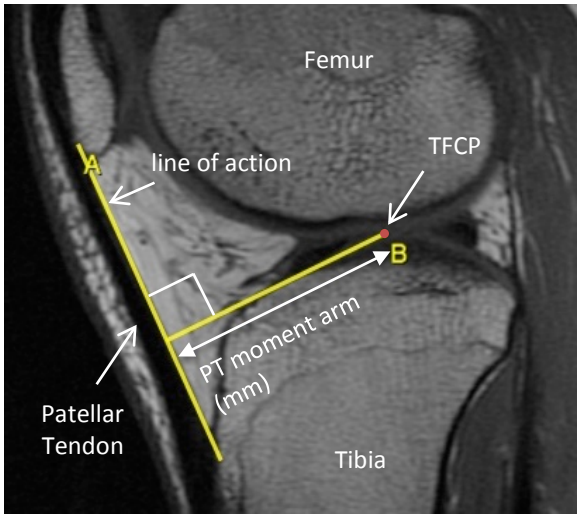

Figure 6.2. Sagittal MRI image of the knee joint: Patellar tendon (PT) moment arm was defined as the perpendicular distance between the tendon line of action and the tibio-femoral contact point (TFCP).

6.2.8. Ramp Contractions for Determination of Tissue Stiffness

Tissue stiffness was derived from synchronous recordings of torque and tissue elongation (see below, corrected for passive tissue displacement via video recording of knee joint changes) during isometric knee extension ramp contractions (experimental set-up; Figure 6.3). Participants completed two sub-maximal practice ramp contractions prior to five maximal attempts with 90-s rest between contractions. Prior to each ramp contraction participants were shown a target torque-time trace on a computer monitor that increased at a constant gradient (50 $Nm.s^{-1}$ loading rate) from zero up to MVT. They were instructed to match the target trace as closely as possible for as long as possible (i.e. up to MVT), and real-time torque was displayed over the target torque-time trace for feedback. The preceding knee extensor MVCs and sub-maximal contractions were considered sufficient to elicit tissue preconditioning. The three most suitable ramp contractions, according to highest peak torque, the closeness to the target loading rate and ultrasound image clarity, were analysed and measurements averaged across these three contractions.

6.2.9. Measurement of Tissue Elongation

Video images from two ultrasound machines and one video camera were captured to obtain tissue and knee joint displacements during ramp contractions. An ultrasound probe (7.5 MHz linear array transducer, B-mode, scanning width 60mm and depth 50 mm; Toshiba Power Vision 6000, SSA-370A: Otawara-Shi, Japan) was fitted into a custom made high-density foam cast that was strapped to the lateral aspect of the thigh with the mid-point of the probe positioned at ~50 % thigh length. The probe was aligned so the fascicles inserting into the vastus lateralis (VL) muscle deep aponeurosis could be visualized at rest and during contraction. An echo-absorptive marker (multiple layers of transpore medical tape) was placed beneath the ultrasound probe to provide a reference for any probe movement over the skin. Another ultrasound probe (5-10 MHz linear array transducer, B-mode, scanning width 92 mm and depth 65 mm, EUP-L53L; Hitachi EUB-8500) was fitted into a custom made high-density foam cast that was held firmly over the anterior aspect of the knee with the probe aligned longitudinal to the patellar tendon such that the patella apex and insertion of the posterior tendon fibres at the tibia could be visualized at rest and throughout the contraction. The ultrasound machines were interfaced with the computer collecting torque data in Spike 2 and the video feeds were recorded synchronously with torque using Spike 2 video capture at 25 Hz. During off-line analysis tissue elongation was tracked frame-by-frame using public-domain semi-automatic video analysis software: Tracker, version 4.86

(www.cabrillo.edu/~dbrown/tracker). VL fascicle deep aponeurosis cross point displacement relative to the skin marker provided a measure of muscle-tendon unit (MTU) elongation (Figure 3). Patellar tendon elongation was determined by the longitudinal displacement of the patella apex and the tendon tibia insertion (Figure 6.3). The distal insertion of the patellar tendon was not monitored for the purpose of estimating overall MTU elongation To enable correction of tissue displacement due to joint angle changes during ramp contractions individual ratios of tissue displacement relative to joint angular displacement (mm/°) were obtained from passive movements (i.e. plotting the tissue displacement-knee joint angle relationship). This ratio was used to determine tissue displacement resulting from knee angle change during ramp contractions, which was subsequently subtracted from total measured displacement. Corrections were only applied to aponeurosis displacement. Tendon elongation under passive conditions was deemed negligible. Passive movements were conducted prior to the ramp contractions. Participants were instructed to completely relax as their knee was moved through 90 to 130°. During passive movements and ramp contractions, knee joint angle (angle between visible markers placed on the greater trochanter, lateral knee joint space and lateral malleolus) was derived from sagittal plane video recorded using a camera mounted on a tripod positioned (1.5 m) perpendicular to the strength-testing chair. The video camera was interfaced with a computer and recorded using spike 2 video capture at 25 Hz (simultaneously with force, EMG, and ultrasound images during the ramp contractions) and analysed via Tracker software.

6.2.10. Calculation of Tendon Force

PT force was calculated by dividing external absolute knee extensor torque by the patellar tendon moment arm length. Direct measures of moment arm where acquired at rest from MRI images as indicated above (*MRI measurement*). Due to constraints in the size of the knee coil, sagittal images were acquired in an extended knee position (~163°). Moment arm length for any specific knee angle measured at rest or during ramp contraction was estimated from previously published data fitted with a quadratic function (Kellis and Baltzopoulos 1999), scaled to each participant's measured moment arm length at 163°. Absolute internal knee extensor torque was given by summing net knee extension torque and the estimated knee flexor co-contraction torque. Antagonist knee flexor torque was estimated by expressing the average knee flexor EMG amplitude (RMS 50 ms moving window) during ramp contractions relative to the knee flexor EMG_{MAX} and multiplying by the knee flexor MVT (assuming a

linear relationship between EMG amplitude and torque). During analysis, torque and EMG amplitude were down-sampled to 25 Hz to match the ultrasound video frequency.

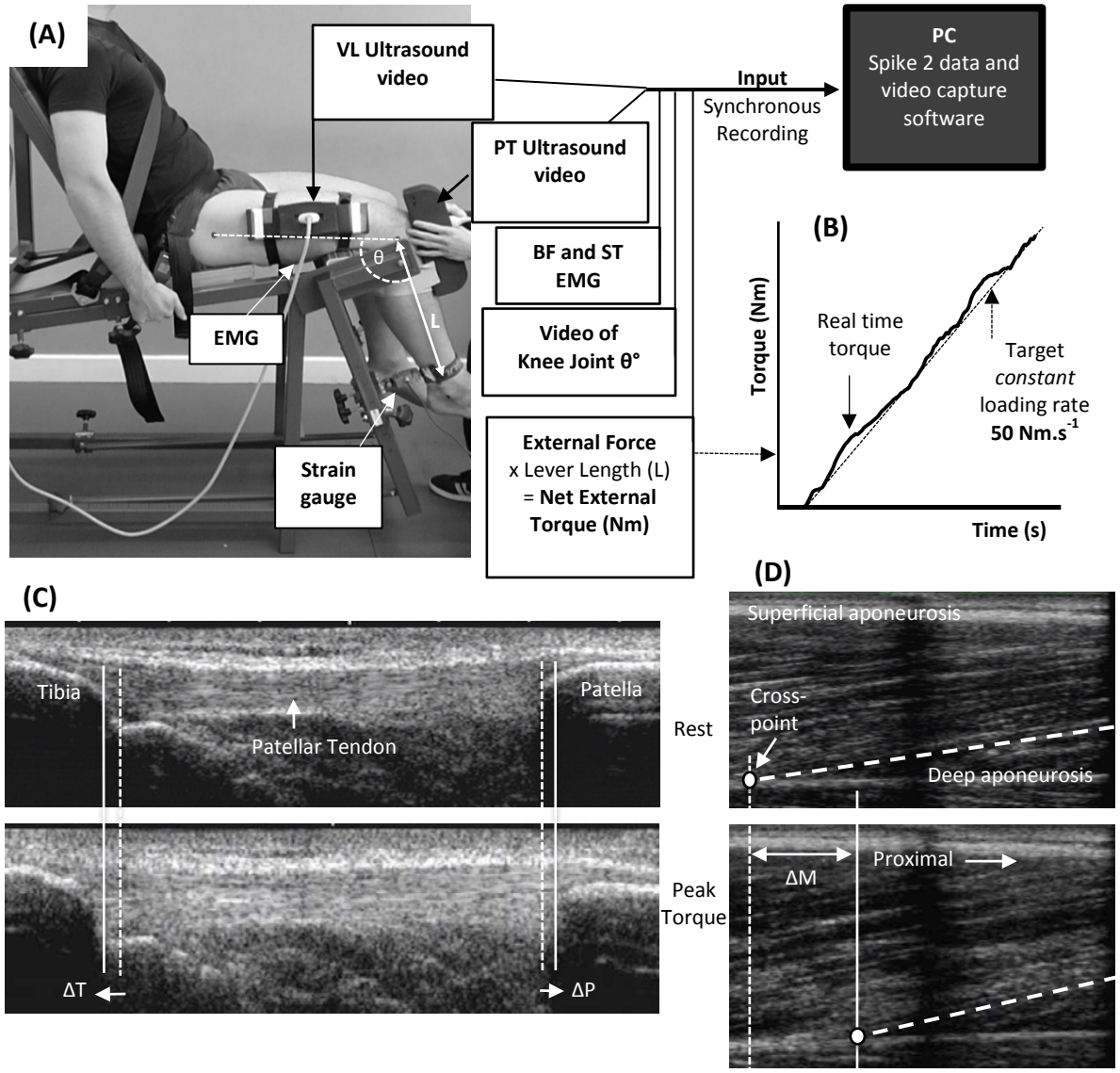

Figure 6.3. The experimental set-up and ultrasound imaging during ramp contractions. Participants were tightly fastened to a rigid isometric strength-testing chair with resting knee and hip angles of 115 and 126° respectively (A). Unilateral knee extensor torque, video of knee joint angle, antagonist muscle (biceps femoris [BF], semitendinosus [ST]) surface electromyography and ultrasound video images were recorded during constant-loading rate isometric ramp knee extensor contractions (example in B). Ultrasound images are of the patellar tendon (PT, C) and vastus lateralis (VL, D) muscle at rest (top) and at peak ramp torque (bottom) and indicate the measurement of PT (tibia-patellar displacement, ΔT + ΔP) and MTU (VL deep aponeurosis fascicle-cross point proximal displacement [ΔM] relative to the echo-absorptive skin marker) elongation.

6.2.11. Calculation of Tissue Stiffness and Tendon Young's Modulus

For each of the three best ramp contractions analysed, MTU (corrected for passive tissue displacement) and PT elongation were plotted against total tendon force (corrected for antagonist force). Force-elongation plots were fitted with a second-order polynomial. Both pre and post-training, tissue stiffness for each individual was calculated as the slope of the force-elongation curve over an absolute tendon force range that equated to 70-80% of pre-training MVT. Tendon stress was obtained by dividing tendon force by mean tendon CSA. Tendon strain was the percentage tendon displacement relative to the resting tendon length. Individual PT stress-strain curves were plotted and PT Young's modulus calculated for each individual as the slope of the stress-strain curve derived over a stress range that corresponded to 70-80% of pre-training MVT. The stiffness and modulus measured from each of the three analysed ramps were averaged to give a representative value.

6.2.12. Statistical Analysis

Data are reported as mean ± standard deviation (SD). Statistical significance tests were conducted using SPSS Version 20.0 (IBM Corp., Armonk, NY), and significance was accepted at $P<0.05$. One-way analysis of variance (ANOVA) tests were conducted on all pre-training variables to determine whether baseline differences existed between groups. Unpaired t-tests were used to assess differences in training variables (loading rate, duration, and magnitude) between ECT and SCT. Within-group changes (absolute values) were evaluated with paired t-tests. Comparison of between-group adaptations to the intervention were initially assessed with repeated measures analysis of variance (ANCOVA; group [ECT vs. SCT vs. CON] x time [pre vs. post]) with corresponding pre-training values used as covariates. When group x time interaction effects displayed $P<0.05$, least significant difference (LSD) post-hoc pairwise comparisons (with Holm-Bonferroni adjustment applied to the P-values adjustment applied to the P-values [LSD_{HB}]) of absolute changes (pre to post) between groups (i.e. ECT vs. SCT, ECT vs. CON, SCT vs. CON) were performed to delineate specific group differences. Effect sizes (ES; specifically Hedges g, incorporating correction for small sample bias; Lakens 2013) were calculated for within-group changes and between-group comparisons. Effect size magnitude was classified as <0.2 = "trivial", 0.2-<0.5 = "small", 0-5-0.8 = "moderate", >0.8 = "large" (Cohen 1988). The reproducibility of measurements (all muscle and tendon variables) was defined by the average within participant co-efficient of variation (CVw, %) calculated between pre-post measurements in the control group.

6.3. RESULTS

6.3.1. Group Characteristics at Baseline

At baseline, no differences (ANOVA, $P \geq 0.579$) were observed between groups for age (ECT 25 ± 2; SCT 25 ± 2; CON 25 ± 3 years) height (ECT 174 ± 7; SCT 175 ± 8; CON 176 ± 6 cm) body mass (ECT 71 ± 10; SCT 70 ± 8; CON 72 ± 7 kg) or habitual physical activity level (ECT 1971 ± 1077; SCT 2084 ± 1256; CON 2179 ± 1588 MET minutes per week). Likewise, ANOVA showed similar MVT ($P = 0.304$), MTU stiffness ($P = 0.328$), PT stiffness ($P = 0.215$), PT Young's modulus ($P = 0.184$), QUADSvol ($P = 0.508$), VL apon area ($P = 0.815$), and PT mean CSA ($P = 0.073$).

6.3.2. Reproducibility of Measurements

The reproducibility of pre and post measures for the CON group over the 12-week intervention period was excellent for MVT (CVw 2.9%) and MTU stiffness (3.9%), and very good for PT stiffness (7.2%) and Young's modulus (6.8%). Excellent reproducibility was also observed for muscle volume (1.7%), aponeurosis area (2.7%) and PT CSA (2.9%).

6.3.3. Training Characteristics for ECT vs. SCT

ECT involved a far greater, ~6.2-fold higher, loading rate per repetition than SCT (8.9 ± 1.4 vs. 1.4 ± 0.1 $\%MVT.s^{-1}$, unpaired t-test $P < 0.001$). Alternatively, loading duration (time >65%MVT) per training session was substantially longer during SCT than ECT (106 ± 12 vs. 8 ± 8 s, unpaired t-test $P < 0.001$). Peak loading magnitude was slightly greater in ECT than SCT (81 ± 4 vs. 75 ± 2% MVT, unpaired t-test $P < 0.001$).

6.3.4. Muscle-Tendon Unit Strength and Size (Tables 6.1 and 6.3, Figure 6.4)

MVT increased after ECT (ES = 1.15 "large", paired t-test $P < 0.001$) and SCT (ES = 1.11 "large", $P < 0.001$), but not following CON (ES = 0.01 "trivial", $P = 0.868$). The absolute increase in MVT was greater than CON for both ECT (ES = 1.90 "large", LSD_{HB} $P < 0.001$) and SCT (ES = 2.64 "large", LSD_{HB} $P < 0.001$), and 45% larger after SCT than ECT (ES = 0.75 "moderate", LSD_{HB} $P = 0.032$).

QUADSvol increased after SCT (ES = 0.47 "small", paired t-test $P = 0.001$) but not following ECT (ES = 0.17, $P = 0.195$) or CON (ES = 0.04, "trivial", $P = 0.661$). There was a group x time effect for QUADSvol (Table 6.1), with the absolute change (Figure 6.4 A) after SCT being greater than CON (ES = 1.12, "large", LSD_{HB} $P = 0.021$), but not statistically

different to ECT (P = 0.074). Absolute changes in QUADSvol after ECT were not greater than CON (ES = 0.31 "small", LSD_{HB} P = 0.479).

VL apon area increased after SCT (ES = 0.32 "small", paired t-test P = 0.015), and also tended to increase after ECT (ES = 0.35 "small", P = 0.060), while remaining unchanged in CON (ES = 0.11 "trivial", P = 0.408). However there was no group x time effect for VL apon area (Table 6.1; Figure 6.4 B).

PT CSA showed a small decrease in CON (ES = 0.27 "small", paired t-test P = 0.028), and after ECT (ES = 0.29 "small", P = 0.012), but was unchanged following SCT (ES = 0.03, "trivial", t-test P = 0.746). However, there was no group x time effect for PT CSA (Table 6.1; Figure 6.4 C).

6.3.5. Tissue Mechanical Properties (Tables 6.2 and 6.3)

6.3.5.1. Patellar Tendon (Figures 6.5, 6.6 and 6.7)

PT elongation at 80% pre-training MVT was less after ECT (ES = 0.75 "moderate", paired t-test P = 0.011; Figure 6.5 A), but was unchanged after SCT (ES = 0.24 "small", P = 0.246) and CON (ES = 0.15 "small", P = 0.331). No group x time effect was observed (Table 6.2).

PT strain (relative elongation) at 80% pre training MVT was also less after ECT (ES = 0.54 "moderate", paired t-test P = 0.01; Figure 6.5 B), but was unchanged after SCT (ES = 0.11 "trivial", P = 0.542) and CON (ES = 0.15 "trivial", P = 0.263). However, there was no group x time effect (Table 6.2).

PT stiffness increased after both ECT (ES = 0.88 "large", paired t-test P = 0.002; 20%) and SCT (ES = 0.74 "moderate", P = 0.019; 16%), but was unchanged in CON (ES = 0.07 "trivial", P = 0.711). Group comparison showed changes (Figure 6.7 A) in both ECT (ES = 1.18 "large", LSD_{HB} P = 0.030) and SCT (ES = 0.73 "moderate", LSD_{HB} P = 0.034) were greater than CON. Positive effects of ECT and SCT on PT stiffness were similar (ES = 0.21, "small", LSD_{HB} P = 0.830).

PT Young's modulus increased after ECT (ES = 1.05 "large", paired t-test P = 0.0004), and SCT (ES = 0.57 "moderate", P = 0.017), and was unchanged in CON (ES = 0.05, "trivial", P

= 0.637). Group comparison showed absolute changes (Figure 6.7 B) were greater in both ECT (ES = 1.38 "large", LSD_{HB} P = 0.012) and SCT (ES = 0.75 "large", LSD_{HB} P = 0.042) than CON. Positive effects of ECT and SCT on PT Young's modulus were similar (ES = 0.21, "small", LSD_{HB} P = 0.830).

6.3.5.2. Muscle-Tendon Unit (Figures 6.8 and 6.9)

MTU elongation at 80% pre-training MVT increased after ECT (ES = 0.89 "large", paired t-test P = 0.003; Figure 6.8 A) but was unchanged after SCT (ES = 0.09 "trivial", P = 0.428) and CON (ES = 0.06 "trivial", P = 0.637). Consequently, there was a group x time interaction effect (P = 0.020; Table 6.1), with changes in ECT being greater than SCT (ES = 1.23 "large", LSD_{HB} P = 0.021) and tended to be greater than CON (ES = 0.80 "large", LSD_{HB} P = 0.098; Figure 6.9 A).

MTU stiffness increased after SCT (ES = 0.50 "moderate", paired t-test P = 0.005) but was unchanged after ECT (ES = 0.02 "trivial", P = 0.938) and CON (ES = 0.03 "trivial", P = 0.695). Consequently, the absolute change in MTU stiffness (Figure 6.9 B) following SCT was greater than ECT (ES = 0.94 "large", LSD_{HB} P = 0.015) and CON (ES = 1.12, "large", LSD_{HB} P = 0.016), while ECT vs. CON changes were equivalent (ES = 0.02 "trivial", LSD_{HB} P = 0.846).

Table 6.1. Muscle-tendon unit maximal strength and size, and patellar tendon moment arm pre and post intervention period in the explosive-contraction strength training (ECT), sustained contraction strength training (SCT) and untrained control (CON) groups.

	ECT		SCT		CON		Two-way ANCOVA Interaction Effect (P-value)
	Pre	Post	Pre	Post	Pre	Post	
MVT, Nm	234 ± 27	273 ± 36***$_{L}$	237 ± 49	293 ± 47***$_{L}$	255 ± 50	256 ± 58	<0.001
QF Volume, cm^3	1778 ± 244	1827 ± 277	1820 ± 273	1967 ± 316***$_{S}$	1897 ± 282	1909 ± 271	0.018
VL Apon area, cm^2	137.1 ± 16.4	143.1 ± 15.2~$_{S}$	136.3 ± 26.1	144.3 ± 21.2*$_{S}$	138.8 ± 13.7	140.5 ± 15.7	0.242
PT mean CSA, mm^2	98.7 ± 10.0	95.9 ± 8.3*$_{S}$	97.3 ± 12.9	97.7 ± 13.0	106.5 ± 9.0	103.6 ± 10.7*$_{S}$	0.129
PT length, mm	47.5 ± 5.7	47.2 ± 5.7	45.4 ± 5.5	45.1 ± 5.5	47.1 ± 5.7	46.6 ± 6.8	0.829
PT moment arm, mm	40.6 ± 2.4	40.7 ± 2.3	42.4 ± 2.9	42.5 ± 2.9	41.2 ± 2.9	41.3 ± 2.9	0.902

Data are mean ± SD. PT MA = moment arm. ECT n = 13; SCT, n = 15 and CON, n = 13.Within-group change: ***Different to pre, P≤0.001, **P<0.01, *P<0.05. ~P=0.051-0.08. Within-group effect size: S = "small" (0.2-0.5), M = "moderate", (>0.5-0.8). Interaction effect: group by time.

Table 6.2. Patellar Tendon (PT) and Muscle-tendon unit (MTU) mechanical properties pre and post intervention period in the explosive-contraction strength training (ECT), sustained contraction strength training (SCT) and untrained control (CON) groups.

	ECT		SCT		CON		Two-way ANCOVA Interaction Effect (P-value)
	Pre	Post	Pre	Post	Pre	Post	
PT							
Elongation at 80% pre-MVT, mm	3.17 ± 0.52	2.82 ± 0.42**$_{M}$	3.23 ± 0.54	3.07 ± 0.64	3.12 ± 0.62	3.02 ± 0.63	0.270
Stiffness, $N.mm^{-1}$	2605 ± 446	3122 ± 632**$_{L}$	2835 ± 444	3239 ± 575*$_{M}$	2534 ± 501	2569 ± 413	0.018
Strain at 80% pre MVT, %	6.8 ± 1.7	6.0 ± 1.1**$_{M}$	7.2 ± 1.4	6.9 ± 1.7	6.6 ± 1.1	6.4 ± 1.1	0.093
Young's Modulus, GPa	1.23 ± 0.18	1.49 ± 0.27***$_{L}$	1.32 ± 0.27	1.51 ± 0.36*$_{M}$	1.14 ± 0.27	1.16 ± 0.20	0.012
MTU							
Elongation at 80% pre-MVT, mm	15.0 ± 2.6	17.4 ± 2.2 **$_{L}$	16.9 ± 4.6	16.4 ± 5.3	16.3 ± 5.7	16.6 ± 4.4	0.020
Stiffness, $N.mm^{-1}$	592 ± 118	595 ± 101	560 ± 177	687 ± 285**$_{M}$	507 ± 130	511 ± 116	0.007

Data are mean ± SD. Elongation and Strain at 80% pre-training MVT. ECT n = 13; SCT, n =14/15 for MTU/PT and CON, n = 13/12 for MTU/PT. ***Different to pre, P≤0.001, **P<0.01, *P<0.05. Effect size: S "small" (0.2-0.5), M = "moderate", (>0.5-0.8). Interaction effect: group by time.

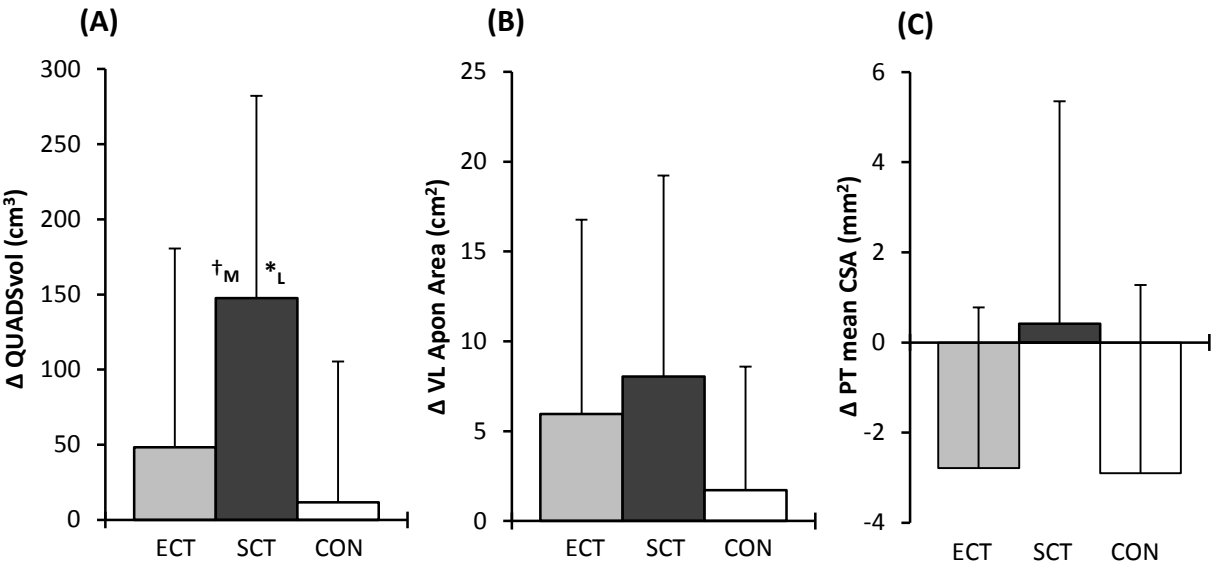

Figure 6.4. Pre to post absolute changes (Δ) in (**A**) Quadriceps Femoris muscle volume (QUADSvol), (**B**) vastus lateralis aponeurosis area (VL Apon Area), and (**C**) Patellar Tendon mean cross-sectional area (PT mean CSA) in response to isometric knee extension explosive-contraction (ECT, n = 13) or sustained-contraction strength training (SCT, n = 14) interventions and in an untrained control (CON) group (n = 13). Symbols indicate group differences: *SCT vs. CON, P<0.05; †ECT vs. SCT, trend 0.05<P<0.09. Letter denotes effect size magnitude: M = moderate (0.5-0.8), L = large (>0.8). Data are mean ± SD.

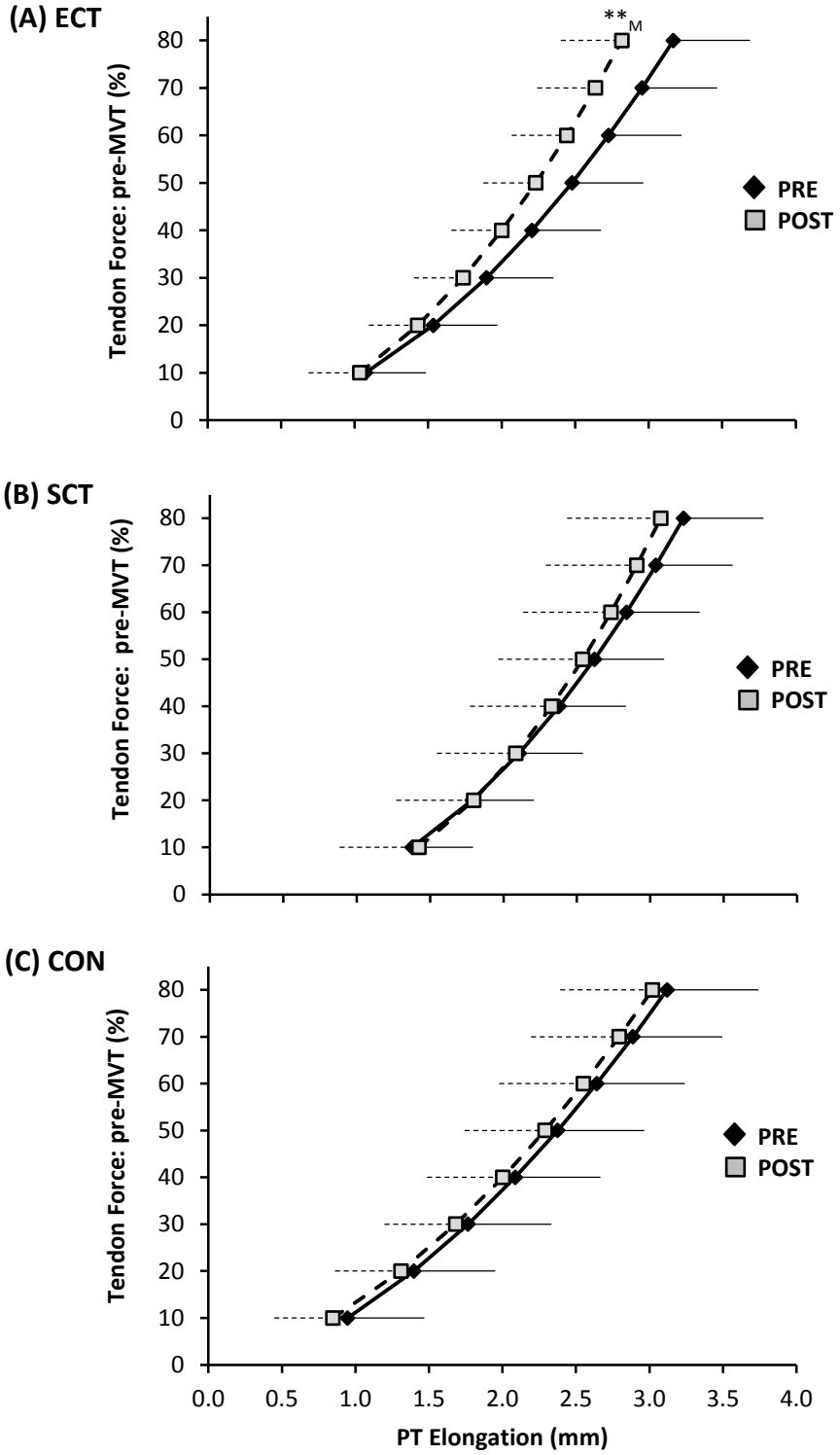

Figure 6.5. Tendon force-patellar tendon (PT) elongation relationships pre (black diamonds) and post (grey squares) 12 weeks isometric knee extension explosive-contraction strength training (ECT, n = 13 [A]) or sustained-contraction strength training (SCT, n = 15 [B]) interventions and in an untrained control group (CON, n = 12 [C]). Data are group mean and SD. Data points are plotted at the elongation corresponding to tendon forces at 10% increments of pre-training maximal voluntary torque (MVT). Within-group effect, PT elongation at 80% pre-training MVT, different to pre **P<0.01. Letter denotes effect size magnitude: M = moderate (>0.5-0.8).

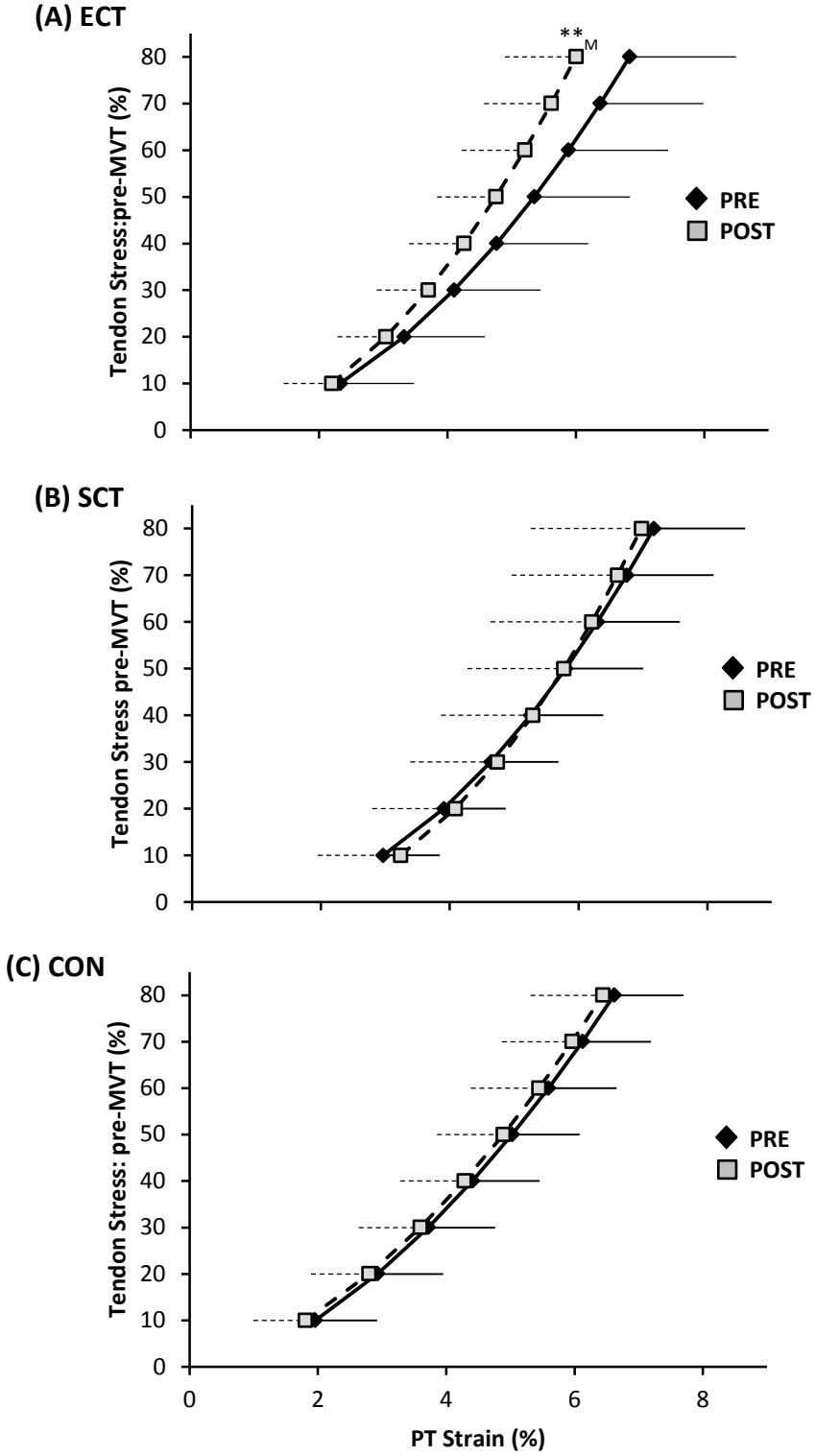

Figure 6.6. Tendon stress-patellar tendon (PT) strain relationships pre (black diamonds) and post (grey squares) 12 weeks isometric knee extension explosive-contraction strength training (ECT, n = 13 [A]) or sustained-contraction strength training (SCT, n = 15 [B]) interventions and in an untrained control group (CON, n = 12 [C]). Data are group mean and SD. Data points are plotted at the elongation corresponding to tendon forces at 10% increments of pre-training maximal voluntary torque (MVT). Within-group effect, PT elongation at 80% pre-training MVT, different to pre **P<0.01. Letter denotes effect size magnitude: M = moderate (>0.5-0.8).

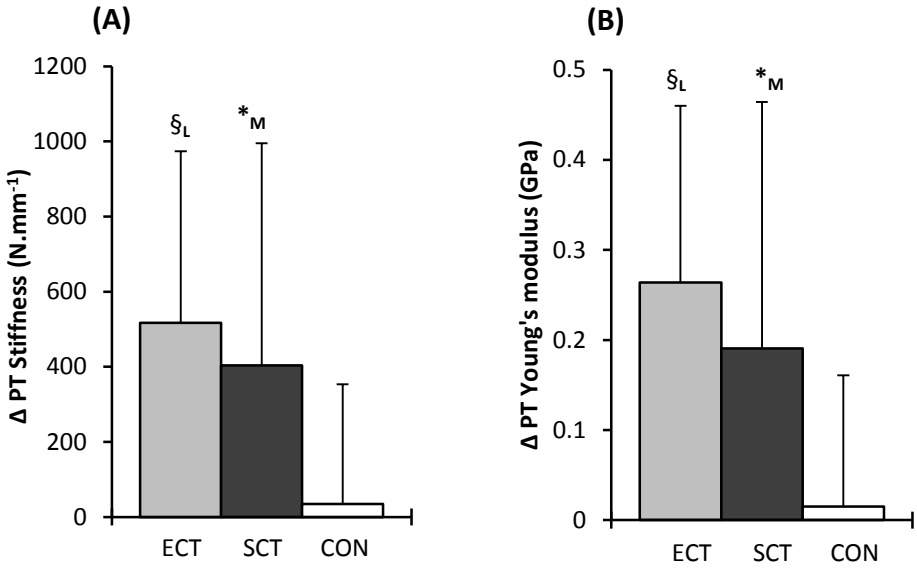

Figure 6.7. Pre to post absolute changes (Δ) in (A) Patellar Tendon (PT) stiffness and (B) PT Young's Modulus, in response to isometric knee extension explosive-contraction strength training (ECT, n = 13) or sustained-contraction strength training (SCT, n = 15) interventions and in an untrained control (CON) group (PT n = 12). Symbols indicate group differences: **§**ECT vs. CON P<0.05; *SCT vs. CON, P<0.05; †ECT vs. SCT P<0.05. Letter denotes effect size magnitude: M = moderate (>0.5-0.8), L = large (>0.8). Data are mean ± SD.

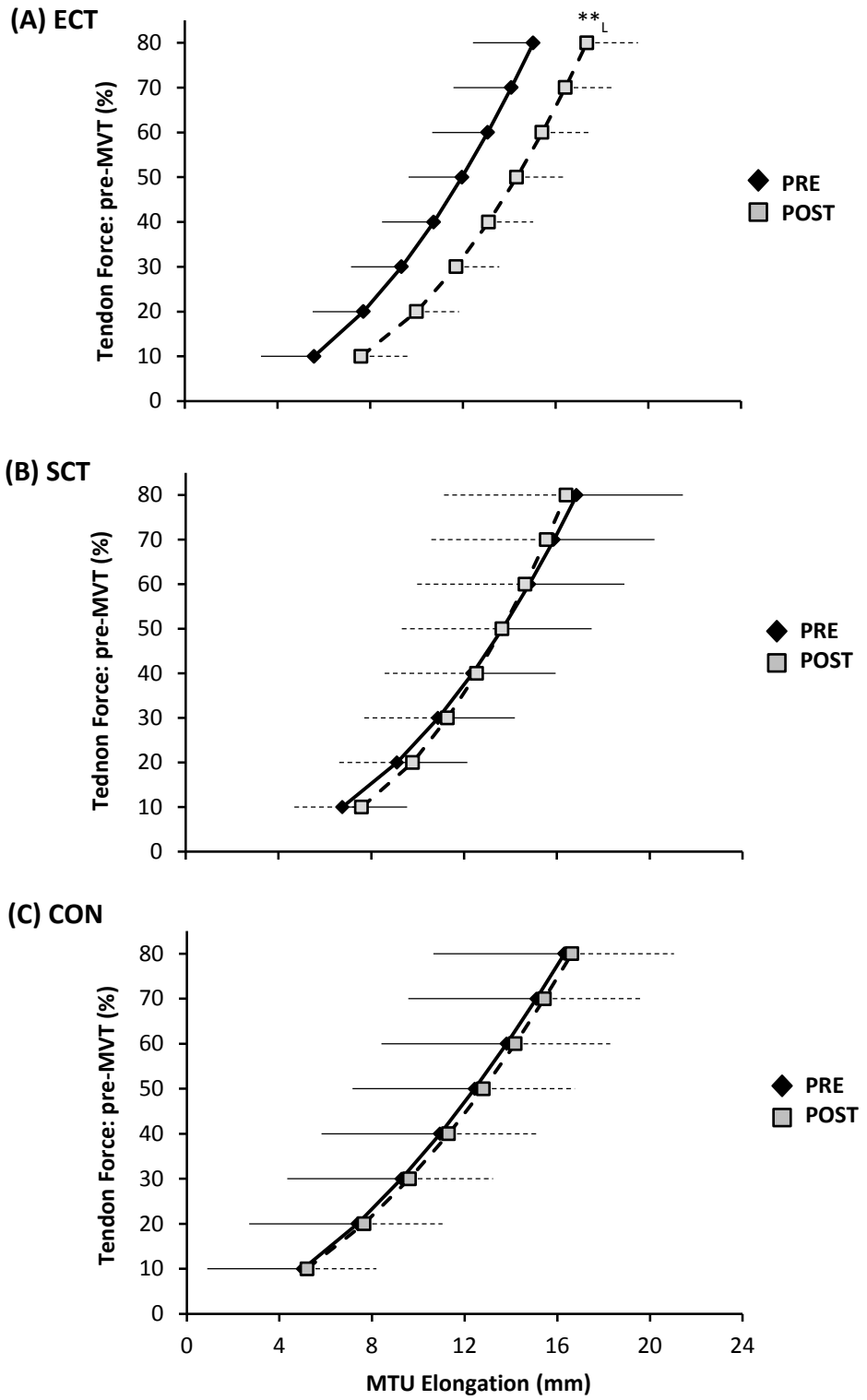

Figure 6.8. Tendon force-muscle-tendon unit (MTU) elongation relationships pre (black diamonds) and post (grey squares) 12 weeks isometric knee extension explosive-contraction strength training (ECT, n = 13 [A]) or sustained-contraction strength training (SCT, n = 15 [B]) interventions and in an untrained control group (CON, n = 13 [C]). Data are group mean and SD. Data points are plotted at the elongation corresponding to tendon forces at 10% increments of pre-training maximal voluntary torque (MVT). Within-group effect, MTU elongation at 80% pre-training MVT, different to pre **P<0.01. Letter denotes effect size magnitude: L = Large (>0.8).

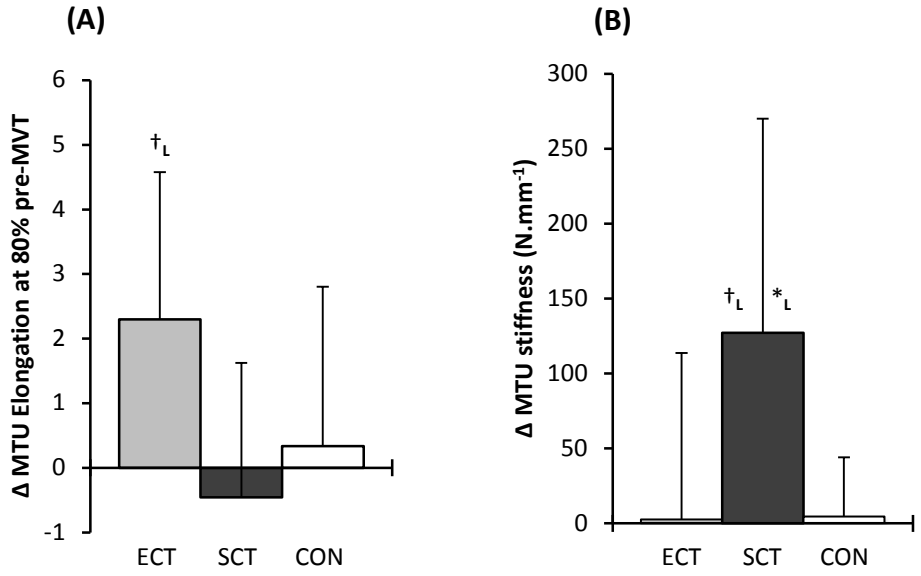

Figure 6.9. Pre to post absolute changes (Δ) in (A) knee extensor muscle-tendon unit (MTU) elongation at pre-training MVT and (B) MTU stiffness (PT) stiffness, in response to isometric knee extension explosive-contraction strength training (ECT, n = 13) or sustained-contraction strength training (SCT, n = 14) interventions and in an untrained control (CON) group (n = 13). Symbols indicate group differences: †ECT vs. SCT P<0.05, *SCT vs. CON, P<0.05; †ECT vs. SCT P<0.05. Letter denotes effect size magnitude: L = large (>0.8). Data are mean ± SD.

Table 6.3. Summary of within-group changes and between-group differences from pre to post training in maximal voluntary strength, muscle-tendon unit hypertrophy and tissue stiffness indices after explosive-contraction strength training, sustained-contraction strength training, and control interventions.

	Within-group changes			Between-group differences
	ECT	**SCT**	**CON**	
Maximal Strength				
MVT, Nm	↑ +17%	↑ +24%	↔	ECT & SCT ↑ > CON
Hypertrophy				
QUADSvol, cm^3	↔	↑ +8%	↔	SCT ↑ > CON
VL Apon Area, cm^2	↔	↑ +7%	↔	-
PT mean CSA, mm^2	↓ -3%	↔	↓ -3%	-
Tissue Stiffness Indices				
PT Elongation at 80% pre-MVT, mm	↓ -10%	↔	↔	-
PT Strain at 80% pre-MVT, %	↓ -11%	↔	↔	-
PT Stiffness, $N.mm^{-1}$	↑ +20%	↑ +16%	↔	ECT & SCT ↑ > CON
PT Young's Modulus, GPa	↑ +22%	↑ +16%	↔	ECT & SCT ↑ > CON
MTU elongation at 80% pre-MVT	↑ +17%	↔	↔	ECT ↑ > SCT
MTU Stiffness, $N.mm^{-1}$	↔	↑ +21%	↔	SCT ↑ > ECT & CON

The directions of the group changes are shown by ↑ or ↑ with the percentage change in the group mean also shown. Non-significant within-/between changes are indicated by ↔/-. ECT, explosive-contraction strength training; SCT, sustained-contraction strength training; CON, control.

6.4. DISCUSSION

The present study compared the efficacy of 12 weeks of ECT vs. SCT to increase PT stiffness and Young's modulus and knee extensor MTU stiffness, as well as elicit tissue (muscle, aponeurosis, and tendon) hypertrophy. Both ECT and SCT similarly increased PT stiffness and modulus (20 and 22% vs. 16 and 16%) whereas only SCT increased MTU stiffness (21.3%). Likewise only SCT increased QUADSvol (8%). A within group increase in VL apon area was also observed after SCT, although this change was not statistically greater to either ECT or CON. Finally, neither ECT nor SCT induced tendon hypertrophy.

SCT produced a distinct increase in tendon stiffness, as has been commonly reported in response to similar conventional SCT regimes (see Wiesinger et al. 2015 review; mean change ~27%). Uniquely we found ECT was equally effective as SCT for promoting tendon adaptation; increases in PT stiffness were similar after ECT (+20%) and SCT (+16%), and both increased by more than CON, with both interventions increasing the gradient of the force-elongation relationship, particularly at high forces. However, neither training intervention induced PT hypertrophy. Thus the increases in PT stiffness were independent of tendon size adaptations. While no previous studies have examined if ECT can induce changes in tendon size, our finding of no change in PT mean CSA with SCT is in agreement with previous studies who equally reported increased tendon stiffness in the absence of altered tendon CSA after a comparable length period of SCT (Arampatzis et al. 2010; Kubo et al. 2012; Bloomquist et al. 2013). In contrast, others have reported small increases in tendon CSA following similar strength training regimes (Arampatzis et al. 2007a; Kongsgaard et al. 2007; Seynnes et al. 2009; Bohm et al. 2014). Though reasons for the discrepant findings are unclear, with regards to our PT CSA data, it is unlikely that our measurements simply failed to detect a change. Pre and post tendon CSA analysis was performed blinded by a single investigator, with precise measurements of tendon CSA made along the full length of the tendon from MRI images, with excellent reproducibility of the measurement (~3% pre-post CVw in CON).

A functionally relevant change in tendon size would manifest from collagen/extracellular matrix protein synthesis and accretion. In support of our findings of no effect of either ECT or SCT on tendon CSA, a couple of studies indicate that resistance exercise may not stimulate *in vivo* production of collagen/or extracellular matrix proteins. For instance, an acute bout of resistance exercise (dynamic knee extension at 70%-RM, 3 x 10 repetitions)

was shown to have no effect on collagen type I messenger RNA expression 24 hours post exercise (Sullivan et al. 2009). Also, 12 weeks of isoinertial squat training failed to increase the concentration of procollagen type 1 N-propetide (biomarker of collagen synthesis) in PT peritendinous tissue (Bloomquist et al. 2013: this study observed no change in tendon CSA). However, there is some evidence that mechanical loading of tendon tissue can induce an increased collagen synthesis measured by peritendinous tissue procollagen peptide levels (Langberg et al. 1999) and via the uptake of labelled amino acids (Miller et al. 2005). Although a collagen synthetic response following an equivalent bout of exercise is not a consistent finding (Didrieksen et al. 2013; Heinemeier et al. 2013a). Therefore, the current evidence suggests mechancial loading *in vivo* does not necessarily trigger the appropriate biochemical response needed to stimulate tendon growth.

In the absence of tendon hypertrophy the increase in PT stiffness with ECT and SCT were due to material stiffness changes, with both interventions producing greater changes in PT Young's modulus than CON. These changes after SCT are in accordance with multiple previous studies (Seynnes et al. 2009; Malliaras et al. 2012; McMahon et al. 2013), although the present study was the first to document increased tendon quality after ECT. Young's modulus changes are thought to reflect the functional consequences of alterations in internal tendon collagenous structure and biochemical composition (Buchanan and Marsh 2002: collagen content, cross-link density, fibril size). However, evidence for changes in tissue intrinsic structure/composition after strength training are lacking, and therefore further investigations to uncover the specific mechanisms for increases in Young's modulus are required.

The similar increases in PT stiffness and Young's modulus for both types of training could perhaps be due to the high loading magnitude in ECT and SCT. Other *in vivo* studies have noted the importance of high loading magnitude for stimulating tendon adaptation (i.e. increased tendon modulus only observed in high vs. low force SCT (Kubo et al. 2003; Kongsgaard et al. 2007; Arampatzis et al. 2007), and it is well recognised that *in vitro* mechanotransduction responses of tenocytes (resident tendon cells responsible for extracellular matrix remodelling) are highly strain magnitude dependent (Arnoczky et al. 2002; Lavagnino et al. 2008). It is perhaps surprising that SCT was not associated with a greater increase in tendon stiffness and modulus than ECT as intuitively a 13-fold greater loading duration in SCT vs. ECT could be expected to induce a more pronounced

mechanostimulatory effect. However, there is currently no *in vivo* data that shows that a greater overall duration of loading is associated with a more pronounced increase in free tendon stiffness. Importantly therefore, our data indicate that brief explosive contractions up to a high loading magnitude are an efficient means of increasing tendon stiffness and Young's modulus, which circumvents any need for sustained, fatiguing muscular contractions to stimulate tendon adaptation. The seeming potency of ECT to elicit an increase in tendon stiffness could be consequent to a greater collagen fibril strain exhibited in response to higher tendon strain rates (Clemmer et al. 2010). Greater fibril strain conceivably provides a greater stimulus to the resident tendon cells to initiate the processes (alterations in extracellular matrix protein composition) that presumably leads to the adaptation of increased tendon stiffness. Our finding therefore highlights that ECT is an efficacious approach to increase tendon stiffness and the less demanding nature of ECT likely makes this training modality preferentially tolerable to older adults and patient groups (e.g. osteoarthritis, tendinopathy) who incidentally may exhibit lesser tendon quality. Moreover, PT strain was reduced after ECT, but not after SCT or CON. Lesser tendon strain in response to a defined stress likely could reduce the susceptibility of the tendon to fatigue damage and overload injury (Ker et al. 1988, 2000; Buchanan and Marsh 2002). ECT may therefore be a useful training modality to adopt to reduce tendon pathology risk and facilitate tendon injury rehabilitation.

Alternative to the tendon responses, ECT was not an effective stimulus for increasing MTU stiffness measured at high forces. An interesting observation was actually that the force-elongation relationship post ECT was shifted to the right (greater elongation at defined forces). The change in elongation in response to the same high force (80% pre-training MVT) after ECT was greater than after SCT and tended to be greater than the CON group change. This suggests that ECT may be leading towards an overall greater compliance in the MTU. The rightward shift in the force-elongation curves after ECT appears to result from a change in elongation at the initial level (10%MVT), that persists throughout the rise in tendon force, as after 10%MVT the gradients of the force-elongation relationships pre-post ECT are equivalent. Nevertheless, consistent with our data, there is some evidence that sprint trained athletes (inherently perform explosive contraction type training) display greater knee extensor MTU compliance at the lowest levels of force (<20%MVT), with subsequent greater elongation values throughout the measured force range (Kubo et al. 2000, 2011). It is possible that this reduction in low force MTU stiffness (i.e. 0-10%MVT) after ECT with no

changes at higher forces indicates changes in tissue collagenous structure/composition that are specific to the highest (earliest) compliance region of the force-elongation relationship. Further work is needed to elucidate whether compliance/force level specific changes in stiffness are possible with different interventions, and whether there is any mechanistic basis for this supposition.

SCT did increase MTU stiffness at the high force level (70-80% pre-training MVT) with greater changes than after ECT or CON, concomitant with a general increase in the gradient of the force-elongation relationship. Alternatively SCT produced no apparent change in the elongation values at a constant high force (80% pre-training MVT), suggesting SCT did not cause a substantial change in stiffness across the whole force range. As per the previous paragraph any influence of SCT on high force stiffness appears to have been diluted by more consistent responses for lower regions of the force-elongation relationship resulting in no change in overall elongation. The increased MTU stiffness in the high force range after SCT is consistent with previous findings (Kubo et al. 2001, 2012; Arampatzis et al. 2007a, 2010; Bohm et al. 2014). The increased MTU stiffness after SCT and not ECT is perhaps due to the substantially longer loading duration in SCT. Previous work has showed greater changes in MTU stiffness after longer vs. short contractions, even though the total loading duration was matched (Kubo et al. 2001; Arampatzis et al. 2007a, 2010; Bohm et al. 2014). Our finding of no change in MTU stiffness after ECT contrasts with two previous studies that reported increased MTU stiffness after merely 4-6 weeks ECT (Burgess et al. 2007; Tillin et al. 2012). It is possible that the increased plantar flexor MTU stiffness observed by Burgess et al. could reflect adaptation of the Achilles tendon, as it accounts for a substantial portion of plantar flexor MTU stiffness (Farcy et al. 2013). Our finding perhaps differs to Tillin et al. because of the different training knee joint angles (115° in our study, vs. 85° in Tillin et al.). Training at longer muscle lengths (more acute angle) has been shown to result in greater MTU stiffness changes (Kubo et al. 2006a).

Collectively, our findings that PT stiffness, but not MTU stiffness increased after ECT, whereas SCT increased both PT and MTU stiffness, indicates a differential adaptive response in the tendinous tissues according to the contrasting loading regime. Further work could attempt to more precisely delineate the specific loading characteristics that could account for the differential adaptations. The contrasting response of PT and MTU stiffness to ECT indicates that MTU stiffness changes are seemingly independent of PT stiffness changes.

This interpretation is reinforced by the simple observation of the small proportion (e.g. 19% pre & post in the SCT group) of MTU elongation being due to the PT, which also suggests a minor contribution of changes in stiffness of the PT, to that of the MTU. Thus MTU stiffness changes perhaps reflect adaptations in the aponeurosis component of the MTU, although the methodology of the present study is insufficient to specifically decipher aponeurosis stiffness changes and could be interesting to explore in future work. However, in accordance with MTU stiffness changes, SCT produced an increase in VL apon area (+7%). This within group increase in VL apon area extends the notion that aponeurosis hypertrophy can occur with SCT, as found in a previous solitary dynamic SCT 12 week intervention (Wakahara et al. 2015). Aponeurosis hypertrophy is thought to be necessary to accommodate an increase in muscle cross-sectional area that occurs in response to strength training (Abe et al. 2012). Consistent with this view, only SCT resulted in an increase in QUADSvol (+8%). Considering the differences in loading characteristics between ECT and SCT, the muscle hypertrophic response to SCT but not ECT is likely a consequence of the greater loading duration (also referred to as time under tension in the wider literature) with SCT. Supportively, in response to bouts of isoinertial knee extensions with equivalent load, a greater loading duration increases the acute amplitude of muscle myofibrillar protein synthesis (Burd et al. 2012). The limited loading duration during ECT therefore seems to account for the lack of muscle hypertrophy in response to this training modality.

In conclusion, while neither ECT nor SCT induced tendon hypertrophy, ECT was equally effective as SCT for stimulating improvements in tendon quality (i.e. material stiffness [Young's modulus]) and stiffness. However, ECT was relatively ineffective for inducing muscular adaptations, as only SCT increased MTU stiffness, and muscle and aponeurosis size. Our results therefore indicate a differential adaptation of MTU component tissues (tendon vs. muscle-aponeurosis) depending upon the loading characteristics of the training completed. Specifically, tendon stiffness changes appeared to be primarily driven by achieving a high loading magnitude, whereas for the muscle and aponeurosis (hypertrophy and stiffness), the duration of loading seemed to be the more important stimulus.

CHAPTER 7

Size and stiffness of the muscle-tendon unit and tendon: influence of short-term and chronic strength training

7.1. INTRODUCTION

The contractile force generated by skeletal muscles is transmitted to the bone via collagenous tendinous tissues (intramuscular aponeurosis and external tendon). The effectiveness of tendons to transmit force is determined by their mechanical stiffness (resistance to deformation). As such we expect that increases in muscle strength induced via training would be accompanied by an increase in tendinous tissue stiffness. Greater tissue stiffness in accordance with stronger muscles would likely be necessary to maintain muscle and tendon force-length interaction, increase tissue maximal tolerable load and restrain the muscle contraction-induced maximal tissue strain within constrained sub-failure physiological limits (Matson et al. 2012; LaCroix et al. 2013).

Short-term strength training (up to 14 weeks) utilising high load sustained contractions has consistently increased both muscle-tendon unit (MTU: Kubo et al. 2001, 2012; Arampatzis et al. 2007a; 2010; Bohm et al. 2014) and external 'free' tendon stiffness (Reeves et al. 2003; Kongsgaard et al. 2007; Seynnes et al. 2009; McMahon et al. 2013). These changes in stiffness of these tendinous tissues could be due to either hypertrophy of the component tissues and/or an increase in their material stiffness. Evidence for aponeurosis hypertrophy is limited and unclear (Wakahara et al. 2015). Whilst the change in tendon size after strength training has been documented by a number of studies, the findings to date are equivocal with reports showing region specific hypertrophy (Kongsgaard et al. 2007; Arampatzis et al. 2007a; Seynnes et al. 2009; Bohm et al. 2014) and no change in tendon size (Arampatzis et al. 2010; Kubo et al. 2012; Bloomquist et al. 2013; Chapter 6). One possible explanation for this controversy is the relatively slow turnover of collagenous tissues (Smith and Rennie 2007; Heinemeier et al. 2013b) such that changes in tendinous tissue size after 8-14 weeks of training are on the threshold of what can be accurately detected. In this case longer durations of training may confirm the potential for tendon hypertrophy in response to strength training. In contrast, numerous studies have shown approximately proportional increases in Young's modulus and tendon stiffness (Reeves et al. 2003; Seynnes et al. 2009; Malliaras et al. 2012; McMahon et al. 2013; Waugh et al. 2014) after short-term strength training, suggesting that changes in material stiffness are the primary adaptation that contributes to the increase in tissue mechanical stiffness. However the potential for further changes in tissue stiffness (mechanical and material) over longer-term periods of training remains largely unexplored.

Long-term intervention studies (>14 weeks) are logistically problematic, therefore an alternative approach is the cross-sectional comparison of chronically strength trained (>5years) vs. untrained males (Weisinger et al. 2013). These authors reported that chronically trained individuals had a 21% greater PT stiffness commensurate with 34% larger tendon CSA (via ultrasound), because Young's modulus was equivalent compared to recreationally active males (Seynnes et al. 2013). However, this study involved small cohorts (n = 8) and measured Young's modulus at a greater tendon stress level (+34%) in the untrained than chronically-trained individuals, which may have confounded the comparison as stress-strain relationships are curvi-linear (e.g. Maganaris and Paul 2000, 2002). Moreover, a more recent study found that tendon CSA measured by MRI for 4/5 different tendons around the body (proximal and distal achilles, patellar and triceps brachii) was no different between strength trained (~10 years) and untrained males despite substantial differences in muscle volume (Fukutani and Kurihara 2015), contrarily implying chronic strength training may therefore not necessarily induce tendon hypertrophy. More robust evidence would ideally measure tendon CSA along the full length of the tendon from MRI (gold standard method: Couppe et al. 2014) images, employing careful segmentation. At present, there is insufficient data to affirm or refute whether high load strength training performed systematically for a number of years is associated with larger tendons. Further there is meagre evidence to show that chronic strength training may clearly induce aponeurosis hypertrophy, with just one study of greater aponeurosis size in weightlifters vs. recreationally active males (Abe et al. 2012). Finally whether MTU stiffness continues to adapt to prolonged strength trained is currently unknown.

The purpose of this study was to compare the mechanical and morphological properties of the patellar tendon (stiffness, Young's modulus, CSA [mean and regional]) and quadriceps femoris muscle-tendon unit (stiffness, muscle volume, vastus lateralis aponeuroses area), between untrained controls, short-term strength trained (post-12 weeks training) and chronic-strength trained (>3 years of systematic training) groups.

7.2. METHODS

7.2.1. Participants

Seventy young men provided written informed consent before completing this study, which was approved by the Loughborough University Ethical advisory committee. All participants were healthy and free from musculoskeletal injury with no previous history of tendon

pathology. An untrained control group (UNT) comprised n = 39 males (no lower body strength training in the >18 months). A short-term strength trained group (SST, n = 15 males) was measured post 12-weeks supervised isometric knee extension strength training (3 x wk, 40 reps of 3-s at 75% MVT). A chronic strength-trained (CST) group comprised n = 16 males with 4.0 ± 0.8 (mean ± SD) years systematic heavy-resistance training experience (~3 x wk of quadriceps sessions; typical exercises were squat, lunge, step-up, leg press). Each CST participant reported some nutritional supplement consumption (predominantly whey protein and creatine), although none declared illegal performance-enhancing substance use. The short format International Physical Activity Questionnaire (IPAQ) was used to assess the regular physical activity of each group (UNT 3661 ± 2404; STT 3510 ± 2124; CST 5558 ± 1460 MET-minutes/week).

7.2.2. Experimental Design

Participants visited the laboratory for a familiarisation session, (STT were familiarised pre-training) and two duplicate measurement sessions. Participants were seated in a custom-built isometric strength-testing chair and completed a series of maximal voluntary contractions (MVCs) and ramp voluntary contractions of the knee extensors as well as knee flexor MVCs of the dominant leg (preferred kicking leg). MVCs established maximal voluntary torque (MVT) and ramp contractions were performed to permit tissue stiffness estimation. Knee joint torque was recorded throughout contractions. Knee flexor surface electromyography was recorded during knee flexor MVCs and knee extensor ramp contractions. Ultrasound images of the vastus lateralis and patellar tendon were recorded throughout the ramp contractions to assess tissue elongation. Measurement sessions were performed at a consistent time of the day (± 2 hrs), separated by at least 2-3 days and started between 12:00–19:00 p.m. Participants were instructed not to participate in strenuous physical activity, consume alcohol/refrain from caffeine consumption in the 36/6 hours before measurement sessions. All participants were instructed to maintain their habitual physical activity and diet throughout the study. For the SST group, post-measurement sessions one and two took place 3-5 and 6-8 days following the last training session. Magnetic resonance imaging (MRI) was performed to assess quadriceps femoris muscle, vastus lateralis aponeurosis, and patellar tendon size. Participants were instructed to refrain from strenuous physical activity in the 24 hours prior to the MRI scan. For the STT group, MRI was conducted 2-3 days after the final training session and prior to post measurement sessions.

7.2.3. SST Group: Sustained Contraction Strength Training Intervention

Training sessions were completed three times per week on the same apparatus used for measurement sessions. After a brief warm-up of sub-maximal contractions of both legs, participants completed four sets of ten unilateral isometric knee-extensor contractions of each leg, with sets alternating between dominant and non-dominant legs until 4 sets per leg had been completed. Contractions were sustained at 75%MVT, with 2 s rest between each contraction. In order to control the torque rise and hold times, participants were presented with a target torque trace 2 s before every contraction and instructed to match this target, which increased torque linearly from rest to 75% MVT over 1 s before holding a plateau at 75%MVT for a further 3 s. MVCs were performed at the start of each training week to re-establish MVT and prescribe training torques.

7.2.4. Torque Measurement

Participants were positioned in an isometric strength-testing chair with knee and hip angles of 115° and 126° (180° = full extension), respectively. Adjustable straps were tightly fastened across the pelvis and shoulders to prevent extraneous movement. An ankle strap (35 mm width reinforced canvas webbing) was placed ~15% of tibial length (distance from lateral malleolus to knee joint space) above the medial malleolus, and positioned perpendicular to the tibia and in series with a calibrated S-Beam strain gauge (Force Logic, Berkshire, UK). The analogue force signal was amplified (x370; A50 amplifier, Force Logic UK) and sampled at 2,000 Hz using an A/D converter (Micro 1401; CED, Cambridge, UK) and recorded with Spike 2 computer software (CED). In offline analysis, force signals were low-pass filtered at 500 Hz using a fourth order zero-lag Butterworth filter, gravity corrected by subtracting baseline force, and multiplied by lever length, the distance from the knee joint space to the centre of the ankle strap, to calculate torque values.

7.2.5. Knee Flexor Electromyography (EMG)

Surface EMG recordings over the biceps femoris (BF) and semitendinosus (ST) were made with a wireless EMG system (Trigno; Delsys Inc, Boston, MA) were made during knee flexor MVCs and knee extensor ramp contractions. Following preparation of the skin (shaving, abrading and cleansing with alcohol) single differential Trigno standard EMG sensors (1-cm inter electrode distance; Delsys Inc, Boston, MA) were attached over each muscle using adhesive interfaces. Sensors were positioned parallel to the presumed frontal plane orientation of the underlying muscle fibres at 45% of thigh length (distance from the

greater trochanter to the lateral knee joint space) measured from the popliteal crease. EMG signals were amplified at source (x300; 20-450 Hz bandwidth) before further amplification (overall effective gain x 909) and sampled at 2000 Hz via the same A/D converter and computer software as the force signal, to enable data synchronization. In offline analysis, EMG signals were corrected for the 48 ms delay inherent to the Trigno EMG system and band-pass filtered (6-500 Hz) using a fourth-order, zero-lag Butterworth digital filter.

7.2.6. Knee Extension and Flexion Maximal Voluntary Contractions

Following a brief warm-up (3-s contractions at 50% [x3], 75% [x3] and 90% [x1] of perceived maximal), participants performed 3-4 MVC's and were instructed to either 'push as hard as possible' (knee extension) or 'pull as hard as possible' (knee flexion) for 3-5-s and rest ≥ 30-s. A horizontal cursor indicating the greatest torque obtained within the session was displayed for biofeedback and verbal encouragement was provided during all MVC's. The highest instantaneous torque recorded during any MVC was defined as MVT. During knee flexor MVC's EMG amplitude was calculated as the root mean square (RMS) of the filtered EMG signal of the BF and ST over a 500 ms epoch at knee flexion MVT (250 ms either side) and averaged across the two muscles to give knee flexor EMG_{MAX}.

7.2.7. MRI measurement of Muscle Tendon Unit Morphology and Moment Arm

T1-weighted MR (1.5 T Signa HDxt, GE) images of the dominant leg (thigh and knee) were acquired in the supine position at a knee angle of 163° (due to constraints in knee coil size) and analysed using OsiriX software (Version 6.0, Pixmeo, Geneva, Switzerland). Using a receiver 8-channel whole body coil, axial images (time of repetition/time to echo 550/14, image matrix 512 x 512, field of view 260 x 260 mm, pixel size 0.508 x 0.508 mm, slice thickness 5 mm, inter-slice gap 0 mm) were acquired from the anterior superior iliac spine to the knee joint space in two overlapping blocks. Oil filled capsules placed on the lateral side of the thigh allowed alignment of the blocks during analysis. The quadriceps femoris (QF) muscles (vastus lateralis [VL] vastus intermedius [VI], vastus medialis, and rectus femoris) were manually outlined in every third image (i.e. every 15 mm) starting from the most proximal image in which the muscle appeared. The volume of each muscle was calculated using cubic spline interpolation (GraphPad Prism 6, GraphPad Software, Inc.). Total QF volume (QUADSvol) was the sum of the individual muscle volumes. As previously described (Abe et al. 2012), the deep aponeurosis of the VL muscle was defined as the visible dark black segment between the VL and VI muscles in the thigh MRI images. The tangent line of

the VL muscle and the dark black segment in each cross-sectional image was traced manually. The length of the black line was defined as VL aponeurosis width and was measured on every third image (i.e. every 15 mm), starting in the most distal image were the aponeurosis was visible. Width measures were plotted against aponeurosis length (distance between most proximal and distal image where the aponeurosis was visible). The area under a spline curve fitted to data points was defined as the VL aponeurosis area (Apon Area).

Immediately after thigh imaging, a lower extremity knee coil was used to acquire axial (time of repetition/time to echo 510/14, image matrix 512 x 512, field of view 160 x 160 mm, pixel size 0.313 x 0.313, slice thickness 2 mm, inter-slice gap 0 mm) and sagittal images (time of repetition/time to echo 480/14, image matrix 512 x 512, field of view 160 x 160 mm, pixel size 0.313 x 0.313, slice thickness 2 mm, inter-slice gap 0 mm) of the knee joint. Contiguous axial images spanned patellar tendon length, which during analysis, were reconstructed to be aligned perpendicular to the line of action of the patellar tendon: straight line from the tendons posterior fibres insertion at the patellar apex to the posterior fibres tibial insertion. Images spanned from 2 cm superior to the patellar apex to 2 cm inferior to the tendon tibial insertion (Figure 7.1 A). Patellar tendon CSA (mm^2) was measured on each contiguous image (e.g. Figure 7.1 B) along the tendons length (first image where the patellar was no longer visible to the last image before the tibial insertion). Images, viewed in greyscale, were sharpened and the perimeter manually outlined (Figure 7.1 C). A spline curve was fitted to the tendon CSA values from each image (Figure 7.1 D) and the average of the spline equated to mean patellar tendon CSA (PT mean CSA). The average of the spline CSA's measured over proximal, middle and distal 3^{rds} was defined as proximal, mid and distal PT region CSA (Figure 7.1 D). Sagittal plane images were used to determined patellar tendon moment arm, the perpendicular distance from the patellar tendon line of action to the tibio-femoral contact point, which was the midpoint of the distance between the tibio-femoral contact points of the medial and lateral femoral condyles (Figure 7.2).

7.2.8. Ramp Contractions for Determination of Tissue Stiffness

Tissue stiffness was derived from synchronous recordings of torque and tissue elongation (see below, corrected for passive tissue displacement via video recording of knee joint changes) during isometric knee extension ramp contractions (experimental set-up; Figure 7.3). Participants completed two sub-maximal practice ramp contractions prior to five maximal attempts with 90 s rest between contractions. Prior to each ramp contraction

participants were shown a target torque-time trace on a computer monitor that increased at a constant gradient (50 $Nm.s^{-1}$ loading rate) from zero up to MVT. They were instructed to match the target trace as closely as possible for as long as possible (i.e. up to MVT), and real-time torque was displayed over the target torque-time trace for feedback. The preceding knee extensor MVCs and sub-maximal contractions were considered sufficient to elicit tissue preconditioning. The three most suitable ramp contractions, according to highest peak torque, the closeness to the target loading rate and ultrasound image clarity, were analysed and measurements averaged across these three contractions.

7.2.9. Measurement of Tissue Elongation

Video images from two ultrasound machines and one video camera were captured to obtain tissue and knee joint displacements during ramp contractions. An ultrasound probe (7.5 MHz linear array transducer, B-mode, scanning width 60mm and depth 50 mm; Toshiba Power Vision 6000, SSA-370A: Otawara-Shi, Japan) was fitted into a custom made high-density foam cast that was strapped to the lateral aspect of the thigh with the mid-point of the probe positioned at ~50 % thigh length. The probe was aligned so the fascicles inserting into the vastus lateralis (VL) muscle deep aponeurosis could be visualized at rest and during contraction. An echo-absorptive marker (multiple layers of transpore medical tape) was placed beneath the ultrasound probe to provide a reference for any probe movement over the skin. Another ultrasound probe (5-10 MHz linear array transducer, B-mode, scanning width 92 mm and depth 65 mm, EUP-L53L; Hitachi EUB-8500) was fitted into a custom made high-density foam cast that was held firmly over the anterior aspect of the knee with the probe aligned longitudinal to the patellar tendon such that the patellar apex and insertion of the posterior tendon fibres at the tibia could be visualized at rest and throughout the contraction. The ultrasound machines were interfaced with the computer collecting torque data in Spike 2 and the video feeds were recorded synchronously with torque using Spike 2 video capture at 25 Hz. During off-line analysis tissue elongation was tracked frame-by-frame using public-domain (www.cabrillo.edu/~dbrown/tracker) semi-automatic video analysis software: Tracker, version 4.86. VL fascicle deep aponeurosis cross point displacement relative to the skin marker provided a measure of muscle-tendon unit (MTU) elongation (Figure 3). Patellar tendon elongation was determined by the longitudinal displacement of the patella apex and the tendon tibial insertion (Figure 7.3). The distal insertion of the patellar tendon was not monitored for the purpose of estimating overall MTU displacement. To enable correction of tissue displacement due to joint angle changes during

ramp contractions individual ratios of tissue displacement relative to joint angular displacement (mm/°) were obtained from passive movements (i.e. plotting the tissue displacement-knee joint angle relationship). This ratio was used to determine tissue displacement resulting from knee angle change during ramp contractions, which was subsequently subtracted from total measured displacement. Corrections were only applied to aponeurosis displacement. Tendon elongation under passive conditions was deemed negligible. Passive movements were conducted prior to the ramp contractions. Participants were instructed to completely relax as their knee was moved through 90 to 130°. During passive movements and ramp contractions, knee joint angle (angle between visible markers placed on the greater trochanter, lateral knee joint space and lateral malleolus) was derived from sagittal plane video recorded using a camera mounted on a tripod positioned (1.5 m) perpendicular to the strength-testing chair. The video camera was interfaced with a computer and recorded using spike 2 video capture at 25 Hz (simultaneously with force, EMG, and ultrasound images during the ramp contractions) and analysed via Tracker software.

7.2.10. Calculation of Tendon Force

PT force was calculated by dividing external absolute knee extensor torque by the patellar tendon moment arm length. Direct measures of moment arm where acquired at rest from MRI images as indicated above (*MRI measurement*). Due to constraints in the size of the knee coil, sagittal images were acquired in an extended knee position (~163°). Moment arm length for any specific knee angle measured at rest or during ramp contraction was estimated from previously published data fitted with a quadratic function (Kellis and Baltzopoulos 1999), scaled to each participant's measured moment arm length at 163°. Absolute internal knee extensor torque was given by summing net knee extension torque and the estimated knee flexor co-contraction torque. Antagonist knee flexor torque was estimated by expressing the average knee flexor EMG amplitude (RMS 50 ms moving window) during ramp contractions relative to the knee flexor EMG_{MAX} and multiplying by the knee flexor MVT (assuming a linear relationship between EMG amplitude and torque). During analysis, torque and EMG amplitude were down-sampled to 25 Hz to match the ultrasound video frequency.

7.2.11. Calculation of Tissue Stiffness and Tendon Young's Modulus

For each of the three best ramp contractions analysed, MTU (corrected for passive tissue displacement) and PT elongation was plotted against total tendon force (corrected for antagonist force). Force-elongation plots were fitted with a second-order polynomial. MTU

and PT stiffness was calculated as the gradient (Δ tendon force [N]/Δ elongation [mm]; $N.mm^{-1}$) of the respective force-strain curve over 80-100% (3360-4200N) of an absolute tendon force (4200N) that corresponded to the lowest common force level attained by all participants during ramp contractions. Tendon stress was obtained by dividing tendon force by mean tendon CSA. Tendon strain was the percentage tendon displacement relative to the resting tendon length. A patellar tendon stress-strain curve was plotted and PT Young's modulus (GPa) calculated as the slope (Δ tendon stress [MPa]/Δ tendon strain [%]) of the stress-strain curve derived over 80-100% of an absolute common stress (40 MPa). The stiffness and Young's modulus measures derived from each of the three ramp contractions analysed was averaged to give each individuals representative values.

7.2.12. Statistical Analysis

For measurements completed in the duplicate measurement sessions, the average value was used for statistical analysis. An a priori significance level of $P<0.05$ was set for all statistical tests which were performed using SPSS Version 20.0 (IBM Corp., Armonk, NY). Descriptive data are presented as mean ± standard deviation (SD) and percentage differences in the group means are given in the text. The influence of group (UNT, STT, CST) on all muscle and tendinous tissue variables was examined by univariate ANOVA. Main group effects were followed by least significant difference (LSD) post-hoc paired comparisons to delineate between group differences; Holm-Bonferroni corrections were applied to LSD *P*-values, and between group Hedges g effect size (ES) was calculated (Lakens 2013). Effect size magnitude was classified as <0.2= "trivial"; 0.2-0.6 = "small"; >0-6-1.2 = "moderate"; >1.2-2.0 = "large"; >2.0 = "very large" (Hopkins et al. 2009).

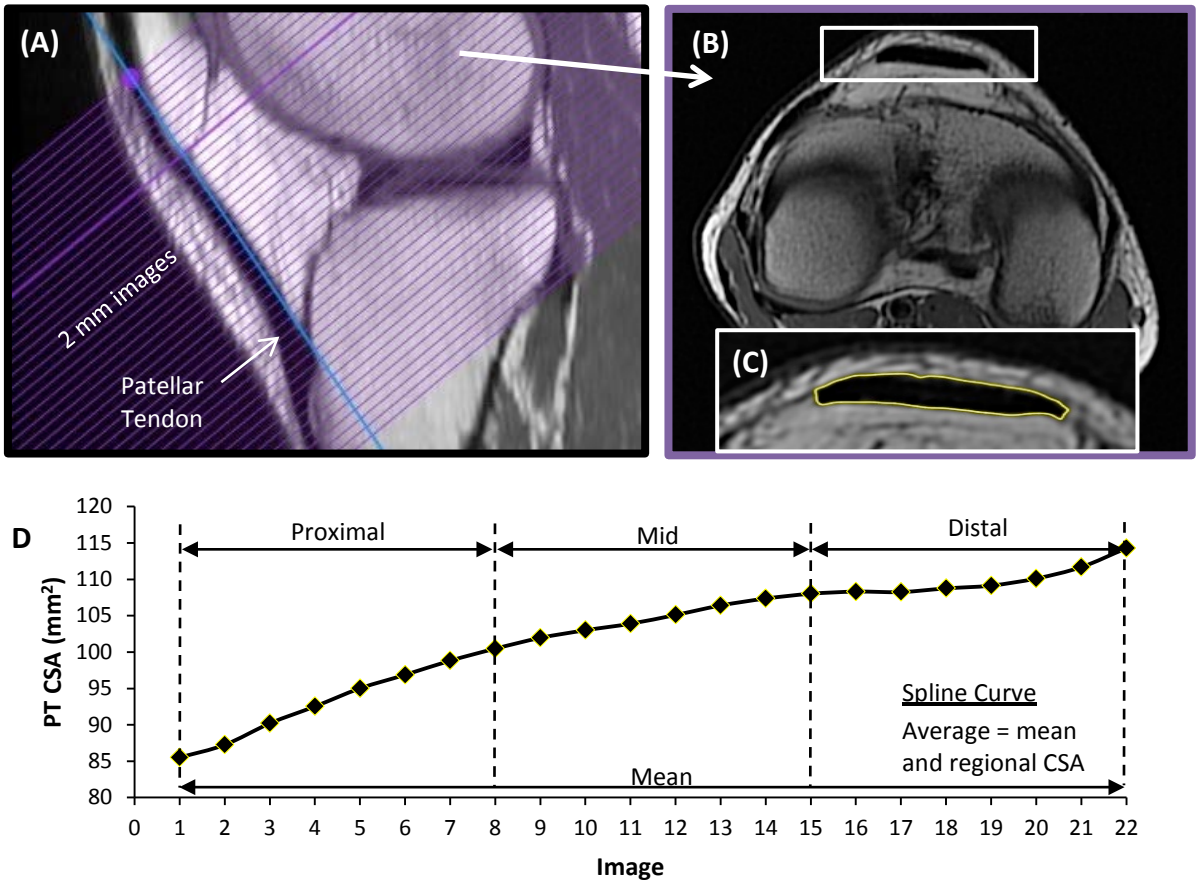

Figure 7.1. Patellar tendon (PT) cross-sectional area (CSA, mm^2) measurement. Axial MRI images spanning tendon length in contigous 2 mm thick slices aligned perpendicular to the tendon (A). In each axial image (e.g. B), the perimeter of the PT which was manually outlined (C), and the CSA's plotted and fitted with a spline curve (D) to interpolate intermediate CSA values and permit standardised regional CSA analysis.. The average of the spline curve in proximal, middle and distal thirds was defined as PT proxmal, mid and distal CSA respectively. The average of all spline CSA's gave PT mean CSA.

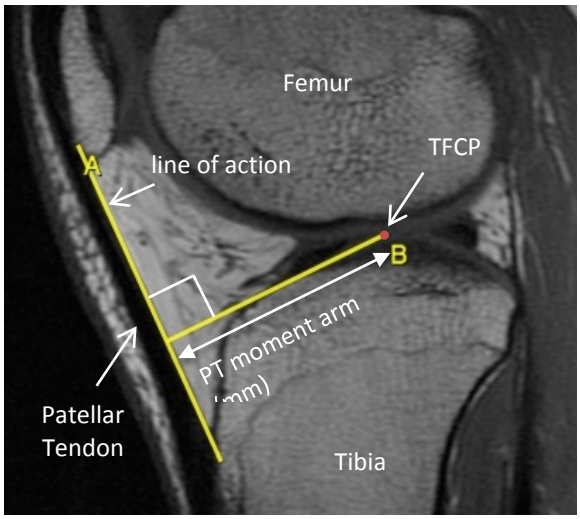

Figure 7.2. Sagittal MRI image of the knee joint: Patellar tendon (PT) moment arm was defined as the perpendicular distance between the tendon line of action and the tibio-femoral contact point (TFCP).

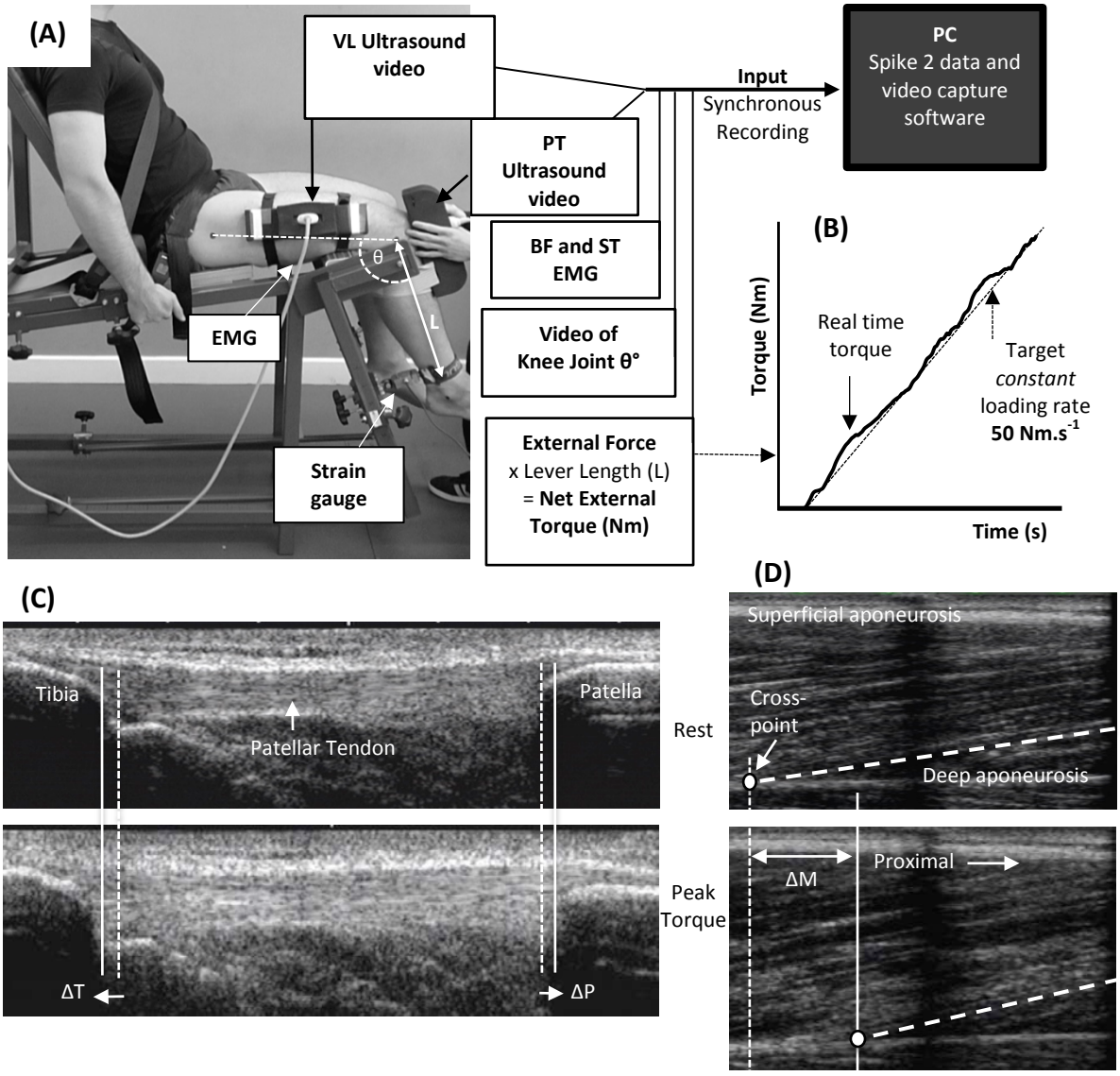

Figure 7.3. The experimental set-up and ultrasound imaging during ramp contractions. Participants were tightly fastened to a rigid isometric strength-testing chair with resting knee and hip angles of 115 and 126° respectively (A). Unilateral knee extensor torque, video of knee joint angle, antagonist muscle (biceps femoris [BF], semitendinosus [ST]) surface electromyography and ultrasound video images were recorded during constant-loading rate isometric ramp knee extensor contractions (example in B). Ultrasound images are of the patellar tendon (PT, C) and vastus lateralis (VL, D) muscle at rest (top) and at peak ramp torque (bottom) and indicate the measurement of PT (tibia-patellar displacement, ΔT + ΔP) and MTU distal tissue (VL deep aponeurosis fascicle-cross point proximal displacement relative to the echo-absorptive marker, ΔM) elongation

7.3. RESULTS

7.3.1. Group Characteristics

Age, height and body mass were similar between UNT and STT groups (P = 0.262, P = 0.488 and P = 0.465 respectively; Table 7.1), while CST were younger, taller and had a larger body mass than UNT and STT (all P ≤ 0.003). MTUdt and PT length were similar between UNT and STT (P = 0.114 and P = 0.195). CST had longer tissue lengths than both UNT and STT (MTUdt: CST 6.5% > UNT and 9.2% > STT, both comparisons P<0.001; PT length CST 9.8% > UNT P = 0.006 and 15.5% > STT P = 0.022).

Table 7.1. Descriptive characteristics of the participants.

	UNT	STT	CST	ANOVA (P)
N =	39	15	16	
Age, years	25 ± 2	25 ± 2	22 ± 2	<0.001
Height, cm	176 ± 6	175 ± 8	183 ± 6	0.001
Body mass, kg	72 ± 9	70 ± 9	90 ± 10	<0.001
MTU distal tissue length, mm	336 ± 16	328 ± 17	358 ± 18	<0.001
PT length, mm	47.7 ± 5.5	45.1 ± 5.5	52.1 ± 5.9	0.005
PT moment arm, mm	43.8 ± 2.7	44.8 ± 3.1	45.8 ± 2.5	0.054

Data are mean ± SD. PT = patellar tendon

7.3.2. Muscle-Tendon Unit Size and Strength

Maximal voluntary torque (Figure 7.4 A) differed between all three groups, being considerably greater in CST than UNT (+58.1%, P < 0.001, ES = 2.90 “very large”) and STT (+34.4%, P < 0.001, ES = 1.66 “large”). STT was also stronger than UNT (+17.6%, P = 0.001, ES = 1.04 “moderate”). Similarly, QUADSvol (Figure 7.4 B) was considerably larger in CST than UNT (+55.7%, P < 0.001, ES = 3.55 “very large”) and STT (+46.2%, P < 0.001, ES = 2.83 “very large”), though SST was similar to UNT (+7%, P = 0.179, ES = 0.42 “small”). Correspondingly VL apon area (Figure 7.4 C) was larger in CST than UNT (+17.3%, P < 0.001, ES = 1.41 “large”) and STT (+13.5%, P = 0.006, ES = 1.09 “moderate”), though STT was not different to UNT (+3.3%, P = 0.331, ES = “small”). In contrast, PT mean CSA (Figure 7.4 D) was similar between groups (ANOVA P = 0.169), and this was also the case for regional PT CSA (Table 7.2).

Table 7.2. Regional patellar tendon cross-sectional area (cm^2)

Region	UNT (n=39)	STT (n=15)	CST (n=16)	ANOVA (P)
Proximal	93.0 ± 9.9	92.0 ± 13.5	98.4 ± 13.1	0.216
Mid	104.4 ± 12.6	97.0 ± 14.3	104.9 ± 13.3	0.146
Distal	110.4 ± 17.9	101.6 ± 14.3	112.1 ± 15.7	0.141

Data are mean ± SD

7.3.3. Patellar Tendon Mechanical Properties (Table 7.3)

The patellar tendon force-elongation relationships (Figure 7.5 A) indicated that PT elongation at the highest common force level (4200N, Figure 7.5 B) was 13.5% less in the CST than UNT (2.6 ± 0.5 vs. 3.0 ± 0.6 mm, P = 0.063, ES = 0.75 "moderate") and 15.4% less in CST than STT (3.1 ± 0.6 mm, P = 0.048, ES = 0.86 "moderate"), indicating less compliance over the whole force range up to 4200N for CST only, whereas STT and UNT were similar (P = 0.698, ES = 0.10 "trivial"). However, PT stiffness measured over a common force range (3360-4200N; Figure 7.5 C) was greater for SST (+24.5%, P = 0.0004, ES = 1.27 "large") and CST (+16.7%, P = 0.021, ES = 0.85 "moderate") than UNT, though similar in CST – STT (P = 0.287, ES = 0.35 "small").

Patellar tendon stress-strain relationships (Figure 7.6 A) revealed that at the common stress level of 40 MPa (Figure 7.6 B), PT strain was less for CST (5.1 ± 1.0%) than UNT by 24.4% (6.4 ±1.4%, P = 0.008, ES = 1.30 "large") and STT by 19.9% (6.7 ± 1.7%, P = 0.006, ES = 0.97 "moderate"), indicating less material compliance over the whole stress range up to 40 MPa for CST only, whereas STT and UNT were very similar (P = 0.369, ES = 0.17 "trivial"). However, PT Young's modulus (Figure 7.6 C) derived over a common stress range (32-40 MPa) was greater for both SST (+21.9%, P = 0.003, ES = 1.00 "moderate") and CST (+23.3%, P = 0.002, ES = 1.13 "moderate") than UNT, but was very similar for CST and STT (P = 0.855, ES = 0.06 "trivial").

7.3.4. Muscle-Tendon Unit Mechanical Properties (Table 7.3)

Tendon force-MTU elongation relationships (Figure 7.7 A) showed that at the common force level of 4200 N (Figure 7.7 B), MTUdt elongation exhibited no main group effect (ANOVA, P = 0.375), indicating similar overall MTU elongation in both strength trained groups as well as the untrained group. Likewise, MTU stiffness (Figure 7.7 C) was not statistically different between groups (ANOVA, P = 0.149).

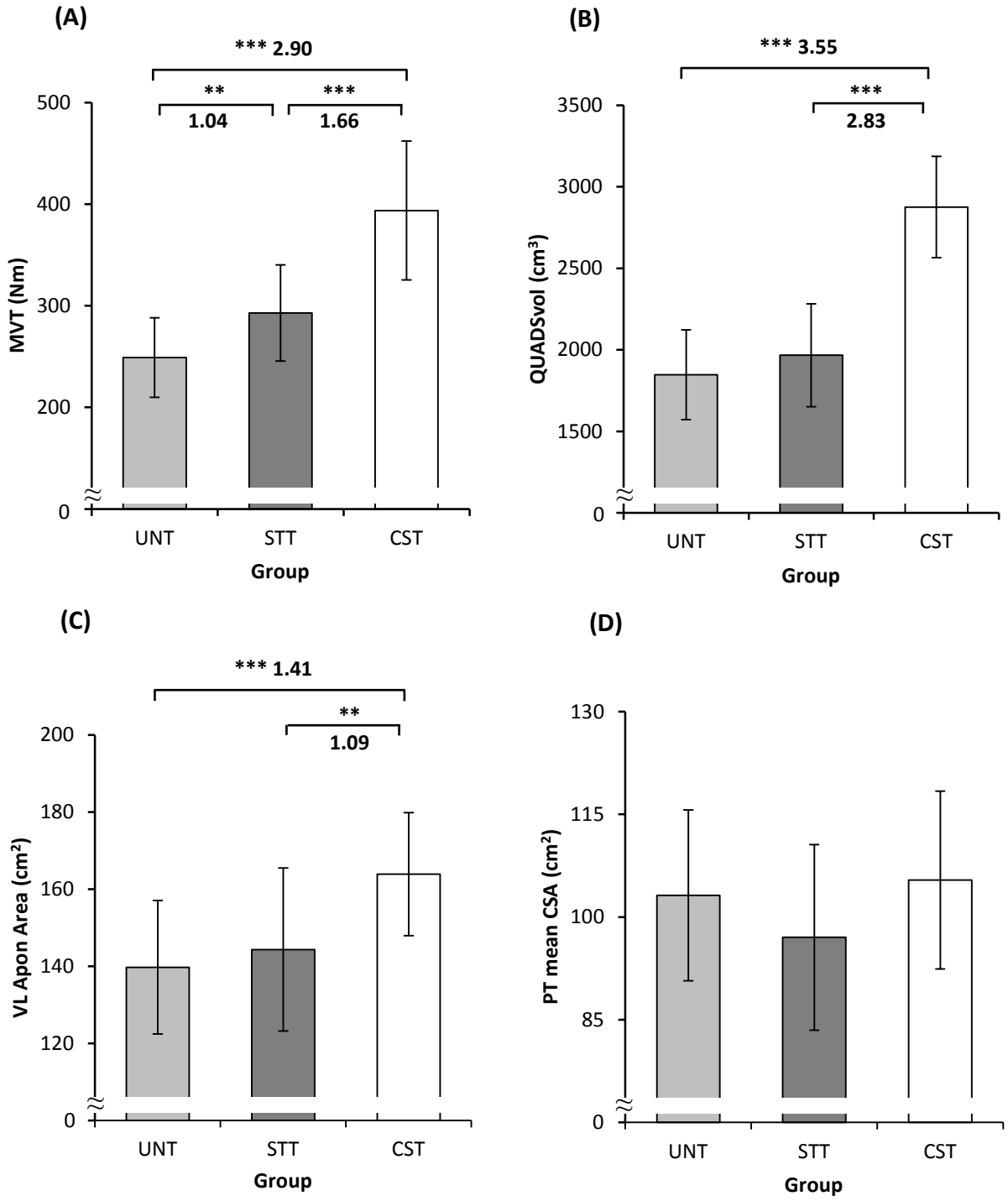

Figure 7.4. Group comparisons: Isometric knee extension maximal voluntary torque (MVT, A), Quadriceps Femoris (QF) muscle volume (B), Vastus Lateralis (VL) Aponeurosis (Apon) area (C) and Patellar Tendon (PT) mean cross-sectional area (CSA, D) for control (UNT, n = 39), short-term strength trained (STT, n = 15) and chronic-strength trained (CST, n = 16) groups. Data are mean ± standard deviation. Bold numbers are between groups hedges g effect size. Post-hoc tests: Least significant difference Holm-Bonferroni corrected P-values. *P<0.05, **P<0.01, ***P<0.001.

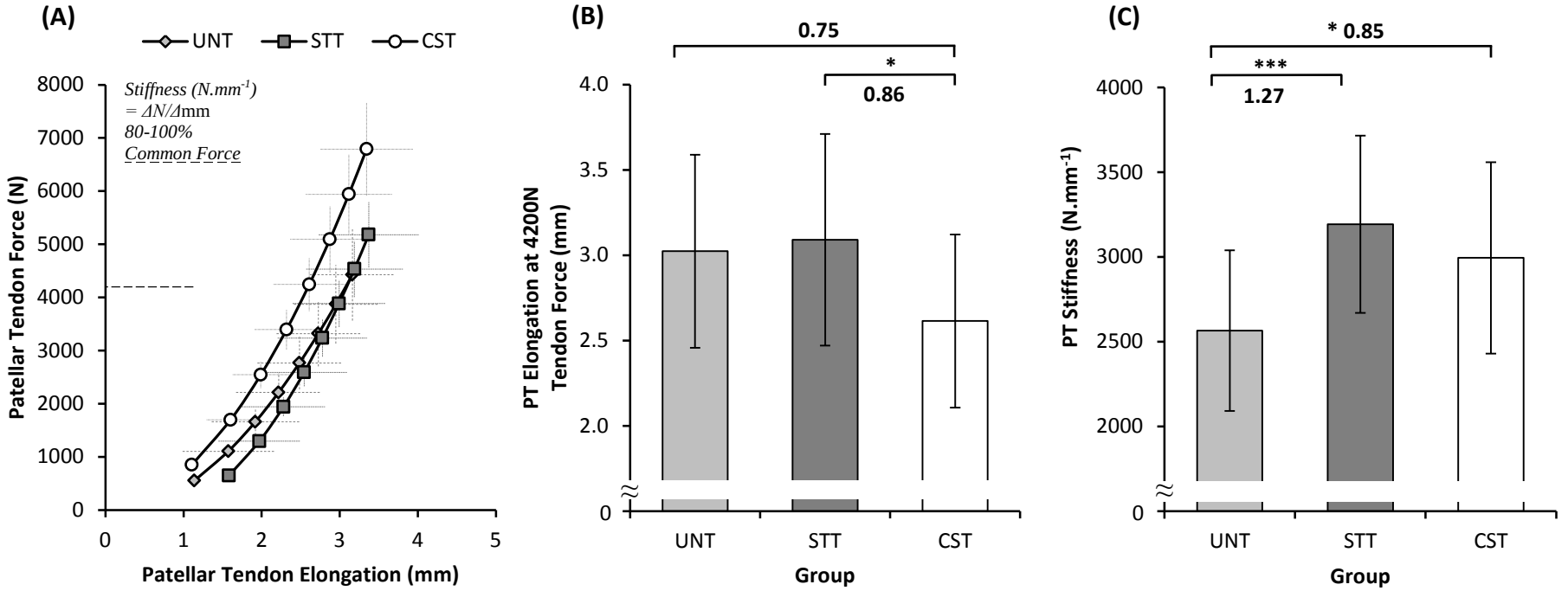

Figure 7.5. (A) Non-linear relationships between estimated patellar tendon force (N) during constant loading-rate isometric ramp knee extension contractions and the resultant patellar tendon elongation in the untrained control (UNT, n = 37), short-term strength trained (STT, n = 15) and chronic strength trained (CST, n = 15) groups. Curves show the group mean relationship. Data points correspond to within group average values for the elongation at 10% intervals of group mean maximal voluntary tendon force, plotted up to 80% (highest common level achieved during ramp contractions). Error bars indicate the within-group standard deviation for force (y-axis bar) and elongation (x-axis bar). Dashed line intercepting the y-axis is the highest common force (4200N) for all participants across each group achieved during ramp contractions. **(B) And (C)** Group comparisons of the PT elongation at the common force level of 4200 N, and PT stiffness (gradient of curves in **A** over 80-100% of the highest common force level [3360-4200N]). Bars are mean ± SD. Bold numbers are the between groups hedges g effect size. Post-hoc tests: Least significant difference Holm-Bonferroni corrected P-values. *P<0.05, ***P<0.001.

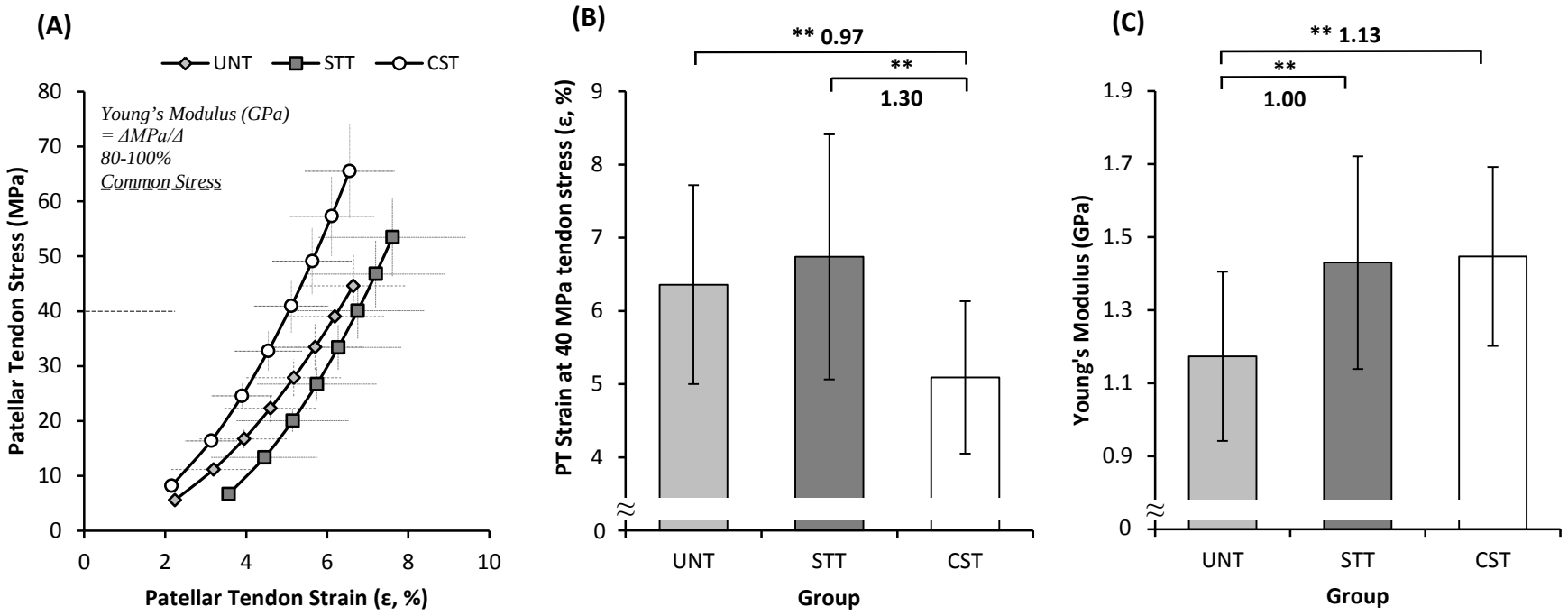

Figure 7.6. (A) Non-linear relationships between estimated patellar tendon stress (MPa [N.mm^2]) during constant loading-rate isometric ramp knee extension contractions and the resultant patellar tendon strain in the untrained control (UNT, n = 37), short-term strength trained (STT, n = 15) and chronic strength trained (CST, n = 15) groups. Curves show the group mean relationship. Data points correspond to within group average values for the strain at 10% intervals of group mean maximal voluntary tendon stress, plotted up to 80% (highest common level achieved during ramp contractions). Error bars indicate the within-group standard deviation for stress (y-axis bar) and strain (x-axis bar). Dashed line intercepting the y-axis is the highest common stress (40 MPa) for all participants across each group achieved during ramp contractions. **(B) And (C)** Group comparisons of the PT strain at the common stress level of 40 MPa, and PT Young's modulus (gradient of curves in **A** over 80-100% common stress level [32-40 MPa]). Bars are mean ± SD. Bold numbers are the between groups hedges g effect size. Post-hoc tests: Least significant difference Holm-Bonferroni corrected P-values. **P<0.01.

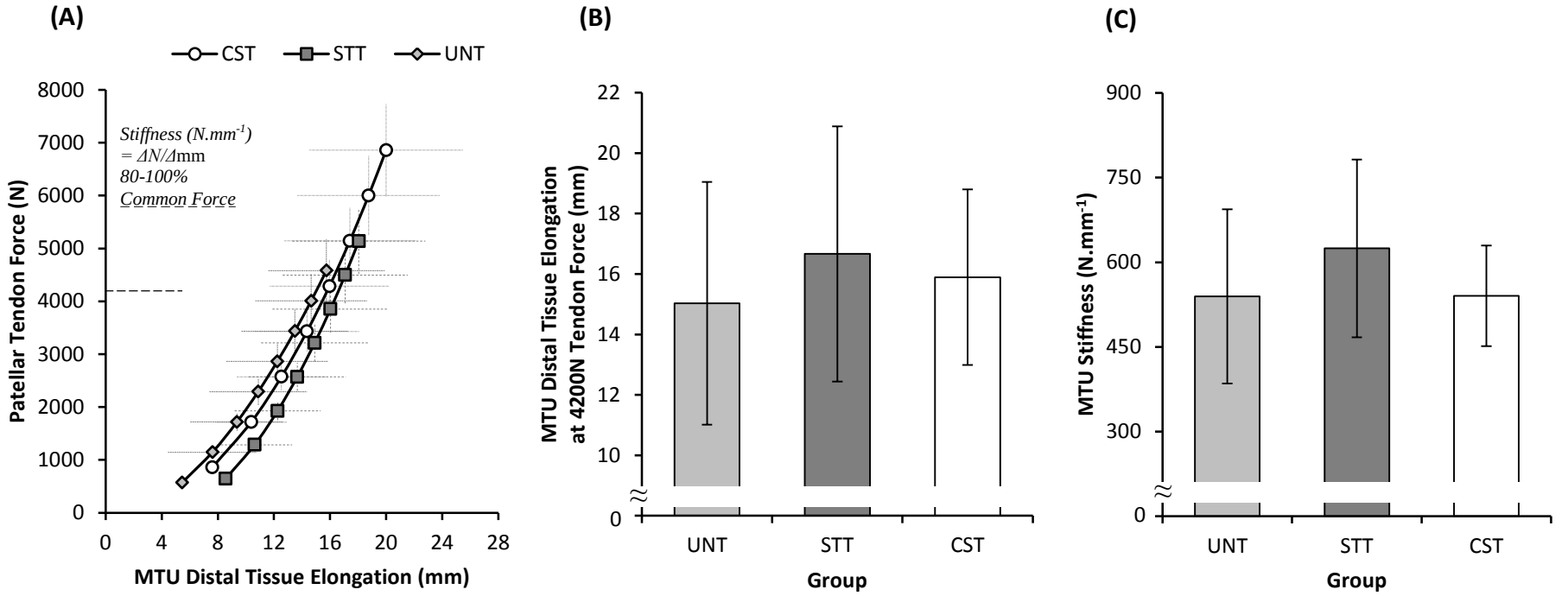

Figure 7.7. (A) Non-linear relationships between estimated patellar tendon force (N) during constant loading-rate isometric ramp knee extension contractions and the resultant muscle-tendon unit (MTU) distal tissue elongation in the untrained control (UNT, n = 37), short-term strength trained (STT, n = 14) and chronic strength trained (CST, n = 16) groups. Curves show the group mean relationship. Data points correspond to within group average values for the strain at 10% intervals of group mean maximal voluntary tendon force, plotted up to 80% (highest common level achieved during ramp contractions). Error bars indicate the within-group standard deviation for force (y-axis bar) and strain (x-axis bar). Dashed line intercepting the y-axis is the highest common force (4200 N) for all participants across each group achieved during ramp contractions. **(B) And (C)** Group comparisons of the MTUdt elongation at the common force level, and MTU stiffness (gradient of curves in **A** over 80-100% common force level [3360-4200N]). Bars are mean ± SD.

Table 7.3. Summary of group differences in maximal strength, muscle tendon unit (MTU) size and tissue (MTU and patellar tendon [PT]) stiffness between chronic strength trained (CST), short-term strength trained (STT) and untrained control (UNT) groups.

Function	
MVT, Nm	CST > STT > UNT
MTU size	
QUADSvol, cm^3	CST > STT & UNT
VL Apon Area, cm^2	CST > STT & UNT
PT CSA, mm^2	-
Indices of Tissue Stiffness	
PT elongation at 4200 N, mm	CST < STT & UNT
PT stiffness, $N.mm^{-1}$	CST & STT > UNT
PT strain at 40 MPa, %	CST < STT & UNT
PT Young's modulus, GPa	CST & STT > UNT
MTU elongation at 4200 N, mm	-
MTU stiffness, $N.mm^{-1}$	-

Significant group differences groups: greater (>) or less (<) than.
PT CSA: both mean and regional CSA measures.

DISCUSSION

The present study compared the mechanical properties of the patellar tendon (PT) and knee extensor muscle-tendon unit (MTU) as well as the size of the MTU components between untrained controls (UNT), short-term strength trained (STT) and chronic strength trained (CST) young males. The main findings were that despite large differences in muscle strength and size, and more modest differences in aponeurosis size, there were no group differences in PT CSA. Both STT and CST had greater PT stiffness and Young's modulus than UNT, though PT stiffness and Young's modulus was similar between STT and CST. Interesting, only CST exhibited lesser PT elongation/strain (compliance) at a comparative tendon force/stress level. Contrary to these differences in tendon mechanics, MTU stiffness and strain was not appreciably divergent between groups.

Greater PT stiffness at high force levels was observed in STT than UNT, and this is consistent with the increases in stiffness observed after short-term (8-12 weeks) strength training studies (Kongsgaard et al. 2007; Seynnes et al. 2009; McMahon et al. 2013). As expected CST also possessed greater PT stiffness than the UNT, which is in accordance with a previous cross-sectional study that found a 21% greater PT stiffness in a smaller cohort of chronically strength trained vs. untrained males (Seynnes et al. 2013). Interestingly however, in the present study the CST did not have greater PT stiffness at high force levels than STT. Taken together, these findings suggest that while short-term training results in a stiffer tendon, further prolonged exposure to strength training does not necessarily stimulate further tendon stiffness adaptation. Therefore the underpinning mechanisms for increased tendon stiffness with short-term training are presumably saturated after 12 weeks. In contrast, the lesser PT elongation at the common force level (4200N) in CST than STT does indicate that chronic strength training impacts the generic stiffness of the tendon across a broader force range. This effect would appear to be due to greater stiffness at particularly low force levels (<1000 N), as the gradients of the force-elongation relationships after the initial most compliant region of tendon deformation were equivalent in STT and CST. These results suggest that there may be force-region specific tendon stiffness adaptations to STT and CST. While STT was sufficient to elicit similar adaptations in high force stiffness to CST, CST had greater stiffness throughout the force-elongation relationship, particularly at low forces, which were not observed after STT.

In the absence of group differences in PT CSA, the greater PT stiffness of STT and CST vs. UNT was ostensibly attributable to the correspondingly greater PT Young's modulus in STT and CST vs. UNT. This affirms that the adaptations in material stiffness are the primary mechanism that causes the increase in mechanical stiffness after strength training, in accordance with previous work (e.g. Reeves et al. 2003; Seynnes et al. 2009; McMahon et al. 2013). Further the difference in modulus between STT and UNT was similar to the mean increase observed after short-term studies (+22%: Weisinger et al. 2015 review). Consistent with the pattern for tendon stiffness measurements, CST had greater Young's modulus over the common stress range (32-40 MPa) than UNT. Our study is the first to document a greater tendon modulus in CST than UNT (at an equivalent tendon stress); a single earlier study failed to equate the stress level for modulus measurement (Seynnes et al. 2013). Intriguingly, CST had similar PT Young's modulus to STT. Similarly explanatory, PT strain exhibited at a comparative stress level was less only in the CST group, thus chronic strength training results in greater generic tendon material stiffness as evidenced by greater resistance to deformation during the lowest levels of loading (<10 MPa). Alternative tendon modulus adaptations at the lowest tendon stresses vs. higher stresses are thus perhaps consequent to different changes to internal tendon structure and/or composition (Buchanan and Marsh 2002; Kjaer et al. 2015) that independently influence contrasting regions of the tendon stress-strain relationship. However, the nature of such changes that can explain an increase in material stiffness (at lower and/or higher stresses) after strength training is presently unknown (Kjaer et al. 2015). Further, a mechanistic basis for why the Young's modulus at higher tendon stresses appears to plateau after short-term strength training yet increases in material stiffness at the lowest stress levels (leading to lesser tendon PT strain at a common stress in CST) presumably occur after 12 weeks is unclear, thus more detailed longitudinal investigations are required.

No difference between groups in PT size is perhaps surprising. Intuitively we might expect the high muscle strength and size values that had occurred after ~4 years of CST to be accompanied by an increase in tendon CSA. However this was not the case with similar PT mean and regional CSA values between groups despite substantial differences in isometric knee extensor MVT (CST 58.1% > UNT) and QUADSvol (55.7% > UNT). This provides convincing evidence that strength training does not induce tendon hypertrophy. Finding no greater PT CSA in STT than UNT is not necessarily unexpected as there is contrasting evidence for tendon hypertrophy after short-term intervention studies (8-14 weeks). Our result corresponds with another isometric strength training study that identified no change in

mean or regional Achilles tendon CSA (Kubo et al. 2012 [12 weeks]), though some studies reported small (typically ~5-6%) increases in tendon CSA (often only in certain regions): patellar (Kongsgaard et al. 2007; Seynnes et al. 2009) and Achilles (Arampatzis et al. 2007a; Bohm et al. 2014). Nevertheless because tendon collagen turnover is relatively slow (Smith and Rennie 2007; Heinemeier et al. 2013b), data from short-term studies are not conclusive. Similar to our data, Fukutani and Kurihara (2015) found that chronic strength trained (~10 years) males did not exhibit greater tendon CSA in all but 1/5 of tendon MRI sites. Only one previous study adopting ultrasound (perhaps less accurate than gold standard MRI; Kruse et al. 2017) tendon CSA measurement documents greater tendon CSA in chronic trained vs. untrained males (Seynnes et al. 2013). In support of our data, tendon MRI was performed along the full length of the tendon and acquired with sensitive spatial resolution (2 mm thick images, 0 mm gap, pixel size 0.313 x 0.313 mm), and careful tendon segmentation performed on each image by a single blinded investigator.

In support of the present studies data, there is some evidence that indicates resistance exercise may not stimulate *in vivo* collagen synthesis in tendon tissue For instance, an acute bout of resistance exercise (dynamic knee extension at 70%-RM, 3 x 10 repetitions) was shown to have no effect on collagen type I messenger RNA expression 24 hours post exercise (Sullivan et al. 2009). Also, 12 weeks of isoinertial squat training failed to increase the concentration of procollagen type 1 N-propetide (biomarker of collagen synthesis) in PT peritendinous tissue (Bloomquist et al. 2013: this study observed no change in tendon CSA). However, there is some evidence that mechanical loading of tendon tissue can induce an increased collagen synthesis measured by peritendinous tissue procollagen peptide levels (Langberg et al. 1999) and via the uptake of labelled amino acids (Miller et al. 2005). These findings are congruent with other studies showing that chronic training can lead to greater tendon size: larger tendon CSA in distance runners vs non-runners (Kongsgaard et al. 2005; Wiesinger et al. 2016) and in the dominant vs. non-dominant leg of the same individual (Couppé et al. 2008), which contrasts the present findings. Perhaps the contrasting findings indicate that the high stress induced during strength training is perhaps not the optimal stimulus for stimulating tendon hypertrophy, and that exposing the tendon tissue to higher volumes of loading than experienced during strength training is a more effective stimulus for tendon growth.

In contrast to tendon size, CST had a much larger VL apon area than both the UNT (+17.3%) and STT (+13.5%). This implies that the substantial muscle hypertrophy in response to many

years of strength training is coincident with increases in aponeurosis size. This suggestion is coherent with the limited previous work suggestive of aponeurosis hypertrophy after strength training (Abe et al. 2012; Wakahara et al. 2015). Between groups differences in QUADSvol (CST, +55.7% vs. UNT and +46.2 vs. STT) were disproportionately greater than the aforementioned differences in aponeurosis area: CST had 3.2 and 3.4-fold greater muscle than aponeurosis size compared to UNT and STT respectively. This is likely attributable to a greater absolute rate of intramuscular myofribrillar than connective tissue collagen synthesis stimulated in response to resistance exercise (Babraj et al. 2005; Smith and Rennie 2007).

Despite greater aponeurosis size and substantial differences in muscle size, the CST did not exhibit a greater MTU stiffness than UNT or STT. Similarly, neither did CST show any difference in MTU elongation at the comparative force level (4200 N) than UNT or STT, indicating no long-term change in MTU stiffness over the wider force-elongation relationship. The present study is the first to document a comparison of MTU stiffness measurements in CST vs. UNT. On the other hand, no difference in MTU stiffness measures in STT vs. UNT is in contrast to previous short-term interventions studies showing increased knee extensor MTU stiffness after 12-14 weeks isometric strength training (Kubo et al. 2001, 2009; Chapter 6). This contrasting result could perhaps be a consequence of the limitations associated with the cross-sectional study design as adopted in the present investigation, as opposed to the short-term studies of within-group changes. No differences in MTU stiffness for CST are perhaps particularly surprising. However, the absolute common force level for MTU stiffness measurement was ~50% MVT for the CST group, and perhaps MTU stiffness changes with training occur preferentially at higher force levels. Prior to my earlier work (Chapter 6), previous studies have measured MTU stiffness changes at absolute force levels relative to maximal strength (e.g. 50-100% MVT). Intriguingly, the present studies result could suggest that perhaps with continued training, STT may experience a subsequent increased MTU compliance to hence account for an equivalent MTU stiffness in UNT and CST. However, a precise explanation for the current studies results is unclear. Detailed longitudinal investigations are needed to further understand MTU stiffness adaptation to sustained-contraction strength training.

The conclusions from the present study are reinforced by our thorough approach. In particular, tissue stiffness estimates were particularly robust; derived from multiple standardised loading rate contractions replicated in duplicate measurement sessions. This

method circumvented introducing bias into stiffness estimates for stronger individuals; stiffness would be greater at higher loading rates and stronger individuals would exhibit a higher loading rate in constant ramp-time contractions. Group comparisons were made of the average of the tissue stiffness/ strain values recorded from both duplicate sessions, which in the context of the complicated method, had good test-retest reliability (coefficients of variation for PT and MTU stiffness and strain, <10%). Further, direct comparisons were facilitated by stiffness/strain measures at equivalent tendon force/stress levels in each group.

In summary, the greater knee extensor MVT and quadriceps size in STT, and in particular, CST than UNT young males was not matched with a correspondingly larger tendon size (no differences in mean or regional PT CSA), indicating that tendon hypertrophy does not occur in response to strength training. However, greater VL aponeurosis area suggests long-term strength training can induce aponeurosis hypertrophy commensurate with muscle growth. Curiously MTU stiffness and strain was similar between groups, with more detailed measurements needed to reconcile this finding. As expected, both STT and CST displayed greater PT stiffness and Young's modulus, at high forces, than UNT although CST was similar to STT for both variables. Alternatively, CST exhibited less compliance and tendon elongation/strain throughout the force/stress range than STT and UNT. These results may suggest that the time course of tendon stiffness adaptations is force/stress region specific with short-term training eliciting increases in high force tendon stiffness, and more prolonged training also promoting increased stiffness at lower forces/stresses and consequently more holistic changes throughout the force/stress range.

CHAPTER 8

General discussion

The present thesis aimed to: (i) document quadriceps femoris (QF) muscle fascicle length (FL) and pennation angle (PA) changes in the transition from rest to isometric maximal voluntary contraction (MVC), and establish if the greater QF effective physiological cross-sectional area ($_{eff}$PCSA) measured during MVC was more strongly correlated, than $_{eff}$PCSA at rest, to maximal isometric strength; (ii) investigate the relationships between QF FL and PA and maximal (isometric and dynamic) and explosive isometric strength; (iii) comprehensively examine whether greater muscle-tendon unit (MTU) and tendon stiffness was associated with higher *in vivo* rate of torque development (RTD); (iv) compare the relative efficacy of explosive-contraction (ECT) vs. sustained-contraction (SCT) strength training to increase MTU and tendon stiffness, and induce MTU (muscle, aponeurosis and tendon) hypertrophy; (v) assess MTU and patellar tendon (PT) size and stiffness in untrained (UNT), short-term strength trained (STT [post-SCT]) and chronic strength trained (CST) males, to gain insight into the capacity of the tendinous tissues to continue to adapt to prolonged exposure to strength training.

The **main findings** of the five empirical studies conducted were:

1. QF FL was -24% lower and PA +40% greater during MVC than at rest. Subsequently QF $_{eff}$PCSA during MVC was +27% greater than at rest. Correlations between maximal strength and $_{eff}$PCSA measured at rest (r = 0.519) and during an MVC (r = 0.530) were similar (Chapter 3).

2. Resting measures of QF FL were inversely related to explosive voluntary, but not evoked, torque (absolute and relative) in just the initial phase (0-50 ms) of contraction (r = 0.433 and 0.453), whereas PA was not associated with explosive strength. Likewise neither FL nor PA was related to maximal isometric or dynamic strength (Chapter 4).

3. PT stiffness was unrelated to voluntary or evoked RTD in either absolute of relative terms. MTU stiffness was also not related to explosive voluntary or evoked octet RTD, relative MTU stiffness was associated with relative RTD assessed over matching torque increments during both explosive voluntary (R^2 = 0.097 – 0.188 between 35 – 55%MVT) and evoked (R^2 = 0.099 – 0.194 between 5 – 45 % MVT) contractions (Chapter 5).

4. Both ECT and SCT resulted in similar increases in PT stiffness (20 and 16%), which was mirrored by the improvements in Young's modulus (22 and 16%). ECT also reduced PT

elongation/strain at the same (pre-post) absolute force/stress. Only SCT increased MTU stiffness (21%), QF muscle volume (8%), and vastus lateralis (VL) aponeurosis area (7%). Neither ECT nor SCT induced PT hypertrophy (Chapter 6).

5. Despite substantially greater muscle strength and QF muscle volume in CST than UNT and even STT (volume: 46% > STT; 56% > UNT) both PT mean and regional cross-sectional area were similar between groups, but VL aponeurosis area was greater (17%) in CST than UNT. PT stiffness and modulus were correspondingly higher in STT (25 and 22%) and CST (17 and 23%) vs. UNT, with no difference between training groups. However, for the CST group PT elongation/strain at a common force/stress level (4200N /40MPa) was less than for both STT (15/20%) and UNT (14/24%). MTU stiffness as well as the MTU elongation at a common force level (4200N) was similar between all groups (Chapter 7).

8.1. Muscle Architecture Variability

An interesting observation that warrants briefly reiterating was the curious finding in Chapter 4 that the intra-individual variability in FL and PA (at rest) within each of the QF component muscles (between subject coefficient of variation [CVb] for FL and PA 12 -17%) was greater than the variation in the subsequently derived whole QF FL (CVb, 7%) and PA (CVb, 9%). This finding suggests that the intra-individual differences in component muscle architecture are counterbalanced once an average QF value is derived; e.g. scenario is one individual with longer FL in VL and VI, but shorter FL in RF and VM than another individual. The result is the average QF FL being more similar between individuals than the inter-individual differences in specific component muscles FL. Intriguingly this observation was made in untrained individuals suggesting that the effect is an innate characteristic. Coincidentally, Chapter 4 also showed that the architecture of component muscles was not related, implying that the architecture of the four QF muscle heads is effectually independent of each other. Thus relating architecture to muscle function would be best accomplished via a holistic muscle architecture appraisal. However, the limited between subject variability in FL and PA (Chapter 4) may have implications for delineating any functional effects of architecture variables in between subject study designs (Chapter 4).

8.2. Determinants of Maximal and Explosive Strength

8.2.1. Maximal Strength

A novel aspect of Chapter 3 was the examination of the maximal isometric strength-muscle size relationship for muscle size ($_{eff}$PCSA) measured during MVC as well $_{eff}$PCSA measured at rest. It was found that QF $_{eff}$PCSA measured during MVC was no more predictive of knee extension isometric MVT, than the more straightforward estimate of $_{eff}$PCSA acquired at rest. Therefore, resting measures of muscle size remain an appropriate morphological descriptor of maximal strength. Following this knowledge, more robust estimates of resting $_{eff}$PCSA than obtained in the present thesis should be sought. For instance, FL and PA were only acquired at one location along the muscle longitudinal axis in the present thesis, therefore discounting any regional heterogeneity. Also, the inability of the planimetric (2-D) ultrasonography to capture three-dimensional muscle structure could limit how well the estimates of $_{eff}$PCSA relate to maximal strength. *In vitro* data show the directly proportionality of $_{eff}$PCSA and maximal isometric muscle force (R^2 = 0.99, Powell et al. 1984). Obtaining more comprehensive estimates of $_{eff}$PCSA at rest may help to reconcile the unresolved issue of which measure of muscle size ($_{eff}$PCSA, ACSA or volume) is the best morphological representative of maximal strength. Capturing three-dimensional muscle architecture measures via diffusion tensor MRI would facilitate future investigations.

As opposed to muscle size, Chapter 4 showed that neither FL nor PA was related to isometric MVT. In contrast, a few studies have found measures of agonist muscle PA to have moderate positive correlations to maximal isometric strength (e.g. Strasser et al. 2013; Ando et al. 2015), although these relationships are most likely coincidental due to a recognised muscle size dependence of PA (Kawakami et al. 2006). Moreover, the finding in Chapter 4 that PA was not related to measures of dynamic strength (concentric torque at 50 and 350°s^{-1}), does not give credence to a hypothetical mechanism of greater PA enhancing the decoupling of muscle and fascicle shortening during concentric muscle contractions, that supposedly favours greater force (Azizi et al. 2008). It is possible that the acuteness (<20°) of the PA's evident in Chapter 4 restrict the importance of the hypothetical mechanism. Lesser PA's favour muscle fascicle shortening rather than fascicle rotation (increased PA; Azizi et al. 2008).

Furthermore, Chapter 4 revealed QF FL was unrelated to knee extension concentric torque at $350^{o}s^{-1}$ or the proportion of low velocity torque developed at $350^{o}s^{-1}$ in accordance with couple of earlier studies (Blazevich et al. 2009b; Baxter and Piazza 2014). This finding contrasts the idea of longer FL allows a lower relative fascicle shortening velocity for a given muscle shortening velocity, which may be expected to facilitate higher velocity force production (Blazevich 2006b). However, even though a recent high-frame ultrasound study has refuted an association of longer FL and slower relative fascicle velocity (Hauraix et al. 2013) it is possible that this mechanism is not relevant at the relatively slow velocities tested. Potentially a quantitative influence of FL on dynamic torque production could be deduced at velocities higher than those tested in chapter 4 and in previous studies. Development of a valid method to establish higher-velocity torque *in vivo* is needed. Alternatively, differences in FL may only seem to have an inconsequential influence because other factors (e.g. muscle size, neural drive, fibre-type composition) are overwhelming dominant predictors of dynamic torque in untrained individuals who incidentally showed limited between subject QF FL variability. Therefore identifying relationships between FL and high velocity torque could have been hindered by the inclusion of a relatively homogenous cohort in Chapter 4. Perhaps FL may represent more of a specialisation for function whose influence could be revealed following a period of training, or it could be an important factor in explaining inter-individual differences across athletic groups or intra-muscular differences in torque production.

8.2.2. Explosive Strength

Both Chapters 4 and 5 aimed to improve our understanding of the physiological determinants of explosive strength, preferentially expressed as the rate of torque development. The primary unique findings were that some measures of voluntary relative RTD were related to both FL (Chapter 4), and relative MTU stiffness (Chapter 5).

Chapter 4 revealed that in contrast to the thought that longer FL with higher shortening velocity potential would favour faster RTD, longer FL was, perhaps counter intuitively shown to negatively influence the earliest phase of voluntary force rise (0-50ms). Curiously FL was subsequently found not to relate to evoked RTD (0-50 ms). At face value, these findings are surprising, as the muscle architecture would be expected to exert a stronger influence on evoked explosive strength. Aside from the suggestion made in Chapter 4; possible the earliest phase of the rising voluntary torque0time curve (0-50ms, 48 ± 17 Nm) that was related to FL was missed by the first measured time point during the evoked

contractions (50 ms, 120 ± 22 ms) when force rises more rapidly, the results present a rather puzzling circumstance to explain. It seems most sensible to suggest more thorough investigation is required to firmly verify the influence of FL on voluntary and evoked RTD. If Chapter's 4 findings are replicated a possible physiological mechanism would need to be confronted.

Alternatively, the clear relation of relative MTU stiffness to evoked relative RTD in Chapter 5 is consistent with the theoretical understanding that stiffer tissues facilitate RTD by slowing muscle shortening and facilitating force production in the lower force region of the force-velocity relationship (Wilkie 1949; Hill 1951; Edman and Josephson 2007). However the limited explained variance (<20%) suggests there are more important determinants of relative evoked RTD (e.g. contractile protein composition, Harridge et al. 1996). The relationship of relative MTU stiffness to evoked relative RTD seemingly explained why voluntary relative RTD was also related to relative MTU stiffness. Contractile properties are known to exert their greatest influence on voluntary RTD during the fastest phase of torque development (50-100 ms; Folland et al. 2014) that corresponded with the positive correlations between relative MTU stiffness and relative RTD.

A positive relation between relative MTU stiffness and relative RTD suggests that an increase in relative MTU stiffness after strength training could partially account for any improvements in relative RTD if there were large improvements in relative MTU stiffness. Given the relatively limited explained variance of relative MTU stiffness to relative RTD (25-50%MVT) in Chapter 5, relative RTD changes after SCT and ECT after 12 weeks (e.g. Tillin et al. 2012, Balshaw et al. 2016) are unlikely to be accounted for by relative MTU stiffness. Indeed, the linear regression equations associated with the results figures (bivariate correlation between relative MTU stiffness and RTD between 25-50%MVT) in Chapter 5 indicated that changes in relative MTU stiffness after SCT (+11%) and ECT (–8.0%) training would produce small changes in voluntary and evoked relative RTD between 25-50%MVT: +4.1 and 5.7% increase after SCT, whereas ECT would yield a decrease of –3.5% and 5.2% respectively. This indication is rather contradictory to a particular importance of MTU stiffness on relative RTD. It seems counterintuitive that training to improve RTD via specific training (i.e. ECT) would subsequently not improve or potentially decrease an underlying physiological determinant.

Despite a relationship between relative MTU stiffness and relative RTD in chapter 5, there was no relation between absolute measures of MTU stiffness and RTD. This is in contrast to previous work (Bojsen-Møller et al. 2005; Waugh et al. 2013; Hannah and Folland 2015). The contrary result was suggested to be a consequence of the previous studies positive correlations being spurious. As highlighted in chapter 5, earlier studies methods likely resulted in a bias towards greater MTU stiffness in stronger individuals that also likely display higher RTD. The more rigorous methodology of Chapter 5 circumvented such bias and therefore revealed that actually absolute MTU stiffness is not a notable determinant of absolute RTD.

Neither QF PA (Chapter 4) nor patellar tendon (PT) stiffness (Chapter 5) related to isometric knee extension voluntary or evoked RTD. Chapter 4 and 5 were the first studies to explore any possible relation of muscle PA and tendon stiffness to *in vivo* RTD. The lack of relation between PA and RTD was deemed consequent to no relation of PA and MVT (Chapter 4). Any hypothetical relation of PA to RTD is not clear apart from a potential indirect link between absolute RTD and PA, owing to an anticipated positive effect of greater PA to increase $_{eff}$PCSA and thus muscle maximal strength, and the recognised positive influence of maximal strength on absolute RTD. As indicated in Chapter 4, the lack of relation between PA and MVT, likely underpinned the subsequent lack of relation between PA and RTD. In general, the results of Chapter 4 suggest that PA has no discernible influence on the *in vivo* muscle strength characteristics examined. The present findings therefore concur with the viewpoint that although PA is a definitive structural descriptor of skeletal muscle, inter-individual differences in PA are unlikely to exhibit any significant functional consequences (Burkholder and Lieber 1994; Lieber and Fridén 2000).

No relation of PT stiffness was attributed to a limited elongation that could not conceivably influence muscle contractile conditions and, the force transmission time through such a short tendon as the PT, being too rapid to noticeably impair RTD. This finding highlights that changes in PT stiffness that occurs after strength training (e.g. Chapter 6 and 7) will not account for improvements in RTD in contrary to the postulations of several studies that have not measured both RTD and PT stiffness simultaneously (Reeves et al. 2003; De Boer et al. 2007; Alegre et al. 2016).

Next to the aforementioned findings regarding FL and MTU stiffness, there appears to be a differential influence of component muscle-tendon unit tissues on RTD. In the context of Chapter 5's method, the relative MTU stiffness relationships, with no apparent influence of tendon stiffness, suggests that the force-length characteristics of the muscle-aponeurosis component of the MTU affected relative RTD to some small extent. However, the ultrasound technique was insufficient to specifically characterise aponeurosis stiffness and delineate its contribution to RTD. Further any possible influence of muscle stiffness (possibly related to FL) could not be captured. Any relation of *in vivo* FL and muscle stiffness has not been examined and any possible effect of muscle stiffness on RTD has been hitherto neglected in the literature, and therefore warrants further consideration.

8.3. Muscle-tendon unit hypertrophic response to strength training

8.3.1. Muscle

Greater muscle size is an obvious and widely documented response to conventional strength training (Folland and Williams 2007; Erskine et al. 2010), as shown by the substantially greater muscle volume in CST individuals (Chapter 7) and the more modest increase in QF muscle size after 12 weeks of SCT (8%, Chapter 6). In contrast the ECT in Chapter 6 was an ineffectual stimulus to induce short-term gains in muscle volume. This finding adds to the evidence that loading duration is an important training variable dictating muscle size changes. Muscle hypertrophy results from the accretion of muscle proteins following repeated bouts of resistance exercise that stimulate a net protein synthetic response (Phillips 2014) and this process is likely amplified by greater muscle time under tension (Burd et al. 2012). Therefore the very limited overall contraction duration inherent to the ECT likely accounts for why it was insufficient to elicit muscle growth. Therefore, if muscle hypertrophy is a desired adaptation, ECT is an inappropriate training regime and the more traditional SCT training would be advantageous.

8.3.2. Aponeurosis

As the aponeurosis is the attachment site for muscle fibres, muscle hypertrophy may implicitly necessitate aponeurosis hypertrophy (Abe et al. 2012). However only one previous study had investigated whether an SCT intervention may enlarge the aponeurosis (Wakahara et al. 2015). Commensurate with the increase in muscle size after SCT in Chapter 6, there was a within-group increase in VL aponeurosis area, which was not observed after ECT.

Nevertheless, the greater aponeurosis size in the CST group in Chapter 7 indicates that with longer periods of training, there is additional aponeurosis growth. To elucidate the time course more detailed longitudinal within-group investigations would be needed to detail aponeuroses size changes. There are some emerging suggestions that aponeurosis size may be a risk factor for MTU injury risk (Fiorentino et al. 2012; Evangelidis et al. 2015). Therefore the evidence in Chapter 6 that aponeurosis size can be increased with appropriate strength training, suggests that further attention should be given to elucidating the potential of strength training to develop aponeurosis size.

8.3.3. Tendon

The present thesis found no evidence that strength training elicits tendon hypertrophy. No change in tendon CSA occurred with either ECT (uniquely documented) or SCT (Chapter 6). Given that tendon collagen turnover is slow, the 12 weeks period of training in Chapter 6 may not have been of sufficient duration to demonstrate conclusively that strength training was not stimulating a gradual accretion of tendon collagen. However, the most robust evidence that strength training does not drive tendon growth was the observation that the CST group in Chapter 7 had a similar tendon size (both mean and regional CSA) to untrained individuals. Therefore it appears that a repeated bout of high stress over several years is not the stimulus for tendon hypertrophy.

Data from multiple short-term intervention studies (small hypertrophy often localised to certain tendon locations: Arampatzis et al. 2007a, Kongsgaard et al. 2007; Seynnes et al. 2009; Bohm et al. 2014, vs. no change across the length of the tendon: Arampatzis et al. 2010; Kubo et al. 2012; Bloomquist et al. 2013), as well as a couple of cross-sectional studies of chronic strength vs. untrained males, (>PT CSA, Seynnes et al. 2013 vs. no differences at multiple tendon sites, Kurihara and Fukutani 2015) have provided controversial data as to the possibility of some limited tendon growth after strength training. In support of the findings of this thesis, PT CSA analysis in Chapters 6 and 7 was conducted with particularly diligence. Sensitive spatial resolution (2 mm thickness, 512 x 512 pixels), of tendon MRI (gives high contrast between tendon and surrounding tissues) images was acquired along the full length of the tendon. Tendon CSA in each image was carefully segmented to yield minimal measurement error in mean PT CSA (~3.0% co-efficient of variation in pre-post control [Chapter 6]). Further complimentary to the results of this finding of no tendon hypertrophy after strength training, is recent evidence that the tendon matrix protein synthesis that would

be required to initiate tendon growth (Svensson et al. 2016) is not stimulated via resistance exercise: no upregulation of collagen messenger RNA post dynamic resistance exercise (Sullivan et al. 2009); and no change in PT peritendinous concentrations of a collagen synthesis biomarker post 12 weeks heavy-squat training (accompanied by no change in PT tendon CSA; Bloomquist et al. 2013). In contrast, endurance exercise has been found to stimulate increases in peritendinous concentrations of collagen synthesis biomarkers (Langberg et al. 1999, 2000, 2001), which may explain the evidence for larger tendon CSA in habitual distance runners than controls (Rosager et al. 2002; Magnusson and Kjaer 2003; Kongsgaard et al. 2005; Wiesinger et al. 2016). The evidence that endurance running and intermittent exercise can induce tendon hypertrophy after years of training (Kongsgaard et al. 2005; Couppé et al. 2008), yet strength training does not (Chapter 7), indicates that tendon hypertrophy is in some way consequent to exposing the tendon to a high volume of loading; rather than merely high infrequently applied stress. In theory, tendon hypertrophy may result from a continuous repair process to restore tendon strength after fatigue induced damage that can occur with prolonged cyclic loading at moderate stress levels (Wiesinger et al. 2015).

8.4. Tendinous Tissue Adaptations to Strength Training

8.4.1. Patellar Tendon

An interesting novel finding of Chapter 6 was that PT stiffness (in this case measured over absolute tendon forces within a high relative force range: 70-80% pre-MVT) was increased similarly after SCT and ECT (i.e. ECT was equally effective for increasing tendon stiffness as SCT). While SCT has been previously shown to increase PT stiffness (e.g. Seynnes et al. 2009; McMahon et al. 2013), Chapter 6 is the first study to indicate that ECT can likewise increase tendon stiffness. The similar tendon stiffness increase after ECT and SCT appears consequent to the similarly high magnitude contractions (≥75% MVT) performed. Neither greater loading rate (i.e. RTD, > in ECT) nor longer loading duration (> in SCT) seemed to influence tendon stiffness adaptations. However it appears that the short-term improvements in PT stiffness after 12 weeks strength training shown in Chapter 6 would not subsequently be furthered with continued training. Chapter 7 uniquely showed that the CST cohort had similar PT stiffness (at the highest common absolute tendon force range) as post 12 weeks of SCT. However, a notable observation in Chapter 6 was that ECT reduced PT elongation/strain at a common force/stress level (80% pre-MVT) whereas SCT had no effect. Although CST also had lesser PT elongation at the comparative force level (4200N) than the

STT group (post SCT). The reduction in tendon elongation implies an increase in the generic tendon stiffness across a broader force range. This adaptation appeared consequent to stiffness changes in the earliest phase of tendon loading (<10% pre-MVT in Chapter 6; <1000N in Chapter 7). Taken together, Chapters 6 and 7 indicate that strength training can reduce PT elongation at a common force level, though SCT requires greater than 12 weeks whereas this adaptation occurs in a shorter period of time with ECT, suggesting a reduction in tendon elongation is an adaptation that occurs faster in response to a high strain rate stimulus.

Because neither ECT nor SCT produced tendon hypertrophy, and the CST had no larger tendon CSA (than untrained [UNT] or STT), the tendon stiffness adaptations are consequent to changes in material stiffness. Accordantly, the PT Young's modulus improvements after ECT and SCT (Chapter 6), as well as the group comparisons in PT modulus in (CST & STT > UNT, but CST = STT), coincided with the results for tendon stiffness. Therefore Chapter 6 was the first study to show that ECT can improve tendon quality. Likewise, Chapter 7 was the first study to indicate: tendon modulus is greater in CST than UNT at an equivalent stress level; CST and STT have remarkably similar Young's modulus, suggesting changes in tendon Young's modulus seemingly occur as a reactive response to short-term (12 weeks) strength training, with no further improvement beyond the intial 12 weeks stimulated by continued exposure to high stress tendon loading.

In an attempt to capture the so-called linear region of the tendon stress-strain relationship (>30MPa: Seynnes et al. 2015), Young's modulus was measured over the highest common stress range for each individual pre and post ECT and SCT (Chapter 6), and for all participants in each group in Chapter 7. When subjected to high levels of stress, tendon strain is thought to result from collagen elongation mechanics (e.g. collagen molecule extension and collagen inter-fibre sliding: Screen et al. 2009; Connizzo et al. 2016). These mechanisms imply that increased collagen content, inter-molecular cross-link concentration and/or collagen fibril size distribution (larger mean fibril diameter) could account for an increased Young's modulus (Buchanan and Marsh 2002; Kjaer et al. 2015). However, whether strength training can alter collagen structure and composition is yet to be clearly elucidated. No studies have examined if tendon collagen structure/ composition is altered in response to strength training in healthy individuals. Although, no difference in PT collagen content or cross-link concentration was found between untrained and chronically (10 ± 1 years)

resistance-trained men (LeMoine et al. 2009), suggesting collagen structure and composition are unlikely to change following strength training. Unfortunately LeMoine et al. did not measure *in vivo* PT Young's modulus so the functional implications of their findings are unclear. Therefore an explanation for the greater Young's modulus post vs. pre strength training (Chapter 6) and in the strength trained vs. untrained groups (Chapter) 7 is unknown and warrants investigation. Further, consideration is yet to be given to any effects of strength training on non-collagenous proteins of the extracellular matrix that could mediate dynamic processes of tendon collagen elongation (Connizzo et al. 2016), and thus influence Young's modulus (Wren and Carter 1998; Thorpe et al. 2013; Connizzo et al. 2016). Regardless of the adaptive mechanisms, no additional functional changes after short-term strength training (i.e. increased Young's modulus) implied in Chapter 7 suggests such mechanisms are saturated after a relatively short period of time, though a precise time-course and the reasons for this limited adaptation are yet to be explored.

In addition to the results for Young's modulus, the lesser PT elongation at a common force level observed after only ECT in Chapter 6 and in CST (than UNT and STT in Chapter 7), was mirrored, and thus explained by, the correspondingly lesser strain at common stress levels. Furthermore, from observation of the stress-strain relationships ECT and longer-term SCT (i.e. CST) appear to increase material stiffness in response to the lowest stress levels (<10%MVT [ECT]; <10MPa [CST]), which leads to an increase in the material stiffness across the broader stress range. The tendon stress-strain relationship in the initial highly compliant (toe) region is thought to reflect the straightening of the crimped collagen fibres and a reorientation of the fibres to align fully in the direction of loading (Wren and Carter 1998; Screen 2009). Our findings suggest that strength training may influence collagen crimp morphology (e.g. angle) as well as the initial collagen fibre alignment, however whether this is the case is unknown. Furthermore, why the underpinning adaptations to explain the lesser strain occur in a shorter period of time after ECT than SCT is unclear. To speculate, initial consideration of the differences in tendon loading characteristics of ECT vs. SCT could have implied that the reduction in tendon strain was related to strain-rate (high in ECT). Though this assumption is not immediately consistent with a reduction in PT strain that presumably occurs after chronic strength training. Perhaps a substantial increase in maximal strength (as with CST) is needed to give rise to a sufficient absolute tendon-loading rate in controlled muscle contractions to elicit adaptations. Hence accounting for why SCT requires a longer period of time than ECT to reduce tendon strain. However, the tendon loading characteristics

that would drive the adaptations to reduced PT strain at a given absolute stress level requires further investigation to be properly understood. Taken together the results of Chapters 6 and 7, suggest that ECT is a more time-efficient approach to elicit equivalent adaptations (increased Young's modulus [higher and initial stress] and reduced PT elongation and strain at equal [pre-post training] absolute forces and stresses) occurring in response to SCT.

8.4.2. Muscle-Tendon Unit

As a first, Chapter 6 found that the contrasting ECT and SCT resulted in force region specific MTU stiffness changes. SCT only increased MTU stiffness at high force levels, where as ECT only increased MTU elongation across the force range suggesting a general increase in MTU compliance. These findings could imply that strain rate (high in ECT), and loading duration (high in SCT) are important mechanical stimuli for the respective MTU stiffness changes.

No change in high force MTU stiffness after ECT contrasts with a previous study (Tillin et al. 2012) that found a significant increase in high force MTU stiffness (50-90% MVT). As noted in Chapter 6, the ECT in the current thesis employed a more extended knee joint position than Tillin et al. (2012). MTU stiffness changes are known to be greater after isometric training with a lengthened MTU (Kubo et al. 2006b). Although whether there is an angle specific interaction with the level of stiffness adaptations is unknown. The change in elongation values after ECT were seemingly consequent to an increased MTU compliance at the lowest force levels, though a mechanism for this is unknown. Nevertheless, there are potential functional implications of this increase in overall MTU compliance. For instance, greater MTU compliance may act to increase the optimal joint-angle for torque production (Lemos et al. 2008), and perhaps reduce the positive strains experienced by muscle-fascicles during MTU length change (Roberts and Konow 2013). These effects could potentially decrease the susceptibility to strain-induced muscle damage during eccentric contractions and thus lessen injury risk. These hypothetical consequences warrant future investigation.

In contrast, SCT training produced no shift in the force-elongation relationship (i.e. no change in elongation at 80% MVT), suggesting no overall change in stiffness after 12 weeks, however the high force MTU stiffness was greater post SCT. These findings are partially consistent with previous work. Greater higher force MTU stiffness has been consistently found in SCT intervention studies and is also typically associated with a general left shift in

the force-elongation relationship (i.e. lesser elongation throughout the range of force levels) (Kubo et al. 2001, 2006b, 2009; Arampatzis et al. 2007a). The increased higher force MTU stiffness in Chapter 6 (+21%) was more moderate than previously reported in the knee extensors after 12 weeks isometric SCT (e.g. +51-58%, Kubo et al. 2001, 2006b, 2009). This discrepancy may be largely accounted for by methodological differences. Specifically, Chapter 6 compared MTU stiffness at the same absolute tendon forces pre-post training, yet these earlier studies measured stiffness over tendon forces relative to MVT (50-100% MVT). Therefore, the previously reported stiffness changes were amplified by increased maximal strength; curvi-linear nature of the force-elongation relationship.

Chapter 7 revealed that MTU distal tissue elongation (at the highest common force) was no different between CST, STT and UNT, suggesting strength training does not lead to changes in lower force region MTU stiffness and the overall force-MTU elongation relationship (overall stiffness). Moreover Chapter 7 intriguingly showed that greater high force stiffness after short-term SCT (Chapter 6) was not replicated in CST vs. UNT individuals (i.e. highest common force MTU stiffness was similar in CST and UNT). This awkwardly questions the validity of strength training to elicit changes in higher force MTU stiffness. Further, this result possibly implies that if the STT group were to continue training, they would experience an increase in MTU compliance at common forces. Longitudinal interventions would be needed to give credence to this supposition, and a precise explanation for the present results is elusive. However it can be implied that considering the aforementioned tendon results from Chapters 6 and 7, the MTU findings are indicative of an influence of strength training on aponeurosis properties. Perhaps herein lies a source of uncertainty regarding how to explain the contrary results. MTU stiffness measurements are rather inexact and indirect estimates derived from measuring muscle-aponeurosis displacement (distal tissue elongation) and presuming aponeurosis force is commensurate with tendon force. During muscle contraction, aponeuroses are known to experience a bi-axial loading pattern, undergoing both longitudinal and transverse strain (Aziz and Roberts 2009). The transverse strain results from muscle lateral expansion proportional to relative muscle force production, and acts to increase the overall longitudinal stiffness of the aponeurosis (Azizi and Roberts 2009). To provide insight into the present results, further investigations could incorporate 3D imaging techniques (ultrasound [Farris et al. 2013] or MRI [Iwanuma et al. 2011]) that can capture the bi-axial aponeurosis strain.

8.5. Summary

Despite theoretically being more physiologically representative, measures of $_{eff}$PCSA during maximal voluntary contraction were no more strongly correlated, than $_{eff}$PCSA measured at rest, to maximal isometric strength. PA seems inconsequential for *in vivo* muscle strength and FL could only explain a small proportion of the large variance in explosive voluntary RTD during the initial phase of rising torque. Likewise, relative MTU stiffness could account for a limited extent of the variance in relative RTD during evoked contractions and the most rapid phase of explosive voluntary contractions. Once the seemingly overwhelming influence of maximal strength was considered, there was no evident relation between absolute MTU stiffness and RTD. Stiffness of the free tendon did not explain any of the substantial inter-individual variability in RTD. However PT stiffness was increased equally following sustained- and explosive-contraction strength training, due to their similar positive effect on tendon material stiffness, as neither training approach elicited tendon hypertrophy. However, tendon elongation/strain at any given absolute tendon force/stress was reduced after explosive training only. In contrast, sustained-contraction, but not explosive, strength training increased MTU stiffness, while neither training modality altered MTU elongation/strain from pre-post training. Tendon size was no greater in a group of chronic strength trained individuals, which provides convincing evidence that strength training does not stimulate tendon hypertrophy. Further this chronic strength trained group possessed similar tendon material (and resultantly mechanical) stiffness to a short-term strength trained group, indicating there may be a plateau in tendon stiffness adaptation following short-term training. However, PT elongation at equal tendon forces was lesser in chronic trained only, implying some longer-term adaptation in the tendon that increases generic tendon stiffness as oppose to the higher force/stress stiffness/modulus. Intriguingly, highest common force muscle-tendon unit stiffness was not apparently greater in the chronic strength trained group, and neither was there any difference in MTU elongation (at a common tendon force) in strength-trained groups, in comparison to untrained individuals. Only sustained-contraction strength training resulted in an increase in aponeurosis size, in concert with muscle hypertrophy, with the potential for longer-term aponeurosis hypertrophy was corroborated by the larger aponeurosis of the chronic strength trained group.

8.6. Future Directions

Following the results of the present thesis, possible suggestions for further research are:

1. ***Further explore the inter-individual variability in muscle architecture.*** The greater variability in the individual constituent quadriceps femoris muscles than the whole muscle group in Chapter 4 was intriguing. This phenomenon of a possible compensation of architecture characteristics between muscles could be explored in more detail and investigated in other muscle groups.

2. ***Investigate the influence of fascicle length on in vivo strength characteristics***. In particular: (a) explore valid protocols to examine high velocity torque production (>700°), than is possible with current isovelocity dynamometry, in order to more thoroughly investigate the relationship of FL with high velocity torque; (b) more detailed examination of the relationship between fascicle length and isometric RTD. A larger cohort (than Chapter 4) would be advantageous, and a more comprehensive estimate of whole muscle FL, by measuring at multiple sites should be derived. Possibly using techniques that account for muscle 3D structure (e.g. 3D ultrasound, or diffusion tensor MRI) could facilitate future investigations.

3. ***More thoroughly investigate the differential PT and MTU adaptations to ECT training***. Chapter 6's results regarding the effects of ECT were only found in a small group. Documenting similar findings in a larger cohort would be needed to firmly corroborate the results. Measurements at multiple time-points could delineate a more accurate time-course for tendinous tissue adaptations. Whether there is a knee-joint angle specific effect of ECT could be explored. Appreciation of adaptations in response to ECT in other population groups (e.g. older adults, tendon pathology) is needed.

4. ***Conduct prolonged SCT interventions.*** The increased high force MTU stiffness after SCT (Chapter 6), yet no difference in highest common force MTU stiffness in CST vs. UNT (Chapter 7) implies a bi-phasic MTU stiffness adaptive response (i.e. increase within 12 weeks, subsequent decrease with more prolonged training) to strength training focused on sustained high force contractions. Moreover, no reduction in PT strain in SCT (Chapter 6), though CST had lesser PT strain than both UNT and STT (Chapter 7)

suggests this adaptation occurs after 12 weeks training. Therefore, the results of Chapters 6 and 7 indicate that longer than 12 weeks strength training is needed to more fully understand the nature of MTU and PT adaptation to SCT training. Intervention periods of 6-9 months would perhaps be feasible.

5. ***Investigate the mechanisms for the increased Young's modulus after strength training.*** The nature of tendon microstructure and/or extracellular matrix biochemical composition changes responsible for material stiffness improvements after strength training needs to be ascertained. Exploring such mechanisms could be logistically challenging owing to requirement for invasive procedures. Perhaps determining the validity of non-invasive methods thought to reflect tendon structure (e.g. MRI signal intensity, Kubo et al. 2012; ultrasound tissue characterisation, Docking et al. 2016) is needed. Appropriate non-invasive imaging markers could perhaps be initially used to refine the time-course of adaptation prior to the use of invasive procedures.

6. ***Explore the possible methods of examining muscle stiffness in vivo, and investigate the relation of muscle stiffness to fascicle length, RTD and the impact of strength training on muscle stiffness.*** Recently, measures of muscle stiffness *in vivo* have been derived from measuring the degree of muscle length change during a rapid stretch or release imposed during an isometric contraction via traditional two-dimensional ultrasonography utilising a relatively high recording frequency (96 Hz ultrasound frame rate, Kubo et al. 2014; or very high 2000 Hz frame rate, Hauraix et al. 2015). Tested hypotheses could include: muscle-stiffness and FL are inversely related; greater muscle stiffness is associated with faster RTD and strength training increases muscle stiffness. Muscle stiffness is thought to relate to the muscle fibre type (greater stiffness in slower contracting fibres: Goubel and Marini 1987), thus simultaneous muscle composition measurements maybe needed.

CHAPTER 9

Appendices

9.1. Isovelocity Torque Analysis

Isovelocity peak torque was determined at angular velocities of 50 and 350°s^{-1}. Before active trials (voluntary contractions), the participant's leg was moved through the test range of motion in a continued passive movement (CPM) trial at both velocities (Figure 9.1) to permit active voluntary torque to be corrected for passive torque contribution a posteriori.

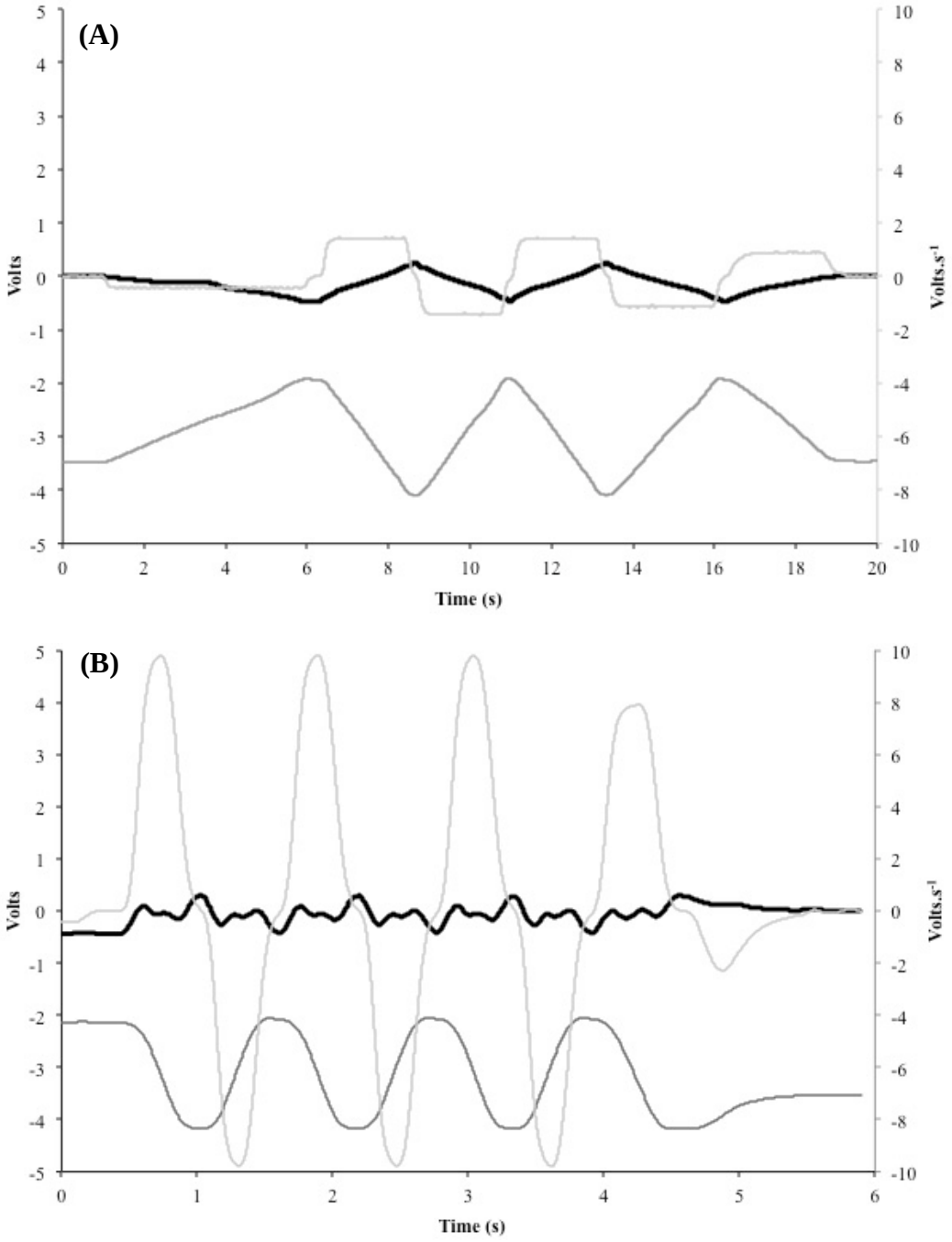

Figure 9.1. Example raw data from continued passive movement trials for 50°s^{-1} (A) and 350°s^{-1} (B). Left y-axis: knee extension torque (black line), crank angle (dark grey line); Right- y-axis = velocity (light grey line). Positive velocity corresponded to the knee extension phase of the movement.

Voluntary isovelocity trials were completed via 2/3 eccentric-concentric contraction cycles at 50/350° s^{-1} (Figure 9.2). The eccentric part of the cycle served as a pre-activation phase to attempt to maximize concentric muscle performance.

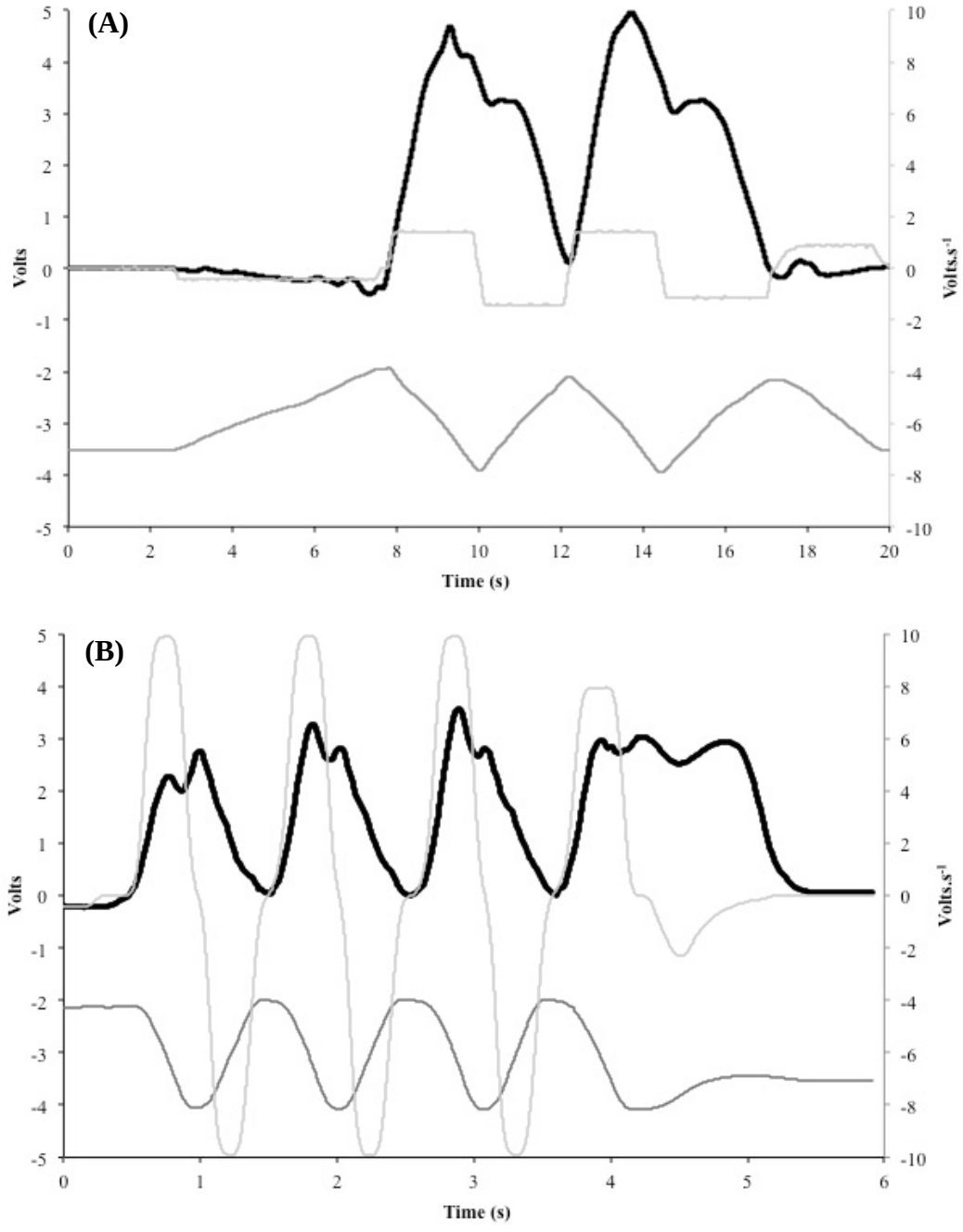

Figure 9.2. Example raw data from active trial (voluntary knee extensor contractions) at 50°s^{-1} (A) and 350°s^{-1} (B). Left y-axis: knee extension torque (black line), crank angle (dark grey line). Right y-axis = velocity (light grey line). Positive velocity corresponds to the concentric contraction phase of the movement.

Upon visual inspection, the concentric contraction with the apparent highest torque was analysed further. The acceleration and deceleration phases of the movement were discounted to identify the isovelocity region (±10% pre-set constant velocity; Figure 9.3). The peak torque within the isovelocity region was then corrected (addition of torque necessary to overcome weight of limb) for passive torque by matching the angle of peak torque within the CPM trial. The corrected active peak torque was then defined as velocity specific maximal concentric torque.

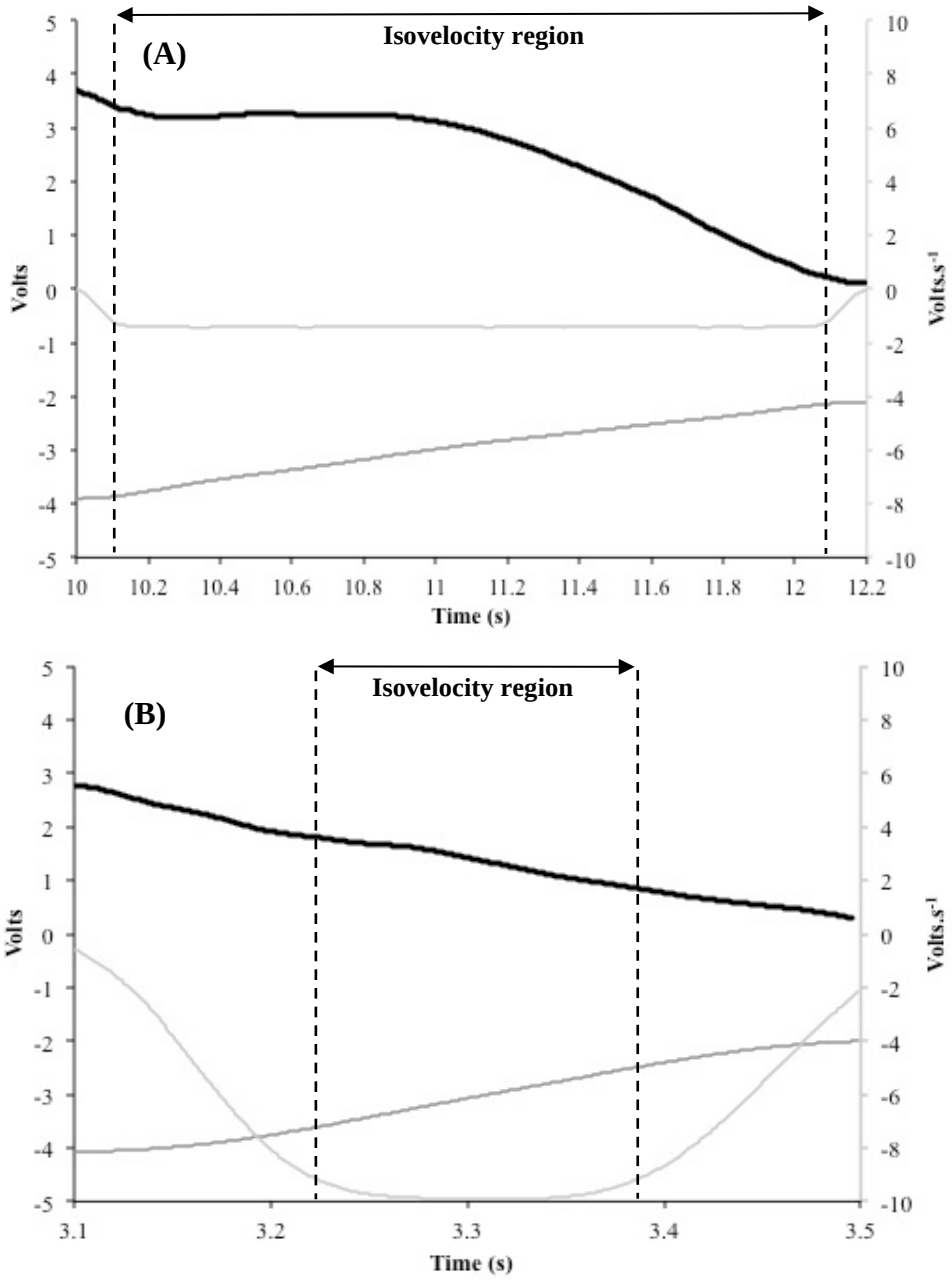

Figure 9.3. Example raw data from isovelocity concentric contractions at $50°s^{-1}$ (A) and $350°s^{-1}$ (B). Left y-axis: knee extension torque (black line), crank angle (dark grey line). Right y-axis = velocity (light grey line). Peak torque within the isovelocity region (±10% pre-set constant angular velocity) was determined.

9.2. Calculation of Tissue Stiffness and Tendon Young's Modulus

9.2.1. Tissue Stiffness

A second-order polynomial with the y-intercept set to zero was fitted to the raw force-elongation data derived by from simultaneous estimations of tendon force and the associated tissue elongation of the patellar tendon (e.g. Figure 9.4) or vastus lateralis aponeurosis (muscle-tendon unit [MTU]; Figure 9.5) displacement during contraction. The associated quadratic equation was used to interpolate the tendon elongation values at designated tendon force levels.

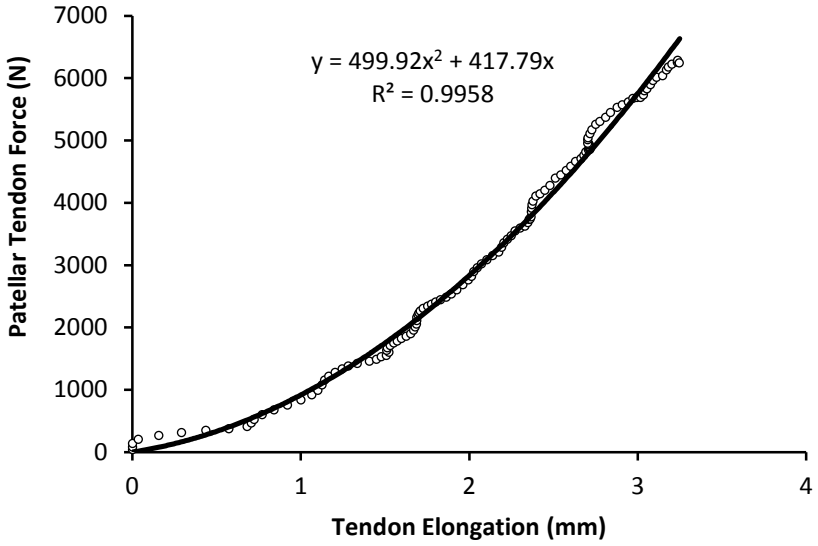

Figure 9.4. Example patellar tendon force-elongation relationship: raw data (circles) are fitted when a second-order polynomial function (black line) force through zero (y-intercept).

Common force level from Chapter 7 = 4200 N; applied to Figure 9.4's quadratic equation:

Tendon elongation at 100% common force (4200 N) = 2.511 mm

Tendon elongation at 80% common force (3360 N) = 2.208 mm

Change in force = 4200 – 3360 = 840 N

Change in elongation = 2.511 – 2.208 = 0.303 mm

Tendon Stiffness = Δ in force (840 N)/Δ in tendon elongation (0.303) = **2777 N.mm^{-1}**

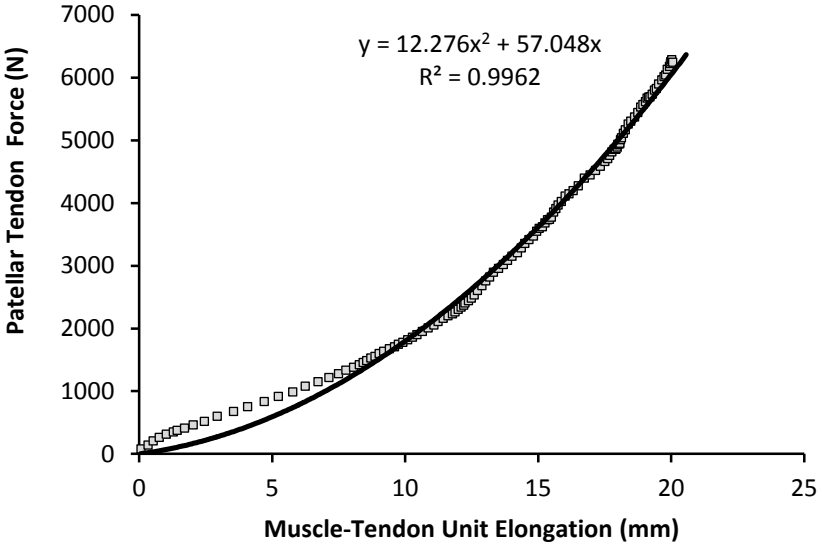

Figure 9.5. Example patellar tendon force- muscle-tendon unit elongation relationship: *raw data* (squares) are fitted when a second-order polynomial function (black line) forced through zero (y-intercept).

Common force level from Chapter 7 = 4200 N; applied to Figure 9.5's quadratic equation:

MTU elongation at 100% common force (4200 N) = 16.32 mm

MTU elongation at 80% common force (3360 N) = 14.38 mm

Change in Force = 4200 – 3360 = 840 N

Change in Elongation = 16.32 – 14.38 = 1.94 mm

MTU Stiffness = Δ in force (840 N)/Δ in tendon elongation (1.94) = **434 N.mm^{-1}**

9.2.2. Patellar Tendon Young's Modulus

Dividing tendon force by the mean tendon cross sectional-area equated to tendon stress, and expressing tendon elongation relative to the initial (resting) length gave tendon strain. A second-order polynomial with the y-intercept set to zero was fitted to the raw stress-strain data (e.g. Figure 9.6). The associated quadratic equation was used to interpolate the tendon strain values at designated tendon stress levels.

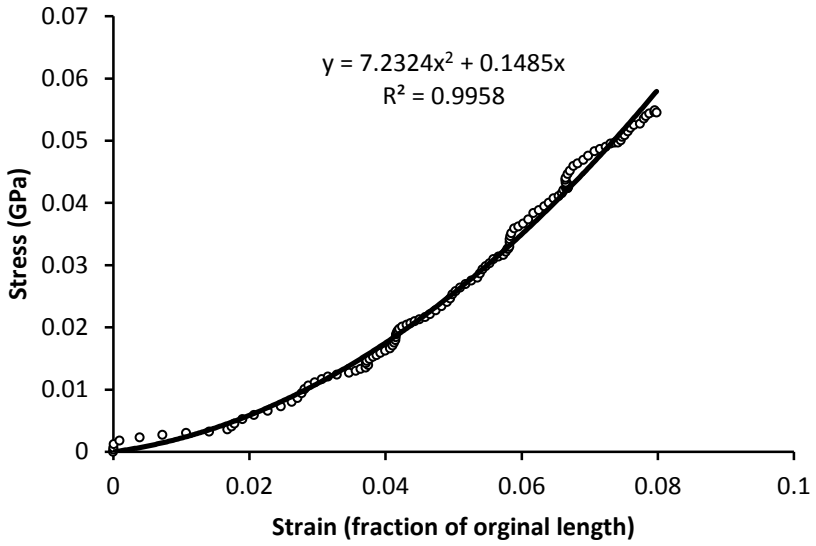

Figure 9.6. Example patellar tendon stress-strain relationship: *raw data* (circles) are fitted when a second-order polynomial function (black line) force through zero (y-intercept).

Common force level from Chapter 7 = 4200 N; applied to Figure 9.6's quadratic equation:

Tendon strain at 100% common stress (40 MPa [0.04 GPa]) = 0.068

Tendon elongation at 80% common stress (32 MPa [0.032 GPa]) = 0.057

Change in stress = 8 MPa [0.008 GPa]) = 0.008

Change in strain = 0.0648 – 0.0570 = 0.078

Tendon Young's Modulus = Δ in stress (0.008)/Δ in strain (0.0.078) = **1.026 GPa**

9.3. Ultrasound Imaging

9.3.1. Vastus Lateralis Aponeurosis Displacement

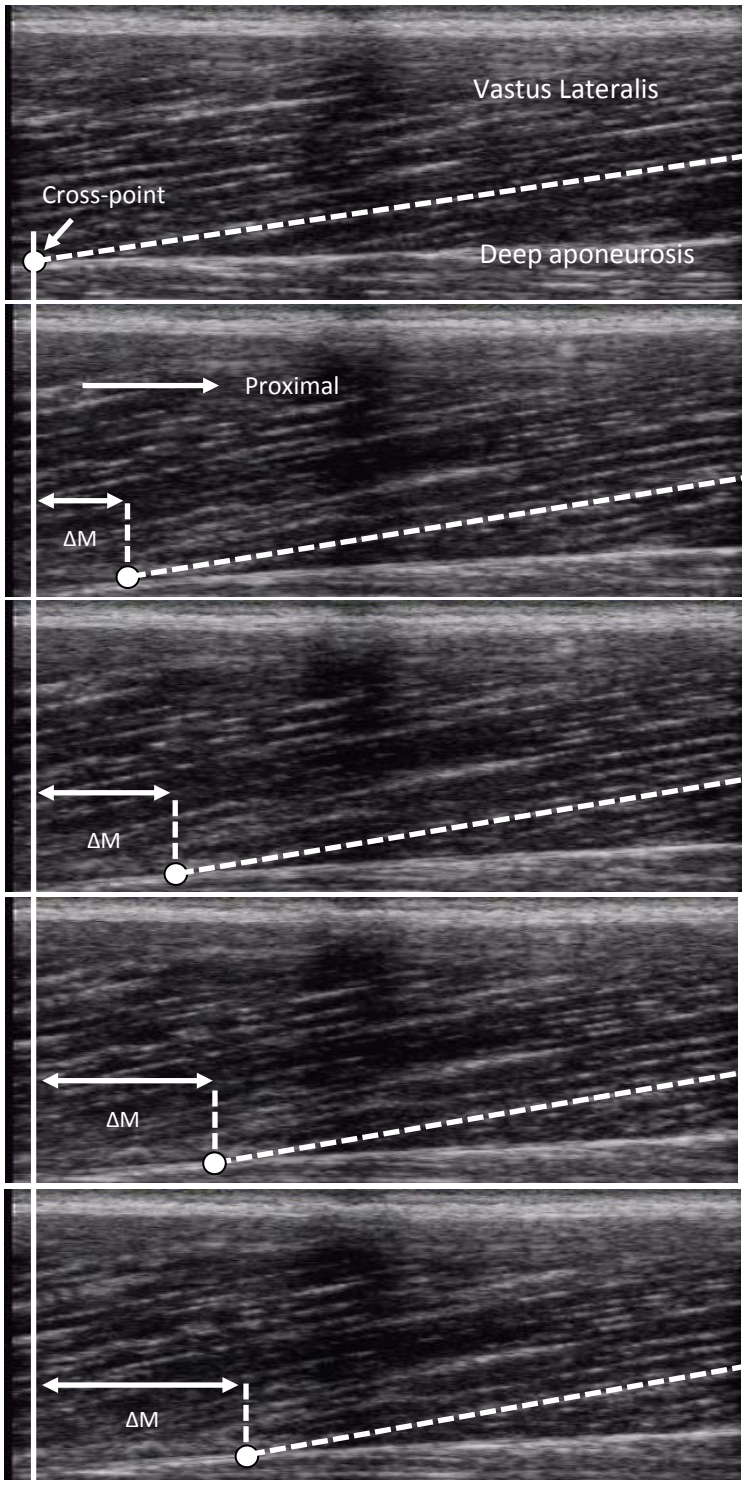

Figure 9.7. Example ultrasound images of the vastus lateralis muscle at rest (A) and various tendon forces (N) during constant loading-rate isometric ramp knee extensor contractions: (B) 1000, (C) 2000, (D) 4000 and (E) 6000N. The proximal displacement (ΔM) of the muscle fascicle-aponeurosis cross point (small white circle) at was defined as the distal muscle-tendon unit elongation.

9.3.2. Patellar Tendon Displacement

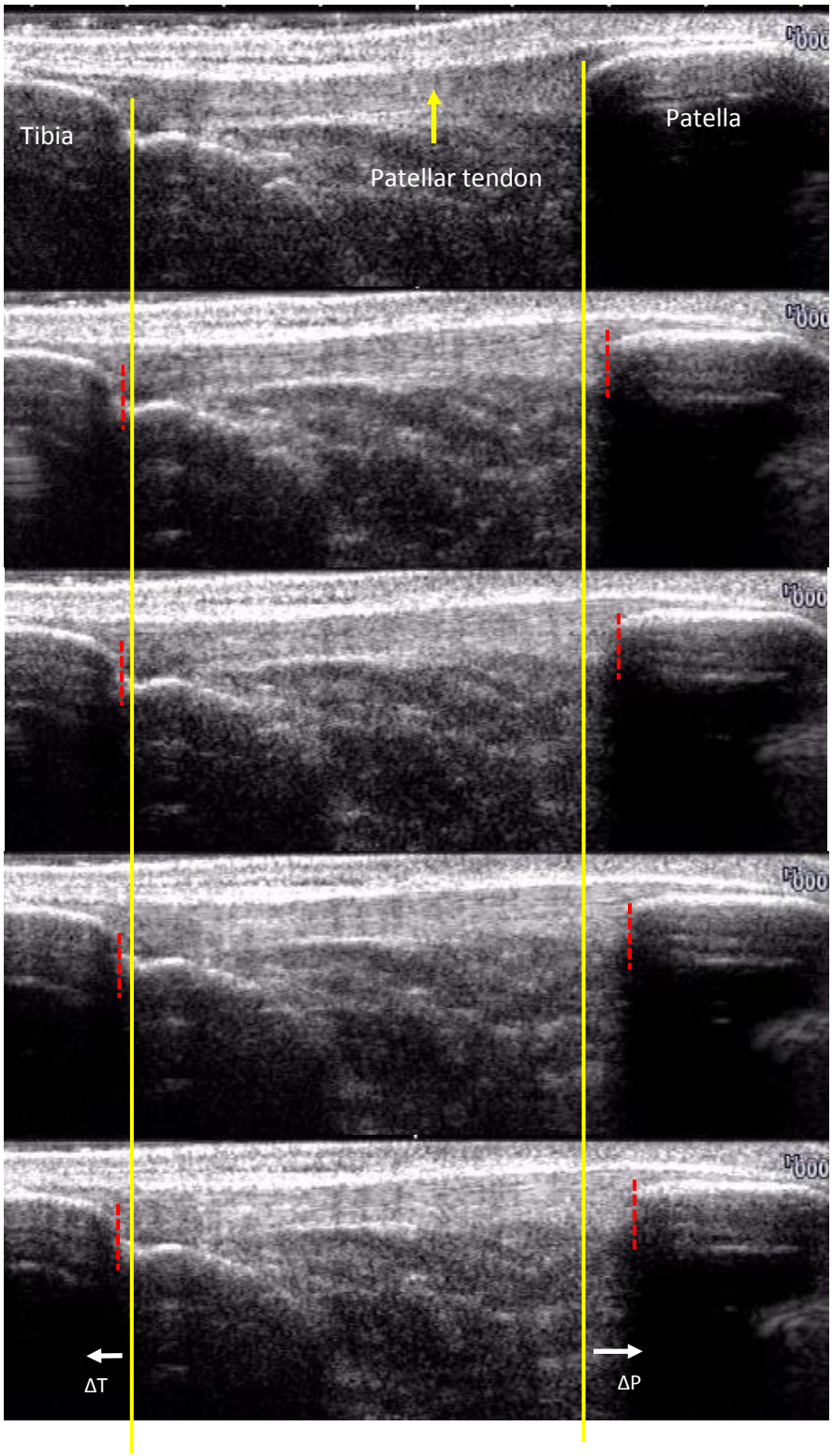

Figure 9.8. Example ultrasound images of the patellar tendon at rest (A) and various tendon forces (N) during constant loading-rate isometric ramp knee extensor contractions: (B) 1000, (C) 2000, (D) 4000 and (E) 6000N. The tendon attachment to the patella and tibia was tracked and the combined proximal and distal displacement of the patella and tibia (ΔP and ΔT) was defined as patellar tendon elongation.

9.3.3. Quadriceps Femoris Muscle Architecture

Architectural parameters (fascicle length [FL; *length of the fascicular path between the aponeuroses attachments*] and pennation angle [PA; *angle between the fascicular path and the muscle's deep lower aponeurosis*]) were measured from ultrasound images of each constituent muscle of the quadriceps femoris: vastus lateralis (VL), vastus intermedius (VI), vastus medialis (VM), rectus femoris (RF), recorded at rest and during maximal voluntary contraction (MVC) (Figures 9.9-9.11, example participant 1), as well as at 20% maximal voluntary torque increments during ramp contractions (Figures 9.12-9.14, example participant 2).

Measurements were performed via manual identification of structural features. Any visible fascicle curvature was included in the fascicle trace. If fascicles extended off the ultrasound field of view, manual linear extrapolation was employed to complete FL measurement.

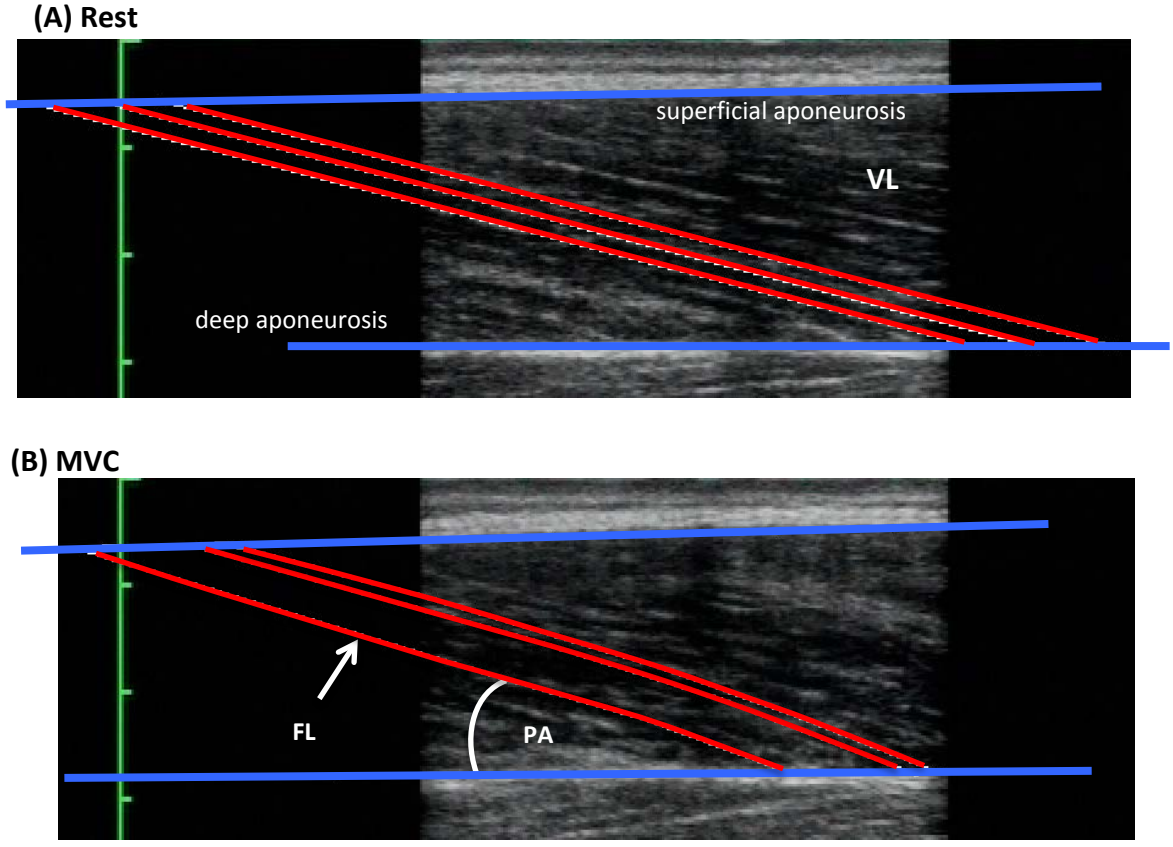

Figure 9.9. Example ultrasound image of the vastus lateralis (VL) muscle at rest (A) and an isometric maximal voluntary contraction (MVC) (B), showing the identification of the muscle aponeuroses and fascicular path to measure architecture: fascicle length (FL) and pennation angle (PA).

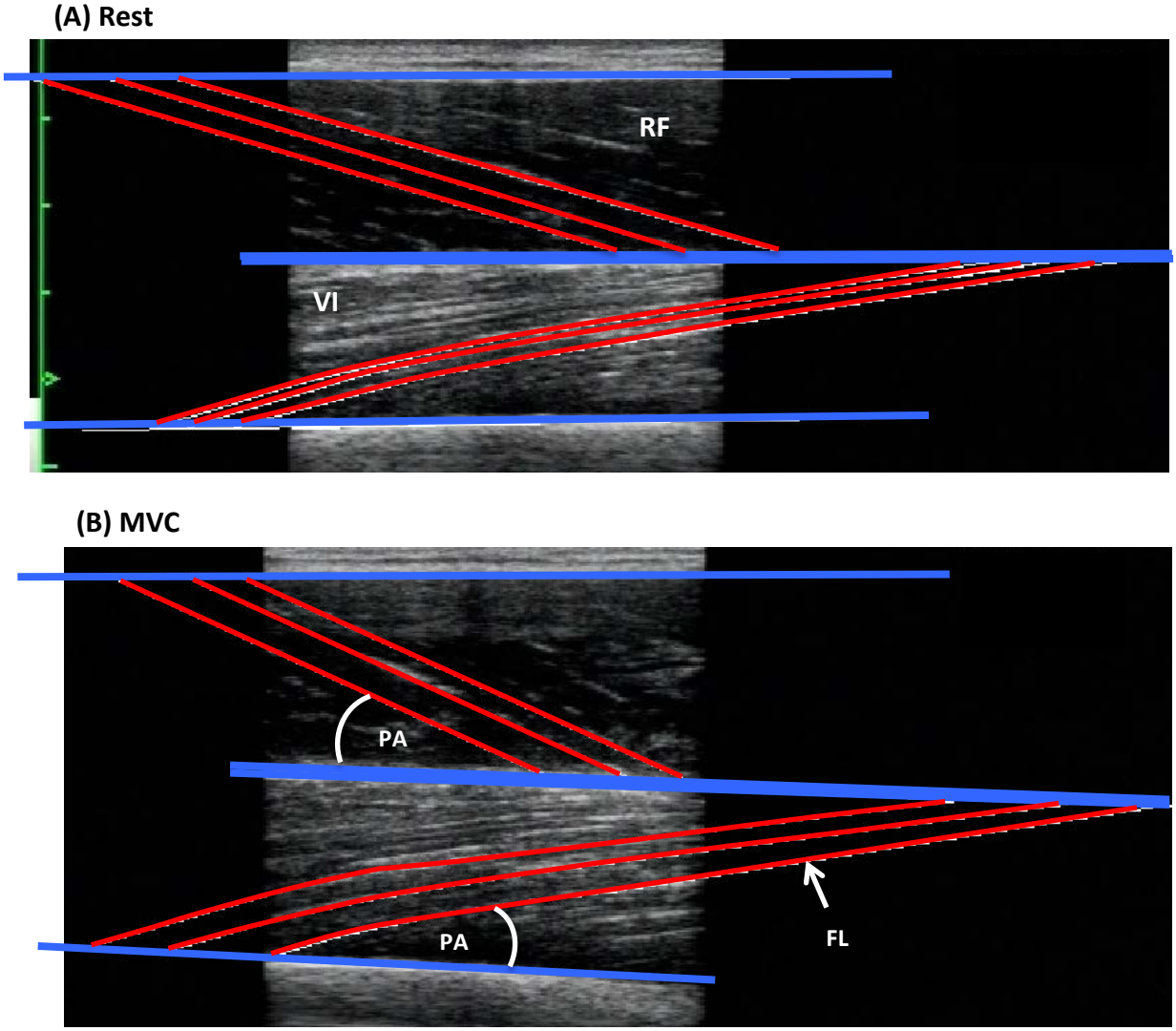

Figure 9.10. Example ultrasound image of the rectus femoris (RF) and vastus intermedius (VI) muscle at rest (A) and (B) depicting the measurements of architecture: fascicle length (FL) and pennation angle (PA).

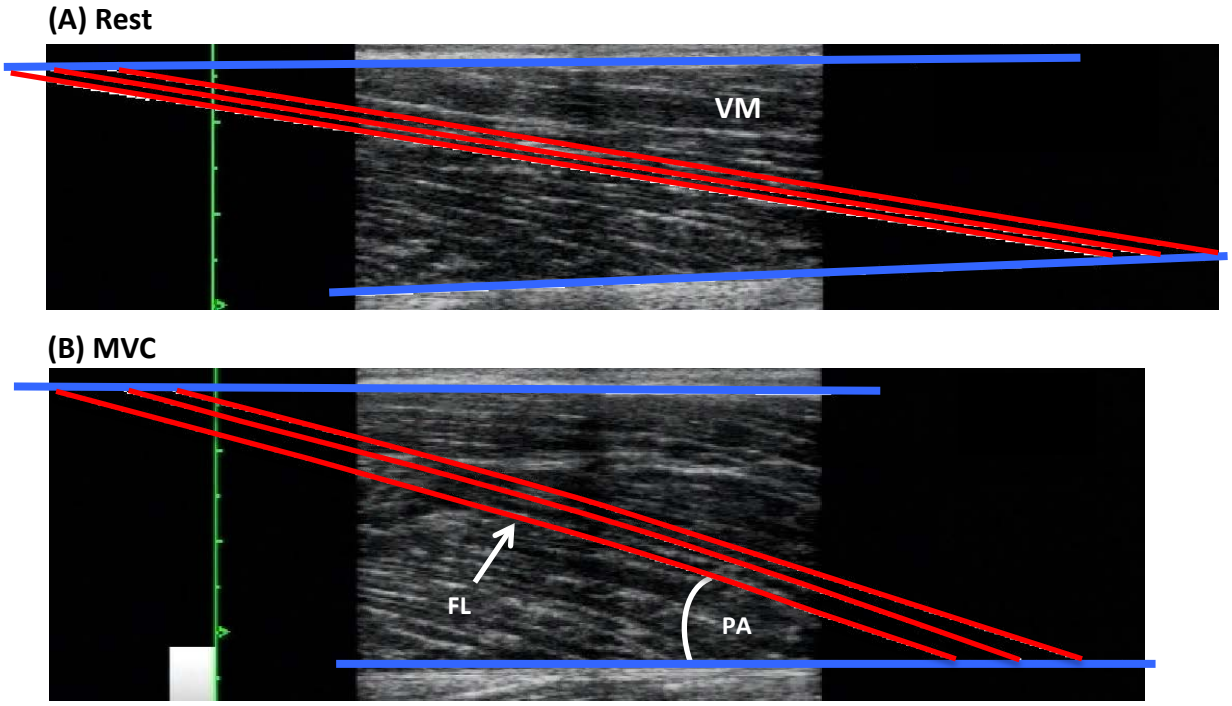

Figure 9.11. Example ultrasound image of the vastus medialis (VM) muscle at rest (A) and during an isometric maximal voluntary contraction (MVC) (B), showing the identification of the muscle aponeuroses and fascicular path to measure architecture: fascicle length (FL) and pennation angle (PA).

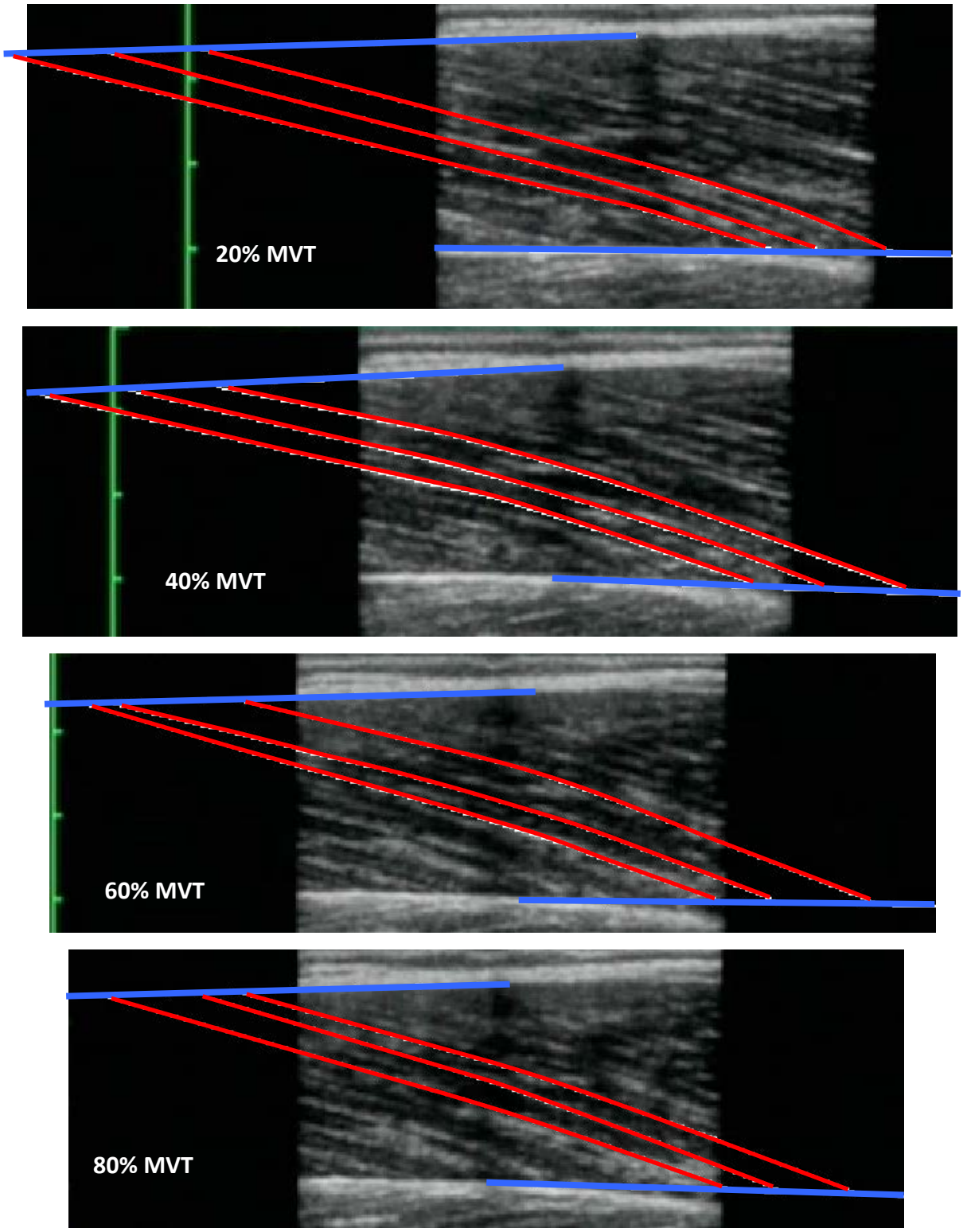

Figure 9.12. Example ultrasound images of the vastus lateralis muscle at 20% maximal voluntary torque (MVT) increments during a isometric ramp contraction, showing the identification of the muscle aponeuroses and fascicular path to measure architecture: fascicle length and pennation angle.

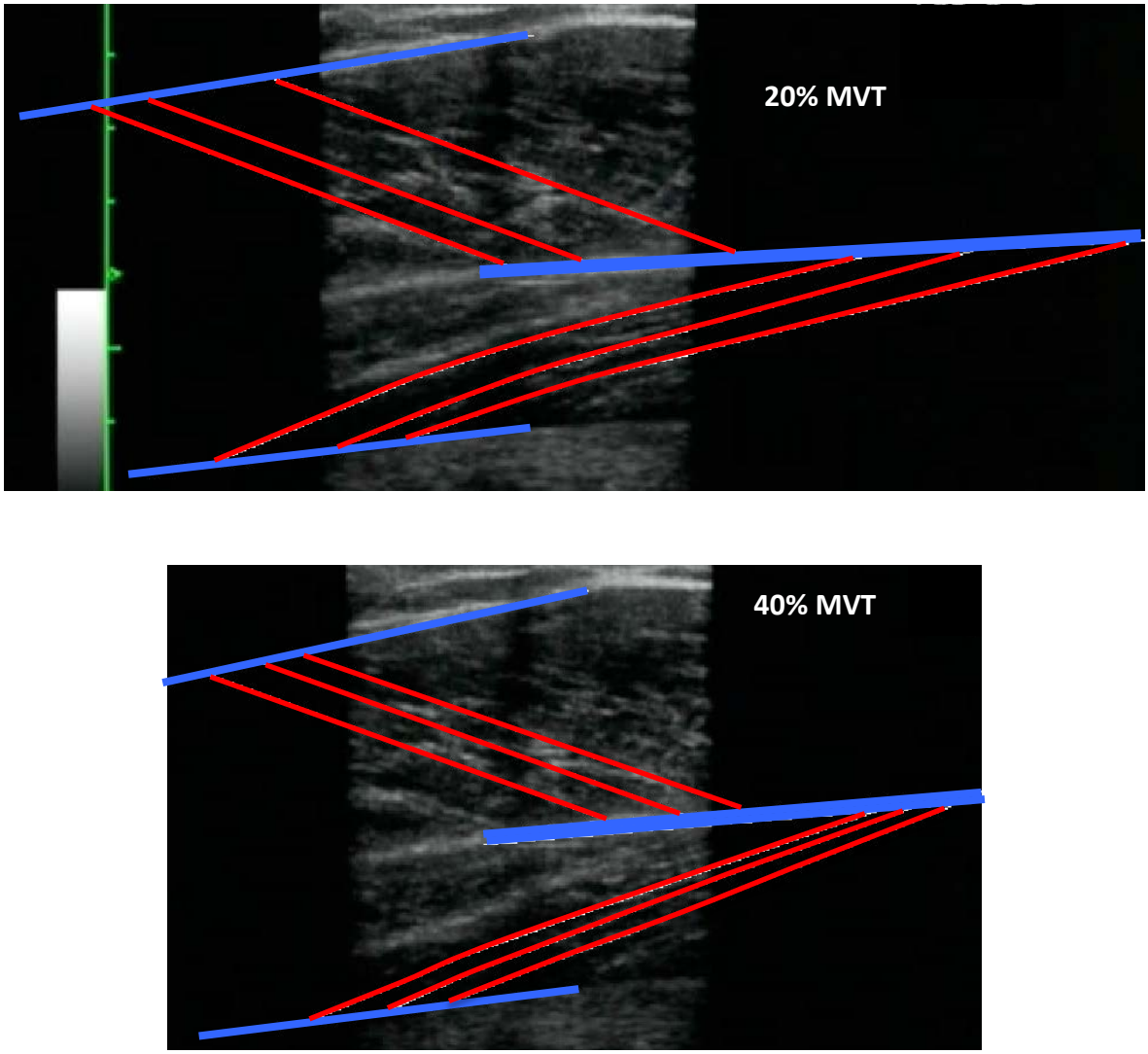

Figure 9.13. Example ultrasound images of the rectus femoris (top) and vastus intermedius (bottom) muscle at 20 and 40% maximal voluntary torque (MVT) increments during a isometric ramp contraction, showing the identification of the muscle aponeuroses and fascicular path to measure architecture: fascicle length and pennation angle.

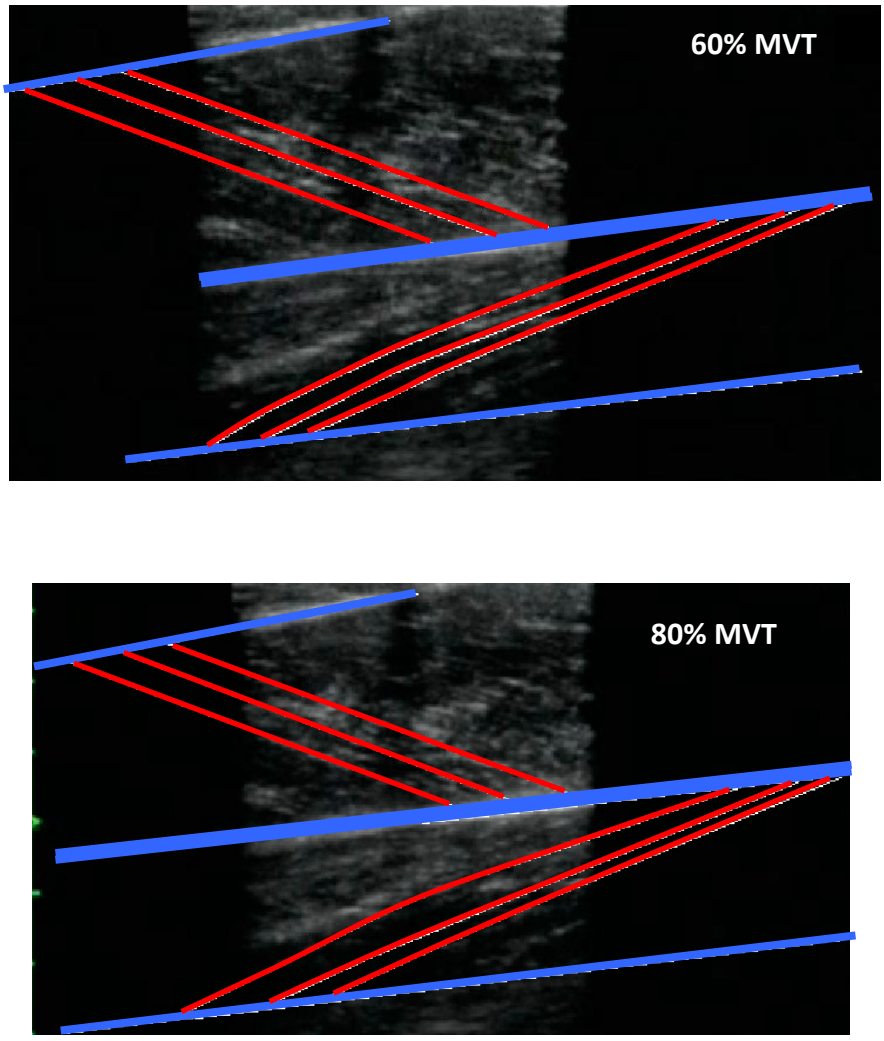

Figure 9.13 cont. Example ultrasound images of the rectus femoris (top) and vastus intermedius (bottom) muscle at 60 and 80% maximal voluntary torque (MVT) increments during a isometric ramp contraction, showing the identification of the muscle aponeuroses and fascicular path to measure architecture: fascicle length and pennation angle.

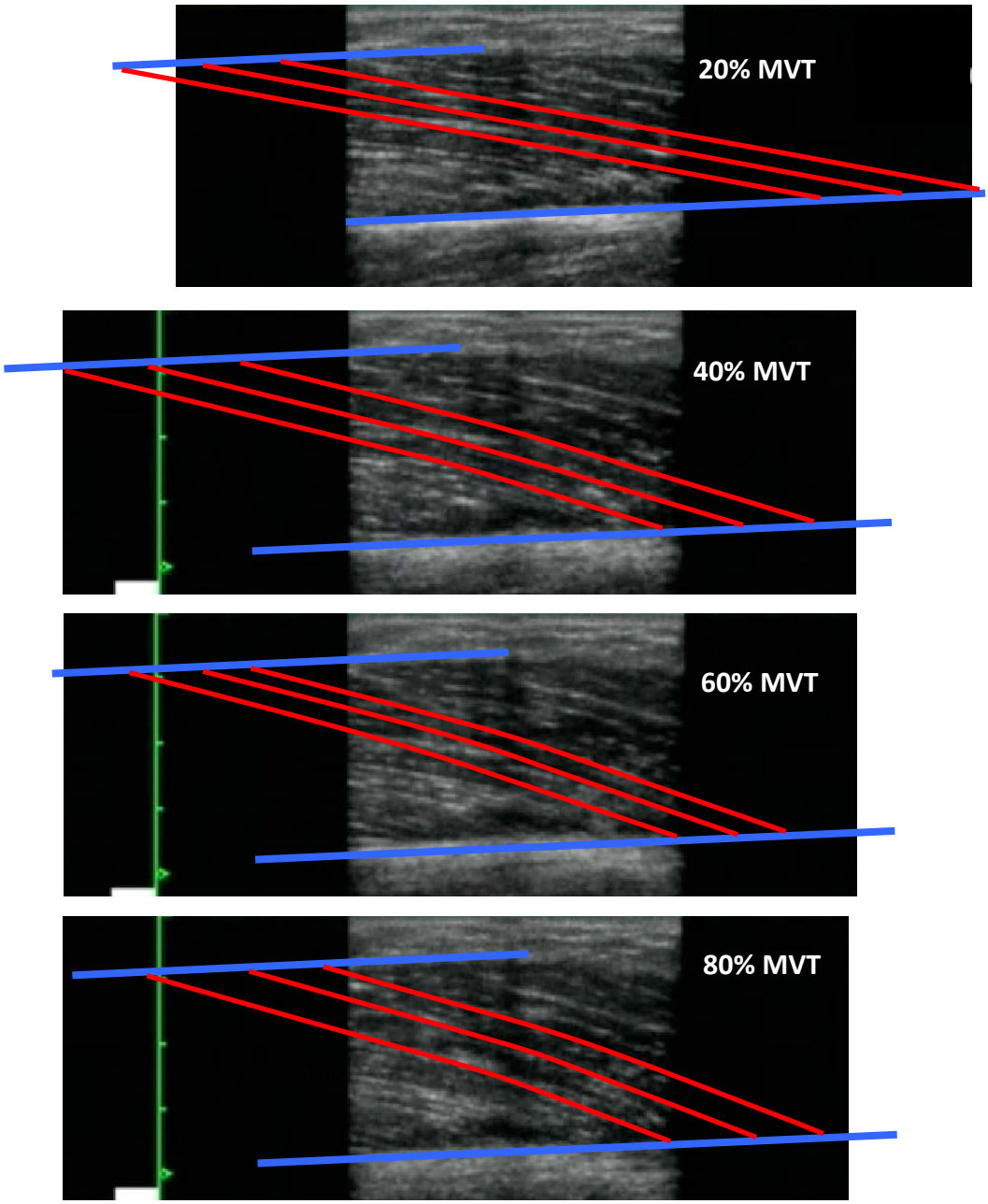

Figure 9.14. Example ultrasound images of the vastus medialis muscle at 20% maximal voluntary torque (MVT) increments during a isometric ramp contraction, showing the identification of the muscle aponeuroses and fascicular path to measure architecture: fascicle length and pennation angle.

9.4. Magnetic Resonance Imaging

9.4.1. Quadriceps Femoris Anatomical Cross-Sectional Area and Volume

The anatomical cross-sectional area (ACSA) of each of the four constituent muscles of the quadriceps femoris (QF) muscle: vastus lateralis (VL), vastus intermedius (VI), vastus medialis (VM) and rectus femoris (RF), were manually outlined (Figure 9.15) on every third axial magnetic resonance image, starting from most proximal image in which the muscle appeared. The volume of each muscle was calculated as the area under ACSA-muscle length (distance between the most proximal and distal MR images in which the muscle was visible) cubic spline curve (Figure 9.16). The sum of the volumes of each constituent muscle gave total quadriceps femoris muscle volume.

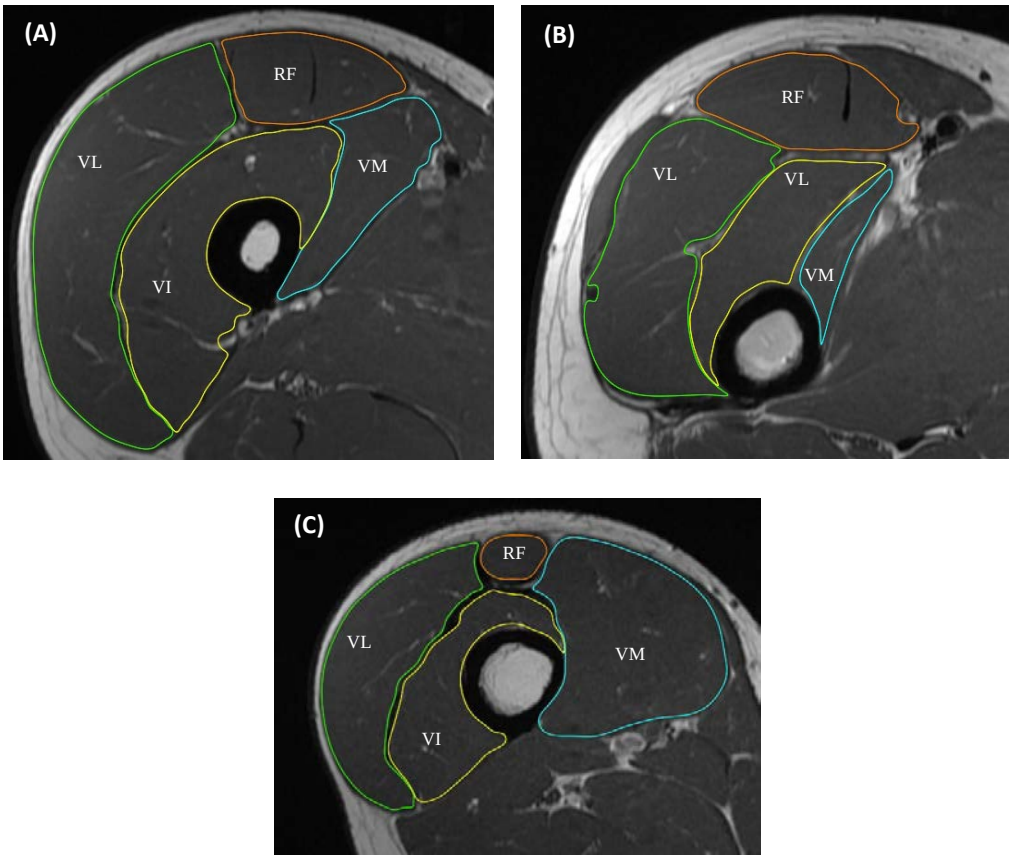

Figure 9.15. Example of the manual segmentation of the constituent muscles of the quadriceps femoris muscle in axial plane magnetic resonance images at (A) proximal, (B) middle, and (C) distal thigh locations.

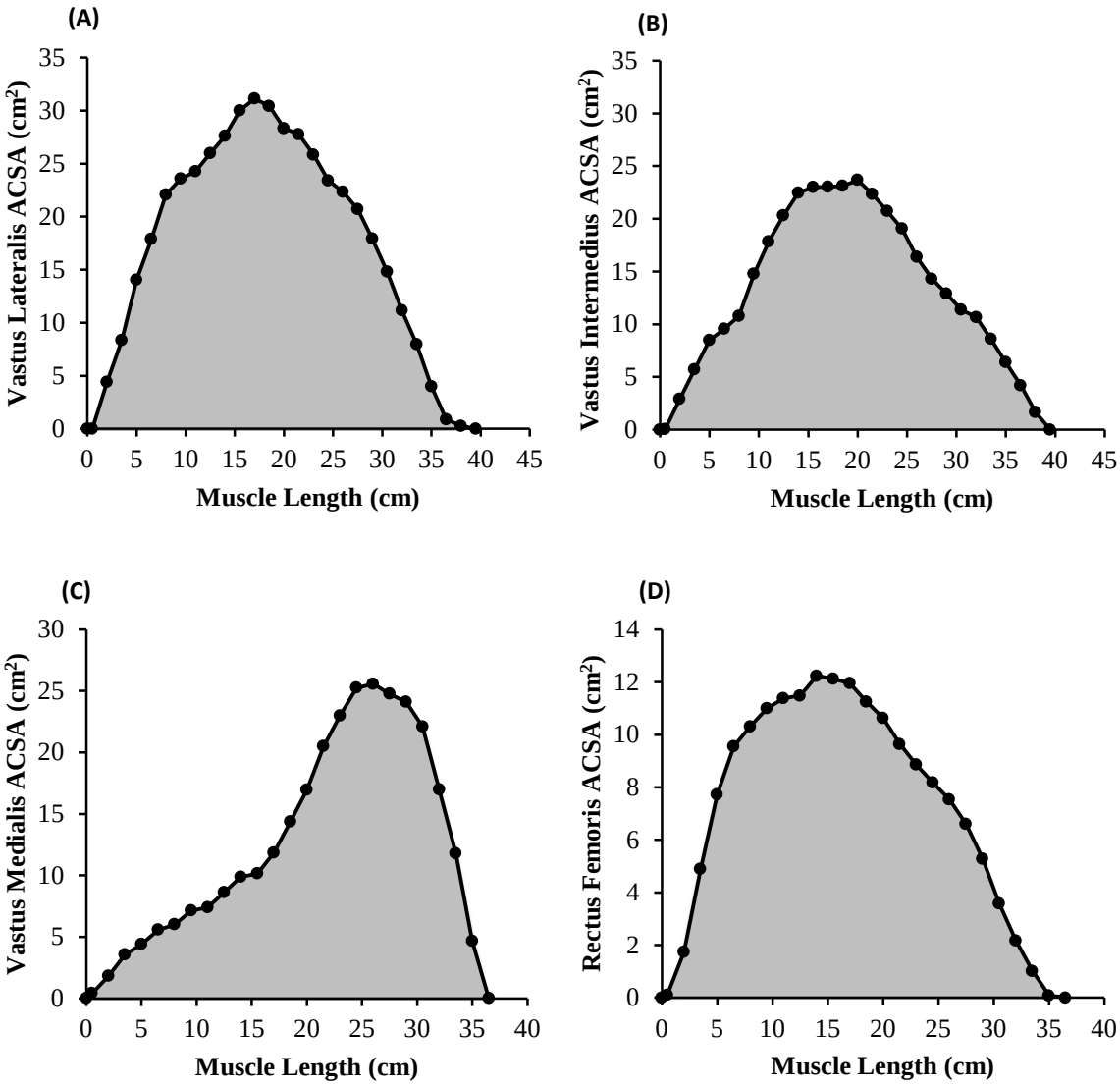

Figure 9.16. Example of quadriceps femoris muscle volume calculation. A cubic spline curve was fitted through the data points defining the anatomical cross-sectional area (ACSA)-muscle length relationship and muscle volume (cm^3) calculated as the area under the curve. Total quadriceps femoris muscle volume equated the sum of the constituent muscles volumes.

9.4.1.1. Quadriceps Femoris Effective Physiological Cross-Sectional Area

For each constituent muscle of the quadriceps femoris muscle, the cross-sectional area of the muscle fascicles perpendicular to the line of action (i.e. physiological cross-sectional area, PCSA) was calculated by dividing its volume by its fascicle length. Subsequently the effective PCSA for each constituent muscle was determined by multiplying the PCSA of the muscle by the cosine of the respective muscles pennation angle.

E.g. Quadriceps Femoris Effective PCSA calculation

Vastus Lateralis
Volume (VOL) = 610 cm^3, FL = 9.7 cm, PA = 15 degs
PCSA (VOL/FL) = 62.9 cm^2
PA (°)/57.2958 radians = 0.262 radians
Cosine PA (radians) = Cos (0.262) = 0.966
Effective PCSA = PCSA*CosPA = 60*0.966 = **60.7 cm^2**

Vastus Intermedius
Volume (VOL) = 560 cm3, FL = 8.3 cm^2, PA 14 degs
PCSA (VOL/FL) = 67.5 cm^2
PA (°)/57.2958 radians = 0.244
Cosine PA (radians = 0.970
Effective PCSA = PCSA*CosPA = 67.5*0.970 = **65.5 cm^2**

Vastus Medialis
Volume (VOL) = 430 cm3, FL = 10.0 cm^2, PA 16 degs
PCSA (VOL/FL) = 43.0 cm^2
PA (°)/57.2958 radians = 0.269
Cosine PA (radians) = 0.961
Effective PCSA = PCSA*CosPA = 42.0*0.961 = **41.3 cm^2**

Rectus Femoris
Volume (VOL) = 300 cm3, FL = 8.5 cm2, PA 18 degs
PCSA (VOL/FL) = 35.3 cm^2
PA (°)/57.2958 radians = 0.314
Cosine PA (radians) = 0.951
Effective PCSA = PCSA*CosPA = 35.3*0.951 = **33.6 cm^2**

Total quadriceps femoris effective PCSA = 60.7 + 65.5 + 41.3 + 33.6 = 201.1 cm^2

E.g. Constituent muscle proportional contributions (effective PCSA/total effective PCSA)
VL = 60.7/201.1 = 0.302
VI = 165.5/201.1 = 0.326
VM = 41.3/201.1 = 0.205
RF = 33.6/201.1 = 0.167

9.4.2. Vastus Lateralis Aponeurosis Area

The width of the deep aponeurosis of the vastus lateralis (VL) muscle was defined as the length of the visible black segment between the VL and vastus intermedius muscle in the thigh MR images (Figure 9.17). VL aponeurosis width was traced manually on every third axial image, starting from most distal image in which the aponeurosis was visible. VL aponeurois area was calculated as the area under aponeurosis width-length (distance between the most proximal and distal MR images in which the aponeurosis was visible) cubic spline curve (Figure 9.18).

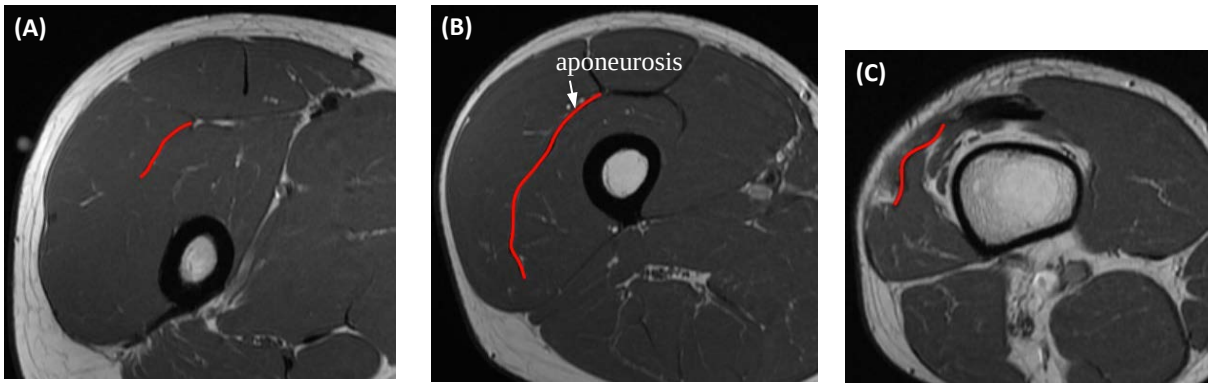

Figure 9.17. Example aponeurosis width measurement. (A) most proximal, (B) middle, and (C) most distal axial magnetic resonance image where the aponeurosis was visible. The visible black segment between the vastus lateralis (VL) and vastus intermedius muscles in the image was defined as the deep aponeurosis of the VL muscle. The length of the visible black segment was measured as aponeurosis width.

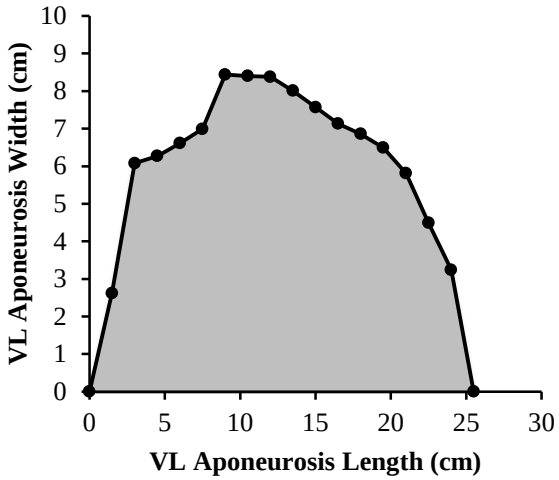

Figure 9.18. Example of vastus lateralis (VL) aponeurosis area calculation. A cubic spline curve was fitted through the data points defining the aponeurosis width-length relationship and the area under the curve defined aponeurosis area (cm^2).

9.4.3. Patellar Tendon Cross-Sectional Area

Patellar tendon cross-sectional area (CSA, mm^2) was measured on each contiguous 2 mm axial image (perpendicular to the tendon) acquired along the whole length of the tendon; from the first image where the patellar was no longer visible to the last image before the insertion of the tendon onto the tibia (e.g. images, Figure 9.19). Mean tendon CSA was defined by the average of each CSA measured on all manually segmented images.

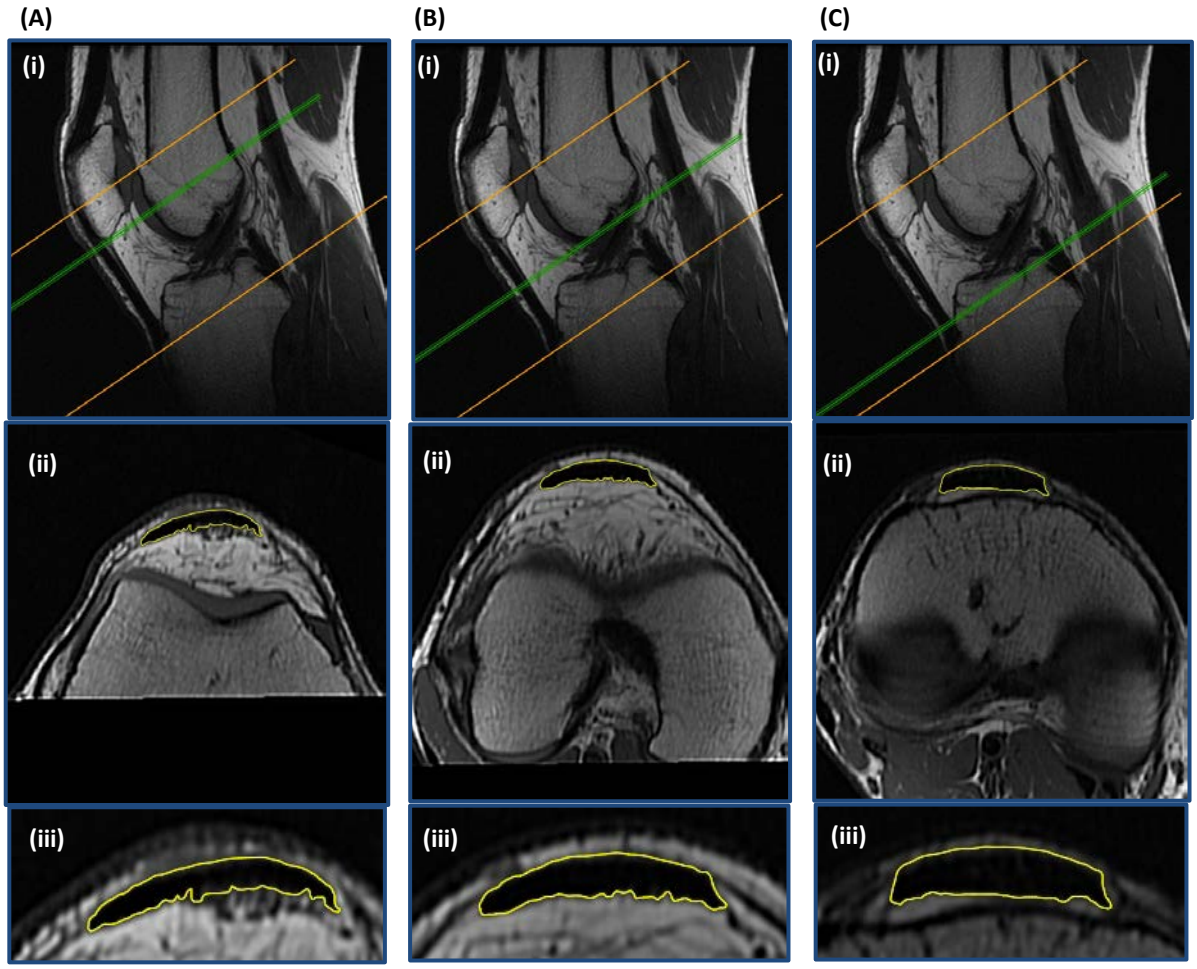

Figure 9.19. Example images of the patellar tendon cross sectional area measurement. Images correspond to (A) proximal; just distal to the apex of the patella, (B) mid-length; 50% distance between patella-tibia attachment, and (C) distal; just proximal to the tendon tibia insertion. Sagittal images showing the position along the tendon length (i), corresponding to where the axial images (ii) were acquired, and tendon cross-sectional area (determined by manual identification of tendon perimeter) was measured (iii).

REFERENCES

Aagaard P, Andersen JL, Dyhre-Poulsen P, Leffers AM, Wagner A, Magnusson SP, Halkjaer Kristensen J, & Simonsen EB. (2001). A mechanism for increased contractile strength of human pennate muscle in response to strength training: changes in muscle architecture. *J Physiol,* 534(Pt.2), 613-623.

Aagaard P, Simonsen EB, Andersen JL, Magnusson P, & Dyhre-Poulsen P. (2002). Increased rate of force development and neural drive of human skeletal muscle following resistance training. *J Appl Physiol,* 93(4), 1318-1326.

Aagaard P. (2003). Training-induced changes in neural function. *Exerc Sport Sci Rev,* 31(2), 61-67.

Abe T, Fukashiro S, Harada Y, & Kawamoto K. (2001). Relationship between sprint performance and muscle fascicle length in female sprinters. *J Physiol Anthropol Appl Hum Sci,* 20(2), 141-147.

Abe T, Kumagai K, & Bemben MG. (2012). Muscle aponeurosis area is hypertrophied and normal muscle. *Journal of Trainology,* 1(2), 23-27.

Abe T, Kumagai K, & Brechue WF. (2000). Fascicle length of leg muscles is greater in sprinters than distance runners. *Med Sci Sports Exerc,* 32(6), 1125-1129.

Akagi R, Iwanuma S, Hashizume S, Kanehisa H, Fukunaga T, & Kawakami Y. (2015). Determination of contraction-induced changes in elbow flexor cross-sectional area for evaluating muscle size-strength relationship during contraction. *J Strength Cond Res,* 29(6), 1741-1747.

Akagi R, Takai Y, Ohta M, Kanehisa H, Kawakami Y, & Fukunaga T. (2009). Muscle volume compared to cross-sectional area is more appropriate for evaluating muscle strength in young and elderly individuals. *Age Ageing,* 38(5), 564-569.

Alegre LM, HAsler M, Wenger S, NAchbauer W, & Csapo R. (2016). Does knee joint cooling change in vivo patellar tendon mechanical properties. *Eur J Appl Physiol,* 116(10), 1921-1929.

Alexander RM & Vernon A. (1975). The dimensions of the knee and ankle muscles and the forces they exert. *J Hum Mov Stud,* 1, 115-123.

Andersen JL & Aagaard P. (2000). Myosin heavy chain IIX overshoot in human skeletal muscle. *Muscle Nerve,* 23(7), 1095-104.

Andersen JL, Aagaard P, Kawakami Y, Abe T, Kuno SY, & Fukunaga T. (1995). Training-induced changes in muscle architecture and specific tension. *Eur J App Physiol Occup Physiol,* 72(1-2), 37-43.

Andersen LL & Aagaard P. (2006). Influence of maximal muscle strength and intrinsic contractile properties on contractile rate of force development. *Eur J Appl Physiol*, 96(1), 44-52.

Andersen LL, Andersen JL, Zebis MK, & Aagaard P. (2010). Early and late rate of force development: differential adaptive response to resistance training? *Scand J Med Sci Sports*, 20(1), e162-169.

Ando R, Saito A, Umemura Y, & Akima H. (2015). Local architecture of the vastus intermedius is a better predictor of knee extension force than that of the other quadriceps femoris muscle heads. *Clin Physiol Funct Imag*, 35(5), 376-382.

Angelozzi M, Madama M, Corsica C, Calvisi V, Properzi G, McCaw S, & Cacchio A. (2012). Rate of force development as an adjunctive outcome measure for return-to-sport decisions after anterior cruciate ligament reconstruction. *J Orthop Sports Phys Ther*, 42(9), 772-780.

Arampatzis A, Karamanidis K, & Albracht K. (2007a). Adaptational responses of the human Achilles tendon by modulation of the applied cyclic strain magnitude. *J Exp Biol*, 210(Pt 15), 2743-53.

Arampatzis A, Karamanidis K, Mademli L, & Albracht K. (2009). Plasticity of the human tendon to short- and long-term mechanical loading. *Exerc Sport Sci Rev*, 37(2), 66-72.

Arampatzis A, Karamanidis K, Morey-Klapsing G, De Monte G, & Stafilidis S. (2007b). Mechanical properties of the triceps surae tendon and aponeurosis in relation to intensity of sport activity. *J Biomech*, 40(9), 1946-1952.

Arampatzis A, Peper A, Bierbaum S, & Albracht K. (2010). Plasticity of human Achilles tendon mechanical and morphological properties in response to cyclic strain. *J Biomech*, 43(16), 3073-3079.

Arellano CJ, Gidmark NJ, Konow N, Azizi E, & Roberts TJ. (2016). Determinants of aponeurosis shape change during muscle contraction. *J Biomech*, 49(9), 1812-1817.

Arnoczky SP, Tian T, Lavagnino M, Gardner K, Schuler P, & Morse P. (2002). Activation of stress-activated protein kinases (SAPK) in tendon cells following cyclic strain: the effects of strain frequency, strain magnitude, and cytosolic calcium. *J Orthop Res*, 20(5), 947-952.

Avlund K, Schroll M, Davidsen M, Løvborg B, & Rantanen T. (1994). Maximal isometric muscle strength and functional ability in daily activities among 75-year-old men and women. *Scand J Med Sci Sports*, 4(1), 32-40.

Azizi E & Brainerd E. (2007). Architectural gear ratio and muscle fiber strain homogeneity in segmented musculature. *J Exp Zool A Ecol Genet Physiol*, 307(3), 145-155.

Azizi E & Roberts TJ. (2009). Biaxial strain and variable stiffness in aponeuroses. *J Physiol*, 587(17), 4309-4318.

Azizi E, Brainerd EL, & Roberts TJ. (2008). Variable gearing in pennate muscles. *Proc Natl Acad Sci,* 105(5), 1745-50.

Babraj JA, Cuthbertson DJ, Smith K, Langberg H, Miller B, Krogsgaard MR, Kjaer M, & Rennie MJ. (2005). Collagen synthesis in human musculoskeletal tissues and skin. *Am J Physiol Endocrinol Metab,* 289(5), E864-869.

Balshaw TG, Massey GJ, Maden-Wilkinson TM, Tillin NA, & Folland JP. (2016). Training-specific functional, neural and hypertrophic adaptations to explosive- vs. sustained-contraction strength training. *J Appl Physiol,* 120(11), 1364-1373.

Bamman MM, Newcomer BR, Larson-Meyer DE, Weinsier RL, & Hunter GR. (2000). Evaluation of the strength-size relationship in vivo using various muscle size indices. *Med Sci Sports Exerc,* 32(7), 1307-1313.

Barry BK, Warman GG, & Carson RG. (2005). Age-related differences in rapid muscle activation after rate of force development training of the elbow flexors. *Exp Brain Res,* 162(1), 122-132.

Baxter J & Piazza S. (2014). Plantar flexor moment arm and muscle volume predict torque-generating capacity in young men. *J Appl Physiol,* 116(5), 538-544.

Bean JF, Leveille SG, Kiely DK, Bandinelli S, Guralnik JM, & Ferrucci L. (2003). A comparison of leg power and leg strength within the InCHIANTI study: which influences mobility more? *J Gerontol A Biol Sci Med Sci,* 58(8), 728-33.

Bénard MR, Becher JG, Harlaar J, Huijing PA, & Jaspers RT. (2009). Anatomical information is needed in ultrasound imaging of muscle to avoid potentially substantial errors in measurement of muscle geometry. *Muscle Nerve,* 39(5), 652-665.

Beyer R, Kongsgaard M, Hougs Kjaer B, Ohlenschlaeger T, Kjaer M, & Magnusson S. (2015). Heavy slow resistance versus eccentric training as treatment for achilles tendinopathy: a randomized controlled trial. *Am J Sports Med,* 43(7), 1704-1711.

Blackburn JT, Norcross MF, Cannon LN, & Zinder SM. (2013). Hamstring stiffness and landing biomechanics linked to anterior cruciate ligament loading. *J Athl Train,* 48(6), 765-772.

Blazevich A & Sharp N. (2005). Understanding muscle architectural adaptation: macro- and micro-level research. *Cells Tissues Organs,* 181(1), 1-10.

Blazevich AJ, Cannavan D, Coleman DR, & Horne S. (2007a). Influence of concentric and eccentric resistance training on architectural adaptation in human quadriceps muscles. *J Appl Physiol,* 103(5), 1565-75.

Blazevich AJ, Cannavan D, Horne S, Coleman DR, & Aagaard P. (2009a). Changes in muscle force- length properties affect the early rise of force in vivo. *Muscle Nerve,* 39(4), 512-520.

Blazevich AJ, Coleman DR, Horne S, & Cannavan D. (2009b). Anatomical predictors of maximum isometric and concentric knee extensor moment. *Eur J Appl Physiol,* 105(6), 869-878.

Blazevich AJ, Gill ND, & Zhou S. (2006a). Intra-and intermuscular variation in human quadriceps femoris architecture assessed in vivo. *J Anat,* 209(3), 289-310.

Blazevich AJ, Gill ND, Deans N, & Zhou S. (2007b). Lack of human muscle architectural adaptation after short-term strength training. *Muscle Nerve,* 35(1), 78-86.

Blazevich AJ, Horne S, Cannavan D, Coleman DR, & Aagaard P. (2008). Effect of contraction mode of slow-speed resistance training on the maximum rate of force development in the human quadriceps. *Muscle Nerve,* 38(3), 1133-1146.

Blazevich AJ. (2006b). Effects of physical training and detraining, immobilisation, growth and aging on human fascicle geometry. *Sports Med,* 36(12), 1003-1017.

Bloomquist K, Langberg H, Karlsen S, Madsgaard S, Boesen M, & Raastad T. (2013). Effect of range of motion in heavy load squatting on muscle and tendon adaptations. *Eur J Appl Physiol,* 113(8), 2133-2142.

Bobbert MF, Mackay M, Schinkelshoek D, Huijing PA, & van Ingen Schenau GJ. (1986). Biomechanical analysis of drop and countermovement jumps. *Eur J Appl Physiol,* 54(6), 566-573.

Bodine SC, Roy RR, Meadows DA, Zernicke RF, Sacks RD, Fournier M, & Edgerton VR. (1982). Architectural, histochemical, and contractile characteristics of a unique biarticular muscle: the cat semitendinosus. *J Neurophysiol,* 48(1), 192-200.

Bohm S, Mersmann F, Tettke M, Kraft M, & Arampatzis A. (2014). Human Achilles tendon plasticity in response to cyclic strain: effect of strain rate and duration. *J Exp Biol,* 217(Pt22), 4010-4017.

Bohm, S, Mersmann, F & Arampatzis, A. (2015). Human tendon adaptation in response to mechanical loading: a systematic review and meta-analysis of exercise intervention studies on healthy adults. *Sports Med - Open,* 1(1).

Bojsen-Møller J, Hansen P, Aagaard P, Kjaer M, & Magnusson SP. (2003). Measuring mechanical properties of the vastus lateralis tendon-aponeurosis complex in vivo by ultrasound imaging. *Scand J Med Sci Sports,* 13(4), 259-265.

Bojsen-Møller J, Magnusson SP, Rasmussen LR, Kjaer M, & Aagaard P. (2005). Muscle performance during maximal isometric and dynamic contractions is influenced by the stiffness of the tendinous structures. *J Appl Physiol,* 99(3), 986-994.

Brainerd E & Azizi E. (2005). Muscle fiber angle, segment bulging and architectural gear ratio in segmented musculature. *J Exp Biol,* 208(17), 3249-3261.

Buchanan CI & Marsh RL. (2002). Effects of exercise on the biomechanical, biochemical and structural properties of tendons. *Comp Biochem Physiol A Mol Integr Physiol*, 133(4), 1101-1107.

Buckthorpe M, Erskine RM, Fletcher G, & Folland JP. (2015). Task-specific neural adaptations to isoinertial resistance training. *Scand J Med Sci Sports*, 25(5), 640-649.

Burd NA, Andrews RJ, West DWD, Little JP, Cochran AJR, Hector AJ, Cashaback JGA, Gibala MJ, Potvin JR, Baker SK, & Phillips SM. (2012). Muscle time under tension during resistance exercise stimulates differential muscle protein sub-fractional synthetic responses in men. *J Physiol*, 590(2), 351-362.

Burgess KE, Connick MJ, Graham-Smith P, & Pearson SJ. (2007). Plyometric vs. Isometric training influences on tendon properties and muscle output. *J Strength Cond Res*, 21(3), 986-989.

Burkholder TJ, Fingado B, Baron S, & Lieber RL. (1994). Relationship between muscle fiber types and sizes and muscle architectural properties in the mouse hindlimb. *J Morphol*, 221 (2), 177-190.

Butler DL, Grood ES, Noyes FR, & Zernicke RF. (1978). Biomechanics of ligaments and tendons. *Exerc Sport Sci Rev*, 6, 125-81

Carroll CC, Dickinson JM, Haus JM, Lee GA, Hollon CJ, Aagaard P, Magnusson SP, & Trappe TA. (2008). Influence of aging on the in vivo properties of human patellar tendon. *J Appl Physiol*, 105(6), 1907-15

Chauhan B, Hamzeh MA, & Cuesta-Vargas AI. (2013). Prediction of muscular architecture of the rectus femoris and vastus lateralis from EMG during isometric contractions in soccer players. *Springerplus*, 2, 548.

Clemmer J, Liao J, Davis D, Horstemeyer MF, & Williams LN. (2010). A mechanistic study for strain rate sensitivity of rabbit patellar tendon. *J Biomech*, 43(14), 2785-2791.

Cohen J. (1988). Statistical power analysis for the behavioral sciences. 2nd ed. Hillsdale (NJ): Lawrence Erlbaum Associates.

Connizzo, B., Adams, S., Adams, T., Jawad, A., Birk, D. and Soslowsky, L. (2016). Multiscale regression modeling in mouse supraspinatus tendons reveals that dynamic processes act as mediators in structure–function relationships. *J Biomech*, 49(9),1649-1657.

Couppé C, Hansen P, Kongsgaard M, Kovanen V, Suetta C, Aagaard P, Kjaer M & Magnusson SP. (2009). Mechanical properties and collagen cross-linking of the patellar tendon in old and young men. *J Appl Physiol*, 107(3), 880-886.

Couppé C, Kongsgaard M, Aagaard P, Hansen P, Bojsen-Moller J, Kjaer M & Magnusson SP. (2008). Habitual loading results in tendon hypertrophy and increased stiffness of the human patellar tendon. *J Appl Physiol*, 105(3), 805-810.

Couppé C, Svensson RB, Sødring-Elbørond V, Hansen P, Kjaer M,& Magnusson SP. (2014). Accuracy of MRI technique in measuring tendon cross-sectional area. *Clin Physiol Funct Imag,* 34(3), 237-241.

Craig CL, Marshall AL, Sjöström M, Bauman AE, Booth ML, Ainsworth BE, Pratt BE, Ekelund U, Yngve A, Sallis JF, & Oja P. (2003). International physical activity questionnaire: 12-country reliability and validity. *Med Sci Sports Exerc,* 35(8), 1381-1395.

Cuoco A, Callahan DM, Sayers S, Frontera WR, Bean J, & Fielding RA. (2004). Impact of muscle power and force on gait speed in disabled older men and women. *J Gerontol A Biol Sci Med Sci,* 59(11), 1200-6.

De Boer MD, Maganaris CN, Seynnes OR, Renniw MJ, & Narici MV. (2007). Time course of muscular, neural and tendinous adaptations to 23 days unilateral lower-limn suspension in young men. *J Physiol,* 582(3), 1079-1091.

de Ruiter CJ, De Korte A, Schreven S, & de Haan A. (2010). Leg dominancy in relation to fast isometric torque production and squat jump height. *Eur J Appl Physiol,* 108(2), 247-255.

de Ruiter CJ, Jones DA, Sargeant AJ, & de Haan A. (1999). Temperature effect on the rates of isometric force development in the fresh and fatigued human adductor pollicis muscle. *Exp Physiol,* 84(6), 1137-1150.

de Ruiter CJ, Kooistra RD, Paalman MI, & de Haan A. (2004). Initial phase of maximal voluntary and electrically stimulated knee extension torque development at different knee angles. *J Appl Physiol,* 97(5), 1693-1701.

de Ruiter CJ, Van Leeuwen D, Heijblom A, Bobbert MF, & de Haan A. (2006). Fast unilateral isometric knee extension torque development and bilateral jump height. *Med Sci Sports Exerc,* 38(10), 1843-1852.

de Ruiter CJ, Vermeulen G, Toussaint HM, & de Haan A. (2007). Isometric knee-extensor torque development and jump height on volleyball players. *Med Sci Sports Exerc,* 39(8), 1336-1346.

Degens H, Erskine RM, & Morse CI. (2009). Disproportionate changes in skeletal muscle strength and size with resistance training and ageing. *J Musculoskelet Neuronal Interact,* 9(3), 123-129.

Del Balso C & Cafarelli E. (2007). Adaptations in the activation of human skeletal muscle induced by short-term isometric resistance training. *J Appl Physiol,* 103(1), 402-411.

Deutekom M, Beltman JGM, de Ruiter CJ, de Koning JJ, & de Haan A. (2000). No acute effects of short-term creatine supplementation on muscle properties and sprint performance. *Eur J Appl Physiol,* 82(3), 223-229.

Dewall RJ, Slane LC, Lee, KS, & Thelen DG. (2014). Spatial variations in Achilles tendon shear wave speed. *J Biomech,* 47(11), 2685-2692.

Dideriksen K, Sindby AK, Krogsgaard M, Schjerling P, Holm L, & Langberg H. (2013). Effect of acute exercise on patella tendon protein synthesis and gene expression. *Springerplus,* 2(1), 109.

Docking SI & Cook J. (2016). Pathological tendons maintain sufficient aligned fibrillar structure on ultrasound tissue characterization (UTC). *Scan J Med Sci Sports,* 26(6), 275-283.

Dudley GA, Harris RT, Duvoisin MR, Hather BM, & Buchanan P. (1990). Effect of voluntary vs. artificial activation on the relationship of muscle torque to speed. *J Appl Physiol,* 69(6), 2215-2221.

Edman KAP (1999). The force bearing capacity of frog muscle fibres during stretch: its relation to sarcomere length and fibre width. *J Physiol,* 591(2), 515-526.

Edman KA & Josephson RK. (2007). Determinants of force rise time during isometric contraction of frog muscle fibres. *J Physiol,* 580(3), 1007-1019.

Ema R, Wakahara T, Miyamoto N, Kanehisa H, & Kawakami Y. (2013). Inhomogeneous architectural changes of the quadriceps femoris induced by resistance training. *Eur J Appl Physiol,* 113(11), 2691-2703.

Enoka RM. (2008). *Neuromechanics of human movement*. 4th ed. Champaign, IL: Human Kinetics.

Erskine RM, Fletcher G, & Folland JP. (2014). The contribution of muscle hypertrophy to strength changes following resistance training. *Eur J Appl Physiol,* 114(6), 1239-1249.

Erskine RM, Jones DA, Maganaris CN, & Degens H. (2009). In vivo specific tension of the human quadriceps femoris muscle. *Eur J Appl Physiol,* 106(6), 827-838.

Erskine RM, Jones DA, Williams AG, Stewart CE, & Degens H. (2010). Inter-individual variability in the adaptations of human muscle specific tension to progressive resistance training. *Eur J Appl Physiol,* 110(6), 1117-1125.

Evangelidis PE, Massey GJ, Pain MT & Folland, JP (2015). Biceps femoris aponeurosis size: a potential risk factor for strain injury? *Med Sci Sports Exerc,* 47(7), 1383-1389.

Evangelidis PE, Massey GJ, Pain MT, & Folland JP. (2016). Strength and size relationships of the quadriceps and hamstrings with special reference to reciprocal muscle balance. *Eur J Appl Physiol,* 116(3), 593-600.

Ezikos A, Papatzika F, Charcharis G, Bohm S, Mersmann F, & Arampatzis A. (2013). Ultrasound does not provide reliable results for the measurement of the patellar tendon cross sectional area. *J Electromyogr Kinesiol,* 23(6), 1278-1782.

Farcy S, Nordez A, Dorel S, Hauraix H, Portero P, & Rabita G. (2013). Interaction between gastrocnemius medialis fascicle and Achilles tendon compliance: A new insight on the quick-release method. *J Appl Physiol,* 116(3), 259-266.

Farris DJ, Trewartha G, McGuigan MP, & Litchwark GA. (2013). Differential strain patterns of human AT determined in vivo with freehand three-dimensional ultrasound imaging. *J Exp Biol,* 216(Pt 4), 594-600.

Farup J, Rahbek SK, Vendelbo MH, Matzon A, Hindhebe J, Bejder A, Ringgard S, & Vissing K. (2014). Whey protein hydrolysate augments tendon and muscle hypertrophy independent of resistance exercise contraction mode. *Scand J Med Sci Sports,* 24(5), 788-798.

Finni T, Hodgson JA, Lai AM, Edgerton VR & Sinha S (2003). Nonuniform strain of human soleus aponeurosis-tendon complex during submaximal voluntary contractions in vivo. *J Appl Physiol,* 95(2), 829-837.

Fiorentino NM, Epstein FH, & Blemker SS. (2012). Activation and aponeurosis morphology affect in vivo muscle tissue strains near the myotendinous junction. *J Biomech,* 45(4), 647-652.

Folland JP & Williams AG. (2007). The adaptations to strength training: morphological and neurological contributions to increased strength. *Sports Med,* 37(2), 145-168.

Folland JP, Buckthorpe MW, & Hannah R. (2014). Human capacity for explosive force production: Neural and contractile determinants. *Scand J Med Sci Sports,* 24(6), 894-906.

Fouré A, Nordez A, & Cornu C. (2010). Plyometric training effects on Achilles tendon stiffness and dissipative properties. *J Appl Physiol,* 109(3), 849-54.

Fouré A, Nordez A, McNair P, & Cornu C. (2011). Effects of plyometric training on both active and passive parts of the plantarflexors series elastic component stiffness of muscle-tendon complex. *Eur J Appl Physiol,* 111(3), 539-48.

Fukunaga T, Ichinose Y, Ito M, Kawakami Y, & Fukashiro S. (1997). Determination of fascicle length and pennation in a contracting human muscle in vivo. *J Appl Physiol,* 82(1), 354-358.

Fukunaga T, Miyatani M, Tachi M, Kouzaki M, Kawakami Y & Kanehisa H. (2001). Muscle volume is a major determinant of joint torque in humans. *Acta Physiol Scand,* 172(4), 249-255.

Fukunaga T, Roy RR, Shellock FG, Hodgson JA, & Edgerton VR. (1996). Specific tension of human plantar flexors and dorsiflexors. *J Appl Physiol,* 80(1), 158-165.

Fukutani A & Kurihara T. (2015). Tendon cross-sectional area is not associated with muscle volume. *J Appl Biomech,* 31(3), 176-80.

Geertsen SS, Lundbye-Jensen J, & Nielsen JB. (2008). Increased central facilitation of antagonist reciprocal inhibition at the onset of dorsiflexion following explosive strength training. *J Appl Physiol,* 105(3), 915-922.

Gerus P, Rao G, & Berton E. (2011). A method to characterize in vivo tendon force–strain relationship by combining ultrasonography, motion capture and loading rates. *J Biomech,* 44(12), 2333-2336.

Gordan AM, Huxley AF, & Julian FJ. (1966). The variation in isometric tension with sarcomere length in vertebrate muscle fibres. *J Physiol,* 184(1), 170-192.

Goubel F & Marini JF. (1987). Fibre type transition and stiffness modification of soleus muscle of trained rats. *Plugers Arch,* 410(3), 321-325.

Gilles AR & Lieber RL. (2010). Structure and function of the extracellular matrix. *Muscle Nerve, 44(3),* 318-331.

Gruber M, Gruber SB, Taube W, Schubert M, Beck SC, & Gollhofer A. (2007). Differential effects if ballistic versus sensorimotor training on rate of force development and neural activation in humans. *J Strength Cond Res,* 21(1), 274-282.

Häkkinen K, Komi, PV, & Alén M. (1985). Effect of explosive type strength training on isometric force- and relaxation-time, electromyographic and muscle fibre characteristics of leg extensor muscles. *Acta Physiol Scand,* 125(4), 587-600.

Häkkinen K, Pakarinen A, Kraemer WJ, Häkkinen K, Valkeinen H, & Alen M. (2001). Selective muscle hypertrophy, changes in EMG and force, and serum hormones during strength training in older women. *J Appl Physiol,* 91(2), 569-580.

Hannah R & Folland JP. (2015) Muscle-tendon unit stiffness does not independently affect voluntary explosive force production or muscle intrinsic contractile properties. *Appl Physiol Nutr Metab,* 40(1), 87-95.

Hannah R, Minshull C, Buckthorpe MW, & Folland JP. (2012). Explosive neuromuscular performance of males versus females. *Exp Physiol,* 97(5), 618-629.

Hansen KA, Weiss JA, & Barton JK. (2002). Recruitment of tendon crimp with applied tensile strain. *J Biomech Eng,* 124(1), 72-77.

Hansen P, Bojsen-Møller J, Aagaard P, Kjaer M, & Magnusson SP. (2006). Mechanical properties of the human patella tendon in vivo. *Clin Biomech (Bristol, Avon),* 21(1), 54-58.

Hansen P, Haraldsson BT, Aagaard P, Kovanen V, Avery NC, Qvortrup K, Krogsgaard M, Kjaer M, & Magnusson, SP. (2010). Lower strength of the human posterior patellar tendon seems unrelated to mature collagen cross-linking and fibril morphology. *J Appl Physiol,* 108(1), 47-52.

Hansen P, Kovanen V, Hölmich P, Krosgaarrd M, Hansson P, Dahl M, Hald M, Aagaard P, Kjaer M, & Magnusson SP. (2013). Micromechanical properties and collagen composition of ruptured human Achilles tendon. *Am J Sports Med,* 41(2), 437-443.

Harridge SD, Bottinelli R, Canepari M, Pellegrino MA, Reggiani C, Esbjornsson M, & Saltin B. (1996). Whole-muscle and single-fibre contractile properties and myosin heavy chain isoforms in humans. *Pflugers Arch,* 432(5), 913-920.

Haugen P & Sten-Knudsen O. (1987). The time course of the contractile force measured during a twitch under fixed sarcomere length. *J Muscle Res Cell Motil,* 8(2), 173-187.

Hauraix H, Nordez A, & Dorel S. (2013). Shortening behavior of the different components of muscle-tendon unit during isokinetic plantar flexions. *J Appl Physiol,* 115(7), 1015-1024.

Hauraix H, Fouré A, Dorel S, Cornu C, & Nordez A. (2015). Muscle and tendon stiffness assessment using the alpha method and ultrafast ultrasound. *Eur J Appl Physiol,* 115(5), 1393-1400.

Heinemeier KM & Kjaer M. (2011). In vivo investigation of tendon responses to mechanical loading. *J Musculoskel Neuonal Interact,* 11(2), 115-123.

Heinemeier KM, Bjerrum SS, Schjerling P, & Kjaer M. (2013a). Expression of extracellular matrix components and related growth factors in human tendon and muscle after acute exercise. *Scand J Med Sci Sports,* 23(3), e150-e161.

Heinemeier KM, Schjerling P, Heinemeier J, Magnusson SP, & Kjaer M. (2013b). Lack of tissue renewal in human adult Achilles tendon is revealed by nuclear bomb (14)C. *FASEB J,* 27(5), 2074-2079.

Herbert RD & Gandevia SC. (1995). Changes in pennation with joint angle and muscle torque: in vivo measurements in human brachialis muscle. *J Physiol,* 482(2), 523-532.

Higashihara A, Ono T, Kubota J, Okuwaki T, & Fukubayashi T. (2010). Functional differences in the activity of the hamstring muscles with increasing running speed. *J Sports Sci,* 28(10), 1085-1092.

Hill AV. (1938). The heat of shortening and the dynamic constants of muscle. *Proc Biol Sci,* 126(843), 136-195.

Hill AV. (1951). The effect of series compliance on the tension developed in a muscle twitch. *Proc Biol Sci,* 138(892), 325-329.

Hodges PW, Pengel LHM, Herbert RD, & Gandevia SC. (2003). Measurement of muscle contraction with ultrasound imaging. *Muscle Nerve,* 27(6), 682-692.

Holtermann A, Roeleveld K, Engstrom M, & Sand T. (2007). Enhanced H-reflex with resistance training is related to increased rate of force development. *Eur J Appl Physiol,* 101(3), 301-31.

Hopkins WG, Marshall SW, Batterham AM, & Hanin J. (2009). Progressive statistics for studies in sports medicine and exercise science. *Med Sci Sports Exerc,* 41(1), 3-13.

Housh DJ, Housh TJ, Johnson GO, & Chu WK. (1992). Hypertrophic response to unilateral concentric isokinetic resistance training. *J Appl Physiol, 73*(1), 65-70.

Hubal MJ, Gordish-Dressman H, Thompson PD, Price TB, Hoffman EP, Angelopoulos TJ, Gordan PM, Moyna NM, Pescatello LS, Visich PS, Zoeller RF, Seip RL, & Clarkson PM.

(2005). Variability in muscle size and strength gain after unilateral resistance training. *Med Sci Sports Exerc,* 37(6), 964-72.

Hug F, Tucker K, Gennisson J, Tanter M, & Nordez A. (2015). Elastography for muscle biomechanics: toward the estimation of individual muscle force. *Exerc Sport Sci Rev,* 43(3), 125-133.

Ichinose Y, Kawakami Y, Ito M, & Fukunaga T. (1997). Estimation of active force-length characteristics of human vastus lateralis muscle. *Acta Anat (Basel),* 159(2-3), 78-83.

Ichinose Y, Kawakami Y, Ito M, Kanehisa H, & Fukunaga T. (2000). In vivo estimation of contraction velocity of human vastus lateralis muscle during "isokinetic" action. *J Appl Physiol,* 88(3), 851-856.

Ito M, Kawakami Y, Ichinose Y, Fukashiro S, & Fukunaga T. (1998). Nonisometric behavior of fascicles during isometric contractions of a human muscle. *J Appl Physiol,* 85(4), 1230–1235

Iwanuma S, Akagi R, Kurihara T, Ikegawa S, Kaneshisa H, Fukunaga T, Kawakami Y. (2011). Longitudinal and transverse determination of human achilles tendon induced by isometric plantar flexion at different intensities. *J Appl Physiol,* 110(6), 1615-1621.

Izquierdo M, Aguado X, Gonzalez R, López JL, & Häkkinen K. (1999). Maximal and explosive force production capacity and balance performance in men of different ages. *Eur J Appl Physiol Occup Physiol,* 9(3), 260-267.

Jones DA, Round JM, & de Haan A. (2004). *Skeletal muscle from molecules to movement*. Churchill Livingstone, London.

Jürimäe J, Abernethy PJ, Blake K, McEniery MT. (1996). Changes in the myosin heavy chain isoform profile of the triceps brachii muscle following 12 weeks of resistance training. *Eur J Appl Physiol,* 74(3), 287-292.

Karamanidis K, Arampatzis A, & Mademli L. (2008). Age-related deficit in dynamic stability control after forward falls is affected by muscle strength and tendon stiffness. *J Electromyogr and Kinesiol,* 18(6), 980-989.

Katz B. (1939). The relation between force and speed in muscular contraction. *J Physiol,* 96(1), 45-64.

Kawakami Y & Lieber RL. (2000). Interaction between series compliance and sarcomere kinetics determines internal sarcomere shortening during fixed-end contraction. *J Biomech,* 33(10), 1249-1255,

Kawakami Y, Abe T, Kanehisa H, & Fukunaga T. (2006). Human skeletal muscle size and architecture: variability and interdependence. *Am J Hum Biol,* 18(6), 845-848.

Kawakami Y, Abe T, Kuno SY, & Fukunaga T. (1995). Training-induced changes in muscle architecture and specific tension. *Eur J App Physiol Occup Physiol,* 72(1-2), 37-43.

Kawakami Y, Abe TA, & Fukunaga T. (1993). Muscle-fiber pennation angles are greater in hypertrophied than in normal muscles. *J Appl Physiol,* 74(6), 2740-2744.

Kawakami Y, Ichinose Y, & Fukunaga T. (1998). Architectural and functional features of human triceps surae muscles during contraction. *J Appl Physiol,* 85(2), 398-404.

Kawakami Y. (2005). The effects of strength training on muscle architecture in humans. *Int J Sport Health Sci,* 3, 208-217.

Kearns CF, Abe T, & Brechue WF. (2000). Muscle enlargement in sumo wrestlers includes increased muscle fascicle length. *Eur J App Physiol,* 83(4-5), 289-296.

Kellis E & Baltzopoulos V. (1999). In vivo determination of the patella tendon and hamstrings moment arms in adult males using videofluoroscopy during submaximal knee extension. *Clin Biomech (Bristol, Avon),* 14(2), 118-124.

Ker RF, Alexander RM, & Bennett MB. (1988). Why are mammalian tendons so thick? *J.Zool,* 216(2), 309-324.

Ker RF, Wang XT, & Pike AV. (2000). Fatigue quality of mammalian tendons. *J Exp Biol,* 203(Pt 8), 1317-1327.

Kinugasa R, Shin D, Yamauchi J, Mishra C, Hodgson JA, Edgerton VR III & Sinha S. (2008). Phase-contrast MRI reveals mechanical behavior of superficial and deep aponeuroses in human medial gastrocnemius during isometric contraction. *J Appl Physiol,* 105(4), 1312-1320.

Kjaer M. (2004). Role of extracellular matrix in adaptation if tendon and skeletal muscle to mechanical loading. *Physiol Rev,* 84(2), 649-698.

Kjaer M, Jørgensen NR, Heinemeier K, & Magnusson SP. (2015). Exercise and regulation of bone and collagen tissue biology. *Prog Mol Biol Transl Sci,*135, 259-291.

Kline P, Morgan K, Johnson D, Ireland M, & Noehren B. (2015). Impaired quadriceps rate of torque development and knee mechanics after anterior cruciate ligament reconstruction with patellar tendon autograft. *Am J Sports Med,* 43(10), 2553-2558.

Koga H, Nakamae A, Shima Y, Iwasa J, Myklebust G, Engebretsen L, Bahr R, & Krosshaug T. (2010). Mechanisms for noncontact anterior cruciate ligament injuries: knee joint kinematics in 10 injury situations from female team handball and basketball. *Am J Sports Med,* 38(11), 2218-25,

Kongsgaard M, Aagaard P, Kjaer M, & Magnusson SP. (2005). Structural Achilles tendon properties in athletes subjected to different exercise modes and in Achilles tendon rupture patients. *J App Physiol,* 99(5), 1965-1971.

Kongsgaard M, Kovanen V, Aagaard P, Doessing S, Hansen P, Laursen AH, Kaldau NC, Kjaer M, & Magnusson SP. (2009). Corticosteroid injections, eccentric decline squat training and heavy slow resistance training in patellar tendinopathy. *Scan J Med Sci Sports,* 19(6), 790-802.

Kongsgaard M, Qvotrup K, Larsen J, Aagaard P, Doessing S, Hansen P, Kjaer M, & Magnusson SP. (2010). Fibril morphology and tendon mechanical properties in patellar tendinopathy: effects of heavy slow resistance training. *Am J Sports Med,* 38(4), 749-756.

Kongsgaard M, Reitelseder S, Pedersen TG, Holm L, Aagaard P, Kjaer M, & Magnusson SP. (2007). Region specific patellar tendon hypertrophy in humans following resistance training. *Acta Physiol,* 191(2), 111-121.

Kösters A, Wiesinger H, Bojsen-Møller J, Müller E, & Seynnes, OR. (2014). Influence of loading rate on patellar tendon mechanical properties in vivo. *Clin Biomech (Bristol, Avon),* 29(3), 323-329.

Kovanen V. (2002). Intramuscular extracellular matrix: Complex environment of muscle cells. *Exerc Sport Sci Rev,* 30(1), 20-25.

Krosshaug T, Nakamae A, Boden BP, Engebretsen L, Smith G, Slauterbeck JR, Hewett TE, & Bahr R. (2007). Mechanisms of anterior cruciate ligament injury in basketball: video analysis of 39 cases. *Am J Sports Med,* 35(3), 359-367.

Kruse A, Stafilidis S, & Tilp M. (2017). Ultrasound and magnetic resonance imaging are not interchangeable to assess the Achilles tendon cross-sectional-area. *Eur J Appl Physiol,* 117(1), 77-82.

Kubo K, Ikebukuro T, Maki A, Yata H, & Tsunoda N. (2012). Time course of changes in the human Achilles tendon properties and metabolism during training and detraining in vivo. *Eur J Appl Physiol,* 112(7), 2679-2691.

Kubo K, Ikebukuro T, Yaeshima K, Yata H, Tsunoda N, & Kaneshisa H. (2009). Effects of static and dynamic training in the stiffness and blood volume of tendon in vivo. *J Appl Physiol,* 106(2), 412-417.

Kubo K, Ikebukuro T, Yata H, Tomita M, & Okada M. (2011). Morphological and mechanical properties of muscle and tendon in highly trained sprinters. *J Appl Biomech,* 27(4), 336-344.

Kubo K, Ikebukuro T, Yata H, Tsunoda N, & Kaneshisa H. (2010a). Time course of changes in muscle and tendon properties during strength training and detraining *J Strength Cond Res,* 24(2), 322-331.

Kubo K, Ikebukuro T, Yata H, Tsunoda N, & Kaneshisa H. (2010b). Effect of training on muscle and tendon in knee extensors and plantar flexors in vivo. *J Appl Biomech,* 26(3) 316-323.

Kubo K, Kanehisa H, & Fukunaga T. (2001). Effect of different duration isometric contractions on tendon elasticity in human quadriceps muscles. *J Physiol,* 536(2), 639-655.

Kubo K, Kanehisa H, & Fukunaga T. (2002a). Effects of resistance training and stretching training programmes on the viscoelastic properties of human tendon structures in vivo. *J Appl Physiol,* 538(1), 219-226.

Kubo K, Kanehisa H, & Fukunaga T. (2003) Effect of low-load resistance training on the viscoelastic properties of tendon-aponeurosis structures in middle aged and elderly women. *Acta Physiol Scand,* 178(1), 25-32.

Kubo K, Kanehisa H, Kawakami Y, & Fukunaga T. (2000). Elasticity of tendon structures of the lower limbs in sprinters. *Acta Physiol Scand,* 168(2), 327-335.

Kubo K, Kawakami Y, & Fukunaga T. (1999). Influence of elastic properties of tendon structures on jump performance in humans. *J Appl Physiol,* 87(6), 2090-2096.

Kubo K, Kawakami Y, Kanehisa H, & Fukunaga T. (2002b). Measurement of viscoelastic properties of tendon structures in vivo. *Scand J Med Sci Sports,* 12(1), 3-8.

Kubo K, Lomuro T, Ishihuro N, Tsunoda N, Sato Y, Ishii N, Kaneshisa H, & Fukunaga T. (2006a). Effects of low-load resistance training with vascular occlusion on the mechanical properties of muscle and tendon. *J Appl Biomech,* 22(1), 112-119.

Kubo K, Morimoto M, Komuro T, Yata H, Tsunoda N, Kanehisa H, & Fukunaga T. (2007). Effects of plyometric and weight training in the muscle-tendon complex and jump performance. *Med Sci Sports Exerc,* 39(10), 1801-1810.

Kubo K, Ohgo K, Takeishi R, Yoshinaga K, Tsunoda N, Kanehisa H, & Fukunaga T. (2006b). Effects of isometric training at different knee angles on the muscle-tendon complex in vivo. *Scand J Med Sci Sports,* 16(3), 159-167.

Kubo K. (2014). Active muscle stiffness in the human medial gastrocnemius muscle in vivo. *J Appl Physiol,* 117(9), 1020-1026.

Kubo, Yata H, Kaneshisa H, & Fukunaga T. (2006c). Effect of isometric squat training on the tendon stiffness and jump performance. *Eur J Appl Physiol,* 96(3) 305-314.

Kumagai K, Abe T, Brechue WF, Ryushi T, Takano S, & Mizuno M. (2000). Sprint performance is related to muscle fascicle length in male 100-m sprinters. *J Appl Physiol,* 96(1), 45-64.

LaCroix AS, Duenwald-Kuehl SE, Lakes RS, & Vanderby R Jr. (2013). Relationship between tendon stiffness and failure: a metanalysis. *J Appl Physiol,* 115(1), 43-51.

Lakens D. (2013). Calculating and reporting effect sizes to facilitate cumulative science: a practical primer for t-tests and ANOVAs. *Frontiers in psychology,* 4, 863.

Langberg H, Rosendal L, & Kjaer M. (2001). Training-induced changes in peritendinous type I collagen turnover determined by microdialysis in humans. *J Physiol,* 534(Pt 1), 297-302.

Langberg H, Skovgaard D, Asp S, & Kjaer M. (2000). Time pattern of exercise-induced changes in type I collagen turnover after prolonged endurance exercise in humans. *Calcif Tissue Int,* 67(1), 41-44.

Langberg H, Skovgaard D, Karamouzis M, Bulow J, & Kjaer M. (1999). Metabolism and inflammatory mediators in the peritendinous space measured by microdialysis during intermittent isometric exercise in humans. *J Physiol*, 515(Pt 3), 919-927.

Lavagnino M, Arnoczky SP, Kepich E, Calballero O, & Haut RC. (2008). A finite element model predicts the mechanotransduction response of tendon cells to cyclic tensile loading. *Biomech Model Mechanobiol,* 7(5), 405-416.

Lee D, Li Z, Sohail QZ, Jackson K, Fiume E, & Agur A (2015). A three-dimensional approach to pennation angle estimation for human skeletal muscle. *Comput Methods Biomech Biomed Engin*, 18(13), 1474-1484.

LeMoine JK, Lee JD, & Trappe TA. (2009). Impact of sex and chronic resistance training on human patellar tendon dry mass, collagen content, and collagen cross-linking. *Am J Physiol Regul Integr Comp Physiol*, 296(1), R119-R124.

Lemos R, Epstein M, & Herzog W. (2008). Modeling of skeletal muscle: the influence of tendon and aponeuroses compliance on the force–length relationship. *Med Biol Eng Comput*, 46(1), 23-32.

Lieber R & Fridén J. (2000). Functional and clinical significance of skeletal muscle architecture. *Muscle Nerve,* 23(11), 1647-1666.

Lieber R, Brown C, & Trestik C. (1992). Model of muscle-tendon interaction during frog semitendinosus fixed-end contractions. *J Biomech,* 25(4), 421-428.

Lieber R, Leonard M, & Brown-Maupin C. (2000). Effects of muscle contraction on the load-strain properties of frog aponeurosis and tendon. *Cells Tissues Organs*, 166(1), 48-54.

Lieber RL & Ward SR. (2011). Skeletal muscle design to meet functional demands. *Philos Trans R Soc Lond B Biol Sci*, 366(1570), 1466-1476.

Lipps DB, Oh YK, Ashton-Miller JA, & Wojtys EM. (2014). Effect of increases quadriceps tensile stiffness on peak anterior cruciate ligament strain during a simulated pivot landing. *J Orthop Res,* 32(3) 423-430.

Litchwark GA & Barclay CJ. (2010). The influence of tendon compliance on muscle power output and efficiency during cyclic contractions. *J Exp Biol*, 213(5), 707-714.

MacDougall JD, Sale DG, Alway SE, & Sutton JR. (1984). Muscle fiber number in biceps brachii in bodybuilders and control subjects. *J Appl Physiol Respir Environ Exerc Physiol,* 57(5), 1399-1403

Maffiuletti N, Aagaard P, Blazevich A, Folland J, Tillin N, & Duchateau J. (2016). Rate of force development: physiological and methodological considerations. *Eur J Appl Physiol,* 116(6), 1091-1116.

Maffiuletti N, Bizzini M, Widler K, & Munzinger U. (2010). Asymmetry in quadriceps rate of force development as a functional outcome measure in TKA. Clin *Orthop Relat Res,* 468(1), 191-198.

Maganaris CC, Baltzopoulos V, & Sargeant AJ. (2002). Repeated contractions alter the geometry of human skeletal muscle. *J Appl Physiol,* 93(6), 2089-2094.

Maganaris CN & Baltzopoulos V. (1999). Predictability of in vivo changes in pennation angles of human tibialis anterior from rest to maximum isometric dorsiflexion. *Eur J Appl Physiol Occup Physiol,* 79(3), 294-297.

Maganaris CN & Paul JP. (1999). In vivo human tendon mechanical properties. *J Physiol,* 521(Pt 1), 307-313.

Maganaris CN & Paul JP. (2000). Load-elongation characteristics of in vivo human tendon and aponeurosis. *J Exp Biol,* 203(Pt 4), 751-756.

Maganaris CN & Paul JP. (2002). Tensile properties of the in vivo human gastrocnemius tendon. *J Biomech,* 35(12), 1639-1646.

Maganaris CN, Baltzopoulos V, & Sargeant AJ. (1998). In vivo measurements of the triceps surae complex architecture in man: implications for muscle function. *J Physiol,* 512(Pt 2), 603-614.

Maganaris CN, Narici MV, & Maffulli N. (2008). Biomechanics of the Achilles tendon. *Disabil Rehabil,* 30(20-22), 1542-1547.

Magnusson SP & Kjaer M. (2003). Region-specific differences in Achilles tendon cross-sectional area in runners and non-runners. *Eur J Appl Physiol,* 90(5-6), 549-553.

Magnusson SP, Hansen P, Aagaard P, Brønd J, Dyhre-Poulsen P, Bojsen-Moller J, & Kjaer M. (2003). Differential strain patterns of the human gastrocnemius aponeurosis and free tendon, in vivo. *Acta Physiol Scand,* 177(2), 185-195.

Magnusson SP, Narici MV, Maganaris CN, & Kjaer M. (2008). Human tendon behaviour and adaptation in vivo. *J Physiol,* 586(1), 71-81.

Malliaras P, Kamal B, Nowell A, Farley T, Dhamu H, Simpson V, Morrissey D, Langberg H, Maffuli N, & Reeves ND. (2013). Patellar tendon adaptation in relation to load-intensity and contraction type. *J Biomech,* 46(11), 1893-1899.

Massey G, Evangelidis P, & Folland J. (2015). Influence of contractile force on the architecture and morphology of the quadriceps femoris. *Exp Physiol,* 100(11), 1342-1351.

Matson A, Konow N, Miller S, Konow PP, & Roberts TJ. (2012). Tendon material properties vary and are interdependent among turkey hindlimb muscles. *J Exp Biol,* 215(Pt 20), 3552-3558.

McMahon GE, Morse CI, Burden A, Winwood K, Onambélé-Pearson GL. (2013). The manipulation of strain, when stress is controlled, modulates in vivo tendon mechanical properties but not systematic TGF-B1 levels. *Physiol Rep,* 1(5): e00091.

McNair PJ, Wood GA, & Marshall RN. (1992). Stiffness of the hamstring muscles and its relationship to function in anterior cruciate ligament deficient individuals. *Clin Biomech (Bristol, Avo*n), 7(3), 131-137.

Miller BF, Olesen JL, Hansen M, Døssing S, Crameri RM, Welling RJ, Langberg H, Fyvbjerg A, Kjaer M, Babraj JA, Smith K, & Rennie MJ. (2005). Coordinated collagen and muscle protein synthesis in human patella tendon and quadriceps muscle after exercise. *J Physiol,* 567(Pt 3), 1021-33.

Mirkov DM, Nedeljkovic A, Milanovic S, & Jaric S. (2004). Muscle strength testing: evaluation of tests of explosive force production. *Eur J Appl Physiol,* 91(2-3), 147-54.

Muramatsu T, Muroaka T, Kawakami Y, Shibayama A & Fukunaga T. (2002). In vivo determination of fascicle curvature in contracting human skeletal muscle. *J Appl Physiol,* 92(1), 129-134.

Muraoka T, Kawakami Y, Tachi M, & Fukunaga T. (2001). Muscle fiber and tendon length changes in the human vastus lateralis during slow pedaling. *J Appl Physiol,* 91(5), 2035-40.

Nagayoshi T, Kawakami Y, Maeda M, Maeda Y, Hidaka S, Ikeda K, & Maruyama A. (2003). The relationships between ankle dorsiflexion torque and muscle size indices. *Int J Sport Health Sci,* 1(2), 216-221.

Narici M & Maganaris C. (2006). Muscle architecture and adaptations to functional requirements. In: Bottinelli R, Reggini C (eds) *Skeletal muscle plasticity in health and disease: from genes to whole muscle*. Springer, Netherlands, 65-288.

Narici M. (1999). Human skeletal muscle architecture studied in vivo by non-invasive imaging techniques: functional significance and applications. *J Electromyogr Kinesiol,* 9(2), 97-103.

Narici MV, Binzoni T, Hiltbrand E, Fasel J, Terrier, & Cerretelli P. (1996a). In vivo human gastrocnemius architecture with changing angle at rest and during graded isometric contraction. *J Physiol,* 496(1) 287–297

Narici MV, Hoppeler H, Kayser B, Landoni L, Claassen H, Gavardi C, Conti M, & Cerretelli P. (1996b). Human quadriceps cross-sectional area, torque and neural activation during 6 months strength training. *Acta Physiol Scand,* 157(2), 175-186.

Narici MV, Roi GS, Landoni L, Minetti AE, & Cerretelli P. (1989). Changes in force, cross-sectional area and neural activation during strength training and detraining of the human quadriceps. *Eur J Appl Physiol Occup Physiol,* 59(4), 310-319.

Nordez A, Gallot T, Catheline S, Guevel A, Cornu, C, & Hug F. (2009). Electromechanical delay revisited using very high frame rate ultrasound. *J Appl Physiol,* 106(6), 1970-1975.

O'Brien TD, Reeves ND, Baltzopoulos V, Jones DA, & Maganaris CN. (2010). Muscle-tendon structure and dimensions in adults and children. *J Anat,* 216(5), 631-632.

Oatis CA (2009). Kinesiology: the mechanics and pathomechanics of human movement, 2nd ed. Philadelphia: Lippincott Williams & Wilkins.

Onambélé GL, Narici MV, & Maganaris CN. (2006). Calf muscle-tendon properties and postural balance old age. *J Appl Physiol,* 100(6), 2048-2056.

Opar DA, Williams MD, Timmins RG, Dear NM, & Shield AJ. (2013). Rate of torque and electromyographic development during anticipated eccentric contraction is lower in previously strained hamstrings. *Am J Sports Med,* 41(1), 116-125.

Pearson SJ, Burgess K, & Onambélé GN. (2007). Creep and the in vivo assessment of human patellar tendon mechanical properties. *Clin Biomech (Bristol, Avon),* 22(6), 712-717.

Peltonon J, Cronin NJ, Stenroth L, Finni T & Avela J. (2013). Viscoelastic properties of the Achilles tendon in vivo. *Springerplus,* 2(1) 212.

Phillips SM. (2014). A brief review of critical processes in exercise-induced muscular hypertrophy. *Sports Med,* 44(1), 71-77.

Powell PL, Roy RR, Kanim P, Bello MA, & Edgerton VR. (1984). Predictability of skeletal muscle tension from architectural determinations in guinea pig hindlimbs. *J Appl Physiol,* 57(6), 1715-1721.

Pucci AR, Griffin L, & Cafarelli E. (2006). Maximal motor unit firing rates during isometric resistance training in men. *Exp Physiol,* 91(1), 171-178.

Purslow PP. (2002). The structure and functional significance of variations in the connective tissue within muscle. *Comp Biochem Physiol A Mol Integr Physiol,* 133(4), 947-966.

Purslow PP. (2010). Muscle fascia and force transmission. *J Bodyw Mov Ther,* 14(4), 411-417.

Rahemi H, Nigam N, & Wakeling J. (2014). Regionalizing muscle activity causes changes to the magnitude and direction of the force from whole muscles – a modeling study. *Front Physiol,* 5: 298.

Randhawa A, Jackman ME, & Wakeling JM. (2013). Muscle gearing during isotonic and isokinetic movements in the ankle plantarflexors. *Eur J Appl Physiol,* 113(2), 437-447.

Rantanen T, Era P, & Heikkinen E. (1994). Maximal isometric strength and mobility among 75-year-old men and women. *Age Ageing,* 23(2),132-137.

Reeves ND, Maganaris CN, & Narici MV. (2003). Effect of strength training on human patella tendon mechanical properties of older individuals. *J Physiol,* 548(3), 971-981.

Rehorn M & Blemker S. (2010). The effects of aponeurosis geometry on strain injury susceptibility explored with a 3D muscle model. *J Biomech,* 43(13), 2574-2581.

Rich C & Cafarelli E. (2000). Submaximal motor unit firing rates after 8 wk of isometric resistance training. *Med Sci Sports Exerc,* 32 (1), 190-196.

Rieder F, Wiesinger HP, Kösters A, Müller E, &Seynnes OR. (2016). Whole-body vibration training induces hypertrophy of the human patellar tendon. *Scand J Med Sci Sports, 26(8),* 902-910.

Roberts TJ. (2002). The integrated function of muscles and tendons during locomotion. *Comp Biochem Physiol A Mol Integr Physiol,* 133(4), 1087-1099

Roberts TJ & Konow N. (2013). How tendons buffer energy dissipation by muscle by muscle. *Exerc Sport Sci Rev,* 41(4), 186-193.

Robinovitch SN, Heller B, Lui A, & Cortez J. (2002). Effect of strength and speed of torque development on balance recovery with the ankle strategy. *J Neurophysiol,* 88(2), 613-620.

Roman WJ, Fleckenstein J, Stray-Gundersen J, Always SE, Peshock R, & Gonyea WJ. (1993). Adaptations in the elbow flexors of elderly males after heavy-resistance training. *J Appl Physiol,* 74(2), 750-754.

Rosager S, Aagaard P, Dyhre-Poulsen P, Neergaard K, Kjaer M, & Magnusson SP. (2002). Load-displacement properties of the human triceps surae aponeurosis and tendon in runners and non-runners. *Scand J Med Sci Sports,* 12(2), 90-98.

Screen HR. (2009). Hierarchical approaches to understanding tendon mechanics. *J Biomech Sci Eng,* 4(4), 481-499.

Schultz AB. (1995). Muscle function and mobility biomechanics in the elderly: an overview of some recent research. *J Gerontol A Biol Sci Med Sci,* 50 (Spec No), 60-3.

Schulze F, Mersmann F, Bohm S, & Arampatzis A. (2012). A wide number of trials is required to achieve acceptable reliability for measurement patellar tendon elongation in vivo. *Gait Posture,* 35(2), 334-338.

Schwartz FP, Bottaro M, Celes RS, Brown LE, & Nascimento FA. (2010). The influence of velocity overshoot movement artifact on isokinetic knee extension tests. *J Sports Sci Med,* 9(1), 140-146.

Scott S & Loeb G. (1995). Mechanical properties of aponeurosis and tendon of the cat soleus muscle during whole-muscle isometric contractions. *J Morphol,* 224(1), 73-86.

Seger JY & Thorstensson A. (2000). Electrically evoked eccentric and concentric torque-velocity relationships in human knee extensor muscles. *Acta Physiol Scand,* 169(1), 63-69.

Seynnes OR, Bojsen-Møller J, Albracht K, Arndt A, Cronin NJ, Finni T, & Magnusson SP. (2015). Ultrasound-based testing of tendon mechanical properties: a critical evaluation. *J Appl Physiol,* 118(2), 133-141.

Seynnes OR, de Boer M, & Narici MV. (2007). Early skeletal muscle hypertrophy and architectural changes in response to high intensity resistance training. *J Appl Physiol,* 102(1), 368-373.

Seynnes OR, Erskine RM, Maganaris CN, Longo S, Simoneau EM, Grosset JF, & Narici MV. (2009). Training-induced changes in structural and mechanical properties of the patellar tendon are related to muscle hypertrophy but not to strength gains. *J Appl Physiol,* 107(2), 523-530.

Seynnes OR, Kamandulis S, Kairaitis R, Helland C, Campbell, EL, Brazaitis M, Skurvydas A, & Narici MV. (2013). Effect of androgenic-anabolic steroids and heavy strength training on patellar tendon morphological and mechanical properties. *J Appl Physiol,* 115(1), 84-89.

Simonsen E B, Klitgaard H, & Bojsen-Møller F. (1995). The influence of strength training, swim training and ageing on the Achilles tendon and m. soleus of the rat. *J Sports Sci,* 13(4), 291-295.

Skelton DA, Kennedy J, & Rutherford OM. (2002). Explosive power and asymmetry in leg muscle function in frequent fallers and non-fallers aged over 65. *Age Ageing,* 31(2), 119-125.

Smith K & Rennie MJ (2007). New approaches and recent results concerning human-tissue collagen synthesis. *Curr Opin Clin Nutr Metab Care,* 10(5) 582-590.

Stafilidis S, Karamanidis K, Morey-Klasping G, Demonte G, Bruggemann GP, Arampatzis A. (2005). Strain and elongation of the vastus lateralis aponeurosis and tendon in vivo during maximal isometric contraction. *Eur J Appl Physiol,* 94(3), 317-322.

Stenroth L, Peltonen J, Cronin NJ, Sipilä S, & Finni T. (2012). Age-related differences in Achilles tendon properties and triceps surae muscle architecture in vivo. *J Appl Physiol,* 113(10) 1537-1544.

Stone MH, Moir G, Glaister M, & Sanders R. (2002). How much strength is necessary? *Phys Ther Sport,* 3(2), 88-96.

Strasser EM, Draskovits T, Praschak M, Quittan M, & Graf A. (2013). Associations between ultrasound measurements of muscle thickness, pennation angle, echogenicity and skeletal muscle strength in the elderly. *Age (Dordr),* 35(6), 2377-2388.

Sullivan BE, Carroll CC, Jemiolo B, Trappe SW, Magnusson SP, Døssing S, Kjaer M, & Trappe TA. (2009). Effect of acute resistance exercise and sex on human patellar tendon structural and regulatory mRNA expression. *J Appl Physiol,* 106(2), 468-475.

Svensson RB, Hansen P, Hassenkam T, Haraldsson BT, Aagaard P, Kovanen V, Krosgaaard M, Kjaer M, & Magnusson SP (2012). Mechanical properties of human patellar tendon at the hierarchical levels of tendon and fibril. *J Appl Physiol,* 112(3), 419-26.

Svensson RB, Heinemeier KM, Couppé C, Kjaer M, & Magnusson SP. (2016). The effect of aging and exercise on the tendon. *J Appl Physiol,* doi: 10.1152/japplphysiol.00328 [Epub].

Theis N, Mohagheghi AA & Korff T. (2012). Method and strain rate dependence of Achilles tendon stiffness. *J Electromyogr Kinesiol* 22(6), 947-953.

Thorpe C, Birch H, Clegg P, & Screen H. (2013). The role of the non-collagenous matrix in tendon function. *Int J Exp Pathol,* 94(4), 248-259.

Tillin NA & Folland JP. (2014). Maximal and explosive strength training elicit distinct neuromuscular adaptations, specific to the training stimulus. *Eur J Appl Physiol,* 114(2), 365-374.

Tillin NA, Jimenez-Reyes P, Pain MT, & Folland JP. (2010). Neuromuscular performance of explosive power athletes versus untrained individuals. *Med Sci Sports Exerc,* 42(4), 781-790.

Tillin NA, Pain MT & Folland JP. (2013a). Explosive force production during isometric squats correlated with athletic performance in rugby union players. *J Sports Sci,* 31(1), 66-76.

Tillin NA, Pain MT, & Folland JP. (2011). Short-term unilateral resistance training affects the agonist-antagonist but not the force-agonist activation relationship. *Muscle Nerve,* 43(3), 375-384.

Tillin NA, Pain MT, & Folland JP. (2013b). Identification of contraction onset during explosive contractions. Response to Thompson et al. "Consistency of rapid muscle force characteristics: Influence of muscle contraction onset detection methodology" [J Electromyogr Kinesiol 2012;22(6):893–900]. *J Electromyogr and Kinesiol,* 23(4), 991-994.

Tillin NA, Pain, MT, & Folland JP. (2012). Short-term training for explosive strength causes neural and mechanical adaptations. *Exp Physiol,* 97(5), 630-641.

Van Cutsem M, Duchateau J, & Hainaut K. (1998). Changes in single motor unit behaviour contribute to the increase in contraction speed after dynamic training in humans. *J Physiol,* 513(Pt 1), 295-305.

Viitasalo JT & Komi PV. (1978). Force-time characteristics and fiber composition in human leg extensor muscles. *Eur J Appl Physiol Occup Physiol,* 40(1), 7-15.

Wakahara T, Ema R, Miyamoto N, & Kawakami Y. (2015). Increase in vastus lateralis aponeurosis width induced by resistance training: implications for a hypertrophic model of pennate muscle. *Eur J Appl Physiol,* 115(2), 309-316.

Wakahara T, Kanehisa H, Kawakami Y, Fukunaga T, & Yanai T. (2013). Relationship between muscle architecture and joint performance during concentric contractions in humans. *J Appl Biomech,* 29(4), 405-412.

Wakeling JM, Blake OM, Wong I, Rana M, & Lee SS. (2011). Movement mechanics as a determinant of muscle structure, recruitment and coordination. *Philos Trans R Soc Lond B Biol Sci,* 366(1570), 1554-1564.

Wang JH. (2006). Mechanobiology of tendon. *J Biomech,* 39(9), 1563-82.

Wang HK, Lin KH, Su SC, Shih TT, & Huang YC. (2012). Effects of tendon viscoelasticity in Achilles tendinosis on explosive performance and clinical severity in athletes. *Scand J Med Sci Sports,* 22(6), e147-e155,

Ward SR, Eng CM, Smallwood LH, & Lieber RL. (2009). Are current measurements of lower extremity muscle architecture accurate? *Clin Orthop Relat Res,* 467(4), 1074-1082.

Waugh CM, Korff T, Fath F, & Blazevich AJ. (2013). Rapid force production in children and adults: mechanical land neural contributions. *Med Sci Sports Exerc,* 45(4), 762-771.

Waugh CM, Korff T, Fath F, & Blazevich AJ. (2014). Effects of resistance training on tendon mechanical properties and rapid force production in prepubertal children. *J Appl Physiol,* 117(3), 257-266.

Westing SH, Cresswell AG, & Thorstensson A. (1991). Muscle activation during maximal voluntary eccentric and concentric knee extension. *Eur J Appl Physiol,* 62(2), 104-108.

Westing SH, Seger JY, & Thorstensson A. (1990). Effects of electrical stimulation on eccentric and concentric torque-velocity relationships during knee extension in man. *Acta Physiol Scand,* 140(1), 17-22.

Westing SH, Seger JY, Karlson E, & Ekblom B. (1988). Eccentric and concentric torque-velocity characteristics of the quadriceps femoris in man. *Eur J Appl Physiol,* 58(1-2), 100-104.

Weyand P, Sandell R, Prime D, & Bundle M. (2010). The biological limits to running speed are imposed from the ground up. *J Appl Physiol,* 108(4), 950-961.

Wickiewicz TL, Roy RR, Powell PL, Perrine JJ, & Edgerton VR. (1984). Muscle architecture and force-velocity relationships in humans. *J Appl Physiol Respir Environ Exerc Physiol,* 57(2), 435-443.

Wiesinger HP, Kösters A, Müller E, & Seynnes OR. (2015). Effects of increased loading on in vivo tendon properties: a systematic review. *Med Sci Sports Exerc,* 47(9), 1885-1895.

Wiesinger HP, Rieder F, Kösters A, Müller E, & Seynnes OR. (2016). Are sport-specific profiles of tendon stiffness and cross-sectional area determined by structural or functional integrity? *PLoS One,* 11(6), e0158441.

Wilkie D. (1949). The relation between force and velocity in human muscle. *J Physiol,* 110(3-4), 249-280.

Wilkinson SB, Tarnopolsky MA, Grant EJ, Correira CE, & Phillips SM. (2006). Hypertrophy with unilateral resistance exercise occurs without increases in endogenous anabolic hormone concentration. *Eur J Appl Physiol,* 98(6), 546-555.

Wilson GJ, Murphy AJ, & Pryor JF. (1994). Musculotendinous stiffness: its relationship to eccentric, isometric, and concentric performance. *J Appl Physiol,* 76(6), 2714-2719.

Winters J & Rudolph K. (2014). Quadriceps rate of force development affects gait and function in people with knee osteoarthritis. *Eur J Appl Physiol,* 114(2), 273-284.

Wren TAL & Carter DR. (1998). A microstructural model for the tensile constitutive and failure behavior of soft skeletal connective tissues. *J Biomech Eng,* 120(1), 55-61.

Wojtys EM, Ashton-Miller JA, & Hustons LJ. (2002). A gender-related difference in the contribution of the knee musculature to sagittal-plane shear stiffness in subjects with knee laxity. *J Bone Joint Surg Am,* 84-A(1), 10-16.

Zajac FE. (1989). Muscle and tendon: properties, models, scaling, and application to biomechanics and motor control. *Crit Rev Biomed Eng,* 17(4), 359-411.

Zatsiorsky V & Prilutsky B. (2012). *Biomechanics of skeletal muscles*. Champaign, IL: Human Kinetics.

Zuurbier CJ & Huijing PA. (1992). Influence of muscle geometry on shortening speed of fibre, aponeurosis and muscle. *J Biomech,* 25(9), 1017-1026.